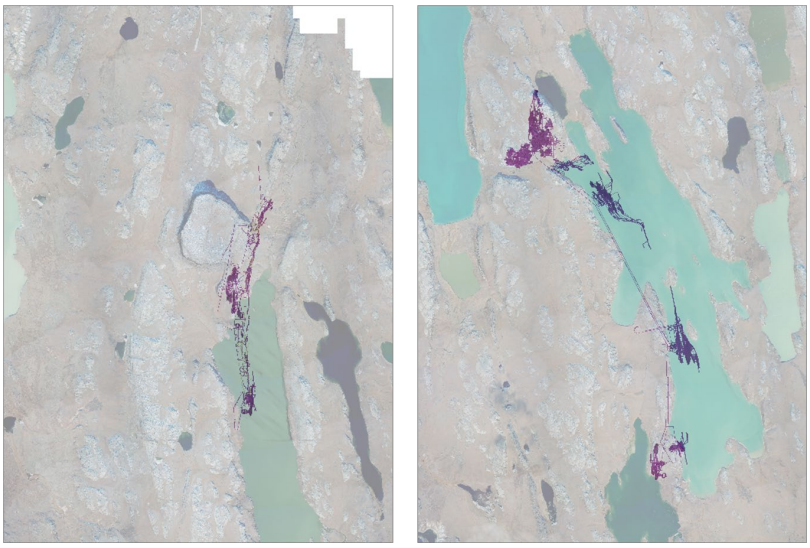
AGNICO EAGLE

2024 Hydrogeological Modeling Update

Prepared for

Agnico Eagle Mines Limited



Prepared by

srk consulting

SRK Consulting (Canada) Inc.
CAPR003296
January 2025

2024 Hydrogeological Modeling Update

January 2025

Prepared for

Agnico Eagle Mines Limited
11600, rue Louis-Bisson
Mirabel, Quebec J7N 1G9
Canada

Tel.: 52 (635) 457 6000
Web: agnicoeagle.com

Prepared by

SRK Consulting (Canada) Inc.
320 Granville Street, Suite 2600
Vancouver, BC V6C 1S9
Canada

Tel.: +1 604 681 4196
Web: www.srk.com

Project No.: CAPR003296

File Name: HopeBay_2025FEIS-GWModel-Addendum_Report_CAPR003296_20240124.docx

Copyright © SRK Consulting (Canada) Inc., 2025

srk consulting

Executive Summary

Agnico Eagle Mines Limited (Agnico Eagle) is planning to restart underground mining operations at the Hope Bay Project (the "Project"), in the Kitikmeot region of western Nunavut, Canada. SRK Consulting Ltd. (SRK) was retained to review the hydrogeological data and update the groundwater conceptual model and numerical model for the Project and estimate groundwater inflow and chloride concentration for an updated mine plan. This information will support the on-going environmental permitting process and serve as a basis to assess the effect of the mines to the groundwater environment and as inputs to the updated Project Water and Load Balance (SRK, 2024).

The Hope Bay greenstone belt hosts three known gold deposits (Doris, Madrid and Boston). Agnico Eagle proposes to expand the Doris mine developed by TMAC between 2017 and 2021 and develop a new underground mine at Madrid.

The Hope Bay belt drains directly into the Arctic Ocean. Numerous lakes and ponds are present, predominantly orientated along a north-south axis. Climate can be described as a sub-Arctic desert with limited rainfall, long dark winters and short bright summers. The Project is within Canada's continuous permafrost region, where permafrost (i.e., frozen ground) can extend to depths of 400 to 500 mbgs (meter below ground surface). Groundwater cannot flow in frozen ground; it can move in the active zone and in features called taliks, where rock is unfrozen. The active zone refers to the layer of ground that undergoes seasonal thawing and freezing. In most cases, taliks are formed by the heat of large water bodies such as lakes; an open talik is an unfrozen zone that penetrates completely and connects to sub-permafrost (i.e., the non-frozen ground below the permafrost).

The regional bedrock geology is composed of a greenstone belt dominated by mafic volcanic rocks. The overburden, up to 30 m in thickness, comprises locally and regionally derived tills and boulder tills with lacustrine and marine sediments and clay up to 15 m thick in the larger valleys. In lake bottoms, limnic sediments range in thickness between a few centimetres to as much as 2 m, under which is a consolidated layer of marine silty clay and clayey silts between 10 and 20 m thick.

Each site, Doris, Madrid, and Boston, has hydraulic conductivity, groundwater level, groundwater quality, and ground temperature data. During operations at Doris, groundwater flow and quality data were also recorded from underground locations.

The hydraulic conductivity (K) dataset includes a total of 190 test measurements in bedrock (i.e., excluding tests in permafrost). These were obtained from surface or underground drilling using slug tests, or short and long-duration packer injection tests. The K values are typically low, at Doris ranging between $<1x10^{-9}$ m/s and $4x10^{-6}$ m/s, with a geomean of $5x10^{-8}$ m/s, and at Madrid ranging between $< 1x10^{-9}$ and $1x10^{-6}$ m/s, with a geomean of $2x10^{-9}$ m/s. The spatial distribution of K values does not show a particular pattern. K values tend to decrease progressively with depth, which is interpreted to a result of reduction of fracture apertures with depth as lithostatic load increases. The probability of encountering higher K can increase in

areas with higher frequencies of fractures, but not always as shown by weak correlation coefficients. The Doris dataset includes fourteen tests, out of a total of 99 tests, that intercept structural features, from gouge-filled fractures to rubble zones; only eight had K greater than the geometric mean ($7x10^{-8}$ to $6x10^{-6}$ m/s). The Madrid dataset shows no evidence of higher K features associated with dyke contacts, major structures or faults, and/or the MDZ.

K measurements in soft lakebed sediments were obtained from 28 pressure dissipation tests conducted during cone penetrometer (CPT) drilling in sediments lining the base of Doris Lake, Patch Lake and Aimakatalok Lake (SRK 2009a) with a geomean of $1x10^{-8}$ m/s. CPT refusals were not associated with bedrock contact, but an indurated layer of lake sediment. Two samples were sent to a laboratory for consolidation testing and had hydraulic conductivity of $4.6x10^{-10}$ and $3.5x10^{-10}$ m/s, respectively (SRK 2009a).

Pre-mining groundwater level data consist of pressure profiles in two Westbay wells, two VWPs, and two drillholes. Groundwater pressure is converted to absolute elevations, but the water is saline and higher density affects the pressure, resulting in an accuracy of ±7 m, corresponding to a density variation of ±0.015 kg/m^3. Pre-mining groundwater levels were approximately at or near the lake levels, and the pressures in Westbay wells suggested a low vertical upward gradient. Additional groundwater pressures were measured during operations in the Doris underground mine and showed effects of mine dewatering, with pressures dropping below the level of Doris Lake as depressurization around the underground developments progressed.

Samples for groundwater quality were collected between 2010 and 2013, in 2022, and in 2023 at Doris, Madrid, and Boston. These samples were analyzed for standard parameters, major cations and anions, and total and dissolved metals. In the period 2010-2013, stable isotopes of oxygen and hydrogen were also analyzed to ensure quality assurance and control (QA/QC) and to assess variations in water source types. Baseline groundwater quality (i.e., 2010-2013) was compared to environmental guidelines[1] with concentrations of ammonia, boron, cadmium, chloride, fluoride, iron, manganese, nickel, selenium, and zinc exceeding guideline concentrations, making them potential constituents of concern. Groundwater samples collected during operations (i.e., 2022-2023) show a dilution of constituents and an increase of alkalinities interpreted to result from the dewatering of the Doris underground.

Ground temperatures have been measured with thermistors at Doris, Madrid and Boston. The active layer is generally less than 1 meter thick, with the depth of zero annual amplitude around 10 m. Freezing point depression based on measured groundwater salinity defined the -2°C isotherm as the boundary between taliks and permafrost.

The base of the permafrost (-2°C isotherm), away from lakes, is at approximately 447 mbgs. The vertical contacts between permafrost and open taliks are located near lake shorelines, at distances driven by thermal dynamics. The boundary slopes outward and downward as it

[1] Canadian Council of Ministers of the Environment (CCME) water quality guidelines for freshwater, irrigation, livestock, and marine (2024) and the Metal and Diamond Mining Effluent Regulations (MDMER) limits for harmful substances (2024)

extends deeper, and permafrost begins to dominate. In cross-section, it takes generally the shape of a parabola with its concave side oriented vertically beneath the lake.

A one-dimensional (1D) steady state analytical thermal model estimated the critical lake dimensions to sustain open taliks underneath water bodies: a) circular water bodies with a diameter greater than 224 m, b) elongated water bodies with a width of at least 104 m, and c) water bodies deeper than 1.3 m. Local 3D configurations of open taliks were estimated in Madrid and Boston areas using 2D thermal modeling in zones where distances between lakes were small and heat from lakes potentially interfering.

SRK reviewed the mine inflow rate and quality monitored during operations at Doris, and the inflows at individual drillholes (i.e., drilling records, packer test or axial velocity measurements), recorded between December 2020 and October 2022, from discrete locations or specific intervals or fractures intercepted by developments. The mine started encountering inflows in January 2018, at an elevation of about -120 masl, when it reached the boundary between permafrost and the Doris Lake open talik; the boundary was approximately vertically below the Doris Lake shoreline when projected downward. The initial concentrations of chloride (22,500 mg/L) were higher than observed prior to mining (6,060 to 14,200 mg/L at -198 masl). The total mine inflow increased progressively as the mine was developed and peaked in January 2020 at about 2,800 m3/day. Between 2020 and 2021 inflow rate plateaued at an average of 1,600 m^3/d.

Most groundwater inflows occurred primarily in the central area and originated from underground diamond drillholes, with flow rates typically within 10 to 50 m^3/d, and a very low percentage of individual holes with up to 2,180 m^3/day. It is uncertain whether inflows from individual features (i.e., drillholes or fractures) decreased over time, which is a behaviour that would be the expected for groundwater released from storage in the fractures rather than a direct connection with Doris Lake. Overall, inflows were highest as mining reached and occurred at its lowest elevations. This suggests the overall increase in inflows was primarily driven by the increase of hydraulic gradient between the mine and Doris Lake, rather than interception of specific geological structures, or exploration drillholes.

Inferences on cause of short-term fluctuations of mine inflow and/or quality that are observed to have occurred found that, 1. while not common, un-grouted surface exploration holes can lead to high inflows, such as during September 2018 when a flow of about 3,650 m^3/d was encountered from a drillhole (hole plugged in October 2018), and 2. the relationships between inflow peaks and structures remain uncertain except at the contact with, or in proximity of, the diabase dyke, which has been frequently reported to produce water. Peaks un-related to drillholes corresponded to short-term temporary increases of both inflow and chloride, suggesting that the features causing these peaks have a limited storage and are connected with deep saline groundwater.

The system is conceptualized as a low-flow, lake-dominated, confined flow system. The widespread, deep permafrost is essentially impermeable. Groundwater flow and connections between surface and deep bedrock groundwater systems occur exclusively in areas where lakes are associated with open taliks or in sub-permafrost zones. Groundwater systems in shallow

active zones have no or minimal influences on inflows to underground mining areas compared to the deeper flow dynamics within the open talik surrounding the underground mine.

K measurements for fractured rock and lake sediments fall within the bounds of published K values. Lake bottoms are draped with low K, fine sediments. At the small scale, bedrock K is fracture controlled, consisting of a low bulk K background intersected by distributed, potentially higher K fractures and geological structures. At the project scale, fractured rock is treated as a single unit, without differentiation between lithologies. This unit is characterized by relatively higher K at shallow depths, gradually decreasing with depth due to increasing confining pressure.

Groundwater is brackish to saline and can have elevated concentrations of major ions and metals. The concentrations of calcium, chloride and sodium show a general trend of increasing concentration with depth; other constituents can also have relatively high concentrations, but do not correlate with depth. Denser saline groundwater requires more energy to move. It tends to sink, move more slowly, and resist upward movement, while lighter freshwater flows more easily. This buoyancy effect can lead to stratification, greater resistance to downward vertical flow, and the formation of slow density-driven convection currents, where saline water sinks and freshwater rises.

During mining operations, the dewatering activities will alter groundwater flow gradients. Depressurization around parts of mines located within taliks or sub-permafrost will extend radially, drawing potentially upward and lateral saline flow from the talik, and downward freshwater flow from the lakes above. The low permeability fine lakebed sediments will limit downward infiltration. Initially, the salinity of the mine inflows will reflect the saline conditions of the surrounding groundwater system and become progressively less saline over time as the relative contribution from shallow freshwaters increases. As K in bedrock decreases with depth, groundwater inflows to the mine are expected to be more significant in shallower regions.

While the mine may intercept geological structures or fractures, historical observations of the Doris mine suggest they will have limited storage capacity and are more likely connected to deep saline groundwater rather than directly to the lakes above. At Doris specifically, the contacts with the diabase dykes are frequently reported to produce water and theorized to be associated with a more permeable contact zone. At Madrid, while no high K structures have been identified, the eastern contact of the MDZ, which typically hosts brittle faults parallel to it, could be theoretically associated with potentially higher K features.

Placement of CRF backfill in the underground will have some influence on mine inflows. Based on experience with similar materials on other projects, hydraulic conductivity of backfill is expected to be within or above the upper range of the shallow bedrock and therefore lead to a low to moderate reduction of inflow at shallow depth and no reduction at depth.

The heat circulated into the underground mines will generate a lateral thaw of the bedrock at distances of about 50 m from the workings. The heat will increase the volume of unfrozen ground around the mines, but it will not generate new open taliks that connect the ground surface to sub-permafrost.

At Closure, dewatering activities will stop. Re-flooding will result in a slow re-equilibration to baseline conditions, driven by the lakes' gradients and density gradients. Some parts of mine workings may continue to act as preferential pathways and may redistribute saline water from deeper zones into shallower regions or adjacent fractured zones. As water fills the mine, the heat will transfer to the surrounding permafrost and the underground areas will be expected to freeze-back where the minimum ground temperature is less than -2°C. It is possible that parts of the underground areas will not completely freeze back. The groundwater contained in unfrozen mined out areas may have its quality modified by the backfill and/or tailings deposited underground. It will become part of the regional groundwater system, and travel though the open taliks via the deep groundwater system. At Post-closure, the groundwater system will have returned to the same conditions as baseline with local influences on flow and groundwater quality immediately around the mines.

The numerical groundwater flow modeling was completed using the software FEFLOW 8.1. The model assumes media is saturated within a confined aquifer and density-dependent flow system. Bedrock is simulated as an equivalent porous media with homogeneous and isotropic hydraulic conductivity within overburden and fractured bedrock. Flow and transport processes are defined by Darcy's Law and advection-dispersion principles; mass transport is modeled using chloride as a conservative tracer; chemical reactions, attenuation processes, or biodegradation were not considered.

The model domain is 71 km^2 (i.e., approximately 18 x 4 km), with an upper surface defined by the topographical surface; the model base is a copy of the topographical surface set to a depth of 1,510 mbgs (between -1542 and -1354 masl), approximately twice the depth below ground of the lowest stopes (approx. 690 mbgs). The finite element mesh is constructed with 32 structured layers, and element width of about 20 m at tunnels and stopes, and 30 m along lake edges. The regional mesh elements are on the order of 30 m wide along lake edges and 100 m in areas away from features of interest. Vertically, the layer thickness ranges between 1 and 200 m.

The permafrost is represented by a selection of elements that matches the 3D geometries of the regional and local permafrost models. These elements are de-activated during simulations; no flow or transport happens through these elements.

The regional flow is simulated by applying constant head boundary conditions to the lakes supporting open taliks. Transport of chloride is simulated by applying an average chloride concentrations of 69 mg/L on the footprints of lakes supporting open taliks, and a vertical profile ranging between 69 and 22,500 mg/L on external borders. Mining is simulated with seepage boundary conditions (i.e., a constant head boundary with a flow constraint that only allows flow out of the model) associated with the mining schedule. The underground mines are represented by nodes aligned with the tunnels and stopes' overall 3D geometries but not explicitly incorporating the mine volume. Reduction in inflow due to grouting is not considered in the model. At the End-of-Mine, the mining boundary conditions are turned off.

The model calibration prioritized the mine inflow rates, and chloride concentrations observed during the 7-years of underground operations at Doris over pre-mining conditions. The pre-mining data, while valuable for the conceptual model, is inherently uncertain, while operational

data reflect the response of the groundwater system to the large stress imposed by mining activities. Calibration was an iterative process of varying the hydraulic conductivity profiles to match the transient observations of mine inflows and chloride concentration recorded between 2018 and 2024. The quality of calibration was rated visually by comparing the model results to observations.

The model replicated well the general trend of increasing and stabilizing mine inflows and the declining trend of chloride concentrations. It was not built to capture the short-term fluctuations, which may be due to episodic factors such as localized inflow with higher or lower salinity, changes in hydraulic connectivity, or interception of distinct water-bearing zones. A comparison between the modelled trend and observed short-term fluctuations showed future developments could potentially intercept additional contributions in the range of 100 to 610 m^3/d for a period of 2 to 8 months.

The base case model forecasts maximum inflows of 2,260 m^3/d in 2031 at Doris, and 750 m^3/d in 2039 at Madrid, and a progressive dilution over time of the chloride concentration with freshwater infiltrating from the lakes. At End-of-Mine, chloride concentrations were lowered to about 1,500 mg/L at Doris, and 9,500 mg/L at Madrid (i.e., equivalent TDS concentrations of 2,650 and 16,780 mg/L respectively). Lake infiltration was greatest for the lakes located directly above the mines, Doris Lake (2,230 m^3/d), Patch Lake (730 m^3/d), and Wolverine Lake (8 m^3/d). Time to reflood the mines at Closure were estimated to range between 4 and 52 years at Doris and Madrid respectively. At Post-closure, groundwater in contact with the Doris Mine will move towards Doris Lake, to the West and North (Roberts Bay), and groundwater in contact with the Madrid mine to Patch Lake, Windy Lake, and Wolverine Lake. Modelled travel times are long. After 1,000 years, no particles are predicted to have reached surface.

Additional scenarios were completed to assess the effects of parameter uncertainties on the calibration and forecasts of mine inflow, mine water quality, lake infiltrations, and reflood period at Closure. The sensitivity scenarios included variations to the permafrost, hydraulic conductivities, geological structures, storage compressibility, and density. The analysis of the model's sensitivity to parametrization showed model calibration and predictions were sensitive to changes in hydraulic conductivity of lakebed sediment or bedrock. These are considered sufficiently constrained by the field data and calibration to current conditions for Doris, but can affect predictions:

- Permafrost variations can influence the predicted leakages for Imniagut Lake and Wolverine Lake.
- Changes in K contrast between shallow and deep bedrock have limited effects on the predicted mine inflows but significant influence on chloride concentration at both Doris and Madrid, as well as leakage from lakes.
- Madrid has less K data than at Doris, but also a lower average than at Doris. Using the Doris K profile (which was calibrated to operational data) at Madrid resulted in significantly higher predicted inflow, but lower chloride concentration due to increased infiltration from Patch Lake.

- The “worst case” scenario combined the most conservative assumptions for the permafrost and hydraulic conductivity field in bedrock at Madrid. This model also resulted in increased flow at Madrid, a subsequent decrease in chloride concentration and a large increase in leakage from Imniagut and Wolverine lakes.
- Models did not explicitly assess the potential for mine inflow from unplugged surface drillholes, either as direct connection to lakes, or as small-scale, local connectors between fractures. Observations from Doris operations indicate an un-grouted surface exploration hole could produce an average flow of about 3,650 m^3/d. Predicting likelihood of any given drillhole to flow is difficult, but Operators were able to divert, manage and stop inflow from the hole within a relatively short time; capacity to manage such events should continue to be incorporated into contingency planning.

Table of Contents

1 Introduction 1
1.1 Scope of Work 1
1.2 Report Layout 1
2 Background 2
2.1 Site History and Mine Plan 2
2.2 Studies Supporting the Characterisation of the Groundwater System 4
3 Baseline Data 5
3.1 Topography, Hydrology and Climate 5
3.2 Permafrost 6
3.3 Geology 7
3.3.1 Regional Geology 7
3.3.2 Doris Bedrock Geology and Structures 8
3.3.3 Madrid Bedrock Geology and Structures 8
3.3.4 Boston Bedrock Geology and Structures 10
3.3.5 Surficial Geology 10
3.4 Doris Groundwater Monitoring Network 13
3.5 Madrid Groundwater Monitoring Network 16
3.6 Boston Groundwater Monitoring Network 18
3.7 Hydraulic Properties 20
3.7.1 Bedrock 20
3.7.2 Lake Sediments 25
3.7.3 Influence of Drillholes on Hydraulic Conductivity 25
3.8 Groundwater Levels 25
3.9 Groundwater Quality 26
3.9.1 Regional Groundwater Quality Data 26
3.9.2 Hope Bay Groundwater Quality Data 27
3.9.3 Freezing Point Depression 32
3.10 Permafrost Boundaries 33
3.10.1 Ground Temperatures 33
3.10.2 Regional Permafrost Model 33
3.10.3 Local Permafrost Models 35
3.11 Underground Inflow Data During Mine Operations 36
4 Conceptual Groundwater Model 38
4.1 Baseline Conditions 39
4.2 Mining Conditions 40

4.3 Closure Conditions 42
4.4 Post-Closure Conditions 42
5 Numerical Groundwater Model 43
5.1 Numerical Model Software 43
5.2 Numerical Model Assumptions 43
5.3 Numerical Model Setup 43
5.3.1 Domain 43
5.3.2 Mesh 44
5.3.3 Permafrost 45
5.3.4 Boundary Conditions 48
5.3.5 Water Density 50
5.3.6 Initial Flow and Mass Conditions 50
5.4 Numerical Model Calibration 51
5.4.1 Approach 51
5.4.2 Transient Calibration 51
5.4.3 Calibrated Properties 53
6 Numerical Model Results 55
6.1 Baseline Conditions 55
6.2 Mining Conditions 57
6.2.1 Mine Inflows 58
6.2.2 Mine Inflow Quality 58
6.2.3 Lake Infiltrations 59
6.3 Closure Conditions 60
6.4 Post-Closure Conditions 61
6.5 Sensitivity to Model Parameters 61
6.5.1 Sensitivity Scenarios 61
6.5.2 Sensitivity Ratings 64
6.5.3 Results 65
6.6 Sensitivity to Flow from Exploration Drillholes 69
7 Conclusions 69
8 References 73

List of Figures

Figure 2-1: Project location 2
Figure 2-2: Plan view and cross-section view of Doris proposed underground developments 3
Figure 2-3: Plan view and cross-section view of Madrid proposed underground developments 3
Figure 3-1: Conceptual drawing of open and closed taliks 7
Figure 3-2: Geological map of the Kitikmeot Region, Nunavut Territory, Canada 9
Figure 3-3: Patch Lake Substrate Classification, August 2023 12
Figure 3-4: Map of hydraulic conductivities measured at Doris from surface drillholes 13
Figure 3-5: Map of hydraulic conductivities measured at Doris from underground drillholes 13
Figure 3-6: Map of groundwater pressure measured at Doris during pre-mining conditions 14
Figure 3-7: Map of groundwater pressures measured at Doris during mining 14
Figure 3-8: Map of ground temperatures measured at Doris 15
Figure 3-9: Map of flow measurements recorded in the Doris underground mine 15
Figure 3-10: Map of hydraulic conductivities measured at Madrid (north area) from surface drillholes 16
Figure 3-11: Map of hydraulic conductivities measured at Madrid (central area) from surface drillholes .. 16
Figure 3-12: Map of hydraulic conductivities measured at Madrid (south area) from surface drillholes 17
Figure 3-13: Map of groundwater pressures measured at Madrid 17
Figure 3-14: Map of ground temperatures measured at Madrid 18
Figure 3-15: Hydraulic conductivity tests measured at Boston from surface drillhole 18
Figure 3-16: Map of ground temperatures measured at Boston 19
Figure 3-17: Hydraulic conductivity versus depth 21
Figure 3-18: Hydraulic conductivity versus fracture frequency 21
Figure 3-19: Hydraulic conductivity versus RQD 22
Figure 3-20: Box plot of the Doris K measurements by geology and structures 23
Figure 3-21: Box plot of the Madrid K measurements by geology and structures 24
Figure 3-22: TDS concentrations with depth in Canada's North 27
Figure 3-23: Chloride concentration versus depth 31
Figure 3-24: TDS vs Chloride 31
Figure 3-25: Potential open taliks in Doris and Madrid areas 34
Figure 3-26: Madrid local permafrost model 35
Figure 3-28: Distribution of flow observations from individual drillholes at the Doris mine 37

Figure 3-29: Mine water flow rates observed between 2017 and 2022 37
Figure 4-1: Hydrogeological conceptual model 38
Figure 4-2: Published K values Vs Hope Bay K measurements 39
Figure 4-3: Lateral Permafrost Thaw from Heated Air in Underground Mining Areas 41
Figure 5-1: Numerical model domain 44
Figure 5-2: Model mesh 45
Figure 5-3: Modelled permafrost 46
Figure 5-4: Permafrost confidence levels at Doris 47
Figure 5-5: Permafrost confidence levels at Madrid in the north area 47
Figure 5-6: Permafrost confidence levels at Madrid in the central area 47
Figure 5-7: Baseline head boundary conditions 49
Figure 5-8: Baseline mass boundary conditions 49
Figure 5-9: Mining head boundary conditions 50
Figure 5-10: Underground mines' bottom elevations versus time 50
Figure 5-11: Modelled versus observed underground inflow rates 52
Figure 5-12: Modelled versus observed chloride concentration of underground inflows 52
Figure 5-13: Calibrated K versus observed 53
Figure 5-14: Modelled calibrated K 54
Figure 5-15: Modelled thicknesses of lake sediments 54
Figure 6-1: Modelled groundwater heads for baseline conditions 55
Figure 6-2: Modelled chloride concentrations for baseline conditions 56
Figure 6-3: Modelled vertical profile of chloride concentrations for baseline conditions 57
Figure 6-4: Modelled groundwater heads at end of mine 57
Figure 6-5: Modelled chloride concentrations at end of mine 58
Figure 6-6: Modelled mine inflows during operations 58
Figure 6-7: Modelled chloride concentrations during operations 59
Figure 6-8: Modelled lake infiltration during operations 59
Figure 6-9: Modelled structures 63
Figure 6-10: Sensitivity K profiles: higher contrast between upper and lower bedrock 63
Figure 6-11: Sensitivity K profiles: lower contrast between upper and lower bedrock 64
Figure 6-12: Sensitivity K profiles: $1x10^{-9}$ m/s cutoff value 64

List of Tables

Table 2-1: Hydrogeological studies 4
Table 3-1: Statistical summary of the hydraulic conductivity dataset 20
Table 3-2: Hydraulic tests intersecting MDZ or other geological structures at Madrid 24
Table 3-3: Hydraulic Conductivity of Doris Lakebed Sediments 25
Table 3-4: Mean baseline groundwater quality (Doris, 10WBW001) 29
Table 3-5: Freezing point depression estimates 32
Table 4-1: Proposed Mine Volumes within and Outside Permafrost 40
Table 5-1: Thicknesses of the model layers 45
Table 5-2: Average elevations of the lakes 48
Table 5-3: Groundwater model properties 53
Table 6-1: Predicted flow rates for baseline conditions 56
Table 6-2: Mine volumes used for reflood estimates 60
Table 6-3: Base Case reflood time estimations 60
Table 6-4: Definitions and significance thresholds for sensitivity models 65
Table 6-5: Sensitivity Results 68

Appendices

Appendix A – Lake Bathymetries

Appendix B – Overburden Data

Appendix C – Hydraulic Conductivity Data

Appendix D – CPT Data

Appendix E – Groundwater Quality Data

Appendix F – Ground Temperature Data

Appendix G - Thermal Models

Appendix H –2020-2022 Doris Inflow Data

List of Abbreviations

°C	degree Celsius
BC	boundary condition
CPT	cone penetrometer test
CRF	cemented rock fill
DDH	diamond drillhole
EOM	end of mine
K	hydraulic conductivity
km	kilometer
LTFT	long-term flow test
m	metre
m/s	metre per second
m^3/d	cubic metre per day
mah	meter along hole
masl	meter above see level
mbgs	meter below ground surface
MDZ	Madrid Deformation Zone
Mg/L	milligram per litre
ML/ARD	metal leaching and acid rock drainage
mm	millimetre
MN	Madrid North
MS	Madrid South
RQD	Rock Quality Designation
SP	Saline Pond
Sx	storage compressibility
STFT	short-term flow test
TIA	Tailings Impoundment Area
TDS	total dissolved solids
UG	underground
VFP	velocity flow profile
MDMER	Metal and Diamond Mining Effluent Regulations

1 Introduction

Agnico Eagle Mines Limited (Agnico Eagle) is planning to restart underground mining operations at its Doris and Madrid Deposits, located at the Hope Bay Project (the “Project”), in the Kitikmeot region of western Nunavut, Canada, approximately 685 km northeast of Yellowknife, Northwest Territories, and 125 km southwest of Cambridge Bay.

The Hope Bay greenstone belt hosts three known gold deposits (Doris, Madrid and Boston). Agnico Eagle proposes to expand the Doris mine developed by TMAC between 2017 and 2021 and develop a new underground mine as well as waste and water management facilities at Madrid. Exploration will continue at Boston, but its development is not planned at this stage.

Agnico Eagle retained SRK Consulting (Canada) Inc. (SRK) to review the hydrogeological data and update the groundwater conceptual model and numerical model of the Project. This information will support the on-going environmental permitting process and serve as a basis to assess the effect of the mines to the groundwater environment and as inputs to the updated Project Water and Load Balance (SRK, 2024).

1.1 Scope of Work

The scope of work consisted of:

- A review, compilation, and discussion of the project-wide hydrogeological data.
- The development of the hydrogeology conceptual site model.
- The development of a groundwater numerical model and calibration to current conditions.
- Simulations of the groundwater system for baseline to the post-closure periods.
- Predictions of mine inflows and effects to the groundwater system.
- An analysis of the sensitivity of the predictions to model parameters.
- Reporting

1.2 Report Layout

The report is organized as follows:

- Section 2: Site history, current land use, and proposed mine designs.
- Section 3: Summary of the hydrogeological studies.
- Section : Compilation of the hydrogeological data supporting the characterization of the groundwater system.
- Section 5: Groundwater conceptual model.
- Section 6: Technical presentation of the numerical groundwater model.
- Section 7: Model forecasts.
- Section 7: Conclusions of the study.

2 Background

2.1 Site History and Mine Plan

The Hope Bay Project (Figure 2-1) covers an area of 1,100 km², approximately 80 km by 20 km, in the Kitikmeot region of Nunavut, Canada, approximately 685 km northeast of Yellowknife and 125 km southwest of Cambridge Bay The Project is within Canada's continuous permafrost region, where permafrost (i.e., frozen ground) can extend to depths of 400 to 500 mbgs (meter below the ground surface) excepted under large water bodies where taliks (i.e., unfrozen ground) are present. At surface, the area is dominated by a tundra ecosystem, rugged terrain with a mix of low hills and flat, barren ground, and numerous lakes and rivers. The current land uses are hunting, fishing, and trapping from the local community in addition to mining activities.

TMAC Resources Inc. started the development of the Doris mine in early 2017. Agnico Eagle took over mining operations in February 2021 and focused on producing from developed stopes and bringing ore to surface until March 2022, at which point operations were scaled back and underground development focused on supporting exploration activities.

The proposed updated mine plan (Agnico, 2024) includes additional developments at the Doris Mine (BCN, and BCO, Figure 2-2), and a new underground mine at Madrid (Figure 2-3), approximately 17 km south of Roberts Bay. Most of the waste rock brought to surface will be used as backfill in the underground mines. At Doris, the backfill will include a mix of previously placed detoxified tailings and cemented rock Fill (CRF). At Madrid it will consist solely of CRF. Mining operations will begin in 2028 and conclude in 2045 after which there will be a 2-year closure period followed by a 3-year post-closure period following operations. At closure, the underground will be flooded and the backfill will be submerged.

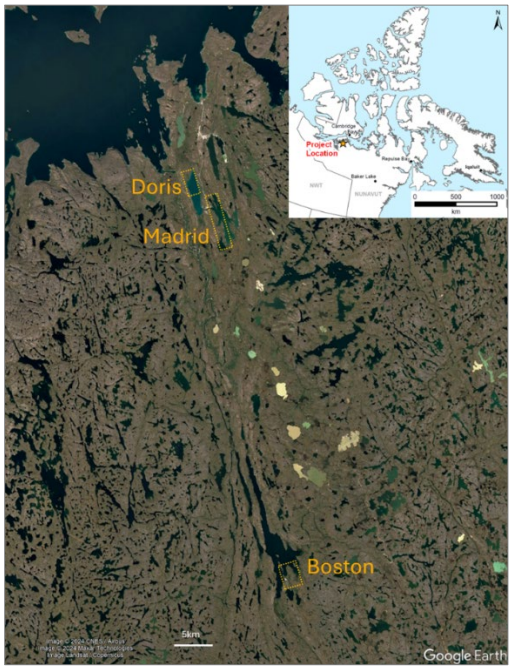


Figure 2-1: Project location

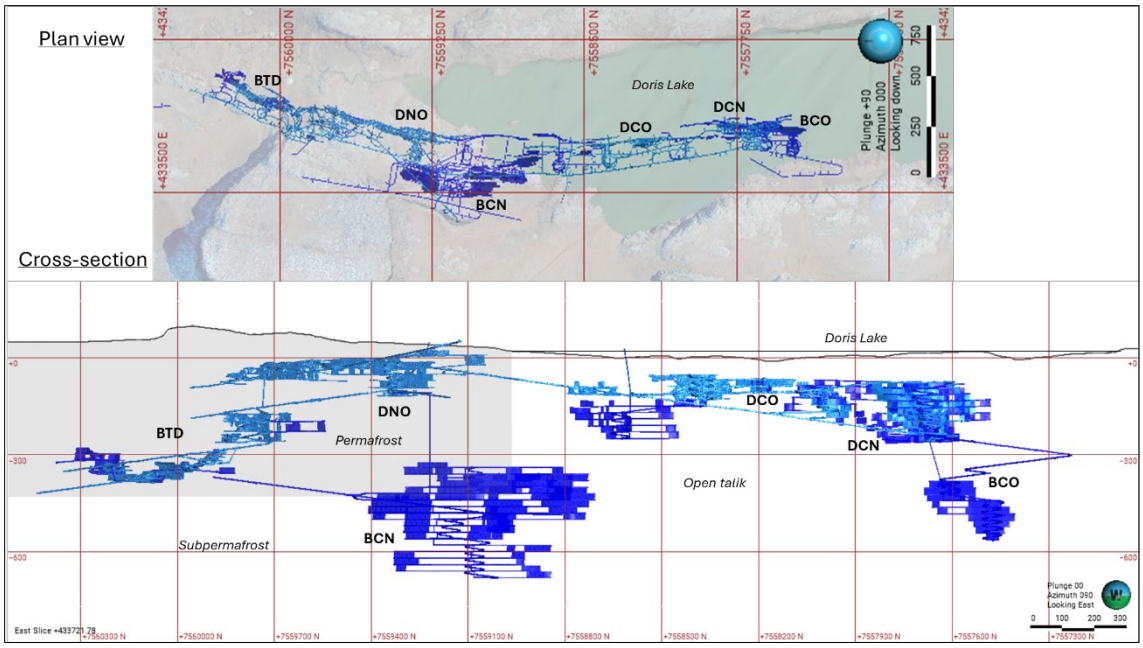


Figure 2-2: Plan view and cross-section view of Doris proposed underground developments

Source: fig_doris_cross-sections_mine,pptx, Leapfrog model ID 12766
(Projection: NAD83 / UTM zone 13N, unit: metre)

Note: Permafrost contacts illustrated based on thermistor data but simplified with vertical wall at the shore of Doris Lake

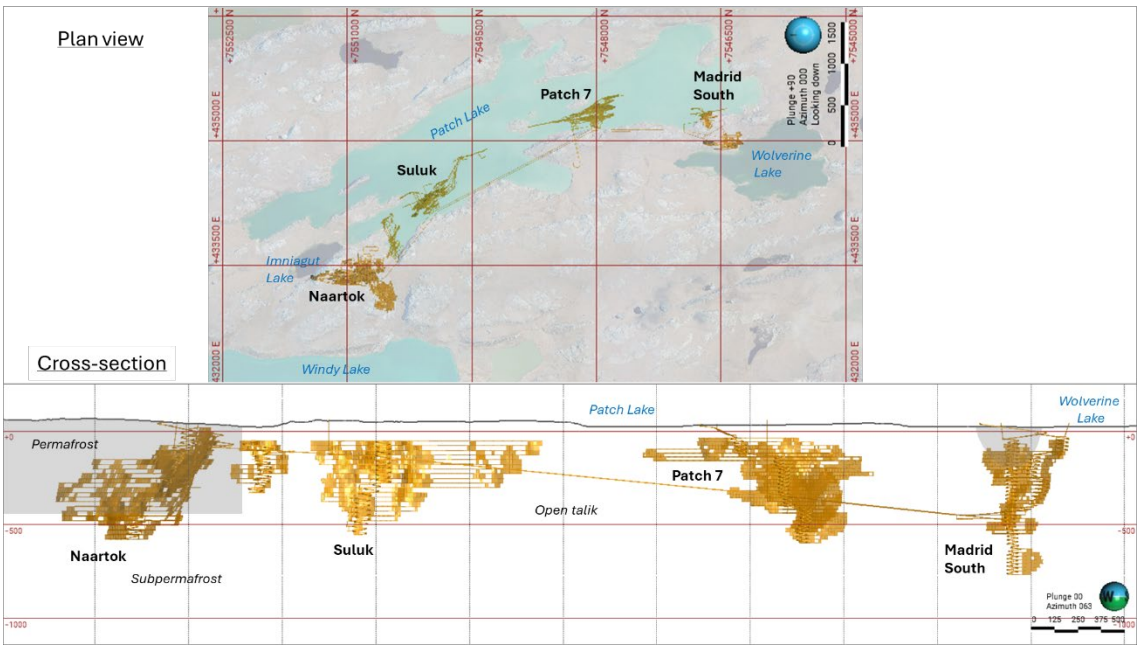


Figure 2-3: Plan view and cross-section view of Madrid proposed underground developments

Source: fig_madrid_cross-sections_mine_rev1.pptx, Leapfrog model ID 12766
(Projection: NAD83 / UTM zone 13N, unit: metre)

Note: Permafrost contacts illustrated based on thermistor data but simplified with vertical wall at the shore of Patch Lake

2.2 Studies Supporting the Characterisation of the Groundwater System

Table 2-1 summarizes hydrogeological studies used to support the Project. Complete references are provided in Section 8.

Table 2-1: Hydrogeological studies

Reference	Description
SRK, 2005	Installation of two thermistor strings at Doris; one in deep permafrost, the other in shallow permafrost.
SRK, 2009 a, b, c, d	Geotechnical and hydrogeological assessments for 1- an open pit at the Boston deposit, 2- an open pit and an underground mine at the Madrid deposit, and 3- an open pit and an underground mine at the Doris deposit. Assessments were based on field studies that included overburden characterisation, detailed structural review, hydrogeological investigations (including installations of additional thermistor), and geotechnical assessments.
SRK 2011a	Field program at Doris and Boston that included hydraulic testing, installation of Westbay multi-level monitoring wells, and groundwater quality sampling.
SRK 2011b	Summary of updated estimates of inflow rates and water quality for Doris, with assessment of potential flow from open exploration drill holes in talik.
SRK 2012	Summary of groundwater quality sampling and analysis results from the three existing Westbay wells: Doris North, Doris Central, and Boston.
SRK 2014	Review of Doris historical data and fieldwork, along with updates to the characterization of geotechnical and hydrogeological conditions. This information supported mine and infrastructure designs for an internal pre-feasibility study.
SRK 2014b	Summary of updated estimates of inflow rates and water quality for the Madrid South and Madrid North mines.
SRK, 2015a	Hydrogeological characterisation and groundwater numerical modeling of the Doris Mine; forecasts of groundwater inflow and quality to support a Type A Water Licence.
SRK, 2015b	Results of a site wide water and load balance for the Doris mine.
SRK, 2017a	Evaluation of the lake talik configurations: regional settings and local thermal modelling at Madrid and Boston.
SRK, 2017b	Hydrogeological characterisation and groundwater numerical modeling of the Madrid and Boston Mines; forecasts of groundwater inflow and quality to support the project site-wide water and load balance.
SRK, 2017c	Madrid-Boston project site-wide water and load balance.
TMAC, 2016	Groundwater management plan describing TMAC's management and work to minimize water that flows into the mine.
TMAC, 2020	Ground Control Management Plan describing TMAC's management and work to reduce the risk of uncontrolled ground failure.
HRI, 2020	Results of a 4-day investigation in the Doris underground, which included pressure measurements, and short- and long-term flow tests (STFT, LTFT) in existing underground open holes.
HRI, 2021	Results of two 14-day investigations in the Doris underground, which included pressure measurements and STFT, velocity flow profiles (VFP), packer tests, and chemical profiles (CP) (i.e., temperature, EC, salinity, and TDS) in existing underground open holes.
SRK, 2022a	Geomechanical design phase 1 review and gap analysis of the Madrid and Boston deposits for the preparation of prefeasibility Studies.

Reference	Description
Agnico, 2022	Groundwater monitoring package of data collected between Dec. 2020 and Oct. 2022. (i.e., mine water flow and quality at stations TL-12, TL-12A and 4926/North Ramp, as well as quantitative and qualitative observations of flows from drillholes or structures intercepted by the mine).
SRK, 2022b	Review of groundwater data collected between Dec. 2020 and May 2021 in the Doris underground mine, including mine water flow and quality, and observations of flows in open drillholes and at intercepted structures; comparisons to the 2015 numerical model predictions; estimation of long-term groundwater flow and chloride concentration with the 2021 as-built mine plan.
SRK, 2023a	Geotechnical and hydrogeological field program at the Madrid deposit. The hydrogeological investigation included hydraulic testing using inflatable packers and installations of thermistors and vibrating wire piezometers.
SRK, 2023b	Hydrogeological inspection of the underground workings of the Doris North mine.
Lorax, 2023a	Field program at Madrid, which included hydraulic testing of one exploration drillhole.
Lorax, 2023b	Results of the groundwater quality samples collected by Agnico in Oct 2022 and July 2023 at the Doris Westbay well 10WBW001.
Lorax, 2024 a,b,c,d	Field programs which included groundwater sampling of the Westbay Well 10WBW001 at Doris, and hydraulic testing of two drillholes at Madrid.

3 Baseline Data

3.1 Topography, Hydrology and Climate

The topography of the Project is typical of coastal lowland, ranging from undulating plains near the coast to massive Archean-age rocks rising to 300 m above sea level in the south. The Hope Bay belt drains directly into the Arctic Ocean and consists of three main watersheds: the Koignuk River (2,937 km^2), Windy-Glenn (48 km^2), and Doris-Roberts (194 km^2).

Numerous lakes and ponds are present along the bottom of elongated valleys separated by bedrock and glacial landforms. The shape of the basins is generally long and narrow and is predominantly orientated along the north-south axis. The main water bodies are the Doris Lake and Tail lakes in the Doris area; Patch, Imniagut, Wolverine, Windy, and Ogama lakes in the Madrid area, and Aimakatalok and Stickleback lakes in the Boston Area. The Tail Lake has been used as a Tailing Impoundment Area (TIA) for the Doris mine (see Section 2.1). Appendix A compiles available maps of the lakes' bathymetry.

Climate of the region can be described as a sub-Arctic desert with limited rainfall, long dark winters and short bright summers. The ground is covered in snow from approximately October to June most years. Extremely cold air temperatures and permafrost cause all rivers and creeks to freeze solid in winter, with ice reaching up to 2 m thick. Streams and rivers typically start flowing in late May or early June when snow and ice melt, peak in June, then decrease steadily until flow cease by October. Runoff occurs only briefly from June to October.

3.2 Permafrost

The Project is located within the zone of continuous permafrost, as delineated by the Geological Survey of Canada (NRCan, 2002). Groundwater cannot flow in frozen ground; it can move in the active zone and in features called taliks where rock is unfrozen.

The active zone refers to the layer of ground that undergoes seasonal thawing and freezing. It is located above the permanently frozen ground. Each year, during the warmer months, the active zone thaws, allowing for movement of water, before refreezing during the colder months. It acts as a dynamic layer where water can infiltrate, be stored, and move. During the thaw period, meltwater from snow and ice can percolate through this layer, potentially recharging shallow aquifers in the active zone. The presence of permafrost limits deeper infiltration, causing groundwater flow to be confined to the active zone.

A talik is defined as “a layer or body of unfrozen ground occurring in a permafrost area due to local anomalies in thermal, hydrological, hydrogeological or hydrochemical conditions” (Van Everdingen, 2005). In most cases, taliks are formed by lakes and other water bodies that cause a local departure in terrestrial ground temperature (Smith and Hwang, 1973; Burn, 2002). Taliks can be closed or open. A closed talik is an unfrozen zone beneath a water body that is enclosed at the base and the surrounding sides by permafrost. An open talik is an unfrozen zone beneath a water body that penetrates the permafrost completely and connects to supra-permafrost (i.e., the layer of ground above permafrost) and sub-permafrost (i.e., the non-frozen ground below the permafrost).

Key factors influencing configurations of taliks include water bottom temperature, lake dimensions, present and past ground thermal regime, and long-term changes to the landscape. Taliks are transient features. Present-day water bathymetry can affect talik configuration where shallow water allows for ice to seasonally freeze to the bottom (bottom-fast ice) and conduct heat from the ground (Burn, 2002, 2005; Stevens, 2010a,b). The long-term thermal and physical evolution of the landscape is a factor in the present-day configuration of taliks. Lunardini (1995) showed temperature at depths up to 600 mbgs can be influenced by surface temperatures as far back as 100,000 years. The boundaries of active zone, taliks, and subpermafrost are discussed in Section 3.10.

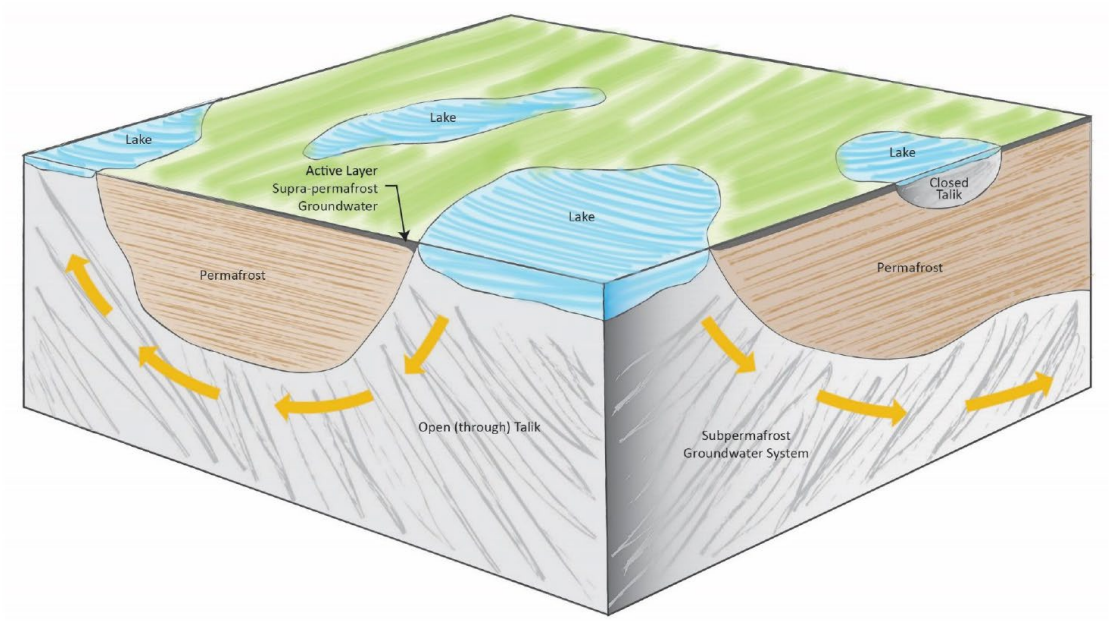


Figure 3-1: Conceptual drawing of open and closed taliks

Source: SRK, 2022a

Note: Orange arrows show potential direction of groundwater flow for illustrative purposes only.

3.3 Geology

3.3.1 Regional Geology

The Hope Bay Volcanic Belt is a greenstone belt located in the northeast portion of the Slave Structural Province (Figure 3-2). Dominated by mafic volcanic rocks, it features massive to pillowed tholeiitic flows interbedded with calc-alkaline felsic volcanic and volcanoclastic rocks, clastic sedimentary rocks, and rarely synvolcanic conglomerate and carbonates.

The Hope Bay area has been affected by successive Laurentide ice sheets during Quaternary ice ages. The last ice sheet began receding about 8,800 years ago (Dyke and Prest, 1986) leaving a blanket of basal till. After deglaciation, the Hope Bay region was submerged approximately 200 metres below present mean sea level (Dyke and Dredge, 1989). Fine sediments from meltwater (rock flour) were deposited as marine clays and silts onto the basal tills, with the greatest thicknesses accumulating in the deeper water zones, now represented by valleys.

Isostatic rebound after deglaciation led to emergent landforms and reworking of unconsolidated marine sediments and tills along the shoreface (EBA, 1996). Sediments were stripped from uplands and redeposited in valleys, forming relatively continuous north-northwest trending bedrock ridges and elongated lakes. The unconsolidated overburden, up to 30 m in thickness, comprises locally and regionally derived tills and boulder tills with lacustrine and marine sediments and clay up to 15 m thick in the larger valleys.

3.3.2 Doris Bedrock Geology and Structures

Gold mineralization is principally hosted by massive and pillowed metabasalt folded around a central coarse gabbroic metavolcanic. The main auriferous quartz vein has an anti-formal shape and appears to be associated with a zone of high strain a few metres wide, plunging 10° north at Doris North, and 25° south at Doris Central. All basaltic and gabbroic rocks are affected by a penetrative foliation, characterized by an alignment of chlorite, sericite, quartz, and carbonate minerals, striking north-south and dipping steeply to the west (i.e., At outcrops, the strike ranges between 175º to 205º and dip between vertical and 80º to the west) (SRK, 2014).

A diabase dyke complex crosscuts the gold mineralization, generally striking north-northeast and dipping both steeply and shallowly to the east. The complex has two distinct geometric features: a vertical dyke and a horizontal dyke. The vertical dyke runs along the west shore of Doris Lake and extends from surface to beyond permafrost maximum depths. The horizontal dyke is mapped between a depth of 339 and 488 mbgs (SRK 2014).

Two sets of sub-vertical dipping brittle faults transect the rock excepted for diabase dykes. The strike is generally northwest and northeast and the dip poorly constrained. All late structures in drill core are typically marked by rubble zones associated with sericitic alteration, slickensides, brecciation, and clay gouge.

3.3.3 Madrid Bedrock Geology and Structures

The stratigraphy of the Madrid area is composed of three major volcanic packages: the Wolverine Group basalts, the Patch Group basalts, and the pale green pillow basalts. Metasedimentary rocks often occur in the Patch Group metavolcanics. Gold mineralization occurs at proximity of a wide package of variably deformed and altered rocks collectively referred as the Madrid Deformation Zone (MDZ). It is not a single planar structure but an anastomosing feature with several splays and local pinch-and-swell textures. Its thickness is about 100 to 140 m and typically comprised of chlorite schist with a strong overprinting (regional) foliation. The eastern contact of the MDZ typically hosts brittle faults parallel to it (i.e., East-West faults at Naartok West and North-South faults at Suluk/Patch 7). Younger diabase dykes are present in the vicinity of Naartok. Apparent discontinuities in alteration, mineralization and lithological units generally define a set of northwest trending steep structures.

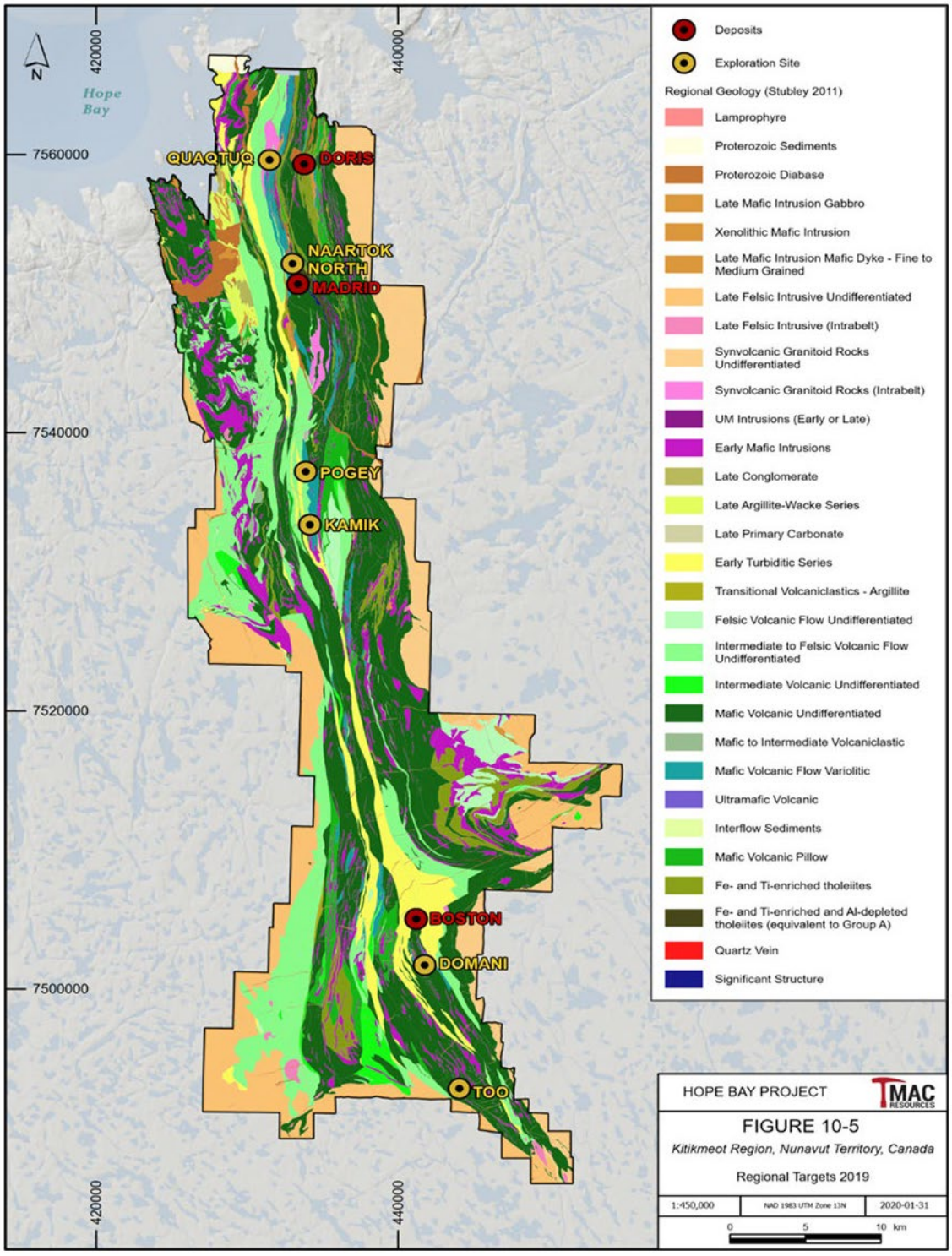


Figure 3-2: Geological map of the Kitikmeot Region, Nunavut Territory, Canada

Source: TMAC, 2020
(Projection: NAD83 / UTM zone 13N, unit: metre)

3.3.4 Boston Bedrock Geology and Structures

The Boston gold deposit is situated in an area dominated by mafic metavolcanics rocks, metasedimentary rock and minor amounts of felsic metavolcanics. The strata are folded and form a large south-plunging synformal anticline. The mafic metavolcanics form the interior of the fold, while synvolcanic metasediments flank the east and the west sides. The transition between the metasediment and metavolcanic packages is variable, with interbedded units of metasediments and metavolcanics.

Gold mineralization is associated primarily with steep deformed quartz veins at the contact between mafic metavolcanics and metasedimentary rocks. Four brittle faults have been modeled to crosscut the Boston area. Additional fault lineaments have been observed in airborne geophysics.

3.3.5 Surficial Geology

Thurber Engineering Limited conducted site-specific surficial geology mapping for the Doris North Project in July 2003. Their study covered an area of 45 km^2 and included air photo interpretation followed by ground reconnaissance. The study indicated that “the active zone earth materials include frost-churned mineral and organic soils mantled by a thin cover of tundra-heath vegetation. Patterned grounds, usually consisting of surface drainage rills, mask the underlying soils. Small, frost-heaved clay-silt polygons are very common. Linear frost cracks are noted in raised marine spit deposits. Ice wedge polygons are common in muskegs. There is evidence of naturally degrading permafrost along two creeks near Roberts Bay and at several other locations. Permafrost degradation is ascribed to past human activity just north of Roberts Lake in the northeast map area.

SRK conducted additional characterization programs on lake sediments and overburden (SRK 2009a, 2011c). Appendix B compiles a map of the locations and tables of sample descriptions. The overburden is described as ice-rich (10 to 30% by volume on average, but occasionally as high as 50%) marine silty clay and clayey silt. The onshore profile consists generally of a thin veneer of hummocky organic soil covered by tundra heath vegetation. Under this organic zone is a layer of marine clay (silty clay and clayey silt) typically between 5 and 20 m thick; however, since the terrain is glaciated with significant bedrock control, there are areas where overburden is less than 5 m thick as well as areas where the overburden exceeds 30 m in thickness. In areas where the overburden exceeds 20 m in thickness, it appears to be underlain by clayey morainal till, which contains moderate amounts of cobbles and boulders. Eskers occur but are not overly common. An esker is a ridge of sediment, generally well sorted sands and gravels, deposited by meltwater streams flowing beneath a glacier. As the glacier retreated, the sediment was left behind in a distinctive long and winding formation.

Onshore, the shallow active zone is disconnected from the deep subpermafrost groundwater system by the permafrost (Figure 3-1). Interactions between surface and groundwater occur only in the shallow active zone or at depths in taliks beneath lakes. For the later, the magnitude of interactions will depend on the type and thickness of lake bottom sediments, particularly fine-grained materials like clay. At lake bottoms, overburden is of the same characteristic as onshore

(i.e., silty clays and clayey silts). There is a layer of limnic sediments ranging in thickness between a few centimetres to as much as 2 m, under which is a consolidated layer of marine silty clay and clayey silts between 10 and 20 m thick (SRK, 2009a).

Minnow Environmental Inc. (2023) conducted baseline field studies in Patch Lake to supplement the existing baseline dataset reported by Rescan (2010). The study involved classifying substrates and preparing a bathymetric map. The shoreline and littoral substrates were visually characterized, sediment sampled from the bottom of Patch Lake was photographed and described, and a hydroacoustic survey was conducted. The visual assessments and sediment samples were used to identify and validate the following substrate types:

- Rock (cobble, boulder, and bedrock) for a high hardness category.
- Fines – Type 1 (sand, silt, and clay intermixed with rock and/or rock overlain with sand, silt, and clay) for a moderate hardness category.
- Fines – Type 2 (sand, silt, clay) for a low hardness category.

Figure 3-3 shows the resulting substrate classification map. Sediment grab sample descriptions, a map of the sample locations, and photos of the samples are included in Appendix B.

The substrate classification map indicated that Type 1 fines, consisting of sand, silt, and clay intermixed with cobble and boulder, were the dominant substrate type in the shallow, littoral areas of Patch Lake. Type 2 fines (sand, silt, and clay) were the second most common substrate type and were generally present in the deeper areas of the lake (typically greater than four metres depth). Rocky substrates (bedrock, boulder, and cobble) were present in shallow areas along the shorelines of islands, in shoals, and along the lake perimeter.

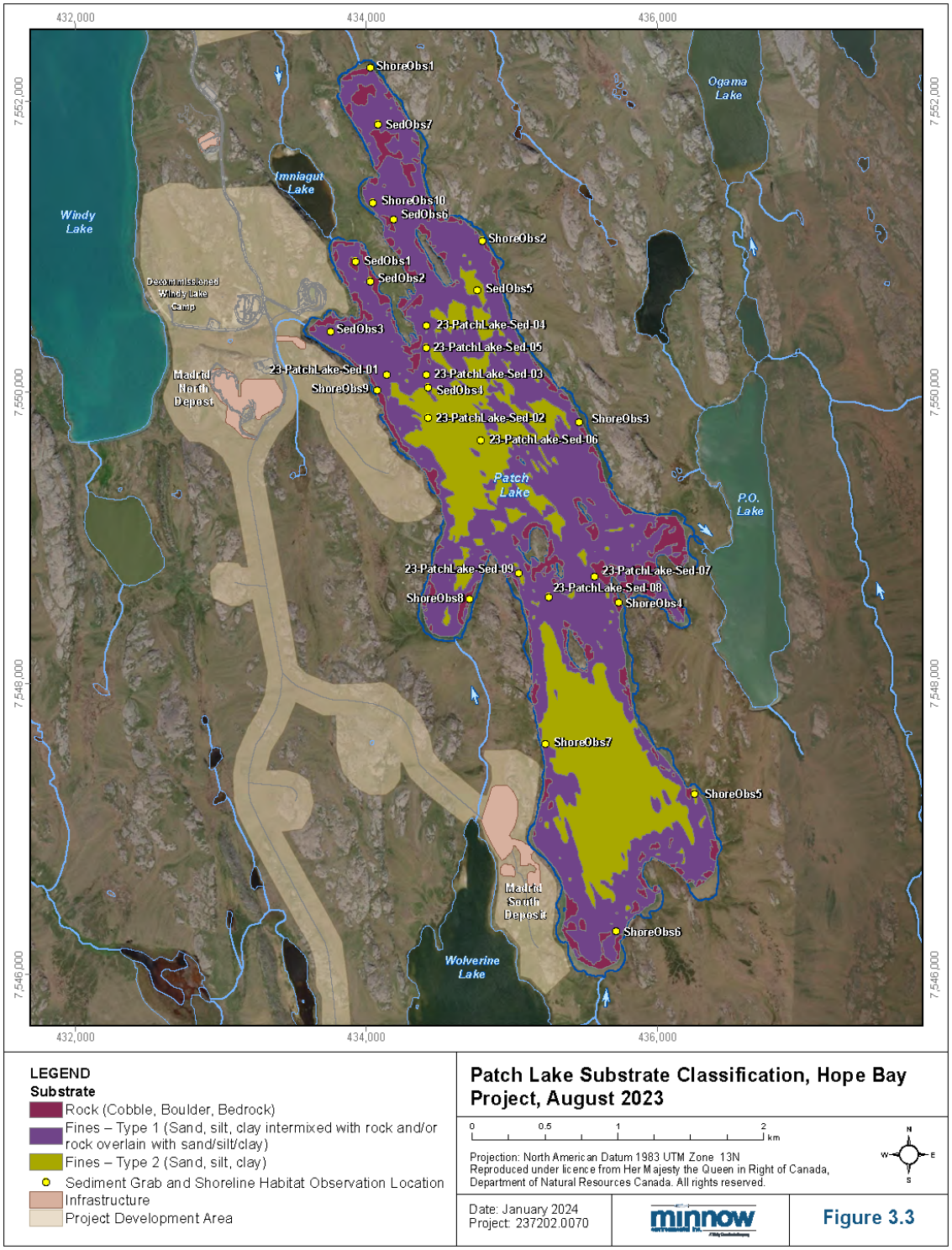


Figure 3-3: Patch Lake Substrate Classification, August 2023

Source: Minnow 2023

3.4 Doris Groundwater Monitoring Network

Figure 3-4 to Figure 3-9 are maps of the hydrogeological data locations at Doris.

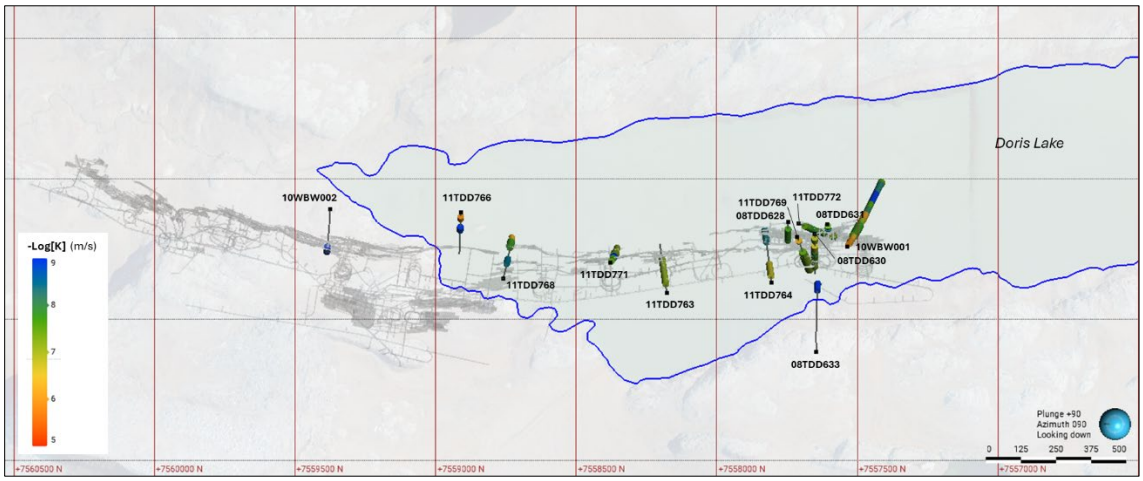


Figure 3-4: Map of hydraulic conductivities measured at Doris from surface drillholes

Source: fig_doris_K_data.pptx, Leapfrog model ID 12766
(Projection: NAD83 / UTM zone 13N, unit: metre)

Note: The map excludes tests in frozen intervals or rated as poor quality due to injection bypass or equipment issues. Variations of sizes for the cylinders representing tests intervals and transparencies are used to display overlapping test intervals; they do not correlate with influence radiuses.
The underground projected footprint corresponds to the proposed mine development.

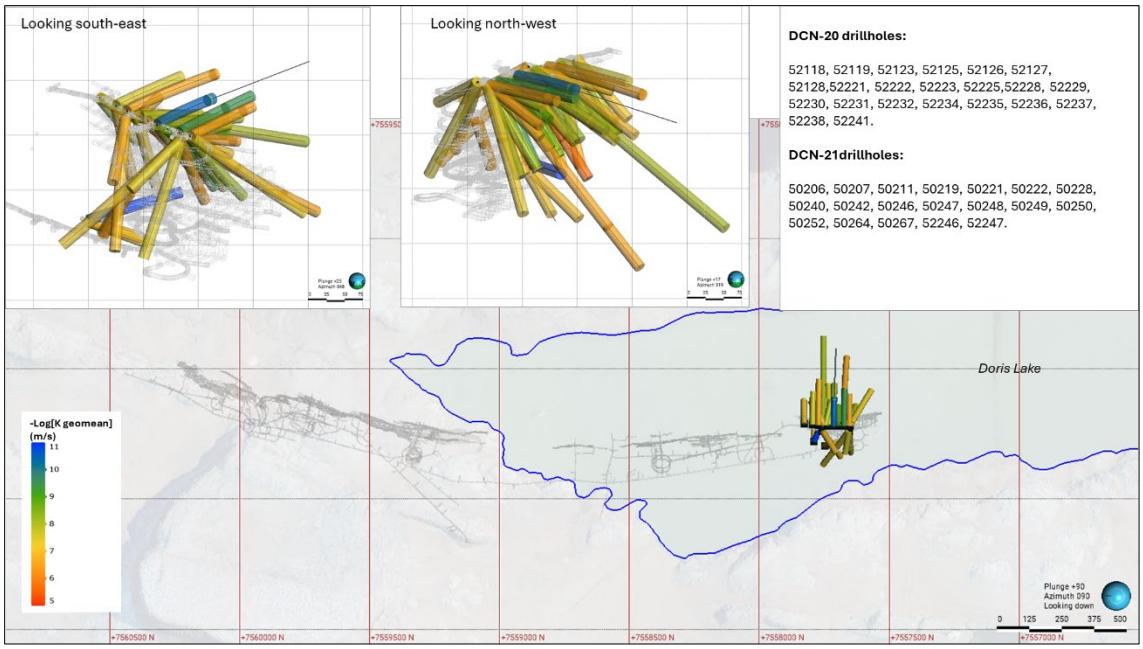


Figure 3-5: Map of hydraulic conductivities measured at Doris from underground drillholes

Source: fig_doris_K_data.pptx, Leapfrog model ID 12766
(Projection: NAD83 / UTM zone 13N, unit: metre)

Note: The underground projected footprint corresponds to the Doris mine developments as of 2022.

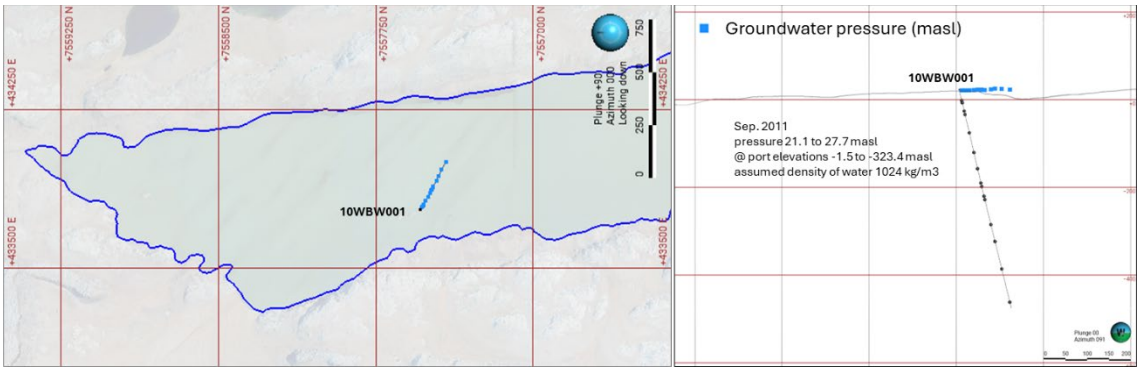


Figure 3-6: Map of groundwater pressure measured at Doris during pre-mining conditions

Source: fig_doris_gwPress_data.pptx, Leapfrog model ID 12766
(Projection: NAD83 / UTM zone 13N, unit: metre)

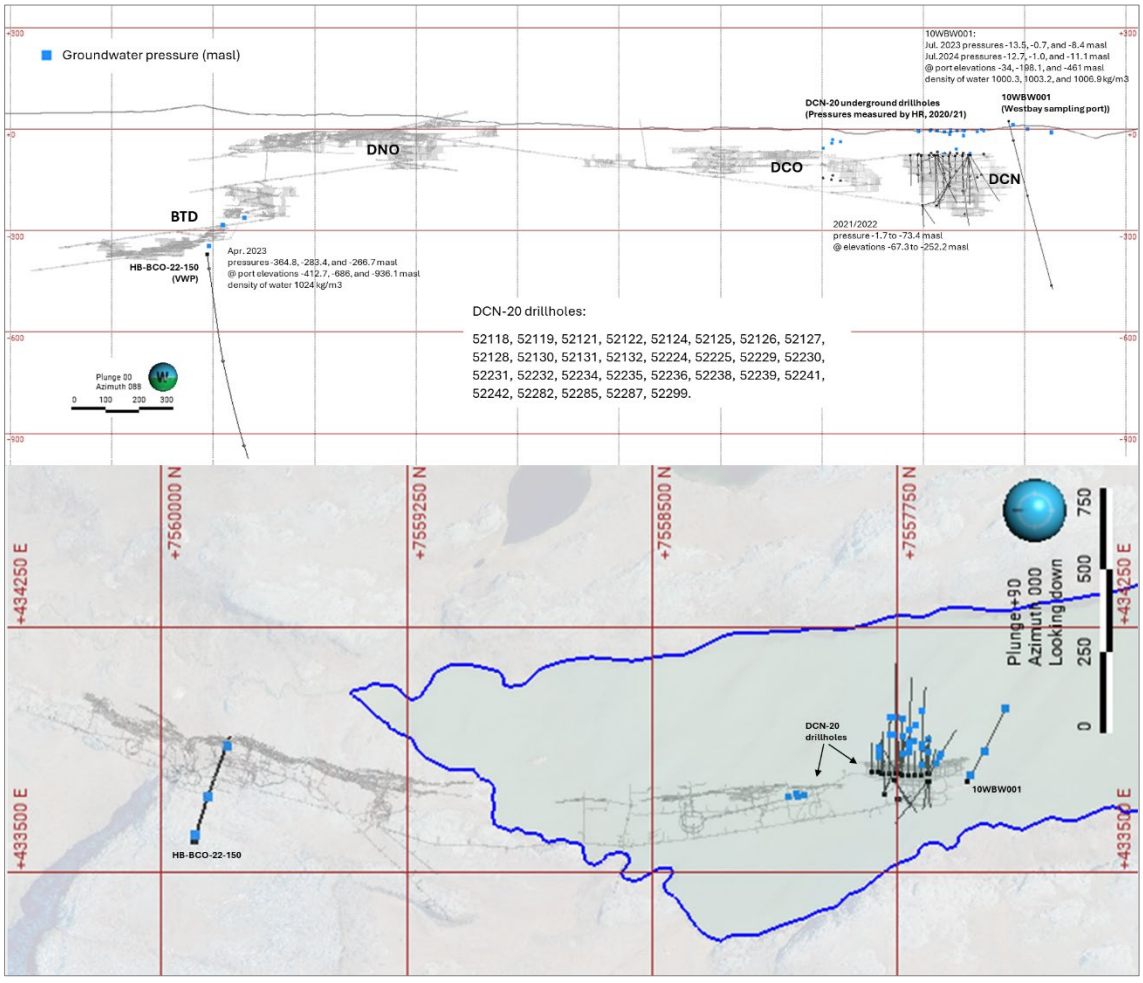


Figure 3-7: Map of groundwater pressures measured at Doris during mining

Source: fig_doris_gwPress_data.pptx, Leapfrog model ID 12766
(Projection: NAD83 / UTM zone 13N, unit: metre)

Note: The underground projected footprint corresponds to the Doris mine developments as of 2022.

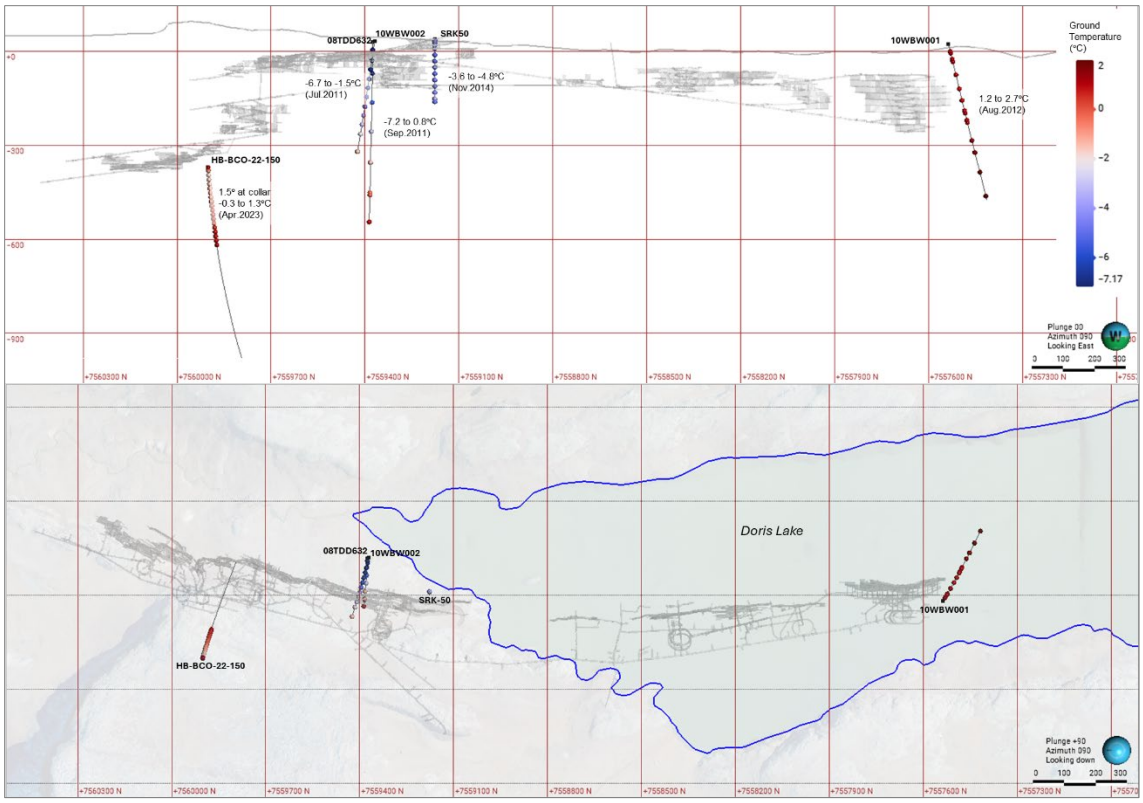


Figure 3-8: Map of ground temperatures measured at Doris

Source: fig_doris_therm_data.pptx, Leapfrog model ID 12766
(Projection: NAD83 / UTM zone 13N, unit: metre)

Note: The underground projected footprint corresponds to the proposed mine developments.

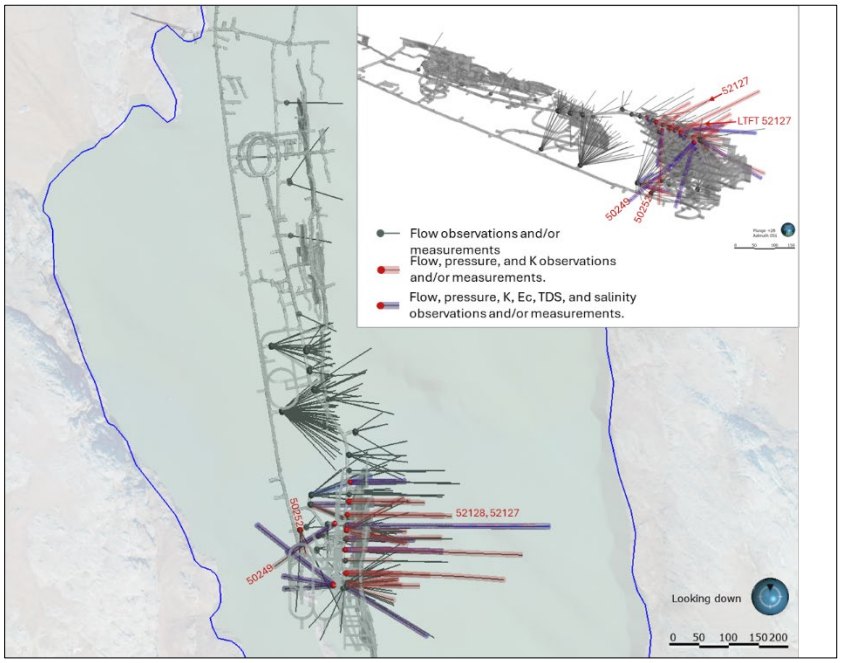


Figure 3-9: Map of flow measurements recorded in the Doris underground mine

Source: fig_doris_flow_data.pptx, Leapfrog model ID 12766
(Projection: NAD83 / UTM zone 13N, unit: metre)

3.5 Madrid Groundwater Monitoring Network

Figure 3-10 to Figure 3-14 are maps of the hydrogeological data locations at Madrid.

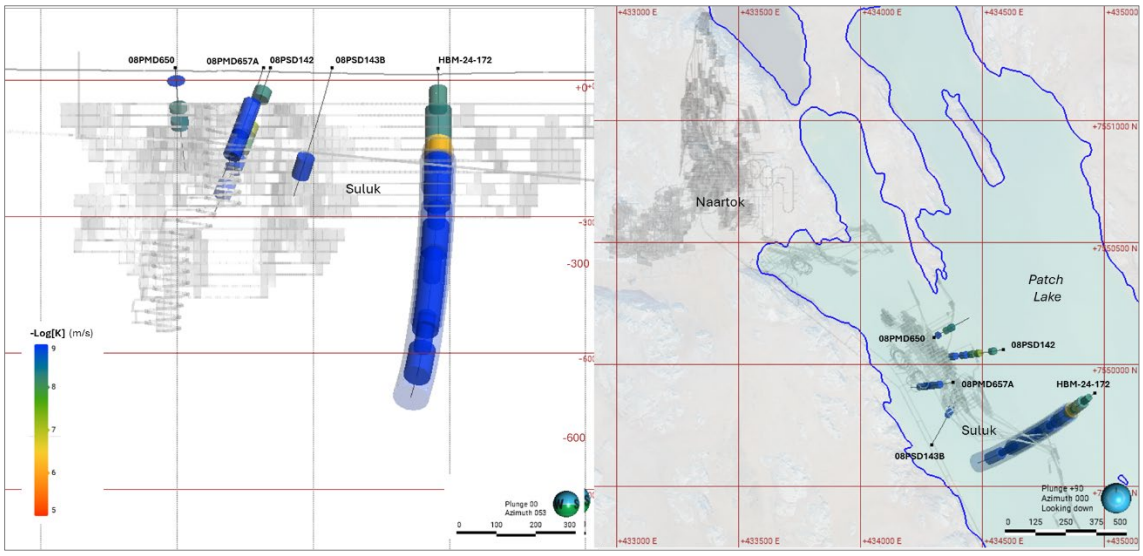


Figure 3-10: Map of hydraulic conductivities measured at Madrid (north area) from surface drillholes

Source: fig_madrid_K_data_rev1.pptx, Leapfrog model ID 12766
(Projection: NAD83 / UTM zone 13N, unit: metre)

Note: The map excludes tests in frozen intervals or rated as poor quality due to injection bypass or equipment issues. Variations of sizes for the cylinders representing tests intervals and transparencies are used to display overlapping test intervals; they do not correlate with influence radiuses.
The underground projected footprint corresponds to the proposed mine development.

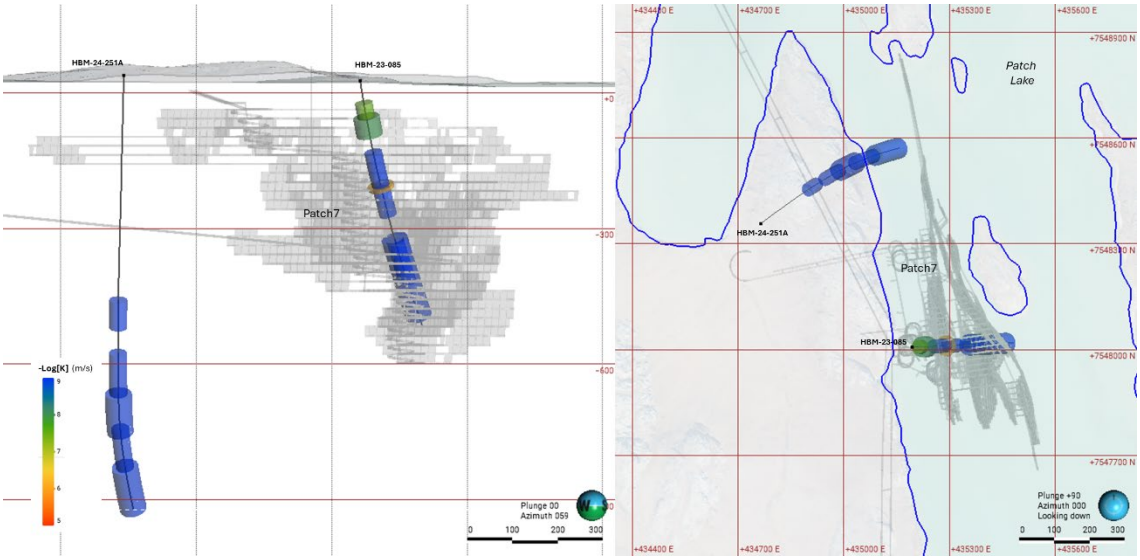


Figure 3-11: Map of hydraulic conductivities measured at Madrid (central area) from surface drillholes

Source: fig_madrid_K_data_rev1.pptx, Leapfrog model ID 12766
(Projection: NAD83 / UTM zone 13N, unit: metre)

Note: The map excludes tests in frozen intervals or rated as poor quality due to injection bypass or equipment issues. Variations of sizes for the cylinders representing tests intervals and transparencies are used to display overlapping test intervals; they do not correlate with influence radiuses.
The underground projected footprint corresponds to the proposed mine development.

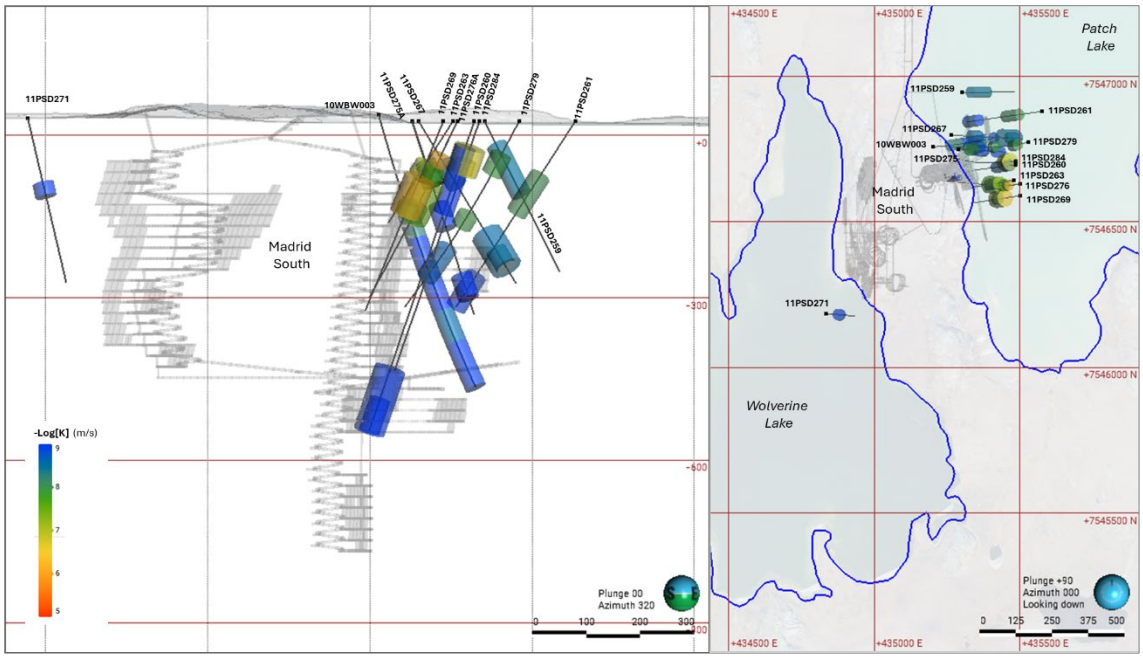


Figure 3-12: Map of hydraulic conductivities measured at Madrid (south area) from surface drillholes

Source: fig_madrid_K_data_rev1.pptx, Leapfrog model ID 12766
(Projection: NAD83 / UTM zone 13N, unit: metre)

Note: The map excludes tests in frozen intervals or rated as poor quality due to injection bypass or equipment issues. Variations of sizes for the cylinders representing tests intervals and transparencies are used to display overlapping test intervals; they do not correlate with influence radiuses.
The underground projected footprint corresponds to the proposed mine development.

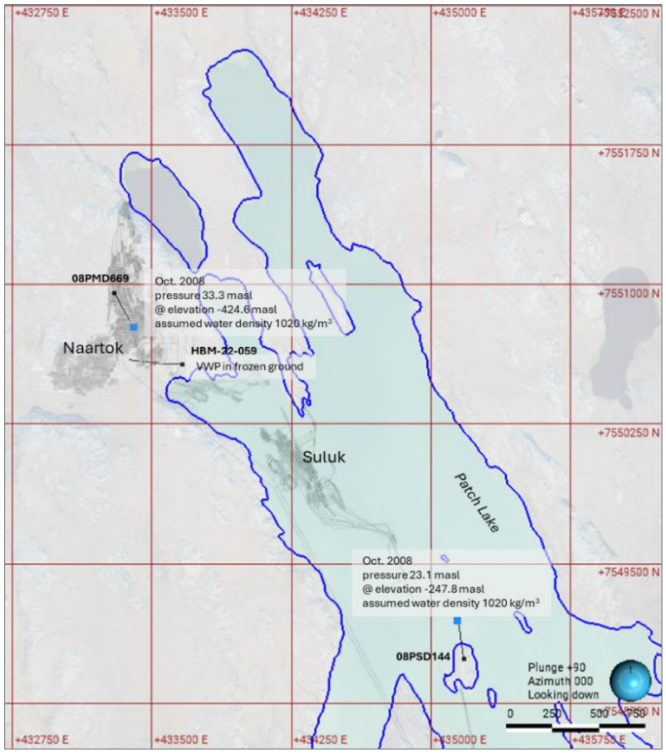


Figure 3-13: Map of groundwater pressures measured at Madrid

Source: fig_madrid_gwPress_data_rev1.pptx, Leapfrog model ID 12766
(Projection: NAD83 / UTM zone 13N, unit: metre)

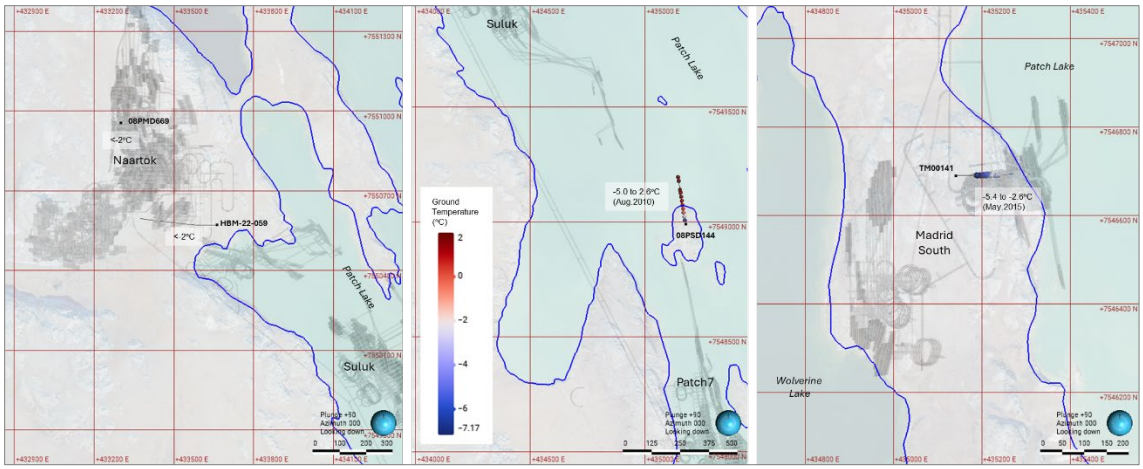


Figure 3-14: Map of ground temperatures measured at Madrid

Source: fig_madrid_therm_data_rev1.pptx, Leapfrog model ID 12766
(Projection: NAD83 / UTM zone 13N, unit: metre)

3.6 Boston Groundwater Monitoring Network

Figure 3-15 and Figure 3-16 show the hydrogeological data locations at the Boston exploration area, located on a peninsula on Aimakatalok Lake, immediately north of Stickleback Lake.

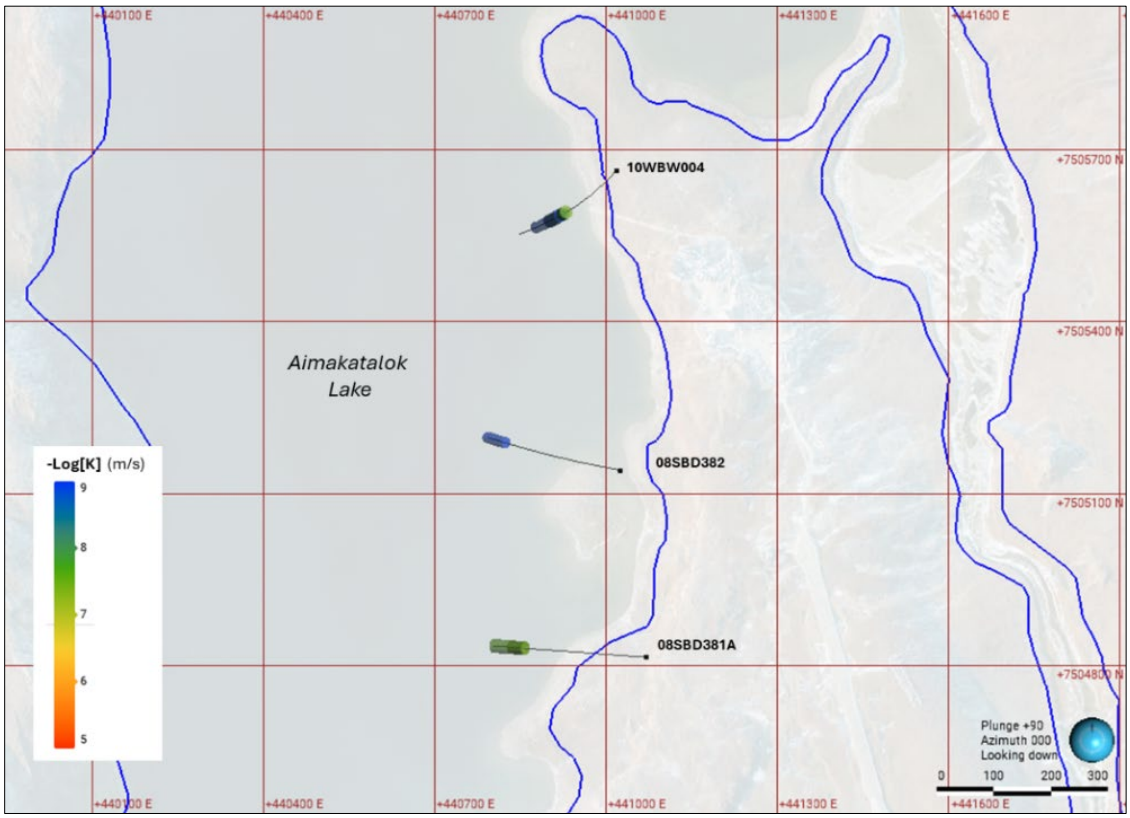


Figure 3-15: Hydraulic conductivity tests measured at Boston from surface drillhole

Source: fig_boston_K_data.pptx, Leapfrog model ID 12766
(Projection: NAD83 / UTM zone 13N, unit: metre)

Note: The map excludes tests in frozen intervals or rated as poor quality due to injection bypass or equipment issues.

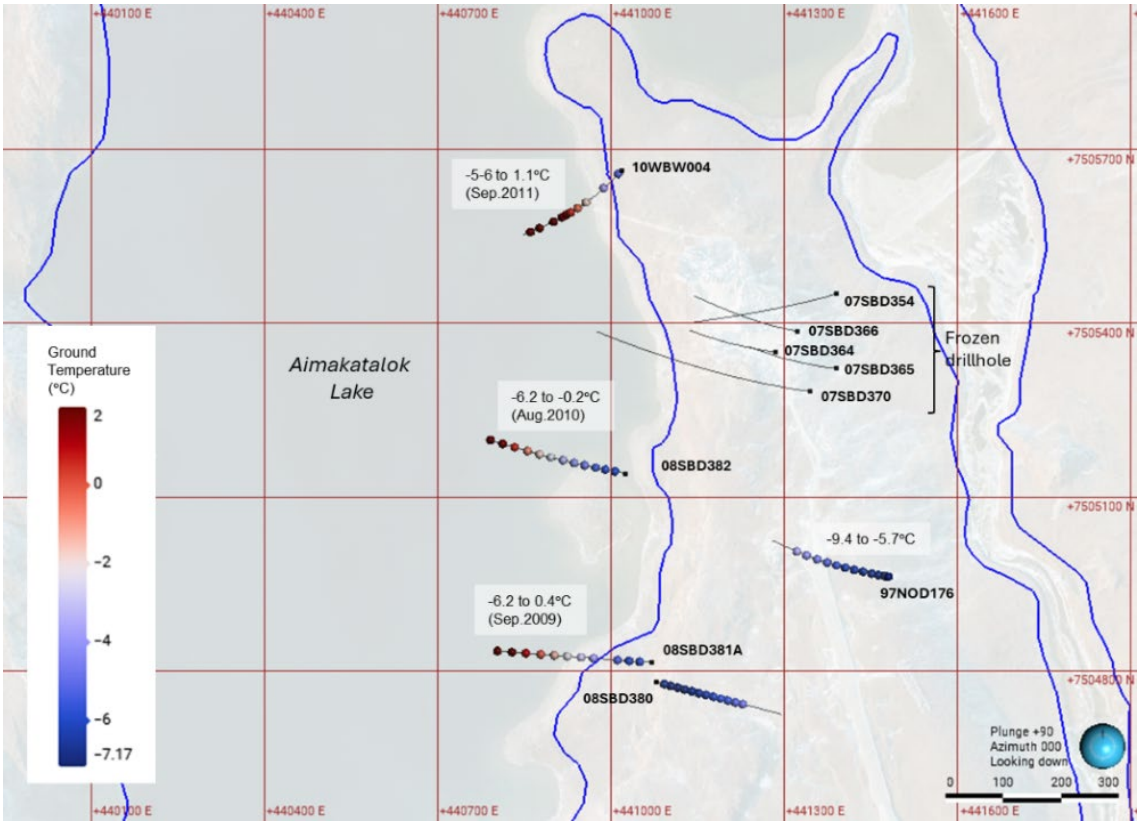


Figure 3-16: Map of ground temperatures measured at Boston

Source: fig_boston_them_data.pptx, Leapfrog model ID 12766
(Projection: NAD83 / UTM zone 13N, unit: metre)

3.7 Hydraulic Properties

The hydraulic conductivity (K) dataset includes a total of 184 test measurements at Doris (Figure 3-4 and Figure 3-5), Madrid (Figure 3-10 to Figure 3-9), and Boston (Figure 3-15), excluding tests in permafrost. These measurements were obtained from surface or underground drilling using slug tests, short and long-duration packer injection tests, pressure dissipation tests in cone penetration tests (CPT), and laboratory permeability measurements. Most tests included more than one lithological unit resulting in the averaging of the individual features or lithologies in the respective test intervals.

3.7.1 Bedrock

Table 3-1 compiles a statistical summary of the K values; individual test results are presented in Appendix C. The arithmetic mean, geometric mean, and harmonic mean are employed to capture different aspects of the hydraulic conductivity variability.

- The arithmetic mean provides a measure of the central tendency of the data. However, the arithmetic mean may not accurately represent the typical behavior in heterogeneous media as extreme values can significantly affect the average. It can be representative of the bulk K along preferential flow directions (i.e., along beddings or vertical fractures).
- The geometric mean is usually considered the best metrics for bulk K values because K is typically log-normally distributed. The geometric mean provides a better representation of the central tendency for log-normally distributed data, giving more weight to the geometrically central values.
- The harmonic mean gives more weight to lower values, making it sensitive to low K zones. In heterogeneous media, this statistic can better reflect the influence of rock with lower K on overall flow.

Table 3-1: Statistical summary of the hydraulic conductivity dataset

Unit	Count (-)	K min. (m/s)	K harm. (m/s)	K geo. (m/s)	K arith. (m/s)	K max. (m/s)
Doris bedrock	99	1.4E-11	5.0E-10	5.0E-08	3.0E-07	4.0E-06
Madrid bedrock	78	1.0E-11	2.4E-10	2.0E-09	5.7E-08	9.0E-07
Boston bedrock	7	1.1E-11	7.2E-11	3.4E-09	2.3E-08	7.0E-08

Source: HopeBay_MASTER_HydrProperties_gf_20250120.xlsx

Note: Min: Min., max: maximum, harm: harmonic mean, geo: geomean; arith: arithmetic mean, max: maximum.

The spatial distribution of K values does not show a particular pattern. Figure 3-17, Figure 3-18 and Figure 3-19 plot the K values versus depth, K values versus fracture frequency, and K values versus Rock Quality Designation (RQD), respectively. K values tend to decrease progressively with depth, which is interpreted to be a result of reduction of fracture apertures with depth as lithostatic load increases (Singhal and Gupta 2010); correlation coefficients between K and depths are weak to moderate. The probability of encountering higher K can increase in areas with higher fracture frequency.

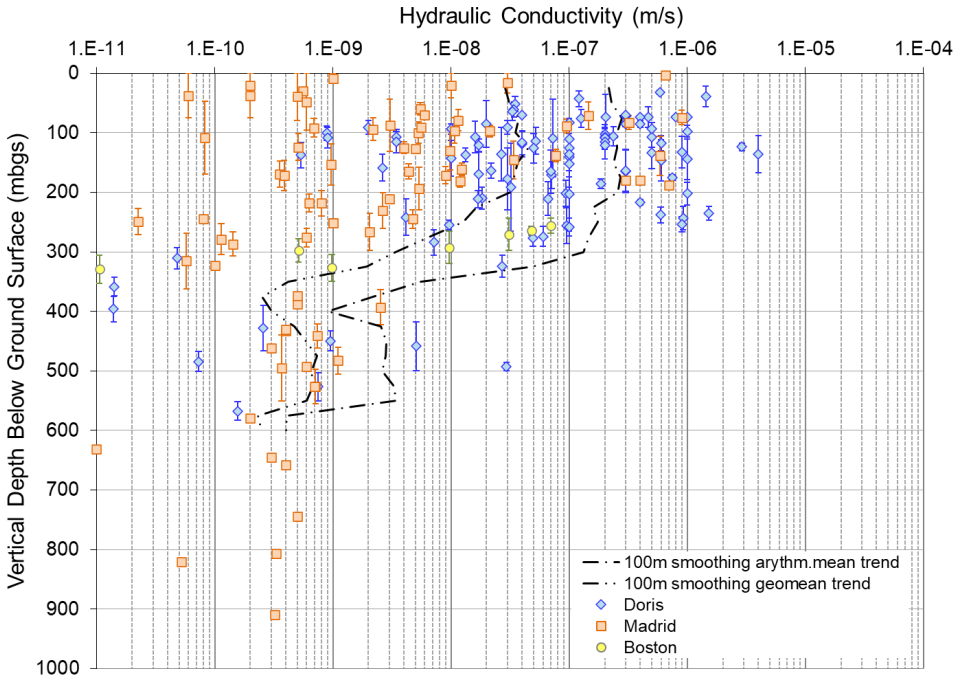


Figure 3-17: Hydraulic conductivity versus depth

Source: HopeBay_MASTER_HydrProperties_gf_20250120.xlsx

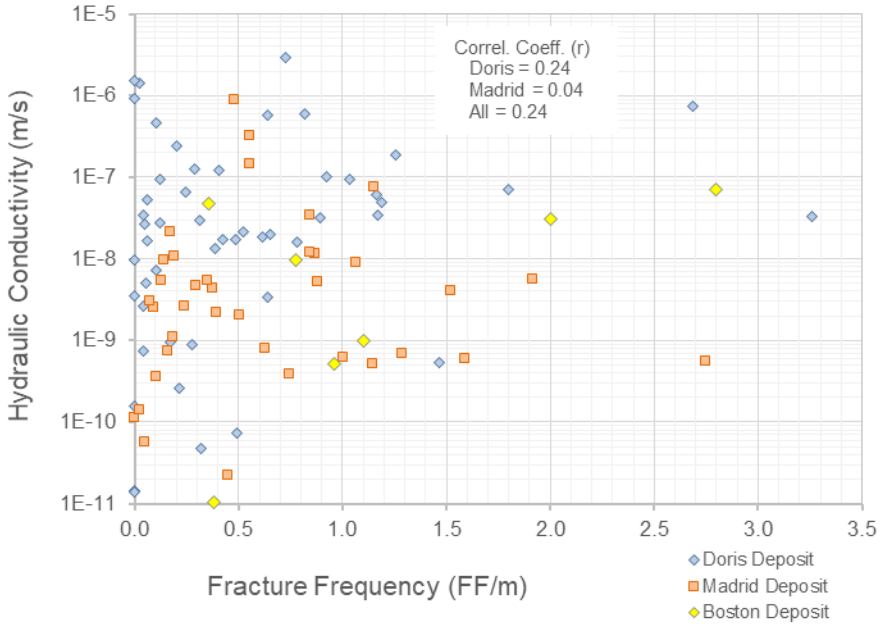


Figure 3-18: Hydraulic conductivity versus fracture frequency

Source: HopeBay_MASTER_HydrProperties_gf_20250120.xlsx

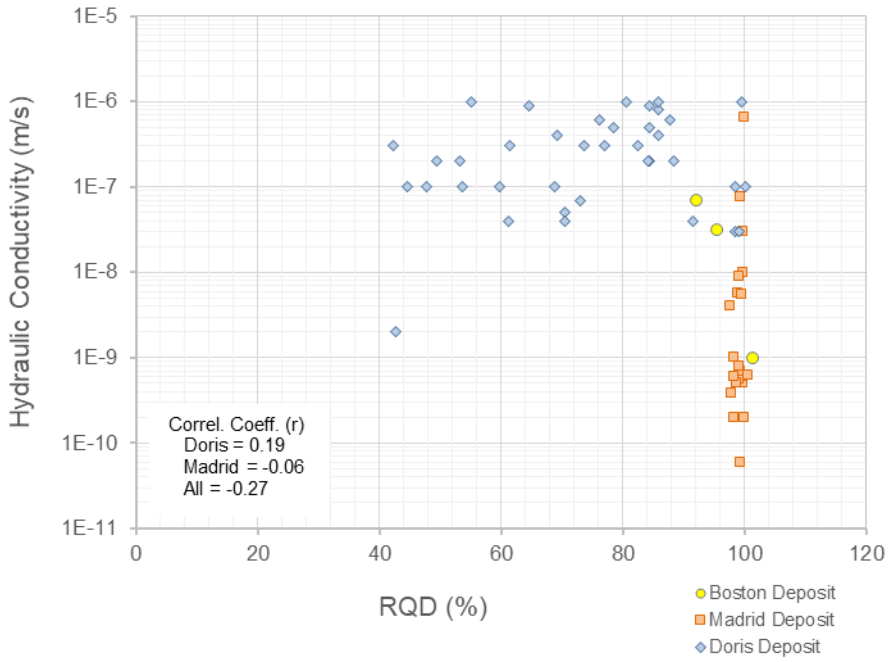


Figure 3-19: Hydraulic conductivity versus RQD

Source: HopeBay_MASTER_HydrProperties_gf_20250120.xlsx

Doris

The K tests performed at Doris (Figure 3-4 and Figure 3-5) show values are typically low, ranging between <1x10^{-9}m/s and 4x10^{-6} m/s, with a geomean of 5x10^{-8} m/s. The diabase dykes appear to have a low bulk rock hydraulic conductivity (1x10^{-11} m/s) but since only two tests were conducted exclusively within the diabase dykes, the statistical confidence remains low.

Out of fourteen hydraulic tests associated with intervals intercepting structural features, from gouge-filled fractures to rubble zones, only eight measurements are greater than the geometric mean.

- At 10WBW001, between 223.1 and 247 mbgs and between 223.1 and 263 mbgs, K was measured respectively as 1.5x10^{-6} m/s and 9.2x10^{-7} m/s. The test interval was described with basalt, quartz and dolomite veins with fractures (no recovery). Loss of pressure or drilling circulation were encountered during drilling.
- At 11TDD769, between 28.0 and 35.2 mbgs, K was measured as 5.9x10^{-7} m/s. The test interval was described as mafic volcanic pillow (foliated basalt) and included a 20 cm shear structure.
- At 11TDD769, between 117.3 and 129.8 mbgs, K was measured as 2.9x10^{-6} m/s. The test interval was described as mafic volcanic pillow (foliated basalt) and included major joints with gouge.
- At 11TDD769, between 170.2 and 179.9 mbgs, K was measured as 7.5x10^{-7} m/s. The test interval was described as mafic volcanic pillow (foliated basalt) with a rubble zone.

- At 11TDD771, between 148.0 and 193.7 mbgs and between 177.3 and 193.7 mbgs, K was measured respectively as $7.1x10^{-8}$ m/s and $1.9x10^{-7}$ m/s. The tests were described as primarily volcanic pillow with quartz, with the ore zone between 166-171m and a structure at the ore zone contact.
- At 11TDD772, between 256.8 and 291.1 mbgs, K was measured as $6.0x10^{-6}$ m/s. The test interval was described as mafic volcanic pillow (foliated basalt) with quartz (ore zone) and intercepted a fault labelled Force 1 in the 2012 structural model.

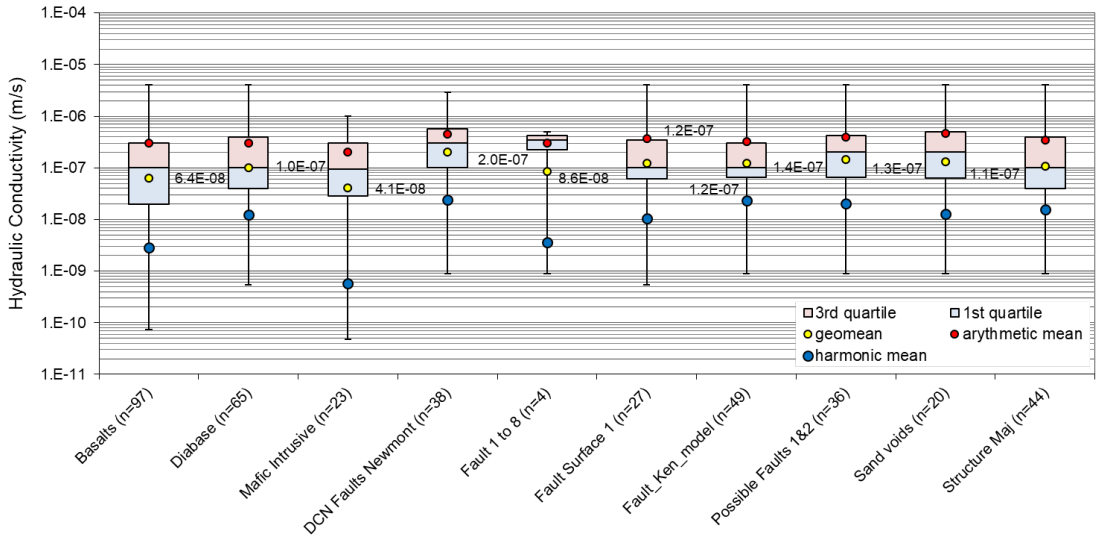


Figure 3-20: Box plot of the Doris K measurements by geology and structures

Source: HopeBay_MASTER_HydrProperties_gf_20250120.xlsx

Madrid

The tests performed at Madrid (Figure 3-10 and Figure 3-21) show K values are typically low, ranging between < $1x10^{-9}$ and $9x10^{-7}$ m/s, with a geomean of $2x10^{-9}$ m/s. The dataset shows no evidence of higher K features associated with dyke contacts, major structures, or faults, and/or the MDZ. The hydraulic tests intersecting geological structures at Madrid are listed in Table 4 3.

Four tests reported a K value above $1x10^{-7}$ m/s:

- At 11PSD269, between 105 and 150 mbgs, K was measured as 6x10-7 m/s. The drillers recorded a loss of return at 137 mah (meter along drillhole), and the geotechnical log indicates the presence of a shear zone at 138 mah.
- At 11PSD276, between 60 and 85 mbgs, K was measured as 9x10-7 m/s. The test interval showed no obvious weak zone; there were no major structures identified, and the number of joints and fractures was low (fracture frequency = 0.3 per m).
- 11PSD284 2, between 70 and 95 mbgs, K was measured as 3x10-7 m/s. The test interval showed no obvious weak zone; there was no major structure identified, and the number of joints and fractures was low (fracture frequency = 0.7 per m).

- HBM-23-085, between 229.7 and 236.6 mbgs, K was measured as 1x10-6 m/s. A zone of increased flow within the test zone was identified by loss of fluid pressure during drilling.

Table 3-2: Hydraulic tests intersecting MDZ or other geological structures at Madrid

ID	Test #	Test Interval (mbgs)	K (m/s)	Notes on the test interval
08PMD650	Test #1	27.7 to 31.2	$5.6x10^{-10}$	Basalt; shattered structure (possibly mechanical); graphite and sediments present.
08PMD650	Test #2	85.7 to 96.1	$5.6x10^{-9}$	Basalt; 4cm fault zone (no gouge).
08PMD657a	Test #1	75.5 to 107.3	$6.9x10^{-10}$	Deformation Zone (Foliated basalt with med-strong sericitic alteration).
08PMD657a	Test #2	100.9 to 146.6	$5.1x10^{-10}$	Deformation Zone (Foliated basalt with med-strong sericitic alteration).
08PMD657a	Test #3	146.8 to 197.4	$3.9x10^{-10}$	Deformation Zone (Foliated basalt with med-strong sericitic alteration).
08PSD142	Test #2	127.8 to 149.1	$6.5x10^{-8}$	Basalt, transition to PGP; set of joints with calcite crystals.
08PSD143B	Test #1	196.8 to 240.0	$8x10^{-10}$	Deformation zone with basalts.
10WBW003	Test #3	227.3 to 270.5	$2.3x10^{-11}$	Highly strained felsic and mafic metavolcanics. Some qtz/carbonate veining, some veins brecciated. Interval intercepted the alteration near the mineralized zone.
11PSD267	Test #1	75.1 to 113.0	$2.2x10^{-9}$	Mafic volcanic and felsic pillows with quartz (discontinuous ore zone 112-118m). Interval intercepted alteration near the mineralized zone, and modelled fault.

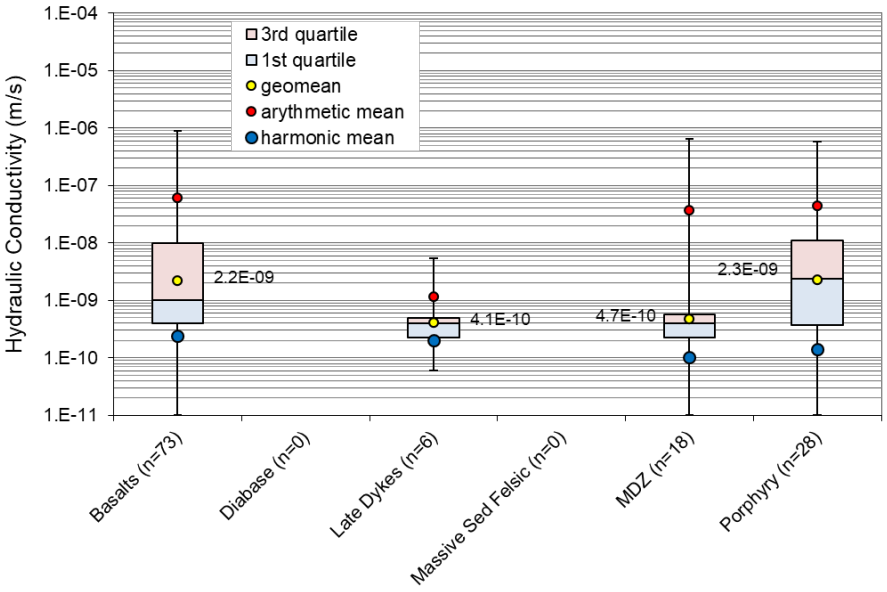


Figure 3-21: Box plot of the Madrid K measurements by geology and structures

Source: HopeBay_MASTER_HydrProperties_gf_20250120.xlsx

Boston

The tests performed at Boston (Figure 3-15) show K values are low, ranging between < $1x10^{-9}$ and $7x10^{-8}$ m/s, with a geomean of $3x10^{-9}$ m/s. The dataset shows no evidence of higher K features associated with geological structures.

3.7.2 Lake Sediments

Table 3-3 presents the estimated hydraulic conductivities of lakebed sediments.

Estimations for soft lakebed sediments were obtained from pressure dissipation tests conducted during CPT drilling in sediments lining the base of Doris Lake, Patch Lake and Aimakatalok Lake (SRK 2009a), and interpreted using the method of Parez and Fauriel (1988). Appendix D compiles the individual results.

CPT refusals were not associated with bedrock contact, but an indurated layer of lake sediment, which is estimated to be on average 3 m thick according to drillhole information. Two samples of the indurated lakebed sediment (SRK-OB-VS-14-S3 and SRK-OB-VS-31-S2) were sent to a laboratory for consolidation testing. The laboratory measured hydraulic conductivity of $4.6x10^{-10}$ and $3.5x10^{-10}$ m/s, respectively (SRK 2009a).

Table 3-3: Hydraulic Conductivity of Doris Lakebed Sediments

Type	Number of Tests	Average Thickness (m)	Hydraulic Conductivity Geometric Mean (m/s)
Soft lakebed sediments	28	17	$1x10^{-8}$
Indurated lakebed sediments	2	3	$4x10^{-10}$

3.7.3 Influence of Drillholes on Hydraulic Conductivity

There have been 1000's of drillholes completed into the different ore bodies over the years in support of exploration, geotechnical studies, etc. A large percentage of these drillholes have been grouted to some extent, but open drillholes can still present a risk for inflow if connected to an appropriate water source. Quantification of how these drillholes could affect the overall bulk K is difficult, if not impossible, but the potential for drillholes to potentially increase bulk K (locally at least) is a consideration.

3.8 Groundwater Levels

Pre-mining groundwater level data (Figure 3-6 and Figure 3-13) consist of pressure profiles in Westbay well 10WBW001 at Doris, groundwater level observations from two drillholes at Madrid, and pressure profiles in Westbay well 10WBW004 and two VWPs at Boston. The water levels collected during hydraulic conductivity tests were not considered representative of in-situ conditions because of influences from drilling. Groundwater pressure measurements are converted to absolute elevations, but as the water is saline, its higher density affects the pressure. To ensure accurate calculations, the pressure is adjusted to account for this increased density. The estimated degree of accuracy of the groundwater pressure measurements

expressed in levels is ±7 m, which corresponds to a variation in density of ±0.015 kg/m^3, as observed in laboratory measurements of Westbay well samples (min. 1.0 and max. 1.03 kg/m3).

Groundwater levels were approximately at or near the lake levels; between 21 and 28 masl at Doris (Doris Lake surface water elevation is ~22 masl), between 23 and 33 masl at Madrid (Patch Lake surface water elevation is ~26 masl), and 56 and 67 masl at Boston (Aimakatalok Lake surface water elevation is ~66 masl). The pressures in 10WBW001 and 10WBW004 suggest a low vertical upward gradient, however this interpretation is uncertain due to density corrections.

Additional groundwater pressures were measured during operations in the Doris underground mine. The dataset (Figure 3-7) includes pressures measured by HR (2020, 2021) in underground exploration drillholes, and pressures measured by Agnico in Westbay well 10WBW001 and VWP HB-BCO-22-150. The measurements show the effect of mine dewatering, with pressures dropping below the level of Doris Lake (-1 to -73.4 masl in the DCO and DCN areas, -266.7 to -364.8 masl in the BTD area) as depressurization around the underground developments progressed.

3.9 Groundwater Quality

Obtaining groundwater quality samples representative of true formation groundwater in low hydraulic conductivity fractured rock within a permafrost environment presents significant challenges. These difficulties arise due to several factors:

- Fractured rock systems with low hydraulic conductivity impede groundwater movement, leading to prolonged residence times and limited flow. This makes it challenging to extract samples that represent natural conditions rather than stagnant or mixed water from the borehole environment.
- Fractures are unevenly distributed and variably interconnected. Samples collected can reflect the water quality of only the more permeable fractures, skewing the representation of the overall system.
- During drilling and sampling, interactions between the borehole environment and surrounding formation water can lead to contamination. For instance, drilling fluids or disturbed fine particles may alter the chemical signature of the extracted groundwater.
- Freezing conditions above and the thermal gradient near the permafrost can alter the groundwater chemistry.

3.9.1 Regional Groundwater Quality Data

A dataset of groundwater Total Dissolved Solids (TDS) concentrations from the Canadian Shield is plotted against depth in Figure 3-22. This dataset includes data from Frape & Fritz (1987) and public data from the following mine projects: Back River (Rescan ERM, 2015), Lupin (Stotler et al., 2009), Meadow Bank (Cumberland Resources, 2005), Meliadine (Golder, 2013), Snap Lake (De Beers, 2002), Ekati (Golder, 2014), Gahcho Kue (De Beers, 2010), and Jay (Golder, 2014).

The distribution of TDS concentrations with depth shows brackish to hypersaline water is common in northern permafrost environments. Salinity, measured as TDS, generally increases with depth, with concentrations reaching up to tens of grams per liter at depths of 500 mbgs beneath continuous permafrost.

The presence of ancient brine water in various locations on the Canadian Precambrian Shield suggests that these deep flow systems are sluggish and slow-moving under natural (pre-mining) conditions (Frape & Fritz, 1987). Gascoyne (2003) reported several potential sources of salinity: (1) rock-water interactions, including reactions with rock matrix minerals and fracture-filling minerals, (2) soluble salts present at grain boundaries and in fluid inclusions, (3) residual saline hydrothermal fluids, and (4) ancient marine fluids or basinal brines that entered rock prior to glaciation. Additionally, in situ cryogenic concentration due to ice and methane hydrate formation may have concentrated the remaining fluids, as observed at the Lupin Mine (Stotler, 2009).

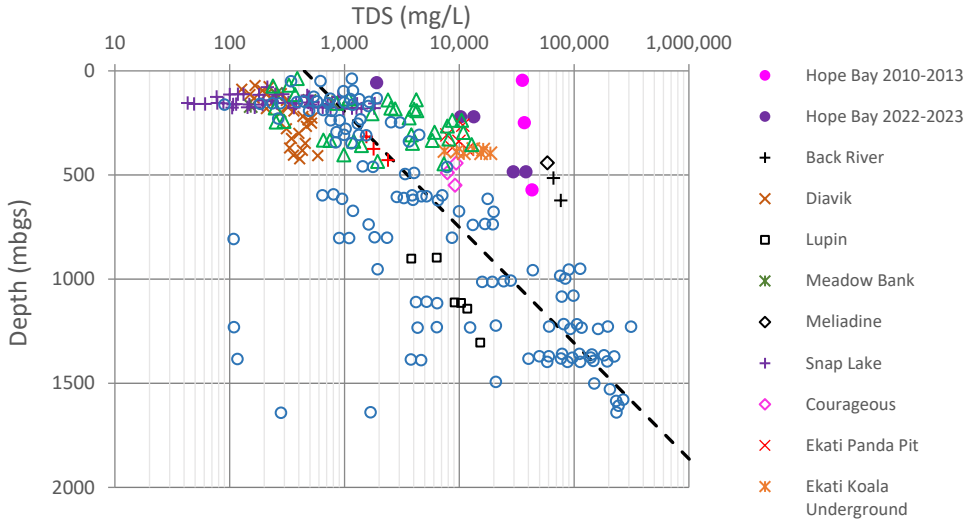


Figure 3-22: TDS concentrations with depth in Canada's North

Source: hopeBay_Compilation of TDS data versus Depth_20241205.GF.XLSX

3.9.2 Hope Bay Groundwater Quality Data

Groundwater samples were collected between 2010 and 2013 at Doris, Madrid, and Boston, and between 2022 and 2024 at Doris. Samples were analyzed for standard parameters, major cations and anions, and total and dissolved metals. In the period 2010-2013 and again in 2024, stable isotopes of oxygen and hydrogen were also analyzed to ensure quality assurance and control (QA/QC) and to assess variations in water source types.

Table 3-4 compiles the mean groundwater concentrations measured in each zone of the Westbay well 10WBW001; Appendix E compiles the individual groundwater quality results (SRK, 2015a, 2017b, c; Lorax 2023b, Lorax 2024c). Comparisons between mean concentrations in 10WBW001 and environmental guidelines[2] indicate that concentrations of ammonia, boron,

[2] Canadian Council of Ministers of the Environment (CCME) water quality guidelines for freshwater, irrigation, livestock, and marine (2024) and the Metal and Diamond Mining Effluent Regulations (MDMER) limits for harmful substances (2024)

cadmium, chloride, fluoride, iron, manganese, nickel, selenium, and zinc exceed the recommended levels, making them potential constituents of concern. Chloride is the only constituent of concern that shows a correlation with depth. Figure 3-23 plots the vertical depth profiles of chloride concentrations, and Figure 3-24 plots TDS Vs chloride concentrations.

The samples collected in 10WBW001 between 2010 and 2013 represent the pre-mining conditions. 10WBW001 underwent significant purging, and QA/QC analyzes concluded samples were representative of true formation groundwater. Although samples from 10WBW004 (Boston) showed comparable chemistry to 10WBW001, they were not considered as representative due to less effective purging. Samples from 10WBW002 (Doris) and 08PMD657a (Madrid) were also not considered representative due to limited purging. Specifically, 10WBW002 had low hydraulic conductivity, and 08PMD657a was a "grab" sample collected using a wireline swabbing method during drilling. The 2010-2013 groundwater quality in 10WBW001 confirmed groundwater was saline and chloride-dominated at all depths, with salinity varying by depth.

The samples collected in 10WBW001 between 2022 and 2024 represent the mining period influenced by the Doris underground operations. In comparison to the pre-mining period, the groundwater quality in Zone 1 (484.8 mbgs) remained the same except for decreases in pH and EC, whereas in Zone 6 and 10 (221 and 57.4 mbgs, respectively), constituents were largely diluted excepted for aluminum and uranium. Almost every major parameter (e.g. Ca, Li, Mg, Fe, SO4, Cl, NH4, Na, Sr) decreased by 60 to 70% in Zone 6 and by 90% in Zone 10. The alkalinity increased to over 200 mg/L in Zone 10 and 6, and from below detection to 14.7 mg/L in Zone 1.

This dilution of constituents and increase of alkalinities are interpreted to result from the dewatering of the Doris underground, which creates a depressurized zone at depth that draws in freshwater from Doris Lake and ultimately leads to an increase of carbonate solubility in the mixed waters. Potential mechanisms are:

- the reduced salinity of freshwater inputs affecting the activity of H+ and thus carbonate dissolution and pH;
- the dissolution of carbonate, specifically dolomite with minor calcite in the quartz veins at depth, by the mixing of surface water previously in equilibrium with the atmosphere (i.e. difference in pCO2) with groundwater;
- the release of groundwater pressures in underground workings and diamond drill holes; and
- various changes in solute concentrations leading to increases in carbonate solubility.

In terms of TDS versus Chloride (Figure 3-24), the increase in the slope from 0.4641 to 0.5662 suggests that chloride concentrations became a larger proportion of the TDS during the mining period. This could indicate that while overall TDS is diluted, chloride is less affected by dilution compared to other constituents. The slight decrease in R^2 from 0.9862 to 0.9823 indicates a minor reduction in the strength of the linear relationship, which could suggest some variability introduced by the mining activities.

Table 3-4: Mean baseline groundwater quality (Doris, 10WBW001)

Parameters		Units	Zone 1 2010-2013 (n = 8)	Zone 1 2022-2024 (n = 3)	Zone 6 2010-2013 (n = 12)	Zone 6 2022-2024 (n = 3)	Zone 10 2010-2013 (n = 9)	Zone 10 2022-2024 (n = 3)[z]	Doris Lake 2003-2016 (n = 8)	*MDMER and CCME Guidelines [mg/L]*
Field Parameters	pH	pH units	7.43	7.12	7.11	7.51	7.23	8.21	-	*6.0 – 9.5 [a2] 7.0 – 8.7 [c2]*
	EC *	µS/cm	52,650	44,431	52,300	17,197	45,050	3,512	-	*N/A*
	DO *	mg/L	11.37	10.27[Y]	10.13	N/A	8.31	8.46	-	*N/A*
	Salinity	%	3.27	2.8	15.1	1.0	15.3	0.2	-	*N/A*
	ORP *	mV	73	74	-66	22	-15	79	-	*N/A*
Lab Physical Parameters	EC *	µS/cm	47,000	47,200 (2022) 23,700 (2023)	45,500	14,600	44,000	3,400 (2023)	-	*N/A*
	Density	kg/m^3	1.03	N/A	1.02	N/A	1.02	N/A	-	*N/A*
	pH	pH units	7.47	6.74	7.48	7.99	7.49	8.23[Y] (2023)	7.62	*6.0 – 9.5 [a2] 7.0 – 8.7 [c2]*
	TDS * (gravimetric)	mg/L	40,700	38,100 (2022) 30,500 (2023/24)	34,400	13,400 (2022) 10,250 (2023/24)	33,700	1,920 (2023/24)	158	*500 – 3,500 [d], 3,000 [e]*
Anions and Nutrients	Alkalinity, Total (as $CaCO_3$)	mg/L	<2	15.3	57.2	288.3	97.5	243.5	29.5	*N/A*
	Ammonia as N	mg/L	0.06	0.01	3.2	2.6	3.6	0.67	<0.005	*1.04-15.3 [b2,F]*
	Chloride (Cl)	mg/L	19,000	19,270	18,000	5,840	17,400	1,000	62	*640 [b1], 120 [b2], 100-710 [d]*
	Fluoride (F)	mg/L	1.2	2.0	0.5	0.9	<0.75	0.8	0.055	*0.12 [b2], 1 [d], 2 [e]*
	Sulfate (SO_4)	mg/L	973	787	1,880	416	1,700	89	3	*1,000 [e]*
Dissolved Metals	Aluminum (Al)	mg/L	<0.005	0.06	<0.005	0.02	<0.005	0.0085	0.055	*0.005 – 0.1 [g]*
	Arsenic (As)	mg/L	<0.002	<0.005	0.033	<0.02	<0.017	0.00062	0.000295	*0.1 [a1], 0.2 [a2], 0.005 [de],*
	Boron (B)	mg/L	3.12	2.97	2.14	2.18	2.32	1.33	0.032	*29 [b1], 1.5 [b2], 0.5 [d], 5 [e]*
	Cadmium (Cd)	mg/L	0.00011	<0.00025	0.00007	<0.0001	0.00013	<0.00001	<0.000005	*0.0086-0.0124 [b1,A], 0.0020-0.0027 [b2,A], 0.00012 [c2], 0.0051 [d], 0.080 [e]*
	Calcium (Ca)	mg/L	4,780	4,630	1,460	310	1520	30	9	*N/A*
	Chromium (Cr)	mg/L	<0.00045	<0.025	0.00047	<0.005	<0.00046	<0.001	<0.0005	*0.001 to 0.0089 [B]*
	Cobalt (Co)	mg/L	0.00015	<0.005	0.00017	<0.002	0.0003	<0.00035	<0.00005	*0.05 [d], 1 [e]*
	Copper (Cu)	mg/L	0.00067	<0.01	<0.0005	0.002	0.00089	0.00071	0.0014	*0.1 [a1], 0.2 [a2], 0.002 [b2,C], 0.2-1.0 [d], 0.5-5.0 [e]*
	Iron (Fe)	mg/L	0.05	2.6	3.5	<0.15	4.7	0.2	0.14	*0.3 [b2], 5 [d]*
	Lead (Pb)	mg/L	0.0004	<0.025	<0.0003	<0.00`075	0.0004	0.0002	<0.00005	*0.08 [a1], 0.16 [a2], 0.001-0.0018 [b2,D], 0.2 [d], 0.1 [e]*
	Lithium (Li)	mg/L	0.38	0.34	0.22	0.064	0.17	0.017	0.004	*2.5 [d]*
	Magnesium (Mg)	mg/L	68	65	1,310	351	1160	36	6.5	*N/A*
	Manganese (Mn)	mg/L	0.72	0.9	1.6	0.3	1.47	0.037	0.02	*Variable [H], 0.2 [d]*
	Mercury (Hg)	mg/L	<0.00002	<0.000005	<0.00003	<0.000005	<0.00002	<0.000005	0.0000007	*0.000026 [b2]. 0.000016 [c2], 0.003 [e]*
	Molybdenum (Mo)	mg/L	0.012	0.01	0.02	<0.00075	0.0095	0.0024	0.0002	*0.073 [b2], 0.01 [d], 0.5 [e]*

Parameters		Units	Zone 1 2010-2013 (n = 8)	Zone 1 2022-2024 (n = 3)	Zone 6 2010-2013 (n = 12)	Zone 6 2022-2024 (n = 3)	Zone 10 2010-2013 (n = 9)	Zone 10 2022-2024 (n = 3)[z]	Doris Lake 2003-2016 (n = 8)	*MDMER and CCME Guidelines [mg/L]*
	Nickel (Ni)	mg/L	0.0017	0.06	0.001	<0.0075	0.0038	0.0015	0.0005	*0.25[a1], 0.5[a2], 0.025-0.150[b2,E], 0.2[d], 1[e]*
	Potassium (K)	mg/L	39	40	213	135	232	30	2.3	*N/A*
	Selenium (Se)	mg/L	<0.002	<0.0025	0.007	<0.00075	<0.002	0.00019	<0.0002	*0.001[b2], 0.02[d], 0.05[e]*
	Sodium (Na)	mg/L	7,000	6,710	8,300	3,060	8,100	680	32	*N/A*
	Strontium (Sr)	mg/L	56	58	19	4.1	16	0.33	-	*N/A*
	Uranium (U)	mg/L	<0.00013	<0.0005	0.00013	0.00021	0.00013	0.00021	0.000035	*0.033[b1], 0.015[b2], 0.01[d], 0.2[e]*
	Zinc (Zn)	mg/L	0.16	0.93	0.22	0.08	0.33	0.09	<0.003	*0.4[a1], Variable[b1b2,I], 5[d], 50[e]*

Source:https://srk.sharepoint.com/sites/FS208/Internal/!Project_Data%20(Not%20Job%20Specific)/04%20Groundwater%20Chemistry/!Master%20WQ%20Database/HopeBay_MASTER_GWQ-DB_jm_ja_spb%20Rev16_pb.xlsx?web=1

Notes:

"<" indicate that measurements were below detection; the average detection limit is the value present.

* EC, Electrical Conductivity; DO, Dissolved Oxygen; ORP, Oxidation-Reduction Potential; TDS, Total Dissolved Solids

1 n, count of values used to calculate statistics. Statistics assumed all values below detection limit were at the detection limit. Some samples taken early in the program with high detection limits were excluded from the statistical summary.

a1 MDMER Maximum authorized monthly mean concentration

a2 MDMER Maximum authorized in a grab sample

b1 CCME Freshwater (Short term)

b2 CCME Freshwater (Long term)

c1 CCME Marine (Short term)

c2 CCME Marine (Long term)

d CCME Irrigation

e CCME Livestock

A Cadmium short term guideline concentration = $10^{[1.016(\log[\text{hardness}])-1.71]}$ µg/L for hardness ≥5.3 and ≤360 mg/L and the long term guideline = $10^{[0.83(\log[\text{hardness}])-2.46]}$ µg/L for hardness ≥17 to ≤280 mg/L

B Chromium Hexavalent 0.001 mg/L and Chromium Trivalent 0.0089 mg/L

C Copper guideline concentration = $0.2*e^{\{0.8545[\ln(\text{hardness})]-1.465\}}$ µg/L for hardness ≥82 to ≤180 mg/L and for hardness <82 mg/L a concentration of 2 µg/L applies

D. Lead guideline concentration = $e^{\{1.273[\ln(\text{hardness})]+4.705\}}$ µg/L for hardness

E. Nickel guideline concentration = $e^{\{0.76[\ln(\text{hardness})]+1.06\}}$ µg/L for hardness >60 to ≤80 mg/L and for hardness ≤60 mg/L a concentration of 0.025 mg/L applies. At hardness >180 mg/L the guideline is 0.150 mg/L.

F Total ammonia guideline pH and temperature dependent

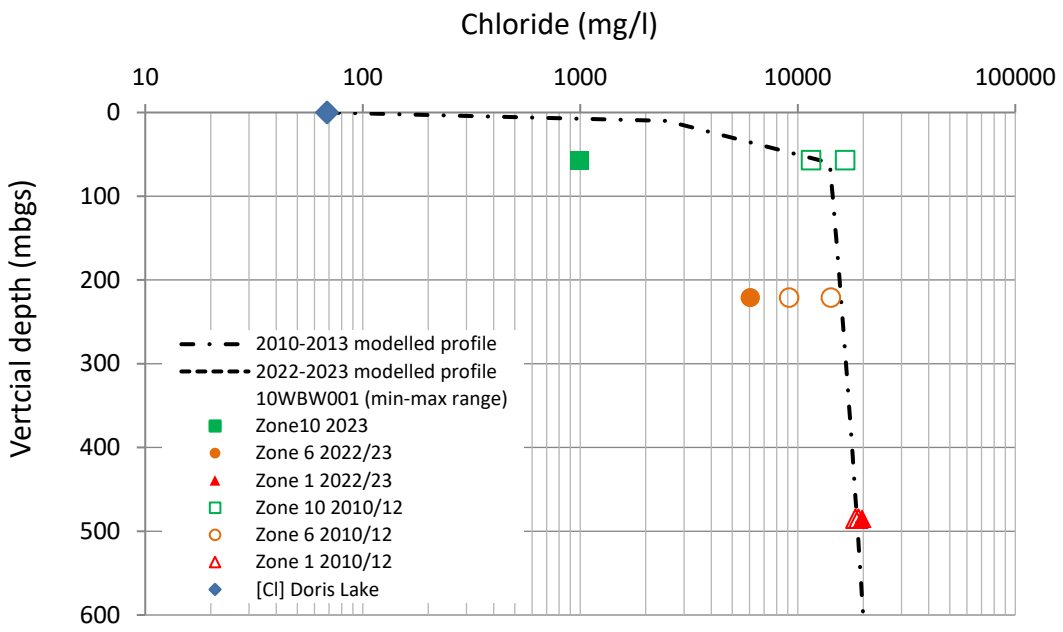
G Aluminum guideline concentrations 0.005 mg/L for pH <6.5 and 0.1 mg/L for pH >6.5

H Benchmark = exp(0.878[ln(hardness)] + 4.76) where the benchmark is expressed in dissolved manganese concentration (µg/L), and hardness is measured as CaCO3 equivalents in mg/L.

I Short-term benchmark is for dissolved zinc and calculated using Benchmark = exp(0.833[ln(hardness mg·L-1)] + 0.240[ln(DOC mg/L)] + 0.526). Long-term CWQG is for dissolved zinc and calculated using CWQG = exp(0.947[ln(hardness mg/L)] – 0.815[pH] + 0.398[ln(DOC mg/L)] + 4.625). Benchmark calculations are limited to a maximum of 250.5 mg/L and 399 mg/L hardness (as $CaCO_3$), for short and long-term concentrations respectfully.

Y Only one value for the date range, not a mean.

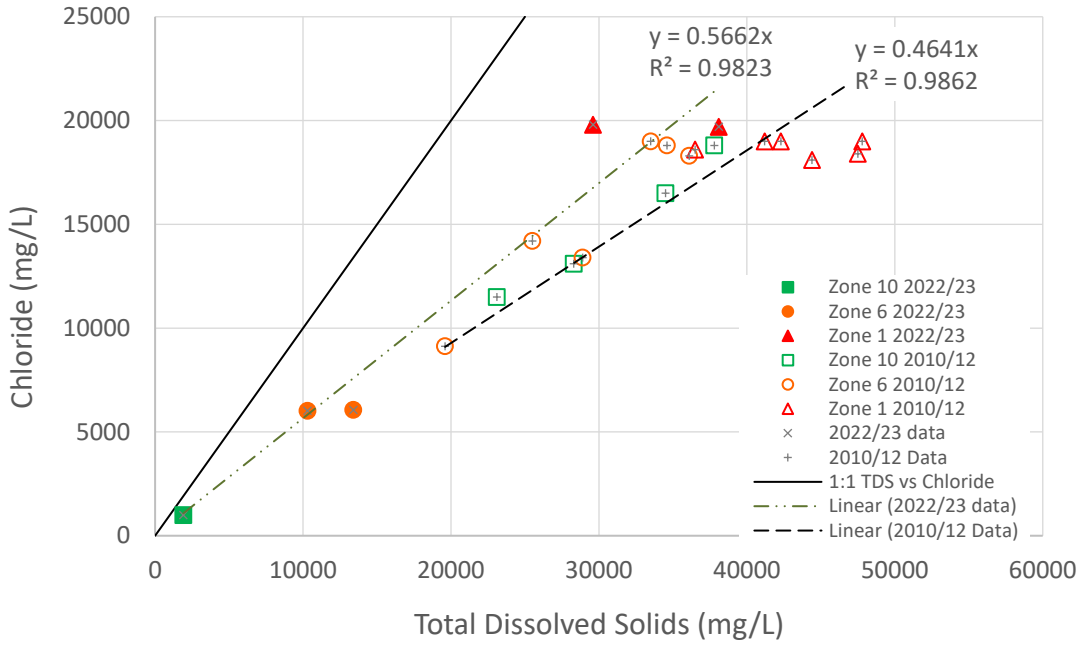
Z Some values were rescinded by the laboratory for improper preservation of sample; one of the sample bottles was acidified when it should not have been. Only parameters affected by this change were removed.



Source: HopeBay_1CT022.004_Chloride_Profile.xlsx

Figure 3-23: Chloride concentration versus depth

Note: Data from Lorax in 2024 was not available at the time of this analysis. The 2024 data in all zones is generally comparable to that of 2022 and 2023, with no significant variations in concentrations in 2024.



Source: HopeBay_MASTER_GWQ-DB_jm_ja_spb Rev16_pb.xlsx

Figure 3-24: TDS vs Chloride

Note: Data from Lorax in 2024 was not available at the time of this analysis. The 2024 data in all zones is generally comparable to that of 2022 and 2023, with no significant variations in concentrations in 2024.

3.9.3 Freezing Point Depression

Salinity lowers the freezing point of water through a process called freezing point depression. The particles of salt interfere with the water's ability to form a solid structure, requiring colder temperatures to freeze. The more salt present, the greater the freezing point depression. Freezing point depression is pertinent when considering the position at which groundwater inflow to a mine could occur, if the mine is advancing from frozen ground into a talik or occurring in the vicinity of a talik frozen-unfrozen boundary. Freezing point depression was calculated using equation (1).

(1) $\Delta T_f = i K_f m$

Where Tf , freezing point depression (ºC)
i, Van't Hoff factor (number of particles the solute dissociates into; for non-electrolytes, i = 1)
Kf, freezing point depression constant of the solvent (ºC.kg/mol)
m, molality of the solution (moles of solute per kilogram of solvent, mol/kg)

Theoretical freezing temperatures were calculated in Table 3-5 based on the 2010/2013 groundwater quality of 10WBW001, prior to mining. The results suggest groundwater freezes at a temperature of between -1°C to -2°C. A freezing point depression of -2°C was assumed for defining talik boundaries.

Table 3-5: Freezing point depression estimates

Parameter	Unit	10WBW001 Zone 1 (548 m)			10WBW001 Zone 6 (246 m)			10WBW001 Zone 10 (63 m)		
		2010/13	2022	2023	2010/13	2022	2023	2010/13	2022[1]	2023
Alkalinity	mg/L	2.0	14.4	15	44.2	260	289	49.7	(1)	229
Calcium	mg/L	4,960	4,400	4,750	749	298	335	1,010	26.9	26.7
Magnesium	mg/L	69.5	64	66.5	702	340	393	849	33.7	36
Potassium	mg/L	39	38.2	41.2	117	94.7	103	160	29.9	29.7
Sodium	mg/L	7,290	6,600	6,830	4,130	2,960	3,370	5,400	664	693
Chloride	mg/L	19,000	19,700	19,800	9,130	6,060	6,020	11,500	(1)	992
Sulphate	mg/L	981	964	476 (2)	940	403	440	1,160	(1)	85.9
Calculated Salinity	%	3.2	2.3 (L)	2.7	3.2	1.4	1.7	2.7	0.2	0.2
Freezing temperature (4)	ºC	-1.9			-0.9			-1.2		

Note: Data from Lorax in 2024 was not available at the time of this analysis. The 2024 data in all zones is generally comparable to that of 2022 and 2023, with no significant variations in concentrations in 2024.

Laboratory measurements affected by improper preservation were removed.

2. Significant variation between ICP-MS Sulfur and Sulfate (80% RPD), assumed to be a laboratory error in the measurement of sulphate.

3. Salinity calculated using linear regression developed in SRK 2022b: y = 0.0006x; with y = salinity in ppt and x the conductivity in µS/cm. 1 ppt = 0.1%.

L. Field conductivity is not available. lab conductivity is used instead. (2010-2013 Data uses mean conductivity - see Table 4-7).

4. Theoretical freezing point calculated based on the 2010/13 groundwater quality.

3.10 Permafrost Boundaries

3.10.1 Ground Temperatures

Ground temperatures have been measured with shallow and deep thermistors at Doris, Madrid and Boston.

At Doris (Figure 3-8, Appendix F):

- Thermistor 08TDD632 and 10WBW002 indicate the -2°C isotherm is between 361 and 366 masl (about 332 and 365 mbgs respectively). Both thermistors are located along the north shore of Doris Lake, which itself influences ground temperatures.
- Westbay well 10WBW001 confirms Doris Lake supports an open talik, with ground temperatures greater than -2°C.
- Thermistor HB-BCO-22-150 was installed from underground, in subpermafrost. It shows ground temperatures are greater than -2°C between 481 and 731 mbgs.

At Madrid (Figure 3-14, Appendix F):

- Thermistor 08PSD144 indicates -2°C isotherm is at 78 mbgs. It is shallow because equipment is located beneath an island centered within Patch Lake, and thus surrounded by heat from the lake.
- Thermistor 08PMD669 is instrumented in permafrost. Its maximum depth is 474 mbgs with temperatures remaining below -2°C.
- The lowermost thermistor sensor of TM00141 measures a ground temperature of -2.6°C at 225 mbgs, projecting a -2°C isotherm at about 346 mbgs. This installation is located between Patch Lake and Wolverine Lakes and influenced by their heat.

At Boston (Figure 3-16, Appendix F):

- At 08SBD382, 08SBD381A, and 10WBW004, the -2°C isotherm is respectively up to 115, 17, and 42 m from the shoreline of Aimakatalok Lake, at depths of 224, 202, and 209 mbgs. The offshore position of the -2°C isotherm cannot be explained by present-day lake configuration nor by lateral heat flow from the adjacent land. It is postulated that the permafrost beneath Aimakatalok Lake has been submerged by lake expansion.
- 08SBD380 and 97NOD176 are in permafrost, with temperature below -2°C down to depths of 241 mbgs and 247 mbgs respectively. The lowermost thermistor sensors indicate relatively cold permafrost temperatures (-5.1°C at 08SBD380 and -5.5°C at 97NOD176).

3.10.2 Regional Permafrost Model

Based on thermistor data, the active layer is generally less than 1 m thick, with the depth of zero annual amplitude around 10 m. The base of the permafrost (-2°C isotherm), away from lakes, is at approximately 447 mbgs. The vertical contacts between permafrost and open taliks are

located near lake shorelines, at distances driven by thermal dynamics. The boundary slopes outward and downward as it extends deeper, and permafrost begins to dominate. In cross-section, it takes generally the shape of a parabola with its concave side oriented vertically beneath the lake.

A one-dimensional (1D) steady state analytical thermal model (Appendix G) estimated the critical lake dimensions to sustain open taliks underneath water bodies.

The model estimated taliks would form under:

- Circular water bodies with a diameter greater than 224 m (radius >112 m); or
- Elongated water bodies with a width of at least 104 m (half-width >52 m); and
- Water bodies deeper than 1.3 m (two-thirds of the mean annual ice thickness).

Figure 3-25 shows the potential open taliks in Doris and Madrid areas according to the above criteria. A default depth of 1.3 m was assumed where the bathymetry of lakes was unknown.

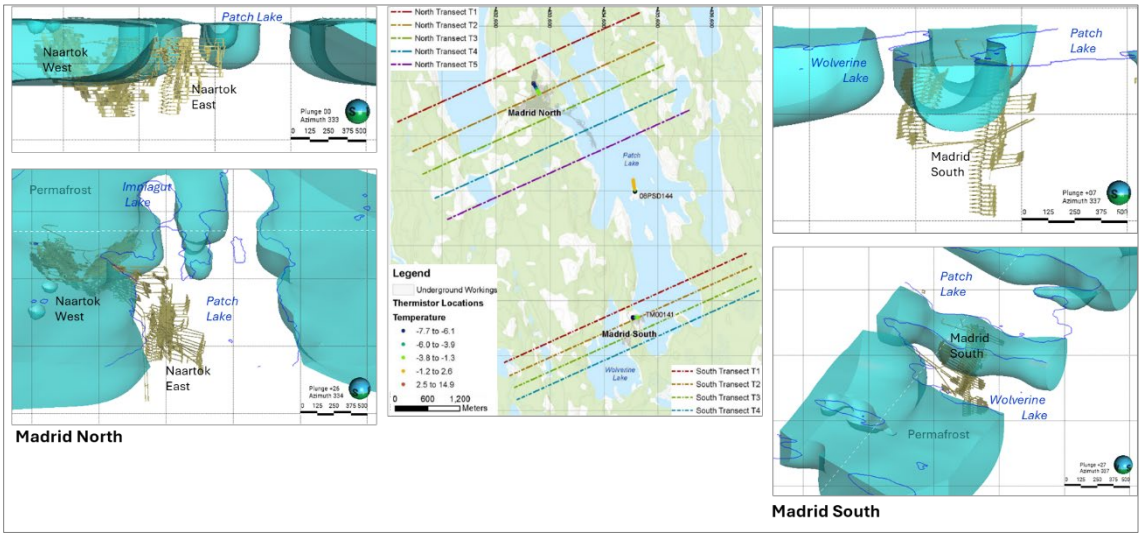


Figure 3-25: Potential open taliks in Doris and Madrid areas

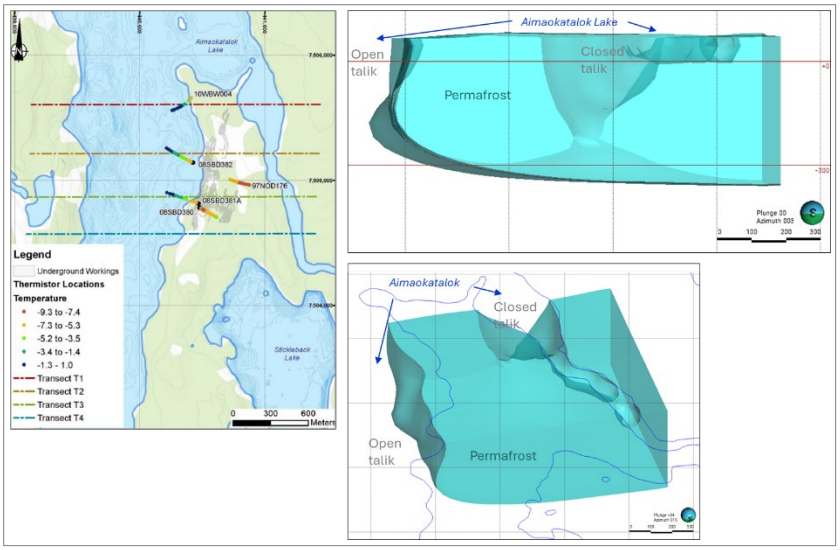
Source: fig_hopebay_potential_openTaliks.pptx

3.10.3 Local Permafrost Models

In 2017, local 3D configurations of the open taliks were estimated in Madrid and Boston areas using 2D thermal modeling (Appendix G) in zones where distances between lakes were small and heat from lakes potentially interfering. Figure 3-26 and Figure 3-27 illustrate the estimated permafrost local 3D-solids. Local 3D estimates were not made for the Doris area at the same time. Assumptions for the Doris area used in modeling are described in Section 6.3.3.



Source: fig_local_prmf_models.pptx



Source: fig_local_prmf_models.pptx

Figure 3-26: Madrid local permafrost model

3.11 Underground Inflow Data During Mine Operations

SRK reviewed the mine inflow rate and quality monitored during operations at Doris, and inflows at individual drillholes (i.e., drilling records, packer test or axial velocity measurements), recorded between Dec.2020 and Oct.2022, from discrete locations or specific intervals or fractures intercepted by developments (Appendix I).

The mine started observing groundwater inflows in January 2018, at an elevation of about -120 masl, when it reached the boundary between permafrost and the Doris Lake open talik; the boundary was approximately vertically below the Doris Lake shoreline when projected downward. The initial concentrations of chloride (22,500 mg/L) were higher than observed prior to mining (6,060 to 14,200 mg/L at -198 masl in 10WBW001 Zone 6). The total mine inflow (Figure 3-29) increased progressively as the mine was developed and peaked in January 2020 at about 2,800 m^3/day. Between 2020 and 2021 inflow rate plateaued at an average of 1,600 m^3/d, and then started decreasing in 2022 as a result of a grouting program.

Most groundwater inflows occurred primarily in the DCN area and originated from underground diamond drillholes (DDH), with flow rates typically within 10 to 50 m^3/d, and a very low percentage of individual DDH with up to 2,180 m^3/day (Figure 3-28). It is uncertain whether inflows from individual features (i.e., drillholes or fractures) decreased over time[(3)], which is a behaviour that would be expected for groundwater released from storage in the fractures rather than a direct connection with Doris Lake.

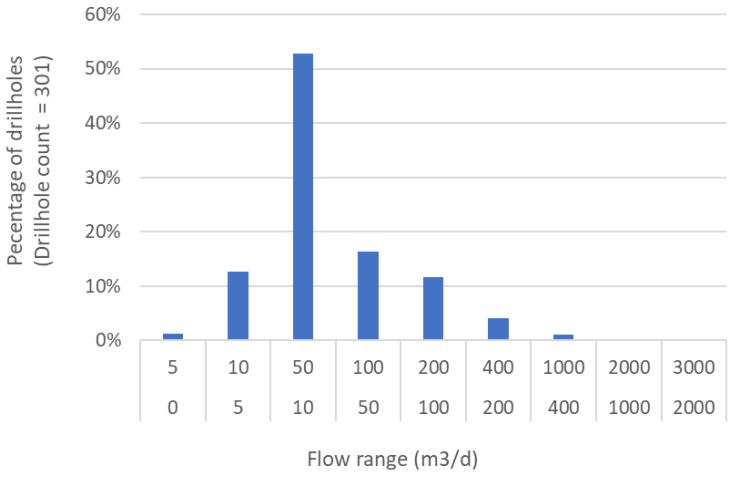
The Figure 3-29 compiles the time series of total mine inflow, chloride load, and chloride concentrations, and shows a cross-section of the Doris mine marked with numbers 1 to 8, corresponding to periodic increases in inflow or events. Overall, the inflows plateaued after the mine reached its lowest elevations, which suggests the overall increase in inflows was primarily driven by the increase of hydraulic gradient between the mine and Doris Lake, rather than interception of specific geological structures, or exploration drillholes.

Based on available information and communication with mine staff, the inferences on causes of the events identified in Figure 3-29 are discussed below:

1. In September 2018, mining at the 114 WLS area intercepted an un-grouted surface exploration hole (TM00083) connected to Doris Lake; the timing of this event is number 2 on Figure 3-29. The drillhole produced an inflow of about 3,650 m3/d and caused some flooding at the bottom part of the DCN decline (pers. Comm. Agnico Jan. 2023). Water was pumped to the North Ramp Sump and subsequently pumped out over time. The hole was plugged in Oct.2018. This event does not correlate with a particularly significant change in total water pumped from the mine, but did correlate with lower mine inflow chloride loads resulting from freshwater inputs.
2. The relationships between the inflow peaks numbered 3 to 8 and structures remain uncertain except at the contact with, or in proximity of, the diabase dyke, which has been frequently

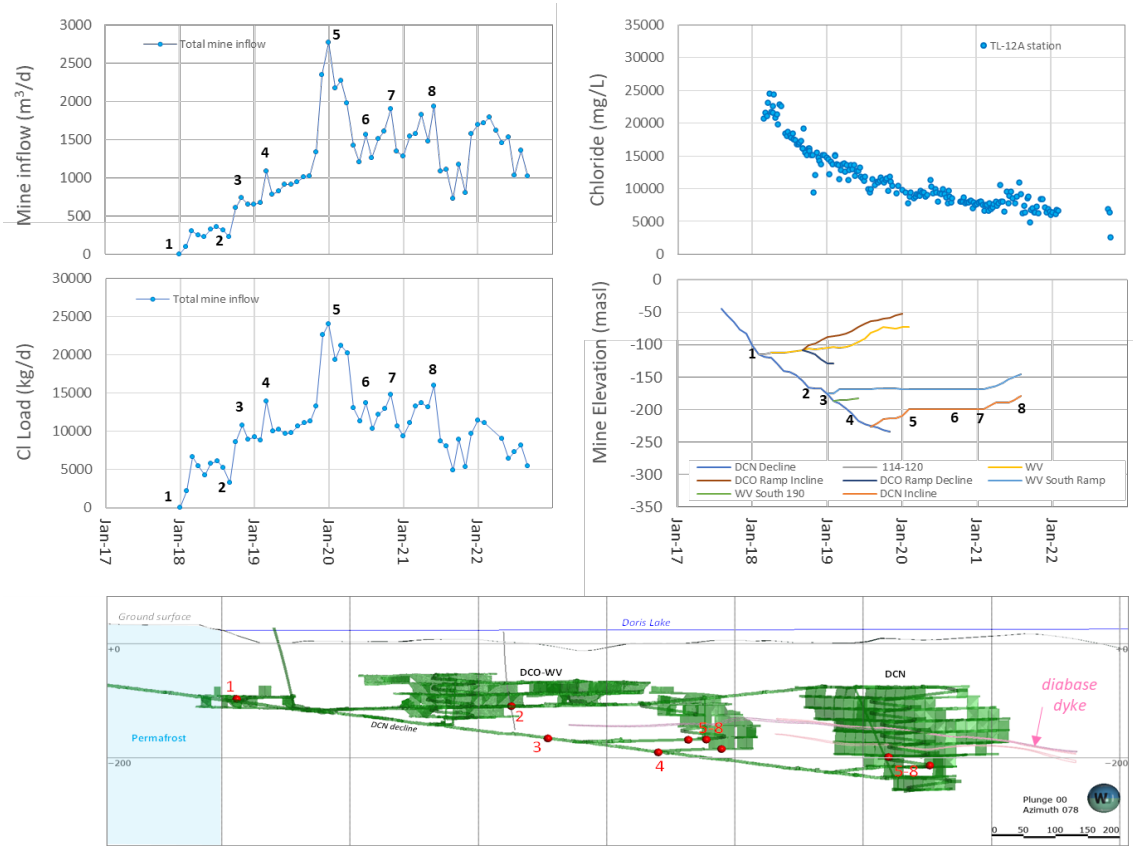
[3] TMAC did not maintain a master database of inflow records or groundwater quality from individual drillholes or fractures. The date and time of the measurements were generally not available, and dataset may contain duplicate records.

reported to produce water. Each peak corresponded to short-term temporary increases of both inflow and chloride, suggesting that the features causing these peaks have a limited storage and are connected with deep saline groundwater. None of these events were correlated with intersection of any specific drillholes.



Source: SRK 2022b

Figure 3-27: Distribution of flow observations from individual drillholes at the Doris mine

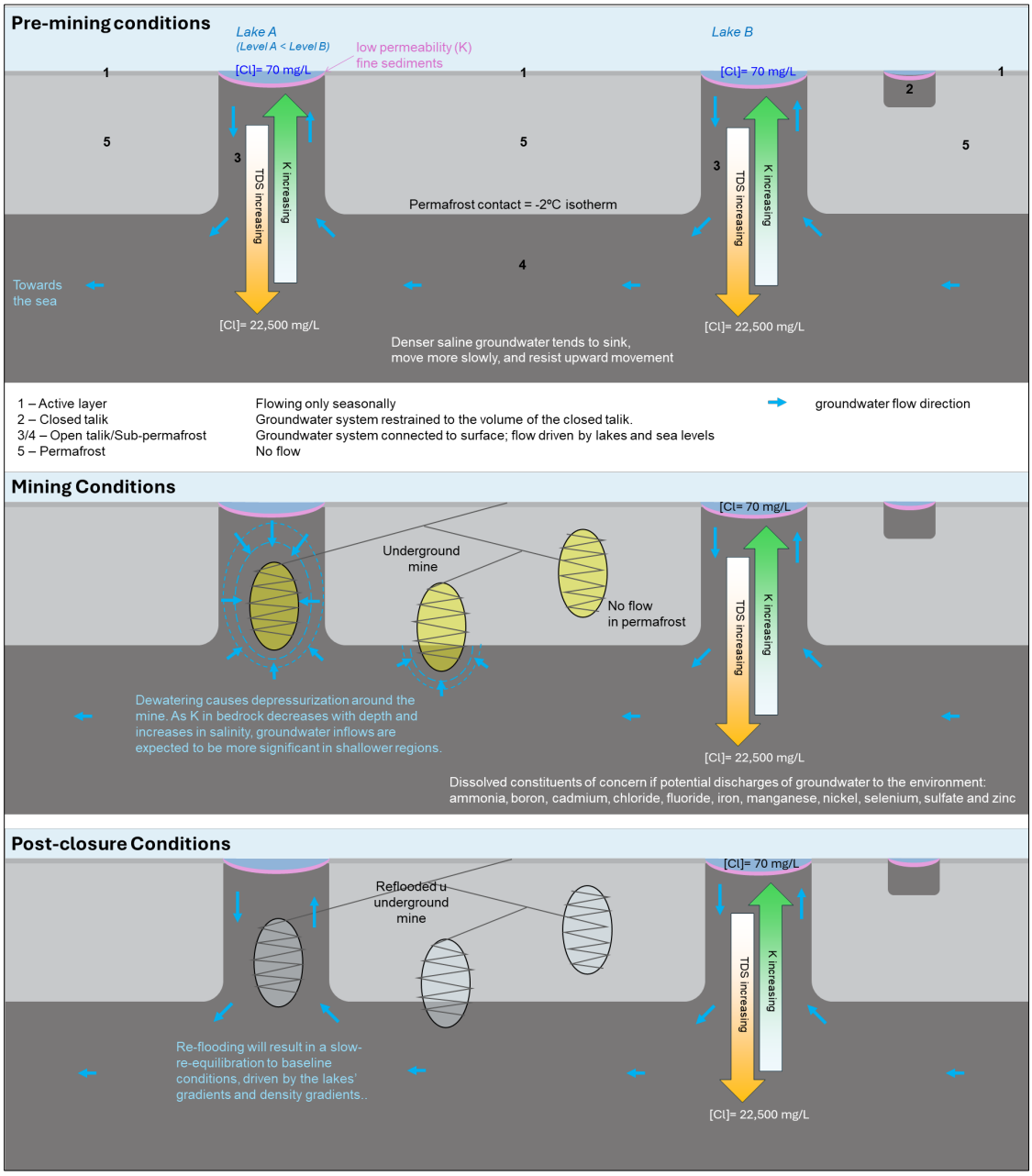


Source: HopeBay_MASTER_Comparison_MineWaterObs-2015Mdl_20221215

Figure 3-28: Mine water flow rates observed between 2017 and 2022

4 Conceptual Groundwater Model

Figure 4-1 illustrates the hydrogeological conceptual model.



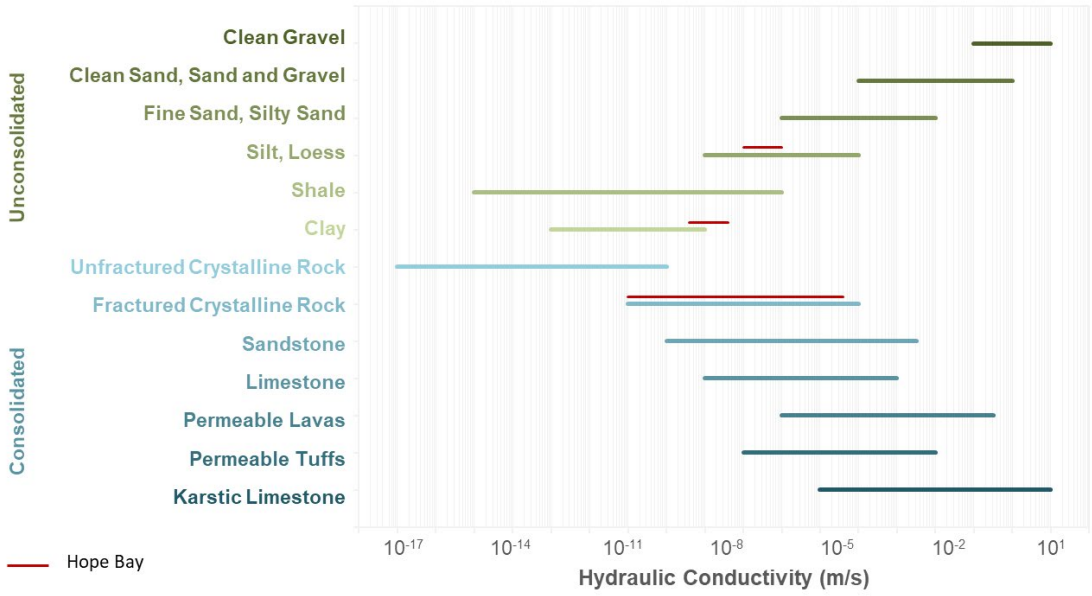
Source: fig_concept_model.pptx

Figure 4-1: Hydrogeological conceptual model

4.1 Baseline Conditions

The system is conceptualized as a low-flow, lake-dominated, confined flow system. The widespread, deep permafrost is essentially impermeable. Groundwater flow and connections between surface and deep bedrock groundwater systems occur exclusively in areas where lakes are associated with open taliks or in sub-permafrost zones. Groundwater systems in shallow active zones have no or minimal influences on inflows to underground mining areas compared to the deeper flow dynamics within the open talik surrounding the underground mine.

K measurements of the fractured rock and lake sediments fall within the bounds of published K values, as shown in Figure 4-2. Lake bottoms are draped with low K, fine sediments. At the small scale, bedrock K is fracture controlled. It consists of a low bulk K background intersected by distributed, potentially higher K fractures and geological structures. At the project scale, fractured rock is treated as a single unit, without differentiation between lithologies. This unit is characterized by relatively higher K at shallow depths, gradually decreasing with depth due to increasing confining pressure.



Source: Hydraulic conductivity ranges from Beale 2014.

Figure 4-2: Published K values Vs Hope Bay K measurements

Deep groundwater is connate, meaning ancient, or emplaced when sediments were originally deposited. Groundwater is brackish to saline, which is common in permafrost environments, and can have elevated concentrations of major ions and metals. The concentrations of calcium, chloride and sodium show a general trend of increasing concentration with depth; other constituents can also have relatively high concentrations, but do not correlate with depth. The dissolved constituents of concern, when looking at potential discharges of groundwater to the environment, are ammonia, boron, cadmium, chloride, fluoride, iron, manganese, nickel, selenium, sulfate and zinc.

Denser saline groundwater requires more energy to move. It tends to sink, move more slowly, and resist upward movement, while lighter freshwater flows more easily. This buoyancy effect can lead to stratification, greater resistance to downward vertical flow, and the formation of slow density-driven convection currents, where saline water sinks and freshwater rises.

As K decreases with depth, inflows are expected to be lower in deeper regions. Chloride concentrations will follow the flow patterns dictated by the hydraulic head and density variations, leading to higher concentrations at depth.

4.2 Mining Conditions

The dewatering activities during underground operations will alter groundwater flow gradients. Depressurization around parts of mines located within taliks or sub-permafrost will extend radially, drawing potential upward and lateral saline flow from the talik, and downward freshwater flow from the lakes above. The low permeability of the fine sediments present at the bottom of lakes will limit downward infiltrations. Table 4-1 lists percentages of mine volumes at the Doris and Madrid areas within and outside permafrost based on the modeled -2°C isotherm.

Table 4-1: Proposed Mine Volumes within and Outside Permafrost

Mine	Volume total	Volume within Permafrost		Volume outside Permafrost	
	m^3	m^3	%	m^3	%
Doris	2,900,000	1,460,000	50%	1,440,000	50%
Madrid	13,640,000	6,660,000	49%	6,980,000	51%

Density-driven flow is likely to slow, delay, and reduce the movement of saline water from depth into the mine. Brackish water at intermediate depths is expected to be mobilized more readily than saline brines at depth, since denser water remains more stagnant and does not mix as freely with fresher water.

Initially, the salinity of the mine inflows will reflect the saline conditions of the surrounding groundwater system. Over time, as the dewatering expands, more freshwater from shallower zones will be mobilized and inflows will become progressively less saline. As K in bedrock decreases with depth, groundwater inflows to the mine are expected to be more significant in shallower regions. Deeper regions, with lower K values, will contribute less water overall, limiting the influx of highly saline groundwater from depth.

While the mine may intercept geological structures or fractures, historical observations of inflow during the development of the Doris mine suggest they will have limited storage capacity and be more likely connected to deep saline groundwater rather than directly to the lakes above. At Doris specifically, the contacts with the diabase dykes are frequently reported to produce water and theorized to be associated with a more permeable contact zone. At Madrid, while no structures have been identified to promote high K, the eastern contact of the MDZ, which typically hosts brittle faults parallel to it, could be theoretically associated with potentially higher K features.

Placement of CRF backfill in the underground will have some influence on mine inflows. Influence is expected to depend on 1) the hydraulic properties of the fractured rock, 2) the type of backfill, and 3) the application methods. The bedrock K is typically low. At Doris, the average K in the top 100 mbgs is $9x10^{-8}$ m/s with some observations between $1x10^{-6}$ to 4×10^{-6} m/s; and at Madrid, it is $1x10^{-8}$ m/s with some observations between $1x10^{-7}$ to 1×10^{-6} m/s. Based on internal knowledge, the CRF backfill K is expected to be within or above the upper range of the shallow bedrock and therefore lead to a low to moderate reduction of inflow at shallow depth and no reduction at depth. In any case, voids left at the contact between backfill and underground walls could still constitute permeable flow pathways.

Effects of Heated Underground Mining

The heat circulated into the underground mines will generate a lateral thaw of the bedrock at some distance from the workings; this distance will be a function of the heated underground air temperature, the initial temperature of the bedrock at each depth, and the duration of time the heat source is applied.

Lateral thaw of permafrost from heated underground mining areas was estimated using a simplified one-dimensional analytical solution of temperature change for a given heat source and the bedrock thermal properties at the Project (SRK, 2017). Based on this analysis, the effects of underground heating on permafrost will be limited. The heat will increase the volume of unfrozen ground around the mines, but it will not generate new open taliks that connects the ground surface to subpermafrost.

The model assumed a constant heat source for the entire duration of mining operations and one-dimensional heat flow in the horizontal direction. Over time, the heat is transferred through the bedrock which contributes to thaw of the surrounding permafrost, with the rate of thaw decreasing with distance from the heat source. Figure 4-3 summarizes expected lateral thaw of the permafrost from underground areas heat over a 4, 12, and 17-year period. The initial bedrock temperatures of -8°C and -4°C represent reasonable end-member ground temperatures measured at the underground mining areas.

Figure 4-3: Lateral Permafrost Thaw from Heated Air in Underground Mining Areas

Heated Air Temperature (°C)	Initial Bedrock Temperature (°C)	Horizontal Thaw from Underground (m)		
		Year 4	Year 12	Year 17
10	-8	18	32	38
10	-4	28	47	57
5	-8	14	24	29
5	-4	23	40	48

Notes:
1. Horizontal thaw based on -2ºC isotherm, with a constant heat source
2. Initial bedrock temperature based on representative end-members measured at the Property

4.3 Closure Conditions

At Closure, dewatering activities will stop. Re-flooding will result in a slow re-equilibration to baseline conditions, driven by the lakes' gradients and density gradients. Some parts of mine workings may continue to act as preferential pathways and may redistribute saline water from deeper zones into shallower regions or adjacent fractured zones.

As water fills the mine, the heat will transfer to the surrounding permafrost and the underground areas will be expected to freeze-back where the minimum ground temperature is less than -2°C. It is possible that parts of the underground areas will not completely freeze back due to the large latent heat requirements combined with relatively warm permafrost temperatures at depth.

The groundwater contained in unfrozen mined out areas may have its quality modified by the backfill and/or tailings deposited underground. It will become part of the regional groundwater system, and travel though the open taliks via the deep groundwater system.

4.4 Post-Closure Conditions

At Post-closure, the groundwater system will have returned to the same conditions as baseline with local influences on flow and groundwater quality immediately around the mines.

5 Numerical Groundwater Model

5.1 Numerical Model Software

The groundwater numerical modeling was completed using FEFLOW 8.1 (DHI, Update 3, May 2024). FEFLOW is a professional software package for modeling fluid flow and transport of dissolved constituents and/or heat transport processes in the subsurface. This program is used extensively for groundwater mining projects around the world. The code is based on a finite element solution of the partial differential equations for flow and transport.

5.2 Numerical Model Assumptions

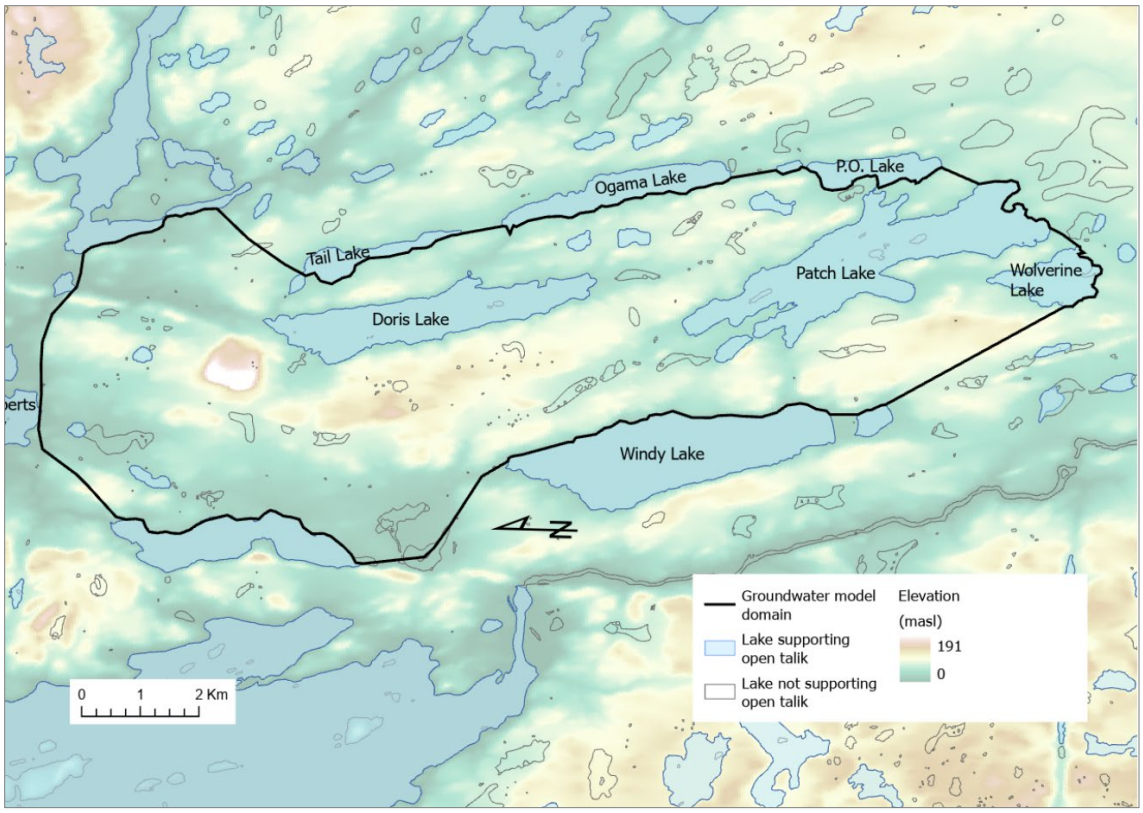
The numerical model assumptions are listed below:

- The media is saturated within a confined aquifer.
- The flow system is dependent on groundwater density.
- Bedrock is simulated as an equivalent porous media. Use of a fracture network model is not justified for a model of this scale and scope.
- The hydraulic conductivity fields within the respective units, overburden and fractured bedrock, are homogeneous and isotropic.
- Steady state or pseudo-steady states define the pre-mining initial conditions. Transient state provides forecasts of mine inflow rates and quality during operations and post-closure conditions.
- Groundwater flow and transport processes can be defined by Darcy's Law and advection-dispersion principles. Mass transport is modeled using chloride as a conservative tracer. The model does not simulate chemical reactions, attenuation processes, or biodegradation.
- The effects of temperature variations, gas migration, and multi-phase flow are not considered.

5.3 Numerical Model Setup

5.3.1 Domain

The model domain is shown on Figure 5-1 and is 71 km^2 (i.e., approximately 18 x 4 km). The upper surface of the model is defined by the topographical surfaces provided by Agnico, which were two high resolution topographical model focused on the Doris and Madrid areas and a topography covering the whole project. The lower surface of the groundwater model is a copy of the topographical surface set to a depth of 1510 mbgs (between -1542 and -1354 masl), approximately twice the depth below ground of the lowest stopes (approx. 690 mbgs).



Source: Hope_Bay_GW_2024.aprx

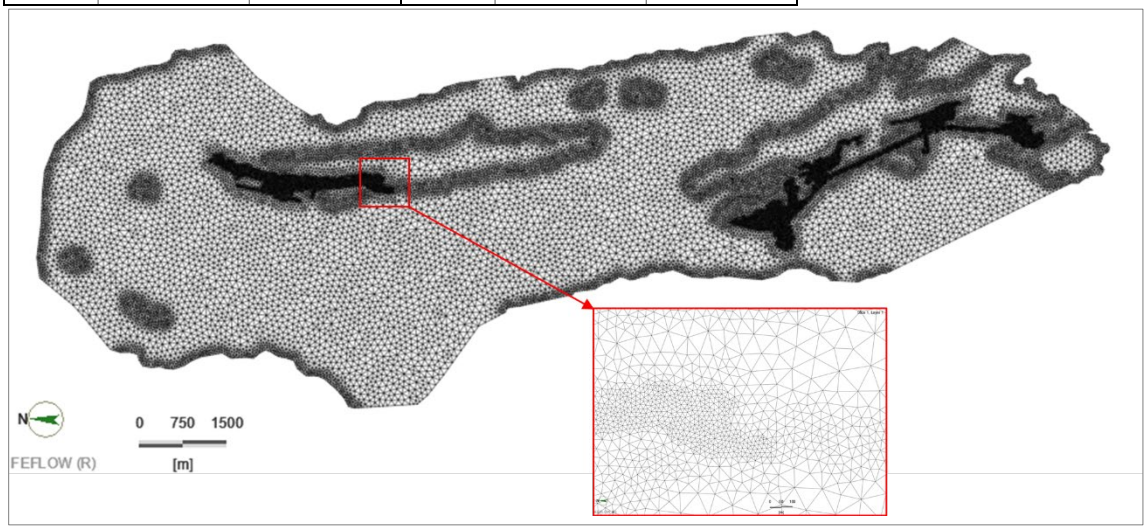
Figure 5-1: Numerical model domain

5.3.2 Mesh

The finite element mesh is shown on Figure 5-2 and has 32 structured layers with 24,312 nodes and 47,579 mesh elements per layer. Horizontally, the element sizes were optimized to obtain a local high resolution at, and immediately around, the Project and along lake edges, and a regional lower resolution near the external borders. The mesh elements are about 20 m wide at tunnels and stopes, and 30 m along lake edges. The regional mesh elements are on the order of 30 m wide along lake edges and 100 m in areas away from features of interest. Vertically, layer thickness increases progressively downwards (Table 5-1, Figure 5-2).

Table 5-1: Thicknesses of the model layers

Layer #	Top Elevation (masl)	Thickness (m)	Layer #	Top Elevation (masl)	Thickness (m)	Layer #	Top Elevation (masl)	Thickness (m)
1	-32 to 156	1	**12**	-262 to -74	40	**23**	-662 to -474	40
2	-33 to 155	3	**13**	-302 to -114	40	**24**	-702 to -514	40
3	-36 to 152	6	**14**	-342 to -154	40	**25**	-742 to -554	40
4	-42 to 146	10	**15**	-382 to -194	40	**26**	-782 to -594	40
5	-52 to 136	20	**16**	-422 to -234	40	**27**	-822 to -634	40
6	-72 to 116	30	**17**	-462 to -274	20	**28**	-862 to -674	80
7	-102 to 86	20	**18**	-482 to -294	20	**29**	-942 to -754	100
8	-122 to 66	20	**19**	-502 to -314	40	**30**	-1042 to -854	100
9	-142 to 46	40	**20**	-542 to -354	40	**31**	-1142 to -954	200
10	-182 to 6	40	**21**	-582 to -394	40	**32**	-1342 to -1154	200
11	-222 to -34	40	**22**	-622 to -434	40			



Source: fig_model_mesh.png

Figure 5-2: Model mesh

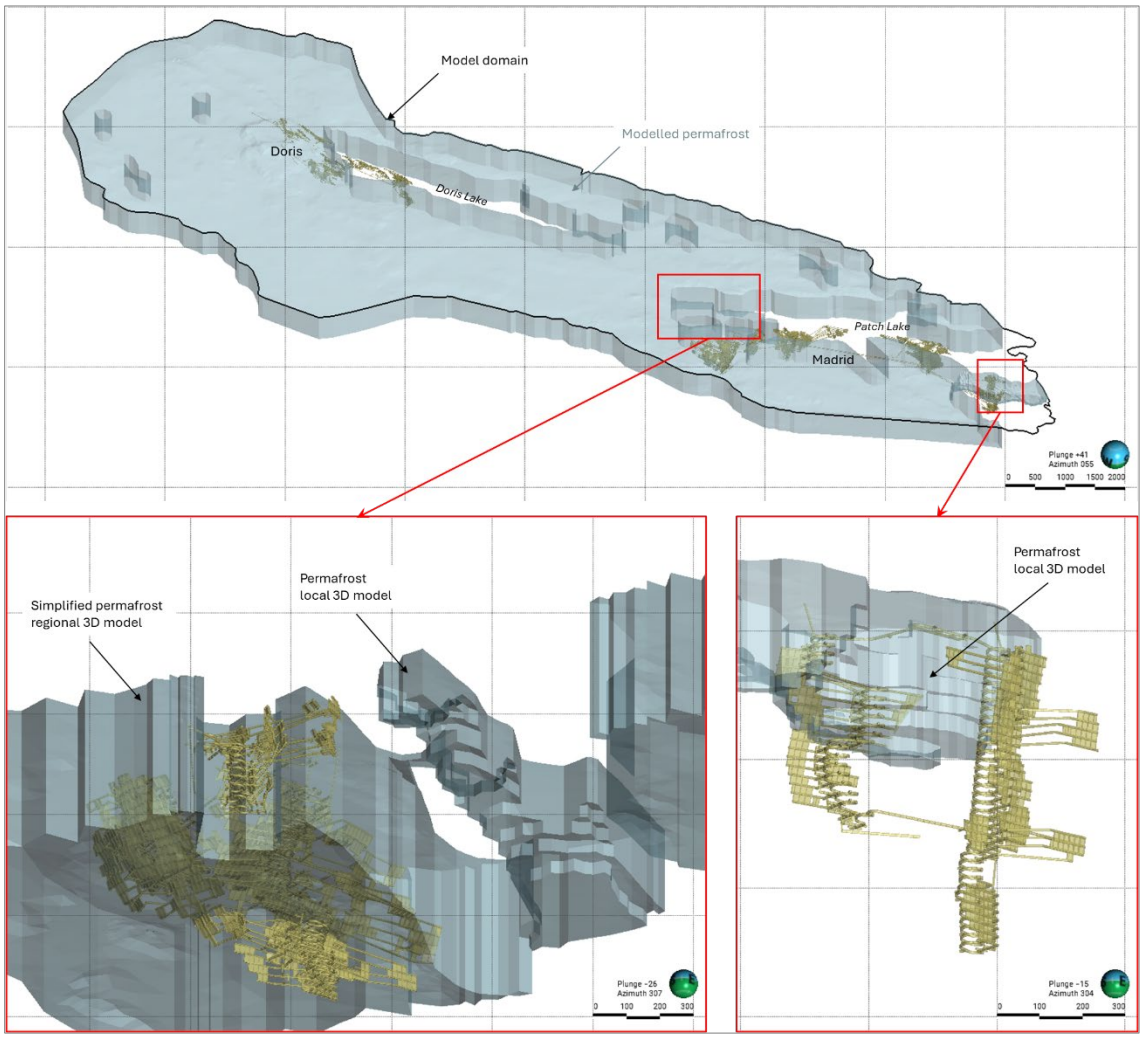
5.3.3 Permafrost

The permafrost is represented by a selection of elements that matches the 3D geometries of the regional and local permafrost models (Section 3.10.2 and 3.10.3). These elements are de-activated during simulations; no flow or transport happens through these elements.

A review of the updated mine plan against thermal data concluded the SRK 2017 3D permafrost models (See Section 3.10.3, Figure 3-26, and Appendix G) captured reasonably well the permafrost geometries in mine areas where ground temperatures are influenced by the heat from adjacent water bodies (i.e., Patch Lake and Imniagut Lake for Madrid North, and Patch Lake and Wolverine Lake for Madrid South). These were replicated in the groundwater numerical model.

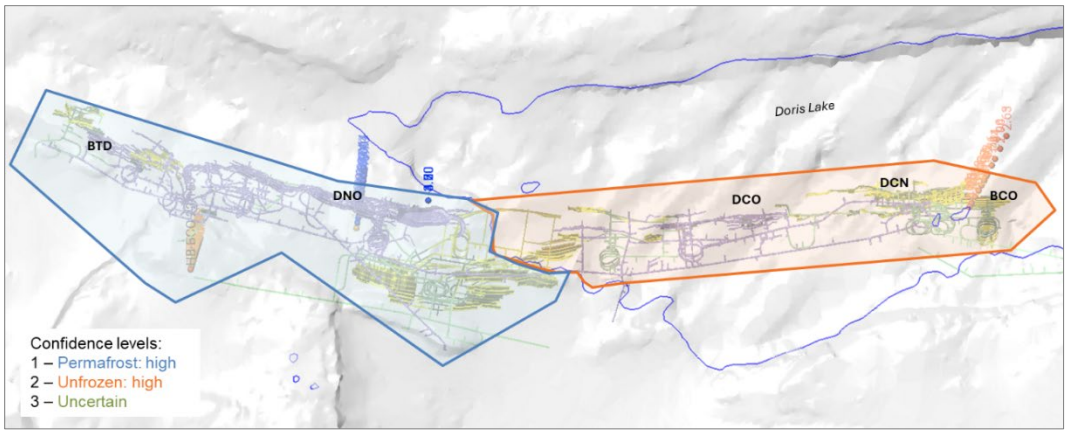
Elsewhere, the 3D geometry of permafrost was simplified: the boundaries between permafrost and open taliks were modeled as vertical and aligned with lake shorelines, while the sub-permafrost base was set at a depth of 450 mbgs.

The global permafrost model is illustrated in Figure 5-3. To evaluate how simplifications can affect inflow rate and quality predictions, mining zones were categorized into confidence levels related to potential interaction with permafrost (Figure 5-4, Figure 5-5, and Figure 5-6) and sensitivity scenarios defined to assess potential influence of model assumptions (Section 6.5). These simulations assessed a) the “uncertain” permafrost areas modeled as open taliks, b) a shallower permafrost base, and/or c) contacts with permafrost placed 100 m inland from the shoreline.



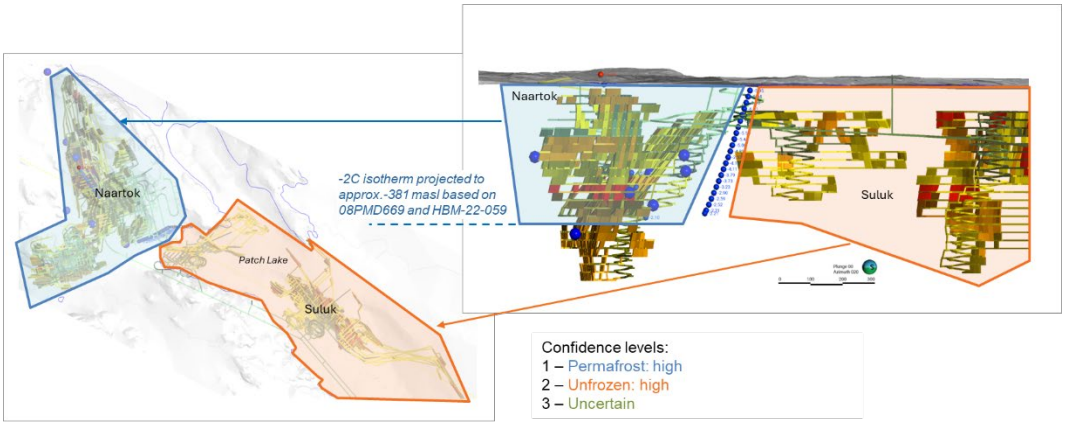
Source: fig_modelled_permafrost_rev1.pptx

Figure 5-3: Modelled permafrost



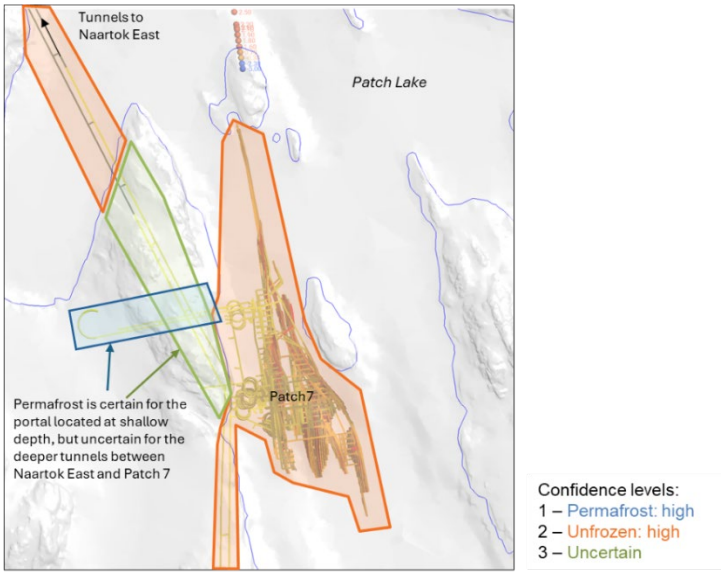
Source: fig_modelled_permafrost_rev1.pptx

Figure 5-4: Permafrost confidence levels at Doris



Source: fig_modelled_permafrost_rev1.pptx

Figure 5-5: Permafrost confidence levels at Madrid in the north area



Source: fig_modelled_permafrost_rev1.pptx

Figure 5-6: Permafrost confidence levels at Madrid in the central area

5.3.4 Boundary Conditions

Baseline Boundaries

- Constant head (i.e., Dirichlet) boundaries (Figure 5-7, Figure 5-8):
- Regional flow is simulated by applying constant head BCs to lakes supporting open taliks. Table 5-2 compiles the water elevations of the main water bodies.

Table 5-2: Average elevations of the lakes

Name	Water level (masl)	Name	Water level (masl)	Name	Water level (masl)
North border	0	Ogama Lake	23.1	Lake #9	42.7
Doris Lake	21.7	P.O. Lake	26.5	Lake #10	47.8
Tail Lake	28.2	Lake #1	20.2	Lake #11	11.4
Patch Lake	26.9	Lake #3	26.7	Lake #12	23.3
Imniagut Lake	28.0	Lake #6	6.3	Lake #14	41.2
Wolverine Lake	32.1	Lake #7	6.0	Lake #15	45.6
Windy Lake	19.0	Lake #8	10.8		

Mass transport:

- Transport of chloride is simulated by applying a constant mass BC of 69 mg/L on the footprints of lakes supporting open taliks, and on external borders constant mass BCs of 69 mg/L for slice 1 to 4, 300 mg/L for slice 3, 2,500 mg/L for slice 4, and 22,500 mg/L for slice 5 to 33.
- No flow (i.e., zero-flux) boundaries:
- All nodes at the top, bottom or external borders other than lakes supporting open taliks.

Mine Boundaries

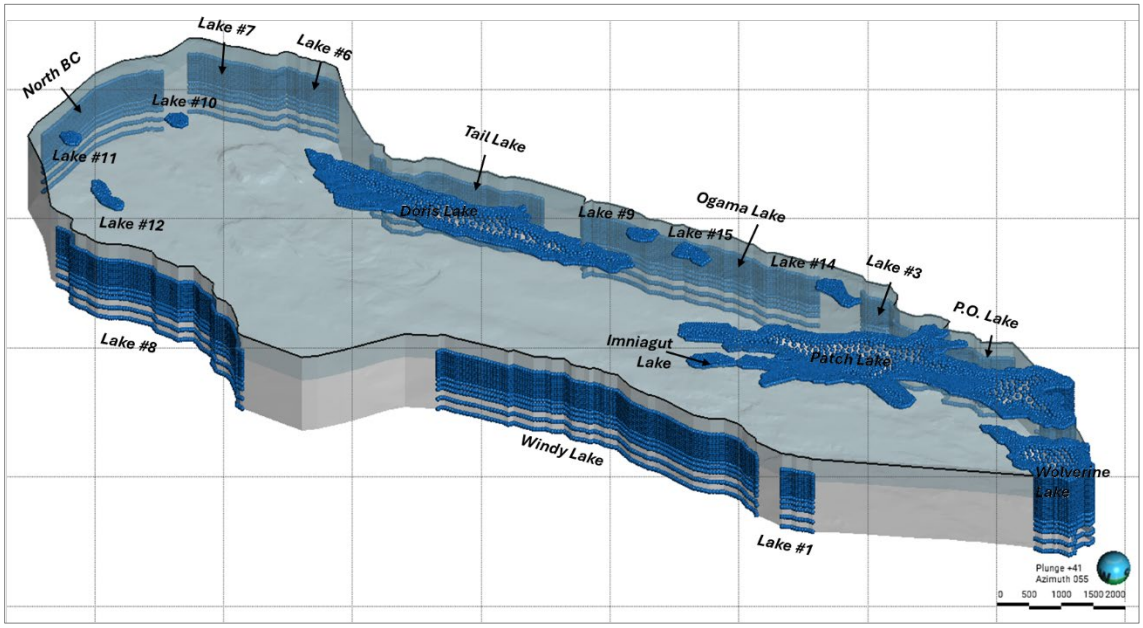
- Boundary conditions are the same as for the baseline model, except for the mining area itself:
- Seepage[4] (i.e., flux constrained Dirichlet) boundaries (Figure 5-9):
- The underground mines are represented by nodes aligned with the tunnels and stopes' 3D geometries that correspond to where water can enter the mine; this method allows for unconstrained flow into the mine where the mathematical solution determines it could occur, allowing assessment of potential impacts on groundwater levels and flow patterns without complex modeling of actual mine volumes.

[4] A seepage boundary is a constant head boundary with a flow constraint that only allows flow out of the model. This represents the fact that undergrounds are exclusively discharge locations.

Each seepage node is associated with a time schedule that matches the proposed progression of the mine. Figure 5-10 illustrates how the minimum elevations in each underground mine progresses over time.

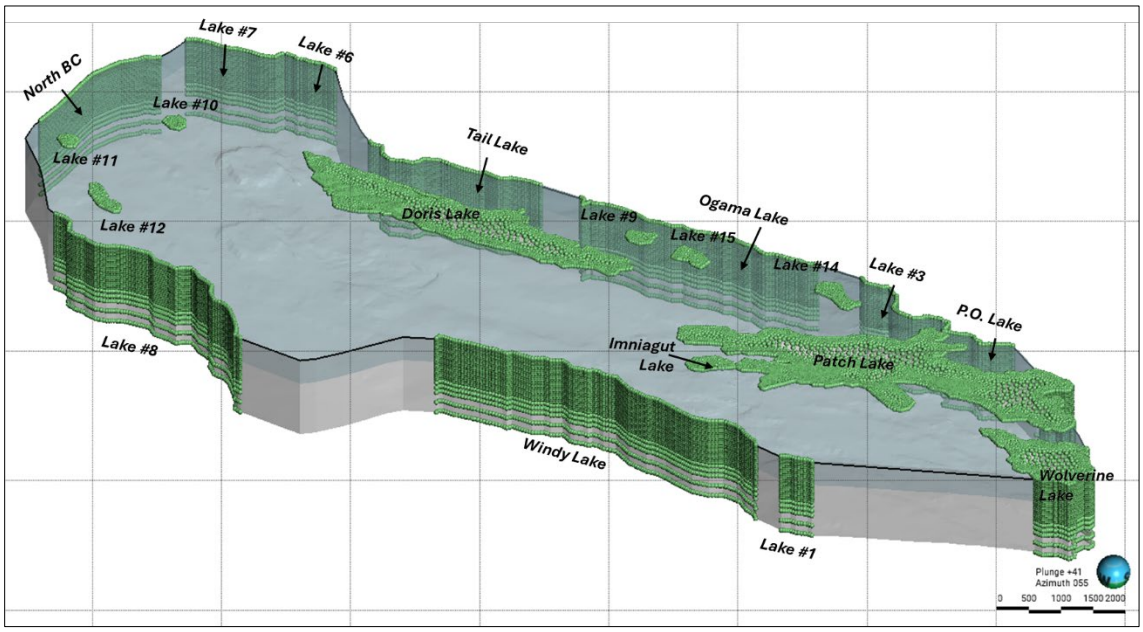
Post-closure Boundaries

At the EOM, the mining boundary conditions are turned off. Boundary conditions are the same as in baseline.



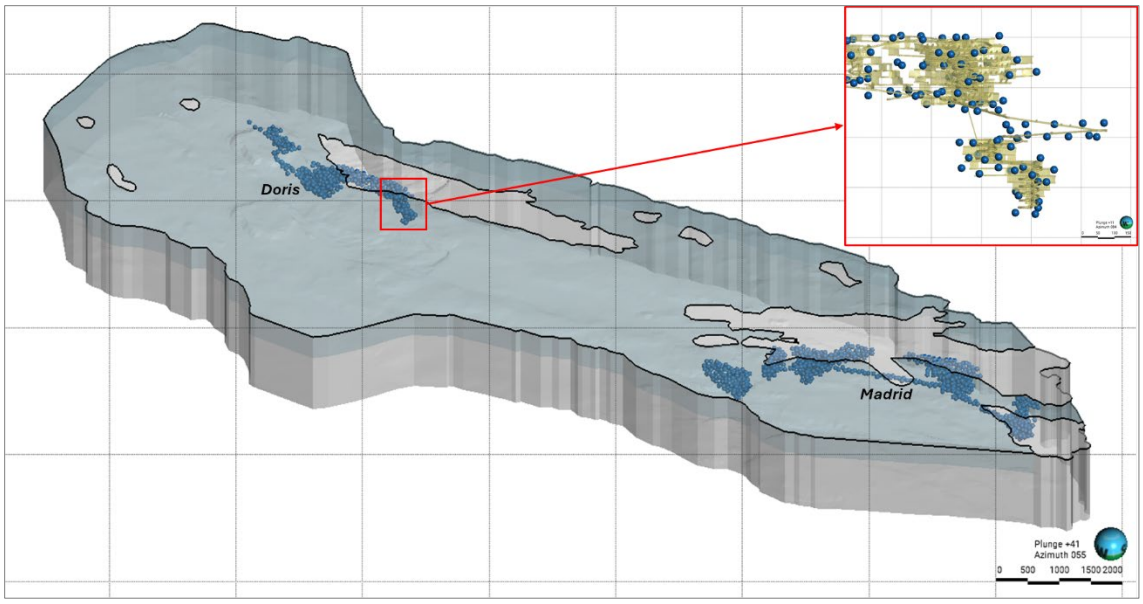
Source: fig_baseline_BC.pptx

Figure 5-7: Baseline head boundary conditions



Source: fig_baseline_BC.pptx

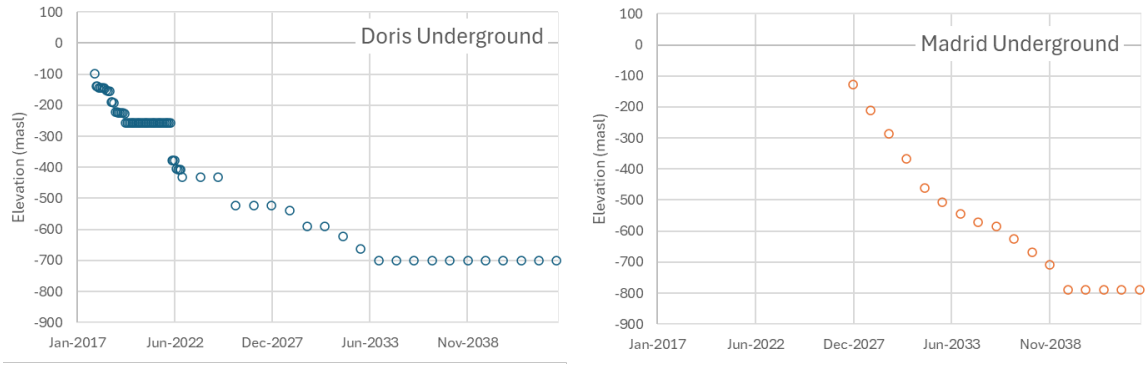
Figure 5-8: Baseline mass boundary conditions



Source: fig_mining_BC_rev1.pptx

Figure 5-9: Mining head boundary conditions

Note: Head boundary conditions assigned to lakes during mining conditions are the same as during baseline. They are hidden to distinguish the seepage nodes assigned to the underground mines.



Source: HB2024_1-ModelSetup_rev1.xlsx

Figure 5-10: Underground mines' bottom elevations versus time

Note: Nodes associated with both underground and permafrost are excluded from the plots.

5.3.5 Water Density

The model was set with a single, uniform density ratio value based on the maximum and minimum densities observed at the Project. This approach simplified the model setup but does not account for local density variability due to infiltration from relatively lower density freshwater lakes. Such infiltration is suspected to occur but not well characterized by monitoring data.

5.3.6 Initial Flow and Mass Conditions

The initial flow field was defined based on steady-state flow predictions under baseline conditions.

The initial mass was set to pseudo-steady state predictions under baseline conditions, with a simulation time of 1,000 years.

5.4 Numerical Model Calibration

5.4.1 Approach

The primary objective of the model is to simulate the hydrogeological behavior of the system under mining conditions, including water inflow rates and solute transport. These outputs will be used to guide mine water management, inform environmental impact assessments, and regulatory compliance.

The model calibration prioritized the mine inflow rates, and chloride concentrations observed during the 7-years of underground operations at Doris over pre-mining conditions. The pre-mining data, while valuable for the conceptual model, is inherently uncertain, while operational data reflect the response of the groundwater system to the large stress imposed by mining activities. Calibrating the model to replicate operational data ensures that the model is fit-for-purpose and enables reliable predictions for ongoing and future mine development scenarios.

The permafrost environment, salinity, and low-permeability fractured bedrock present significant challenges for data collection and interpretation. These complexities exacerbate the uncertainties in pre-mining data, particularly with respect to groundwater flow dynamics and solute distribution. The pre-mining groundwater pressures converted to absolute elevations are uncertain due to assumptions about water density, and the fact that chloride concentrations were significantly greater when the Doris mine intercepted the open talik suggest a limitation in capturing true hydrogeological conditions before operations. Even with its limitations, this data provided a valuable understanding of groundwater pressures, flow patterns, and baseline chloride concentrations, and established a starting point for interpreting deviations observed during mining operations.

5.4.2 Transient Calibration

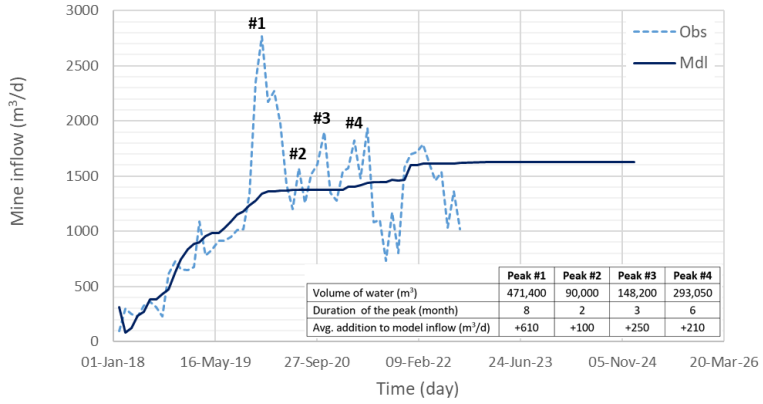
The transient calibration was an iterative process that consisted of varying the hydraulic conductivity profiles to match the transient observations of mine inflows and chloride concentration ([Cl]) recorded between 2018 and 2024 (i.e., year 2017 was not included because the mine was in permafrost and not yet intercepted inflows). The quality of calibration was rated visually by comparing observed and modelled inflow rates and [Cl].

Initially, the model was configured with two hydraulic conductivity profiles (Figure 5-13) defined using K geomeans and expert judgment. One profile was assigned to the Doris area based on the Doris K dataset, and the other to the Madrid area using the Madrid K dataset. A transition zone of approximately 2 km allowed for a gradual shift in hydraulic conductivities between the two areas. During calibration, adjustments to hydraulic properties were applied uniformly across the entire model.

Figure 5-11 and Figure 5-12 show calibration results. The results were considered reliable for predicting the average mine inflows and long-term chloride trends but limited in resolving short-term variabilities.

The model replicated well the general trend of increasing and stabilizing mine inflows but not the sharp peaks and variabilities. These are interpreted as temporary increases caused by local interception of structural bedrock features with limited storage capacity, leading to temporary inflow events. The model does not attempt to replicate the discrete fracture network, focusing instead on capturing the overall trend of mine inflows, but the comparison between the global average trend and the observed peaks provides insights into the potential additional volumes of inflow that may be intercepted occasionally and temporarily by the future developments. The analysis of water volumes associated with peaks shows additional contributions to the overall model inflows could range between 100 to 610 m^3/d for a period of 2 to 8 months.

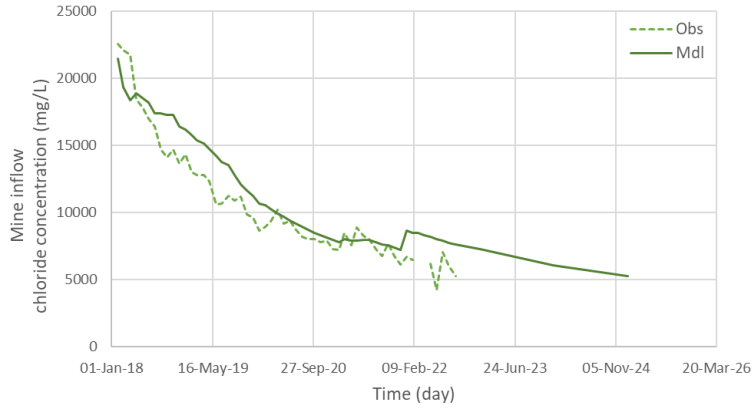
The model replicated well the overall declining trend of chloride concentrations which reflects the gradual dilution of chloride in mine inflows over time. The model did not reproduce the short-term fluctuations, which may be due to episodic factors such as localized inflow with higher or lower salinity, changes in hydraulic connectivity, or interception of distinct water-bearing zones.



	Peak #1	Peak #2	Peak #3	Peak #4
Volume of water (m^3)	471,400	90,000	148,200	293,050
Duration of the peak (month)	8	2	3	6
Avg. addition to model inflow (m^3/d)	+610	+100	+250	+210

Source: HB2024_2-ModelResultsCalib.xlsx

Figure 5-11: Modelled versus observed underground inflow rates



Source: HB2024_2-ModelResultsCalib.xlsx

Figure 5-12: Modelled versus observed chloride concentration of underground inflows

5.4.3 Calibrated Properties

Table 5-3 compiles the properties of the calibrated numerical model. Figure 5-14 shows the modelled calibrated file of hydraulic conductivities. All the parameters fall within the range of the field observations and, if not measured, within the range of literature values.

Table 5-3: Groundwater model properties

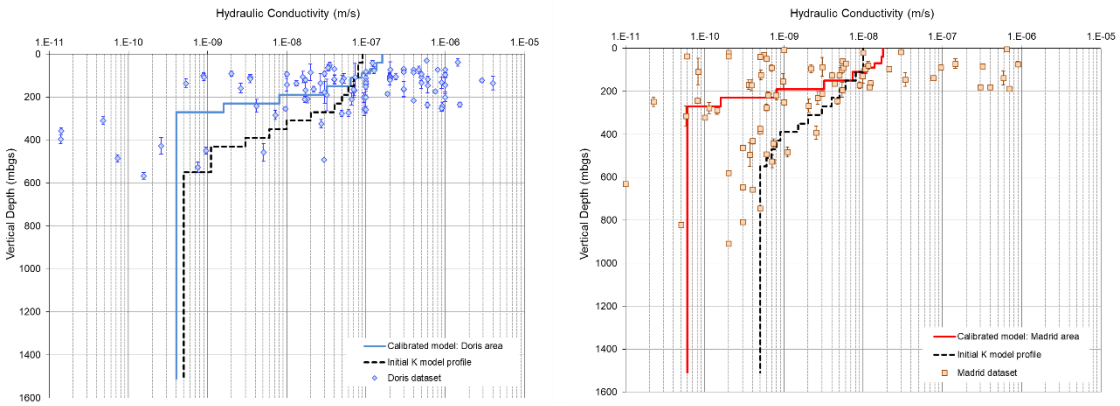
Unit	K_{xyz} (m/s)	S_x [1] (-)	Porosity (-)	Density ratio (-)
Lake sediments [layer 1 to 4]	$1x10^{-8}$	$1.0x10^{-5}$	0.2	0
Fractured bedrock [layer 1 to 32]	*See Figure 5-13*	$3.0x10^{-7}$	0.03	$8.1418x10^{-3}$

Note:

The modelled thickness of lake sediments (Figure 5-15) vary between 0.5 and 20 mbgs, with shallow thickness at the edges, and a gradual decrease towards the center of the lakes.

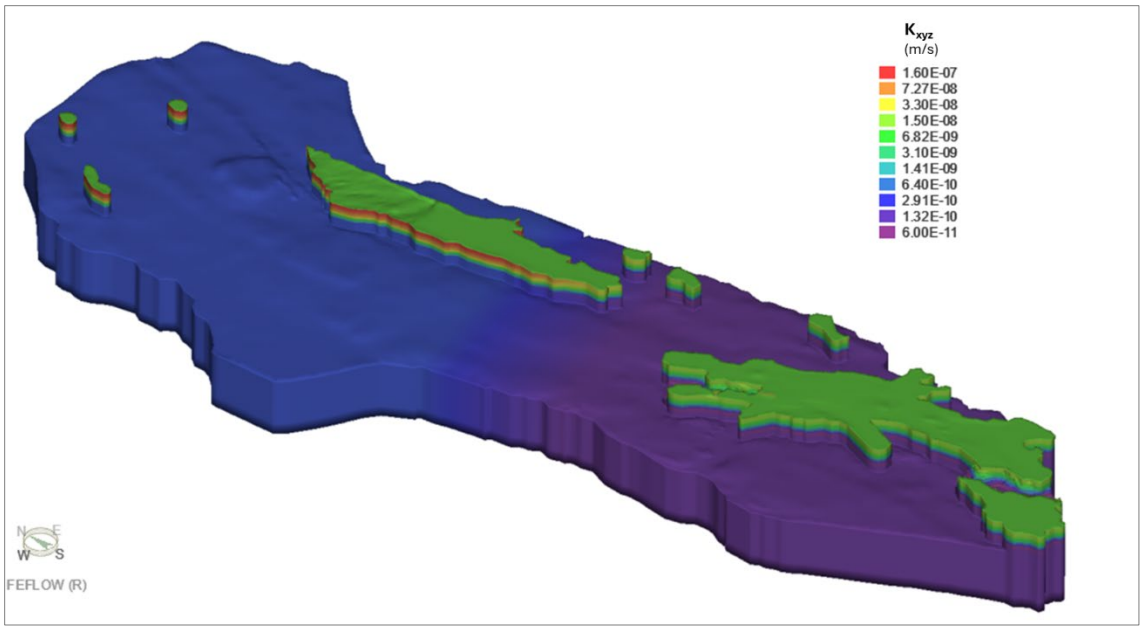
1 Storativity (or specific storage), influences the "drainability" of surficial material. There are no site-specific overburden storativity value measurements. A value of $1x10^{-5}$ m^{-1} was assumed based on scientific literature (Singhal and Gupta, 2010).

Density ratio estimates based on minimum density calculated for a chloride concentration of 69 mg/L and a maximum chloride concentration of 22,056 mg/L.



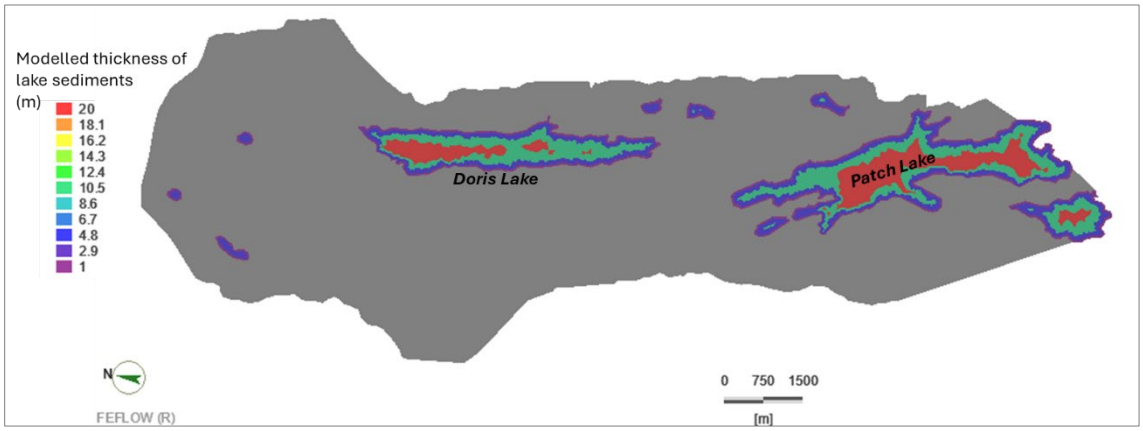
Source: HopeBay_MASTER_HydrProperties_gf_20250120.xlsx

Figure 5-13: Calibrated K versus observed



Source: fig_model_K_rev1.pptx

Figure 5-14: Modelled calibrated K



Source: fig_model_thickn_sedimLakes.pptx

Figure 5-15: Modelled thicknesses of lake sediments

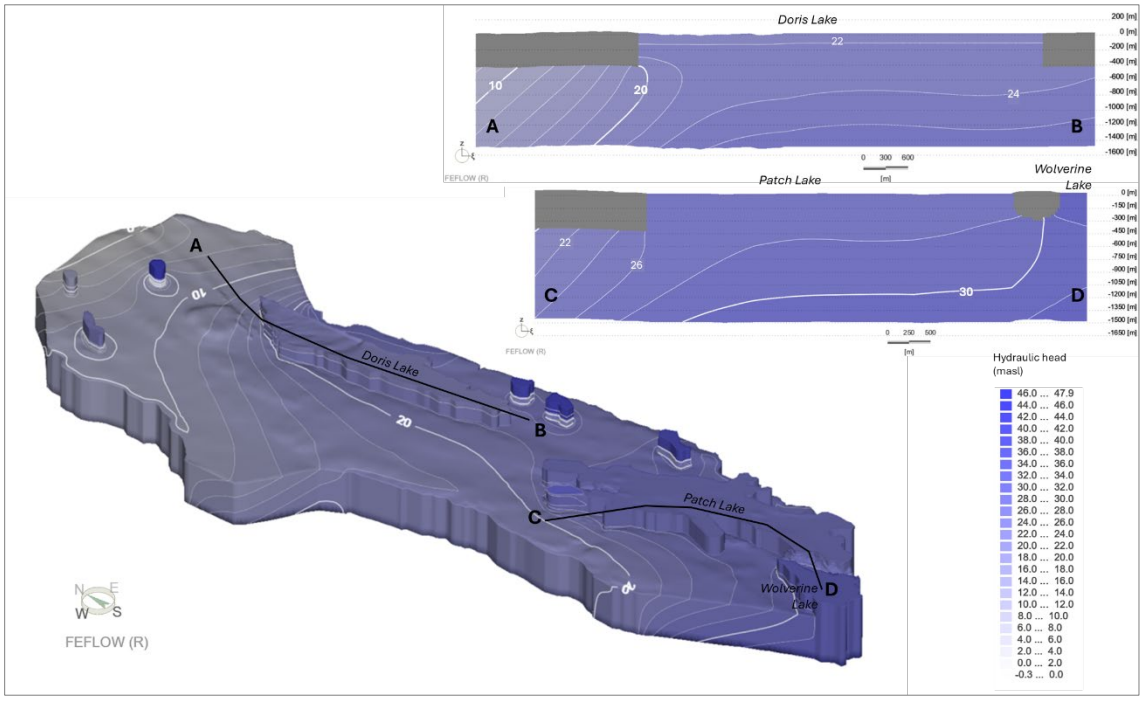
6 Numerical Model Results

The base case modeling scenario consists of a single model run, set to the calibrated properties presented in Section 5.4.3 and simulating the full mining development schedule, from 2018 to 2043, and a 500-year post-closure period. The permafrost model corresponds to the model illustrated in Figure 5-3, with the mining areas rated with an “uncertain” permafrost confidence levels simulated as frozen. The predictions were used to estimate the average annual mine inflows and support the evaluation of Project’s potential impacts on the environment. Particle tracking was used to estimate the flow paths of contact water and their potential discharge points and contribution to lakes.

Section 6 will present alternative scenarios with the most conservative permafrost settings and parameter variabilities.

6.1 Baseline Conditions

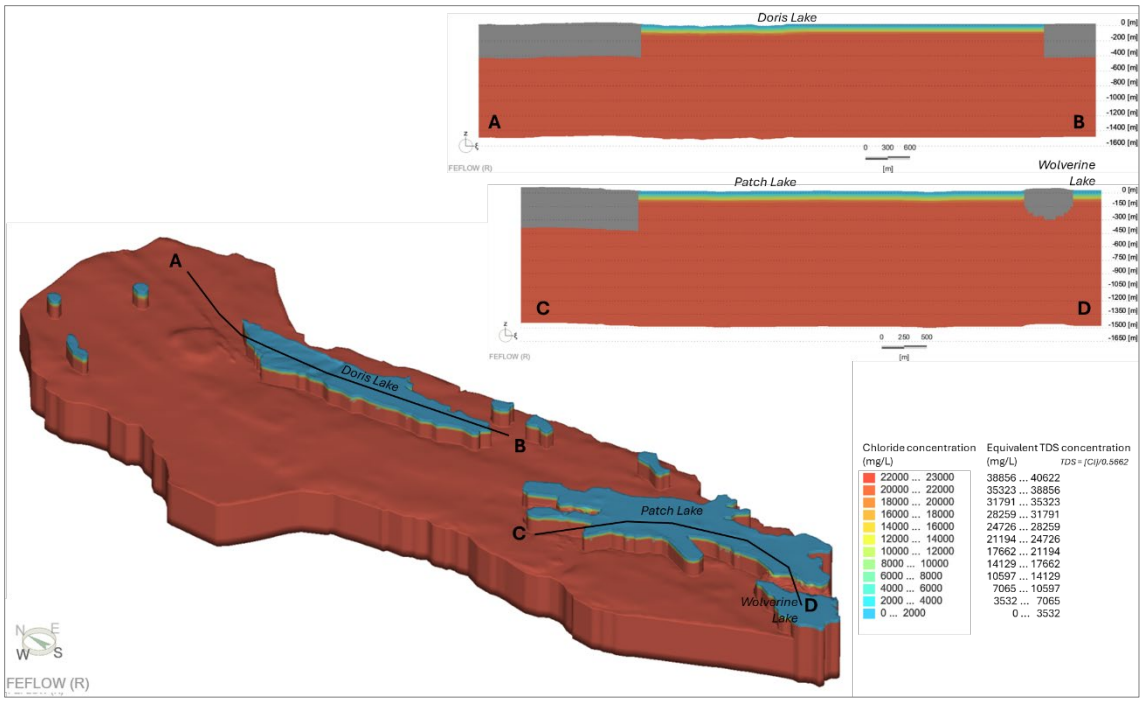
Figure 6-1 and Figure 6-2 present the modelled hydraulic heads and chloride concentrations for baseline conditions. Groundwater flow and mass balances were good (<0.1% and 0.9% respectively), and the predictions consistent with the groundwater conceptual model. Modelled groundwater flows from the south to the north, towards the coast, at a slow rate (Table 6-1). The chloride concentration in groundwater is increasing with depth as shown in the vertical profile (Figure 6-3).



Source: fig_mdl_baseline_head_rev1.pptx, HB2024_3DgwMdl_03-00_rev2_[InitHeadMass]_trsnt1000yr.dac

Figure 6-1: Modelled groundwater heads for baseline conditions

Note: Permafrost elements are not shown in the 3D view.



Source: fig_mdl_baseline_mass_rev1.pptx, HB2024_3DgwMdl_03-00_rev2_[InitHeadMass]_trsnt1000yr.dac

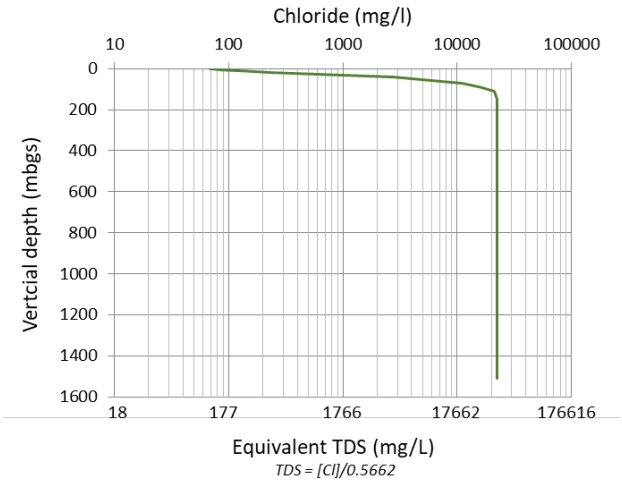
Figure 6-2: Modelled chloride concentrations for baseline conditions

Note: Permafrost elements are not shown in the 3D view.

Table 6-1: Predicted flow rates for baseline conditions

Name	**Outflow Rate** (*Discharge*) (m^3/d)	**Inflow Rate** (*Infiltration*) (m^3/d)	**Name**	**Outflow Rate** (*Discharge*) (m^3/d)	**Inflow Rate** (*Infiltration*) (m^3/d)
Model domain	4.3	4.3	Lake #1	<0.1	<0.1
North border	0.8	<0.1	Lake #3	<0.1	<0.1
Doris Lake	0.3	0.8	Lake #6	0.2	<0.1
Imniagut Lake	0.0	0.2	Lake #7	0.2	<0.1
Patch Lake	0.8	0.9	Lake #8	0.7	0.1
P.O. Lake	<0.1	<0.1	Lake #9	0.0	<0.1
Ogama Lake	0.3	<0.1	Lake #10	0.0	0.3
Tail Lake	<0.1	0.8	Lake #11	0.0	<0.1
Wolverine Lake	0.5	0.5	Lake #12	0.0	0.2
Windy Lake	0.4	<0.1	Lake #14	0.0	<0.1
			Lake #15	0	0.1

Source: HB2024_3DgwMdl_03-00_rev2_[InitHeadMass]_trsnt1000yr.fem

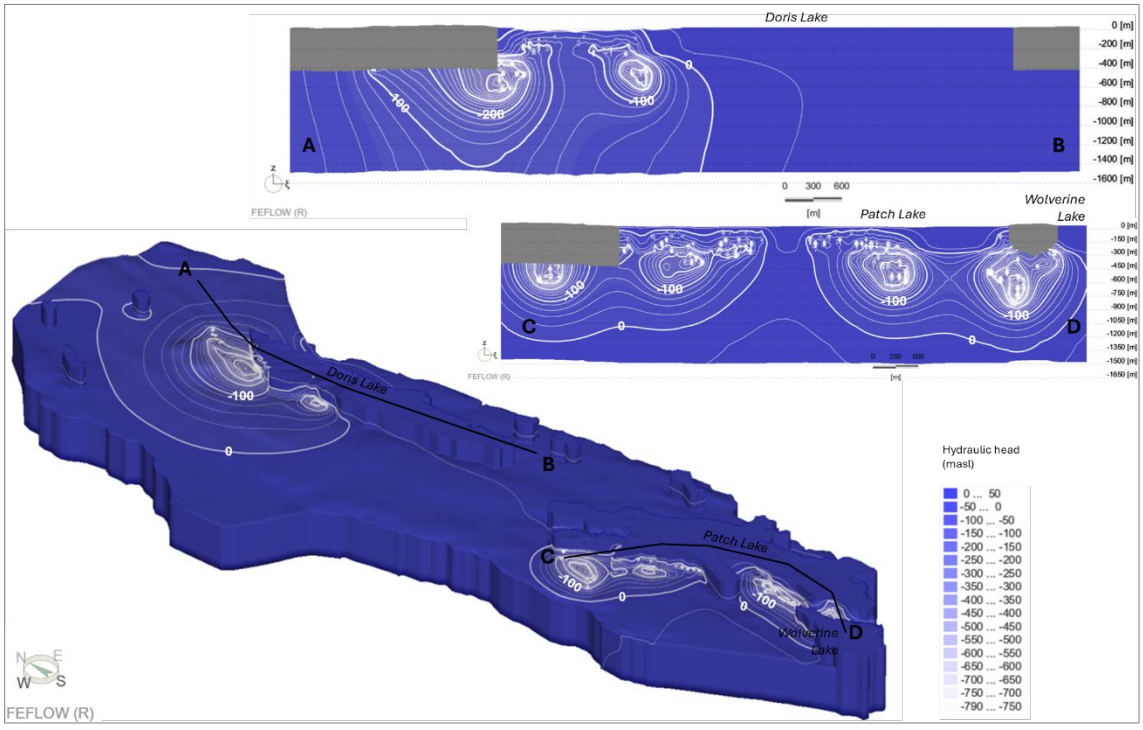


Source: HB2024_2-ModelResultsCalib.xlsx

Figure 6-3: Modelled vertical profile of chloride concentrations for baseline conditions

6.2 Mining Conditions

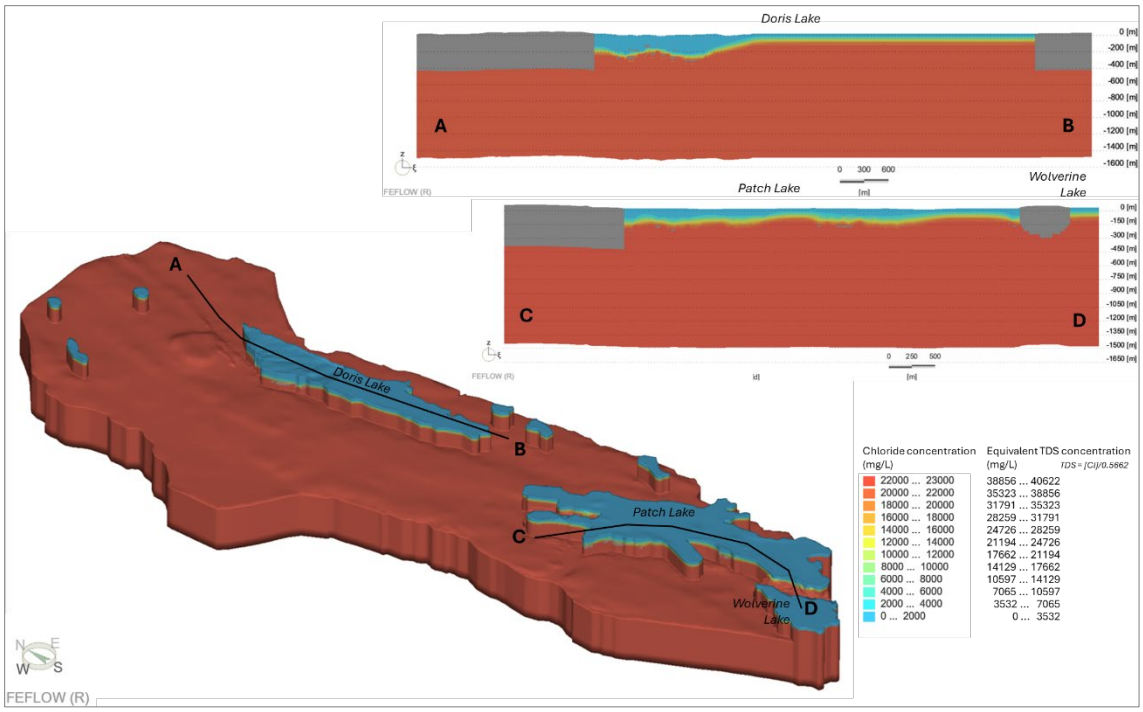
Figure 6-4 and Figure 6-5 show the modelled hydraulic heads and chloride concentrations at the end of mine (i.e., end of year 2043). Groundwater flow and mass balance of the simulation were reasonable; flow imbalance <0.1% and mass <10% until mid-2020, then 10 to 15% except for the period 2024-2029 between 16 and 23% and 2044-2046 between 16 and 17%. Some oscillations occurred at distance from the mine dewatering areas, but predictions remained stable.



Source: fig_mdl_eom_head_rev1.pptx, HB2024_3DgwMdl_04-01m_rev3_histFutrMng_[03-27m_rev1]_trsnt.dac

Figure 6-4: Modelled groundwater heads at end of mine

Note: Permafrost elements are not shown in the 3D view.



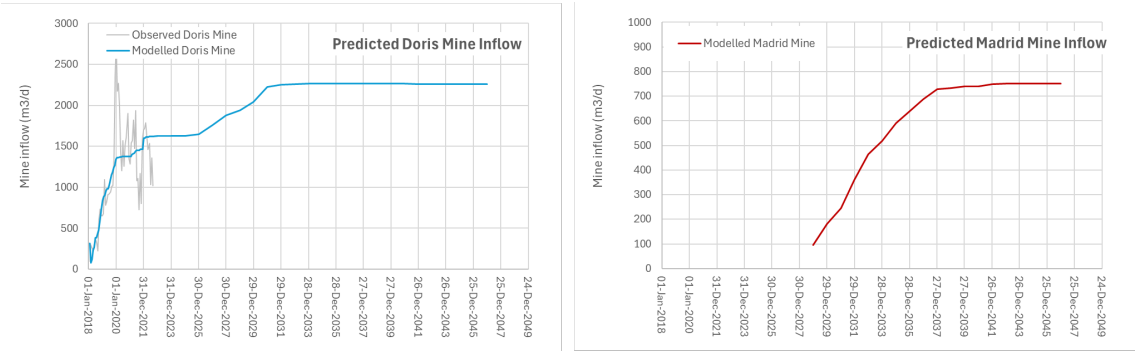
Source: fig_mdl_eom_head_rev1.pptx, HB2024_3DgwMdl_04-01m_rev3_histFutrMng_[03-27m_rev1]_trsnt.dac

Figure 6-5: Modelled chloride concentrations at end of mine

Note: Permafrost elements are not shown in the 3D view.

6.2.1 Mine Inflows

Figure 6-6 plots the modelled average inflow rates during operations. The model forecasts a maximum inflow of 2,260 m^3/d in 2031 at Doris, and 750 m^3/d in 2039 at Madrid. As discussed in Section 5.4.1, the model captures the overall trend of mine inflows and not suitable to predict temporary inflow events from discrete structures. Based on history of inflows at Doris, additional inflows between 100 m^3/d to 600 m^3/d could occur for periods of 2 to 8 months.



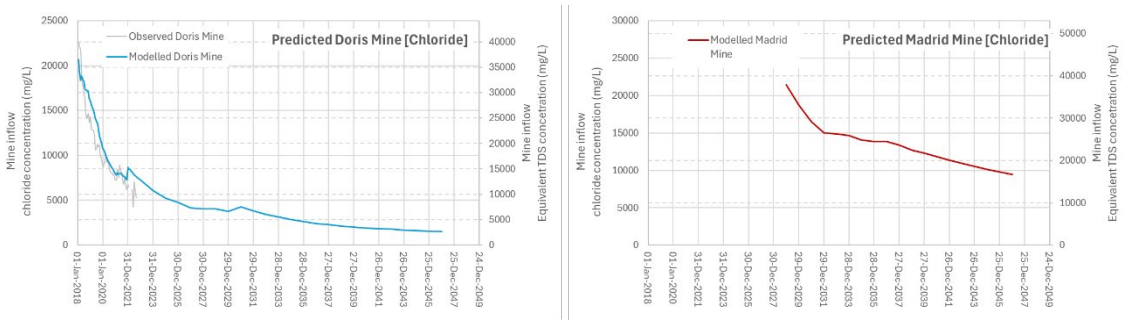
Source: HB2024_3-ModelResultsPredictions_04-01m_rev3.xlsx

Figure 6-6: Modelled mine inflows during operations

6.2.2 Mine Inflow Quality

Figure 6-7 plots the modelled chloride concentrations during operations. The model forecasts a progressive dilution of the chloride concentration with freshwater infiltration from the lakes. At

end of mining, chloride concentrations are lowered to about 1,500 mg/L at Doris, and 9,500 mg/L at Madrid (i.e., equivalent TDS concentrations of 2,650 and 16,780 mg/L respectively).

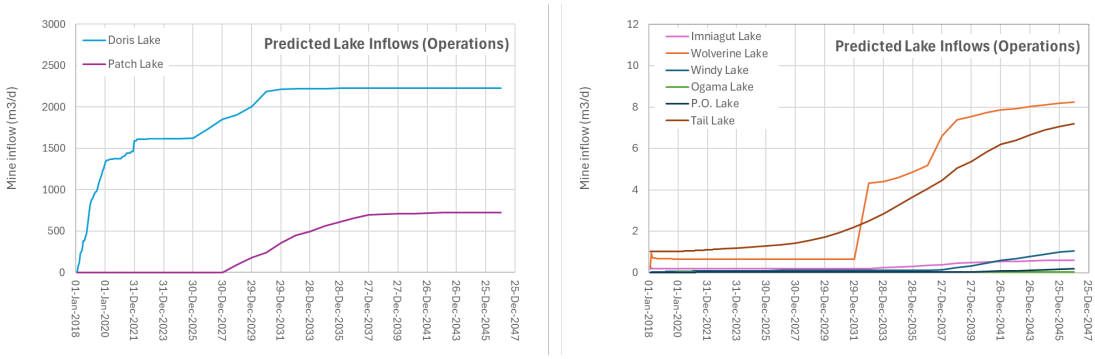


Source: HB2024_3-ModelResultsPredictions_04-01m_rev3.xlsx

Figure 6-7: Modelled chloride concentrations during operations

6.2.3 Lake Infiltrations

Figure 6-8 plots the modelled infiltration rates from the main lakes. The model forecasts a progressive increase of freshwater infiltration from the lakes over time. Changes to lake infiltration are greater for the lakes located directly above the mines: Doris Lake, Patch Lake, and Wolverine Lake.



Source: HB2024_3-ModelResultsPredictions_04-01m_rev3.xlsx

Figure 6-8: Modelled lake infiltration during operations

6.3 Closure Conditions

Mine Reflood Time Estimation

At Closure, mine dewatering will be deactivated and the mine areas allowed to flood. The duration of the reflood period will be a function of inflow rate, the volume of the mine void and equilibration of pressures to a state similar to pre-mining conditions in the surrounding rock mass. Time to re-flood incorporating the mine void were estimated using an exponential decay function, the predicted mine inflow rates, and the void volumes of the mine workings including backfill; equation (2):

(2) $\Delta h_r(t) = \Delta h_{eom}\, e^{-t\frac{Q_{eom}}{V_{mine}}}$

Where $\Delta h_r(t)$, final reflood time to the reflood level (calculation in days, then converted to years)
Δh_{eom}, drawdown at end of mining (maximum mine depth; meters)
Q_{eom}, inflow rate at the end of mining (m^3/d)
V_{mine}, effective mine volume to reflood (total void minus backfill; m^3)
t, time since end of dewatering (days)

Effective volume of the mine at the end of operations (V_{mine}) was estimated based on the proposed mine plan and backfill volumes. Mine volumes were estimated from annual mine plans using MineSight 3D and Rhino 3D. Backfill volumetric quantities were based on the LOM plan assuming a bulk density of 1,990 kg/m^3. Estimated volumes rounded to the nearest 1,000 m^3 are listed in Table 6-2.

Table 6-2: Mine volumes used for reflood estimates

Component	Unit	Doris	Madrid
Total Mine Void	m^3	2,824,000	13,973,000
Backfill Volume	m^3	1,671,000	9,325,000
Unfilled Volume	m^3	1,153,000	4,648,000
Unfilled Volume	% of Total	41%	33%

Source: CAPR003296_DorisMadrid-reflood_calculations_REV01.xlsx

Table 6-3 compiles the input parameters and reflood time estimations for the proposed mine areas based on Base Case calibrated model. The significant difference in reflood time between the Doris and Madrid areas reflects the significantly larger open mine volume at Madrid, combined with significantly lower inflow rate compared to Doris.

Table 6-3: Base Case reflood time estimations

Parameters	Unit	Doris	Madrid
V_{mine}	m^3	1,153,000	4,648,000
Δh_r[1]	mbgs	50	30
Δh_{eom}	mbgs	680	635
(Q_{eom})	m^3/d	2,260	750
t_1 reflood	year	4	52

Source: CAPR003296_DorisMadrid-reflood_calculations_REV01.xlsx

Note:
[1] Reflood level defined as top of mine void, thus values reflect crown pillar thickness below lake level.

6.4 Post-Closure Conditions

Final Receptors

Once the mine voids are reflooded and groundwater conditions have re-equilibrated, the groundwater flow system will return to a state similar to pre-mining conditions. Water in contact with mine areas will move in a down gradient direction.

At Doris, the model forecasts groundwater will flow towards Doris Lake, towards lake #8 to the west, and towards Roberts Bay to the north. At Madrid, the model forecasts groundwater will flow towards Patch Lake, as well as westwards towards Windy Lake and Wolverine Lake. While flow directions are towards lakes, the travel times are very long. Assuming parameters used in the Base Case calibrated model, no particles are predicted to have reached these lakes after 1,000 years.

6.5 Sensitivity to Model Parameters

Additional scenarios were completed to assess the effects of parameter uncertainties on the calibration and forecasts of mine inflow, mine water quality, lake infiltrations, and reflood period at Closure. The goal was to evaluate the impact of key parameters, providing a basis for understanding the robustness and limitations of the groundwater flow model under different conditions. This information is important for decision-making and model refinement, ensuring the model accurately represents the hydrogeological system.

6.5.1 Sensitivity Scenarios

Sensitivity scenarios are listed below by category:

Permafrost Model (P)

- P1: The depth of the sub-permafrost is raised by about 90 m.
- P2: The depth of the sub-permafrost is raised by about 180 m.
- P3: Mining zones where permafrost has been rated as "uncertain" are assumed part of the open taliks (unfrozen).
- P4: The permafrost model is modified to place the contacts between permafrost and open taliks approximately 100 m inland from shorelines.

Permeable Structures (S)

- S: Hypothetical permeable ($K=1x10^{-6}$ m/s) geological structures, approximately five-metre-thick, intercept the Doris and Madrid mines (Figure 6-9). At Doris, the structure is hypothesised to match the upper diabase dyke. At Madrid, the structure is hypothesised to match the MDZ eastern wall.

Hydraulic Conductivities (K)

- K1: Hydraulic conductivity is increased by one order of magnitude in the overburden unit (K_{ovb} = 1x10^{-7} m/s).
- K2: Hydraulic conductivity is decreased by one order of magnitude in the overburden unit (K_{ovb} = 1x10^{-9} m/s).
- K3: Hydraulic conductivity is increased globally by one order of magnitude in bedrock.
- K4: The contrast of hydraulic conductivity between the upper and lower bedrock is increased by 50% (Figure 6-10).
- K5: The contrast of hydraulic conductivity between upper and lower bedrock is decreased by 50% (Figure 6-11).
- K6: The hydraulic conductivity profile is cutoff with a low value of 1x10^{-9} m/s (i.e., typical limit of testing equipment, Figure 6-12).
- K7: The hydraulic conductivity profile applied at Doris is applied to Madrid.

Storage Compressibility (Sx)

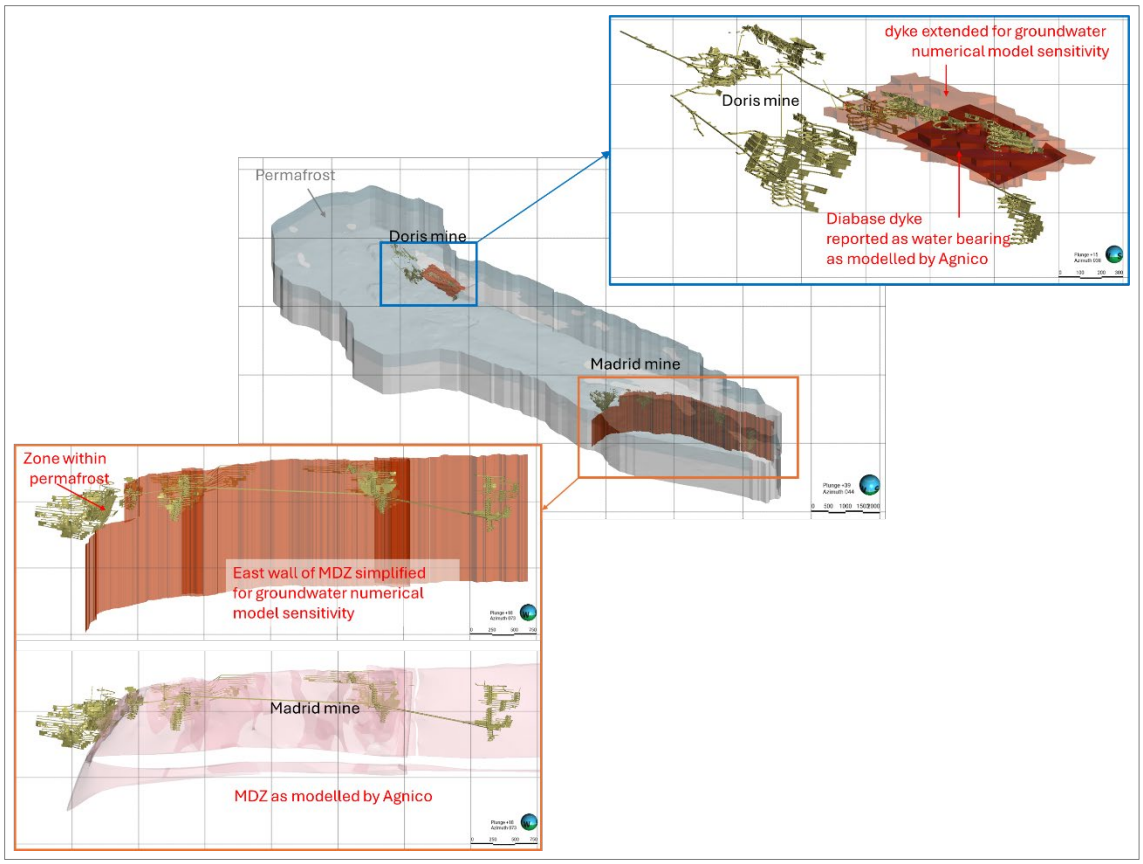
- Sx1: Storage compressibility is increased by one order of magnitude in overburden (Sx_{ovb} = 1x10^{-4} m/s).
- Sx2: Storage compressibility is decreased by one order of magnitude in overburden (Sx_{ovb} = 1x10^{-6} m/s).
- Sx3: Storage compressibility is increased by one order of magnitude in bedrock. (Sx_{bdr} = 3x10^{-6} m/s).
- Sx3: Storage compressibility is decreased by one order of magnitude in bedrock. (Sx_{bdr} = 3x10^{-8} m/s).

Density Dependent Flow Assumption (D)

- D1: Water density is not accounted for (density ratio = 0)
- D2: Higher density ratio based on 69 mg/L at surface and 35,000 mg/L at depth.

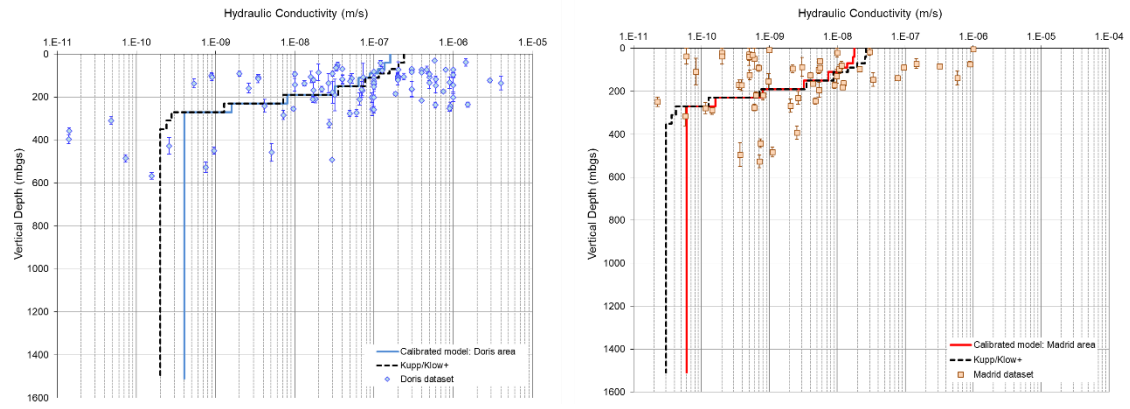
Worst Case Scenario (W)

- W: The hydraulic conductivity profile applied at Doris is applied at Madrid; mining zones where permafrost has been rated as "uncertain" are assumed part of the open taliks (unfrozen); the permafrost model assumes contacts between permafrost and open taliks are approximately 100 m inland from shorelines; and the calibrated hydraulic conductivities are cutoff to a lower limit of 1x10^{-9} m/s.



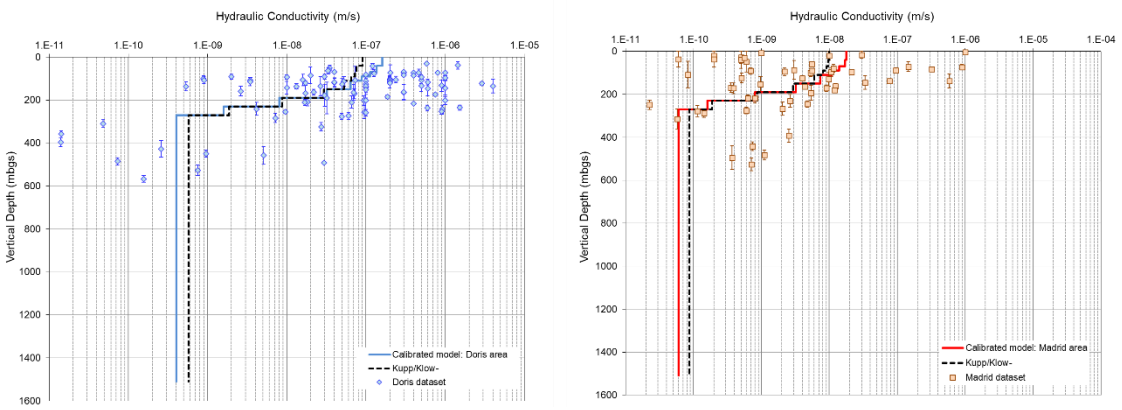
Source: fig_mdl_svy_structure.pptx

Figure 6-9: Modelled structures



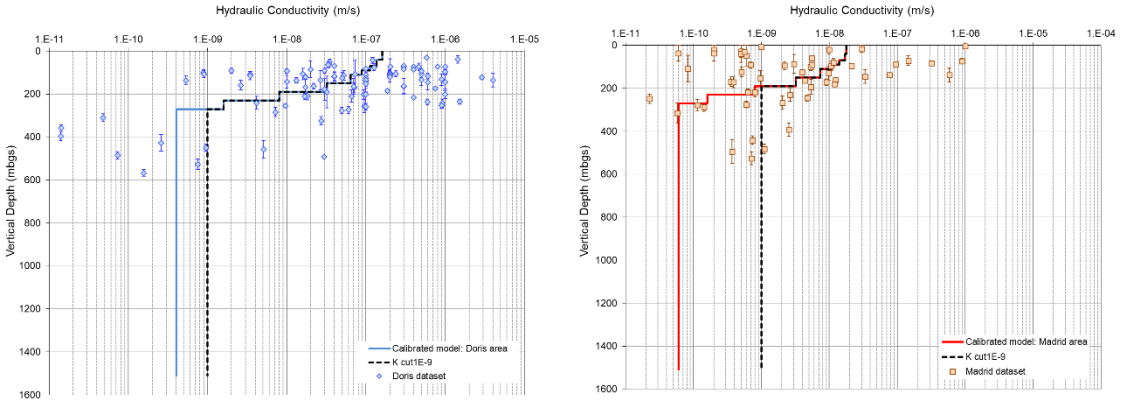
Source: HopeBay_MASTER_HydrProperties_gf_20241120.xlsx

Figure 6-10: Sensitivity K profiles: higher contrast between upper and lower bedrock



Source: HopeBay_MASTER_HydrProperties_gf_20241120.xlsx

Figure 6-11: Sensitivity K profiles: lower contrast between upper and lower bedrock



Source: HopeBay_MASTER_HydrProperties_gf_20241120.xlsx

Figure 6-12: Sensitivity K profiles: 1x10^{-9} m/s cutoff value

6.5.2 Sensitivity Ratings

The sensitivity of each scenario was rated as either significant or not significant according to the thresholds defined in Table 6-4, then classified into sensitivity types as defined by Brown (1996) and presented below.

Type I: There are no significant effects for both model calibration and predictive model results. In other words, within a reasonable range of parameter values, the model outcomes are not significantly affected. This parameter type does not need further data collection or monitoring. Type I sensitivities are of little concern because the impact on predictions is insignificant.

Type II: There is a significant effect on model calibration, but no significant effect on predictive model results (relative to modelling objectives). The model calibration is affected so the parameter has an effect on the calibration goodness of fit. However, the results of the predictive model are still insensitive to this parameter. Type II sensitivities are of little concern because the impact on predictions is insignificant.

Type III: There are significant effects on both model calibration and model prediction results. The parameter has an effect on the calibration goodness of fit and a corresponding effect on the predictive model results. Type III sensitivity is of concern only for an uncalibrated model, or where a wide range of calibrations are possible, and proper calibration of this parameter is the solution. The sensitivity is important, but it is known and can be avoided by model calibration.

Type IV: There is no significant effect on model calibration, but a significant effect on predictive model results. The model calibration is not affected and does not help constrain this parameter value, while the results of the predictive model are sensitive to this parameter. Type IV sensitivity is cause for concern because of the non-uniqueness. The model input may allow for a range of valid calibrations, but the choice of value significantly impacts model prediction. It is important to determine the actual value of this parameter and not rely on model calibration to estimate this parameter. It should be measured with robust data.

Table 6-4: Definitions and significance thresholds for sensitivity models

Definition	Calibration	Predictions
Information evaluated	• Mine inflow rate at the end of year 2022. • Mine inflow chloride concentration at the end of year 2022.	• Average annual mine inflow rate at EOM (2046). • Average annual mine inflow chloride concentration at EOM (2046) • Infiltrations for the Doris Lake, Patch Lake, and Wolverine Lake at EOM (2046). • Mine closure reflood time.
Significant Change	• +/- 300 m^3/d variations to mine inflows compared to observed (i.e., approximately 10% of the modelled base case total inflows for the Project). • +/- 20% variations to chloride concentrations compared to observed.	• +/- 300 m^3/d variations compared to modelled base case (i.e., approximately 10% of the modelled base case total inflows for the Project). • +/- 20% variations to mine inflow chloride concentration compared to modelled base case. • +/- 10% and greater than 0.5 m^3/d variations to lake infiltration rates compared to modelled base case. • +/- 5-year variations to reflood time compared to modelled base case.

6.5.3 Results

Table 6-5 lists results from sensitivity model runs categorized into sensitivity type III and IV. Some parameters were either not sensitive to both calibration and predictions (Type I), sensitive to both calibration and predictions (Type III), or not sensitive to calibration but sensitive to predictions (Type IV). Parameters showing significant effects on both calibration and prediction results (Type III) or prediction alone (Type IV) require careful consideration.

Key observations are:

Type I sensitivities: Models in this category had changes to both calibration and predictions but less than the defined significance thresholds.

- P1, P3 included a change to depth of the base of permafrost. Since most of the future mining occurs within the Doris Lake or Patch Lake taliks, permafrost boundaries at distance from the mines would not be expected to have a significant effect on flow; results also indicate minimal effect on chloride concentration.
- Sx1 and Sx2 changed storage compressibility in the lakebed sediment. Results suggest that pressure changes from dewatering (thus water release from overburden storage) do not extend significantly into the lakebed (this does not mean leakage does not occur, just that it is not sensitive to storage compressibility).
- Sx4 simulated a decreased storage compressibility in bedrock. Results show predictions are not particularly sensitive to lower storage compressibility in bedrock.
- D1 and D2 related to water density. Results show predictions are not particularly sensitive to density. Changes to chloride concentrations were minimal, likely because the flow system was not significantly affected.

Type II sensitivities: There were no models in this category, with significant effect on calibration but not predictions.

Type III sensitivities: Models in this category have significant effects on both model calibration and model prediction.

- Scenarios K1, K2, K3 and K4 fall in this category, and all reflect changes in hydraulic conductivity, of lakebed sediment or bedrock. Significant sensitivities are seen for both flow and chloride concentration. The largest changes in flow occurred for K1 and K3, both of which reflect increases in K, for lakebed sediment and bedrock, respectively; K3 shows the most significant increase in flow for any sensitivity run and reflects that model results are most sensitive to this assumption. Chloride concentrations responded inversely to flow, decreasing for sensitivity runs that indicate increase in flow and increasing for sensitivity runs that indicate decrease in flow. This relationship is a function of increased flow from shallower, lower concentration waters when K is higher and higher leakage from overlying lakes. The uncertainty on K assumptions is reduced by the fact that modelled hydraulic conductivity fields are well aligned with Project data and calibrated to the historical records of mine inflows and chloride concentrations at Doris.
- The structures simulating hypothetical permeable conduits in the Scenario S influence both the model calibration and predictions. At End-Of-Mine, the inflows are increased to 2,780 m^3/d at Doris and 2,810 m^3/d at Madrid. Chloride concentrations respond inversely to flow at Madrid, decreasing to 4,560 mg/L. Concentrations at Doris are not affected significantly.

Type IV sensitivities: Models in this category have no significant effect on model calibration, but a significant effect on model prediction; these sensitivities are considered the most important because the parameter variation cannot be constrained by model calibration and accurate input is data is needed.

- Scenarios related to permafrost, P2 and P4 only showed changes for leakage from Imniagut Lake and Wolverine Lake, suggesting permafrost assumptions influenced predictive outcomes for these lakes.
- Scenarios K5, K6 and K7 reflect changes in K contrast between shallow and deep bedrock, a low K cutoff of $1x10^{-9}$ m/s (testing instrument limits) or the relatively high calibrated K for Doris applied to Madrid. With the exception of K7 (calibrated K for Doris applied to Madrid) change to flow was not significant but change to inflow chloride concentration was, at both Doris and Madrid areas. These models also had significant changes on leakage from lakes.
- Scenario K7 highlights the potential effect of higher K at Madrid. K in the Base Case model was set to match Madrid data, which has on average lower K than Doris; increasing K at Madrid to match the average at Doris has a significant effect on predicted inflow.
- Scenarios Sx3 (storage compressibility in bedrock) affected leakage from Wolverine Lake, but not to the same degree as models K5, K6 and K7.
- Scenario W is a “worst case” scenario combining changes to the most conservative assumptions for the permafrost and bedrock hydraulic conductivity field at Madrid. It resulted in increased flow at Madrid, a subsequent decrease in chloride concentration (significantly greater leakage from Patch Lake) and also large increases in leakage from Imniagut and Wolverine lakes. Results again indicate sensitivity to K, but not in a way that would affect model calibration; K in the Madrid area is not as well constrained as in the Doris area.

Reflooding durations in Doris were not sensitive to parameter changes. Sensitivity K3 (global increase in K by one order of magnitude) does decrease the time to reflood Doris by a factor of five, but not technically within the selected sensitivity threshold. The reflood duration for the Base Case is significantly longer for Madrid (50 years) than Doris (4 years) due to a larger open area and lower inflow. Increasing K, thus increasing inflow can significantly shorten the time to reflood (K3, K7 and W), as expected.

Sensitivity results clearly indicate that model calibration and predictions are affected by K assumption, and subsequently have an effect on predicted chloride concentrations. Such K changes can be in either bedrock or lakebed sediments, or by the assumed location of the boundary with permafrost (though not as significantly as bedrock K in general). This is generally consistent with results of modelling for many other projects and can be particularly important at Hope Bay when considering that mining occurs underneath lakes.

There was no specific sensitivity model run to address the potential for flow from drillholes, as this is generally more uncertain than other parameters, but this is discussed in Section 6.6.

Table 6-5: Sensitivity Results

ID	Description	Calibration		Predictions												Sensitivity Ratings		
		End of 2022 Mine Inflow		End of Mine 2046 Mine Inflow			End of Mine 2046 UG [Cl]			End of Mine 2046 Lake Infiltrations				Closure		Ratings		Type
		Flow (m^3/d)	[Cl] *(TDS)* [a] (mg/L)	Total inflow (m^3/d)	Doris inflow (m^3/d)	Madrid inflow (m^3/d)	Total [Cl] *(TDS)* [a] (mg/L)	Doris [Cl] *(TDS)* [a] (mg/L)	Madrid [Cl] *(TDS)* [a] (mg/L)	Doris Lake (m^3/d)	Patch Lake (m^3/d)	Imniagut Lake (m^3/d)	Wolverine Lake (m^3/d)	UG reflood Doris (year)	UG reflood Madrid (year)	Calibration (S/NS)	Prediction (S/NS)	
-	Base case model	1621	7644 *(13501)*	3014	2262	752	3492 *(6167)*	1509 *(2665)*	9457 *(16703)*	2231	727	0.6	7.8	3.6	51.6	-	-	-
P2	Depth of subpermafrost raised by about 180m	1639	7796 *(13769)*	3047	2287	760	3658 *(6461)*	1729 *(3054)*	9465 *(16717)*	2246	730	**1.7**	8.3	3.6	51.1	NS	**S**	IV
P4	Contacts between permafrost and open taliks approx. 100 m inland from shorelines.	1714	7685 *(13573)*	3211	2383	827	3750 *(6623)*	1726 *(3048)*	9581 *(16922)*	2354	795	**2.1**	**14.1**	3.5	47.0	NS	**S**	IV
S	Structures intercepting the mines x simulated as potential conduits	**2184**	7694 *(13589)*	**5595**	**2782**	**2812**	3038 *(5366)*	1499 *(2647)*	**4561** ***(8055)***	**2749**	**2765**	0.4	**8.6**	3.8	**6.9**	**S**	**S**	III
K1	Hydraulic conductivity increased in overburden (K_{ovb} = 1x10^{-7} m/s)	**2220**	**5240** ***(9255)***	**4030**	**3217**	813	**2490** ***(4398)***	**949** ***(1676)***	8586 *(15164)*	**3187**	788	0.6	7.8	2.6	47.8	**S**	**S**	III
K2	Hydraulic conductivity decreased in overburden (K_{ovb} = 1x10^{-9} m/s)	**966**	**12488** ***(22056)***	**1847**	**1273**	574	**6140** ***(10844)***	**3302** ***(5832)***	**12434** ***(21960)***	**1238**	**546**	0.6	7.4	6.5	**67.7**	**S**	**S**	III
K3	Hydraulic conductivity increased globally by one order of magnitude in bedrock	**9608**	**2818** ***(4977)***	**18329**	**12656**	**5673**	**1650** ***(2914)***	**1013** ***(1789)***	**3070** ***(5422)***	**12399**	**5501**	**8.0**	**81.7**	0.7	**6.8**	**S**	**S**	III
K4	Contrast of hydraulic conductivity between the upper and lower bedrock increased by 50%	**1995**	6497 *(11475)*	**3709**	**2740**	970	2856 *(5044)*	**1078** ***(1904)***	7881 *(13919)*	**2717**	**926**	0.7	**9.5**	3.0	**40.1**	**S**	**S**	III
K5	Contrast of hydraulic conductivity between the upper and lower bedrock decreased by 50%	1474	8453 *(14929)*	2899	2106	793	**4992** ***(8817)***	**2243** ***(3961)***	**12292** ***(21710)***	2042	690	**1.5**	**10.8**	3.9	49.0	NS	**S**	IV
K6	hydraulic conductivity profile is cutoff with a low value of 1x10^{-9} m/s	1631	7736 *(13663)*	**3350**	2329	1021	**5451** ***(9627)***	**2135** ***(3771)***	**13015** ***(22987)***	2261	**894**	**5.7**	**30.9**	3.5	**38.0**	NS	**S**	IV
K7	hydraulic conductivity profile applied at Doris applied to Madrid	1621	7644 *(13501)*	**7223**	2262	**4960**	**2402** ***(4242)***	1513 *(2672)*	**2808** ***(4959)***	2231	**4857**	**4.4**	**60.2**	3.6	**7.8**	NS	**S**	IV
Sx3	Storage compressibility is increased in bedrock (Sx_{bdr} = 3x10^{-6} m/s)	1625	7644 *(13501)*	3037	2273	763	3583 *(6328)*	1588 *(2805)*	9521 *(16816)*	2226	720	0.3	**6.6**	3.6	50.9	NS	**S**	IV
W	Worst case: combination of scenarios P3, P4, K6 and K7	1724	7771 *(13725)*	**8295**	2465	**5830**	3259 *(5756)*	**2432** ***(4295)***	**3609** ***(6374)***	2402	**5599**	**25.1**	**133.7**	3.3	**6.7**	NS	**S**	IV

Source: HB2024_4-ModelResultsSummaryReport.xlsx

Note:

[a] Equivalent TDS concetration calculated using equation [TDS] = [Cl] / 0.5662 (See Section 3.9.2)

A value in bold red font indicates the modelled result is above the criteria listed in Table 6-4.

GWL, groundwater level; UG, underground

NS, Not Significant; S, Significant.

6.6 Sensitivity to Flow from Exploration Drillholes

As noted previously, there are a significant number (>1000) of drillholes into the ore bodies that represent potential flow conduits. Uncertainties exist regarding flow potential, either as direct connections between the lake and the mine, or as small-scale, local connectors between fractures that can influence bulk K. Most surface holes should have been plugged using a method that involved setting a Van Ruth–type plug approximately 35 m into bedrock and then emplacing cement on top of the plug, but a certain number are also known to have not been cemented or have no written records of methods for cementing; nor are there as-built-type descriptions of what was actually done. In 2017, SRK had estimated that the Madrid prefeasibility mine layouts had a more than 50% probability to intercept old open exploration holes in the north area (Naartok East), and a low probability in the south area.

Predicting likelihood of any given drillhole to act as a connector to surface (or a lake) is difficult and can be best addressed through management planning for such events. Observations from mining at Doris suggest the likelihood for such an event is low but possible. The scale of inflow that could be encountered is indicated by the September 2018 inflow event at Doris, when workings intercepted an un-grouted surface exploration hole producing an averaged flow on the order of 3,650 m^3/d until it was plugged in Oct.2018. While this event happened despite efforts to proactively identify zones where such intercepts can occur, it showed Operators were able to divert, manage and stop the inflow from that hole within a relatively short time.

7 Conclusions

This study reviewed hydrogeological data to update the groundwater conceptual model and refine estimates of groundwater inflow and chloride concentrations in alignment with the updated Hope Bay mine plan. The objective was to support the ongoing environmental permitting process, provide a basis for assessing the mine's effects on the groundwater environment, and supply inputs to the updated Project Water and Load Balance. The level of detail, methods, and quality of the hydrogeological data supporting the conceptual and numerical models were deemed adequate for these purposes.

The system is conceptualized as a low-flow, lake-dominated, confined flow system. The widespread, deep permafrost is essentially impermeable. Groundwater flow and connections between surface and deep bedrock groundwater systems occur exclusively in areas where lakes are associated with open taliks or in sub-permafrost zones. The primary controls on the groundwater system are the hydraulic conductivities of the overburden and bedrock, and the 3D geometries of permafrost and open taliks. K measurements for lake sediments and fractured rock fall within the bounds of published K values. The lakebeds are draped with fine sediments characterized with an average low K of $1x10^{-8}$ m/s. The fractured rock is characterized by K ranging between $<1x10^{-9}$ m/s and $4x10^{-6}$ m/s, with a higher K geomean at Doris than at Madrid, $5x10^{-8}$ m/s and $2x10^{-9}$ m/s respectively. Clear distinction between bedrock lithologies or geological structures are not observed, at least not consistently. At the project scale, fractured rock is treated as a single unit, with relatively higher K at shallow depths, gradually decreasing with depth due to increasing confining pressure. Groundwater is brackish to saline and can have

elevated concentrations of major ions and metals. The dissolved constituents of concern, when looking at potential discharges of groundwater to the environment, are ammonia, boron, cadmium, chloride, fluoride, iron, manganese, nickel, selenium, sulfate and zinc. The concentrations of chloride show a general trend of increasing concentration with depth; other constituents do not correlate with depth.

The dewatering activities during underground operations will alter groundwater flow gradients. Depressurization around parts of mines located within taliks or sub-permafrost will extend radially, drawing potential upward and lateral saline flow from the talik, and downward freshwater flow from the lakes above. The low permeability of the fine sediments present at the bottom of lakes will limit downward infiltrations. Initially, the salinity of the mine inflows will reflect the saline conditions of the surrounding groundwater system. Over time, as the dewatering expands, more freshwater from shallower zones will be mobilized and inflows will become progressively less saline. While the mine may intercept geological structures or fractures, historical observations of inflow during the development of the Doris mine suggest they will have limited storage capacity and be more likely connected to deep saline groundwater rather than directly to the lakes above.

At Closure, dewatering activities will stop. Re-flooding will result in a slow re-equilibration to baseline conditions, driven by the lakes' gradients and density gradients. At Post-closure, the groundwater system will have returned to the same conditions as baseline with local influences on flow and groundwater quality immediately around the mines.

The groundwater numerical model constructed by SRK was calibrated to the mine inflow rates, and chloride concentrations observed during the 7-years of underground operations at Doris. The calibrated model resulted in reasonable model fit to the observations. The calibrated model predicted the following:

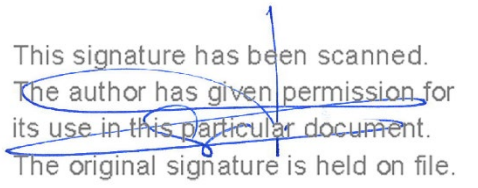
- A maximum annual average inflow of 2,260 m^3/d in 2031 at Doris, and 750 m^3/d in 2039 at Madrid.
- The model captures the overall trend of mine inflows, but not temporary inflow events from discrete structures. Additional inflows between 100 m^3/d to 600 m^3/d could occur for periods of 2 to 8 months based on the historical mine inflow records of Doris.
- Dilution of inflow chloride concentration over time due to freshwater infiltration from the lakes. At End-Of-Mine, chloride concentrations are about 1,500 mg/L at Doris, and 9,500 mg/L at Madrid (i.e., equivalent TDS concentrations of 2,650 and 16,780 mg/L respectively).
- An increase in freshwater infiltration from lakes over time with greater changes for the lakes located directly above the mines: Doris Lake, Patch Lake, and Wolverine Lake.
- At Closure, underground reflood periods of 4 years at Doris and about 50 years at Madrid.
- At Post-Closure, the groundwater flow system will return to a state similar to pre-mining conditions. The model forecasts groundwater will flow very slowly towards the lakes in

close proximity and towards Roberts Bay to the north. No particles are predicted to have reached surface water bodies after 1,000 years.

The analysis of the model's sensitivity to parametrization showed model calibration and predictions were sensitive to changes in hydraulic conductivity of lakebed sediment or bedrock. These are considered sufficiently constrained by the field data and calibration to current conditions for Doris, but can affect predictions:

- Permafrost variations can influence the predicted leakages for Imniagut Lake and Wolverine Lake.
- Changes in K contrast between shallow and deep bedrock, or a low K cutoff of $1x10^{-9}$ m/s (testing instrument limits) have limited effects on the predicted mine inflows but significant influence on chloride concentration at both Doris and Madrid, as well as leakage from lakes.
- Madrid has less K data than at Doris, but also a lower average than at Doris. Using the Doris K profile (which was calibrated to operational data) at Madrid resulted in significantly higher predicted inflow, but lower chloride concentration due to increased infiltration from Patch Lake.
- The "worst case" scenario combined the most conservative assumptions for the permafrost and hydraulic conductivity field in bedrock at Madrid. This model also resulted in increased flow at Madrid, a subsequent decrease in chloride concentration and a large increases in leakage from Imniagut and Wolverine lakes.
- Models did not explicitly assess the potential for mine inflow from unplugged surface drillholes, either as direct connection to lakes, or as small-scale, local connectors between fractures. Observations from Doris operations indicate an un-grouted surface exploration hole could produce an average flow of about 3,650 m^3/d. Predicting likelihood of any given drillhole to flow is difficult, but Operators were able to divert, manage and stop inflow from the hole within a relatively short time.

This report, 2024 Hydrogeological Modeling Update, was prepared by



Gregory Fagerlund, MSc., PGeo.
Associate Geologist

and reviewed by



Daniel Mackie, MSc. PGeo (BC)
Principal Consultant, Canada GeoEnvironmental
Practice Lead

All data used as source material plus the text, tables, figures, and attachments of this document have been reviewed and prepared in accordance with generally accepted professional engineering and environmental practices.

SRK Consulting (Canada) Inc. Engineers and Geoscientists BC Permit to Practice No: 1003655

Disclaimer—SRK Consulting (Canada) Inc. has prepared this document for Agnico Eagle, our client. Any use or decisions by which a third party makes of this document are the responsibility of such third parties. In no circumstance does SRK accept any consequential liability arising from commercial decisions or actions resulting from the use of this report by a third party.

The opinions expressed in this document have been based on the information available to SRK at the time of preparation. SRK has exercised all due care in reviewing information supplied by others for use on this project. While SRK has compared key supplied data with expected values, the accuracy of the results and conclusions from the review are entirely reliant on the accuracy and completeness of the supplied data. SRK does not accept responsibility for any errors or omissions in the supplied information, except to the extent that SRK was hired to verify the data.

8 References

Agnico Eagle, 2022. Hydro Reports and groundwater monitoring data package

Agnico Eagle, 2024. Hope Bay updated mine plan. Provided by Agnico Eagle.

Beale, G. and J. Read, 2014. Guidelines for Evaluating Water in Pit Slope Stability. CRC Press.

Burn CR. 2002. Tundra lakes and permafrost, Richards Island, western Arctic coast, Canada. Canadian Journal of Earth Sciences 39: 1281–1298.

Burn CR. 2005. Lake-bottom thermal regimes, western arctic coast, Canada. Permafrost and Periglacial Processes 16: 355–367.

Cumberland Resources Ltd., 2005. Meadowbank Gold Project: Final Environmental Impact Statement.

De Beers Canada Inc. 2002. Snap Lake Diamond Project: Environmental Assessment Report. Submitted to the Mackenzie Valley Review Board. Feb. 2002.

De Beers Canada Inc. 2010. Gahcho Kue Project: Environmental Impact Statement. Dec. 2010.

Dyke, A.S., and Prest, V.K. 1986. Late Wisconsin and Holocene retreat of the Laurentide Ice Sheet. Geological Survey of Canada, Map 1702A

Dyke, A.S., and Dredge, L.A. 1989. Quaternary Geology of the Northwestern Canadian Shield. In Quaternary Geology of Canada and Greenland. Ed. R.J.Fulton. Ottawa: Geological Survey of Canada.

EBA. 1996. Report on the Boston Gold Project. Surficial geology and Permafrost features. Prepared for Rescan Environmental Services Ltd. Vancouver, BC.

Frape, S., & Fritz, P., 1987. Geochemical trends for groundwater from the Canadian Shield, in saline water and gases from crystalline rocks. Geological Association of Canada Special Paper, 33, 19-38.

Gacoyne M., 2003. Hydrogeochemistry, groundwater ages and sources of salt in a granitic batholith on the Canadian Shield, southeastern Manitoba. Applied Geochemistry 19 (2004) 519-560.

Golder Associates Inc., 2013. Meliadine Draft Environmental Impact Statement - Volume 7 Freshwater Environment - Appendix 7.2-A Groundwater Quality Baseline Report.

Golder Associates Inc., 2014. Hydrogeology Baseline Report for the Jay Project. Sep. 2014.

Hydro-Ressources Inc. (HRI), 2020. Letter from Julien Cameroon to TMAC. Subject: Hydrogeology TMAC. Date: Feb.2nd 2020.

Hydro-Ressources Inc. (HRI), 2021. Letter from Philemon Desrochers-Gagnon to Agnico Eagle. Subject: Mine water control – Hope Bay. Date: Nov.22nd 2021.

Lorax Environmental. 2023a. 2023 Patch Lake Hydrogeological Field Investigation. Technical Memorandum prepared for Agnico Eagle. A674-3. Oct.16, 2023.

Lorax Environmental. 2023b. Westbay Installation 10WBW001 Groundwater Sampling Review. Technical Memorandum prepared for Agnico Eagle. A674-3. Nov.22, 2023.

Lorax Environmental. 2024a. 2022 Hope Bay, Hydrogeological Field Investigation. Technical Memorandum prepared for Agnico Eagle. A674-2. Jan.10, 2024.

Lorax Environmental. 2024b. 2024Patch Lake Hydrogeological Investigation. Technical Memorandum prepared for Agnico Eagle. A674-5. Jul.19, 2024.

Lorax Environmental. 2024c. 2024 Hope Bay Groundwater Sampling Review – Westbay Installation 10WNW001. Technical Memorandum prepared for Agnico Eagle. A674-7. Nov.18, 2024.

Lorax Environmental. 2024d. 2024 Q3 Patch Lake Hydrogeological Investigation. Technical Memorandum prepared for Agnico Eagle. A674-5. Dec.13, 2024.

Lunardini V.J. 1995. Permafrost Formation Time. CRREL Report 95-8, US Army Corps of Engineers, Cold Regions Research & Engineering Laboratory, April 1995.

Minnow Environmental Inc. “2023 Patch Lake Aquatic Baseline”. Report prepared for Agnico Eagle Mines Ltd. Project 237202.0070. Feb. 2023

Rescan Environmental Services Ltd. (Rescan). 2009 Freshwater Fish and Fish Habitat Baseline Report, Hope Bay Belt Project. Vancouver, BC. Report Prepared for Hope Bay Mining Limited. May 2010.

Natural Resources Canada (NRCan). Canadian Permafrost Thickness, Geological Survey of Canada [digital resource: vector]. Natural Resources Canada, 2002. Retrieved from http://geo.scholarsportal.info/#r/details/_uri@=1250329824.

Parez and Fauriel (1988). "Le piézocone améliorations apportées à la reconnaissance de sols." Revue Francaise de Geotech 44: 13-27.

Rescan ERM, 2015. Back River - 2014 Sub-permafrost Groundwater Quality Baseline Report. Jun. 2015.

Smith, M.W. and Hwang, C.T., 1973. Thermal Disturbance Due To Channel Shifting, Mackenzie Delta. N.W.T., Canada; in Proceedings Second International Permafrost Conference, North American Contribution; National Academy of Sciences, Washington, D.C., p51-60.

SRK Consulting (Canada) Inc., 2003. Preliminary Groundwater Inflow Study Doris Crown Pillar. Prepared for: Miramar Mining Corporation. Sep. 2003.

SRK Consulting (Canada) Inc., 2005. Groundwater Assessment, Doris North Project, Hope Bay Nunavut, Canada. Report prepared for Miramar Hope Bay Limited. 1CM014.006. Oct. 2005.

SRK Consulting (Canada) Inc. 2009a. Hope Bay Gold Project Overburden Characterization Report. Prepared for Hope Bay Mining Limited. Project No.: 1CH008.002. Jun. 2009.

SRK Consulting (Canada) Inc. 2009b. Geotechnical and Hydrogeological Assessment for the Boston Open Pit, Nunavut, Canada. Prepared for Hope Bay Mining Limited. Project No. 2CH009.000. Jun. 2009.

SRK Consulting (Canada) Inc. 2009c. Geotechnical and Hydrogeological Assessment for the Madrid Open Pit and Underground, Nunavut, Canada. Prepared for Hope Bay Mining Limited. Project No. 2CH009.000. Jun. 2009.

SRK Consulting (Canada) Inc. 2009d. Geotechnical and Hydrogeological Assessment for the Doris North Open Pit and Doris Central Underground, Nunavut, Canada. Prepared for Hope Bay Mining Limited. Project No. 2CH009.000. Jun. 2009.

SRK Consulting (Canada) Inc., 2011a. Hope bay 2010 Westbay Program Data Report. Report prepared for Hope Bay Mining Limited. 1CH008.013. Feb. 2011.

SRK Consulting (Canada) Inc., 2011b. Groundwater Inflows and Inflow Water Quality for the Revised Doris North Project Water Licence Amendment Package. 2011.

SRK Consulting (Canada) Inc., 2011c. Geochemical Characterization of Lake Sediments and Overburden, Hope Bay Project. Draft Prepared for Hope Bay Mining Limited. 1CH008.043. Apr.2011

SRK Consulting (Canada) Inc., 2012. Hope Bay 2011 Groundwater Quality Report. Report prepared for Hope Bay Mining Limited. 1CH008.060. Apr. 2012.

SRK Consulting (Canada) Inc., 2014a. 2011 Stage 2 Geotechnical and Hydrogeological Assessment for Doris Central and Connector Underground Mines. Report prepared for TMAC Resources Inc. 1CT022.001. Apr. 2014.

SRK Consulting (Canada) Inc., 2014b. Hope Bay Project: Madrid Advanced Exploration Project: Underground Inflow Estimates. Memo prepared for TMAC Resources Inc. 1CT022.001. Oct. 2014.

SRK Consulting (Canada) Inc., 2015a. Hydrogeological Modeling of the Proposed Doris North Project, Hope Bay, Nunavut. Report prepared for TMAC Resources Inc. 1CT022.002. Jun. 2015.

SRK Consulting (Canada) Inc., 2015b. Doris North Project, Hope Bay - Water Quality Model Report. Report prepared for TMAC Resources Inc. 1CT022.002. May 2015.

SRK Consulting (Canada) Inc., 2017a. Hope Bay Project, Lake Talik Configuration. Memo prepared for TMAC Resources Inc. 1CT022.013. Nov. 2017a.

SRK Consulting (Canada) Inc., 2017b. Hydrogeological Characterization and Modeling of the Proposed Boston, Madrid South and Madrid North Mines, Hope Bay Project. Report Prepared for TMAC Resources Inc. 1CT022.013. Nov. 2017b.

SRK Consulting (Canada) Inc., 2017c. Madrid-Boston Project Water and Load Balance, Hope Bay Project. Report Prepared for TMAC Resources Inc. 1CT022.013. Nov. 2017c.

SRK Consulting (Canada) Inc. 2020. Hope Bay Operational Water Management Model – 2019 Validation. Memo prepared for Agnico Eagle Mines Ltd. 1CT022.066. March 2020.

SRK Consulting (Canada) Inc. 2022a. Hope Bay Geomechanical Design Phase I Review and Gap Analysis. Report prepared for Agnico Eagle Mines Ltd. 2CA027.001. Jan. 2022.

SRK Consulting (Canada) Inc., 2022b. Hope Bay Near-Term Water Treatment Review. Technical memo prepared for Agnico Eagles Mines Ltd. 1CT022.078. Feb. 2022.

SRK Consulting (Canada) Inc. 2022c. Hope Bay Climate Update. Technical memo prepared for Agnico Eagles Mines Ltd. 1CT022.066. Apr. 2022.

SRK Consulting (Canada) Inc. 2022d. Hope Bay Operational Water Management Model – 2021 Validation. Draft Technical memo prepared for Agnico Eagles Mines Ltd. CAPR001817. July. 2022.

SRK Consulting (Canada) Inc., 2023a. Hope Bay 2022 Drilling Program Factual Data Report – Final, prepared for Agnico Eagles Mines Ltd. CAPR001941. Mar. 2023.

SRK Consulting (Canada) Inc., 2023b. 2022 Annual Hydrogeological Inspection of Underground Workings – Doris North, Hope Bay, Draft memo, prepared for Agnico Eagles Mines Ltd. CAPR002135. Apr. 2023.

SRK Consulting (Canada) Inc., 2024. Mine Plan Operational Update: Water and Load Balance Model. Hope Bay Project, Cambridge Bay, NU, Canada. Report prepared for Agnico Eagle Mines Limited. CAPR003305. December 2024

Stevens C. W. 2010a. Interannual Changes in Seasonal Ground Freezing and Near-surface Heat Flow beneath Bottom-fast Ice in the Near-shore Zone, Mackenzie Delta, NWT, Canada. Permafrost and Periglacial Processes 21: 256-270.

Stevens C. W. 2010b. Modeling Ground Thermal Conditions and the Limit of Permafrost within the Nearshore Zone of the Mackenzie Delta, Canada. Journal of Geophysical Research. 115: F04027.

Stotler R.L., Shaun K. Frape, Ruskeeniemi T., Ahonen L., Onstott T.C., Hobbs M.Y. 2009. Hydrogeochemistry of groundwaters in and below the base of thick permafrost at Lupin, Nunavut, Canada. Journal of Hydrology 373 (2009) 80–95.

TMAC Resources, 2016. Hope Bay Project Groundwater Management Plan, Hope Bay, Nunavut. Aug. 2016.

TMAC Resources, 2020. Hope Bay – Doris Mine and Madrid Exploration Ramp, Ground Control Management Plan. Oct. 2020. Report No 001-2020.

Van Everdingen, 1998 revised May 2005. Multi-language Glossary of Permafrost and Related Ground-ice Terms. Boulder, CO: National Snow and Ice Data Center.

Appendix A – Lake Bathymetries

Appendix V5-3A

Lake Bathymetry Surveys in the LSA and RSA

MAC RESOURCES

Figure V5-3C-1
Doris Lake

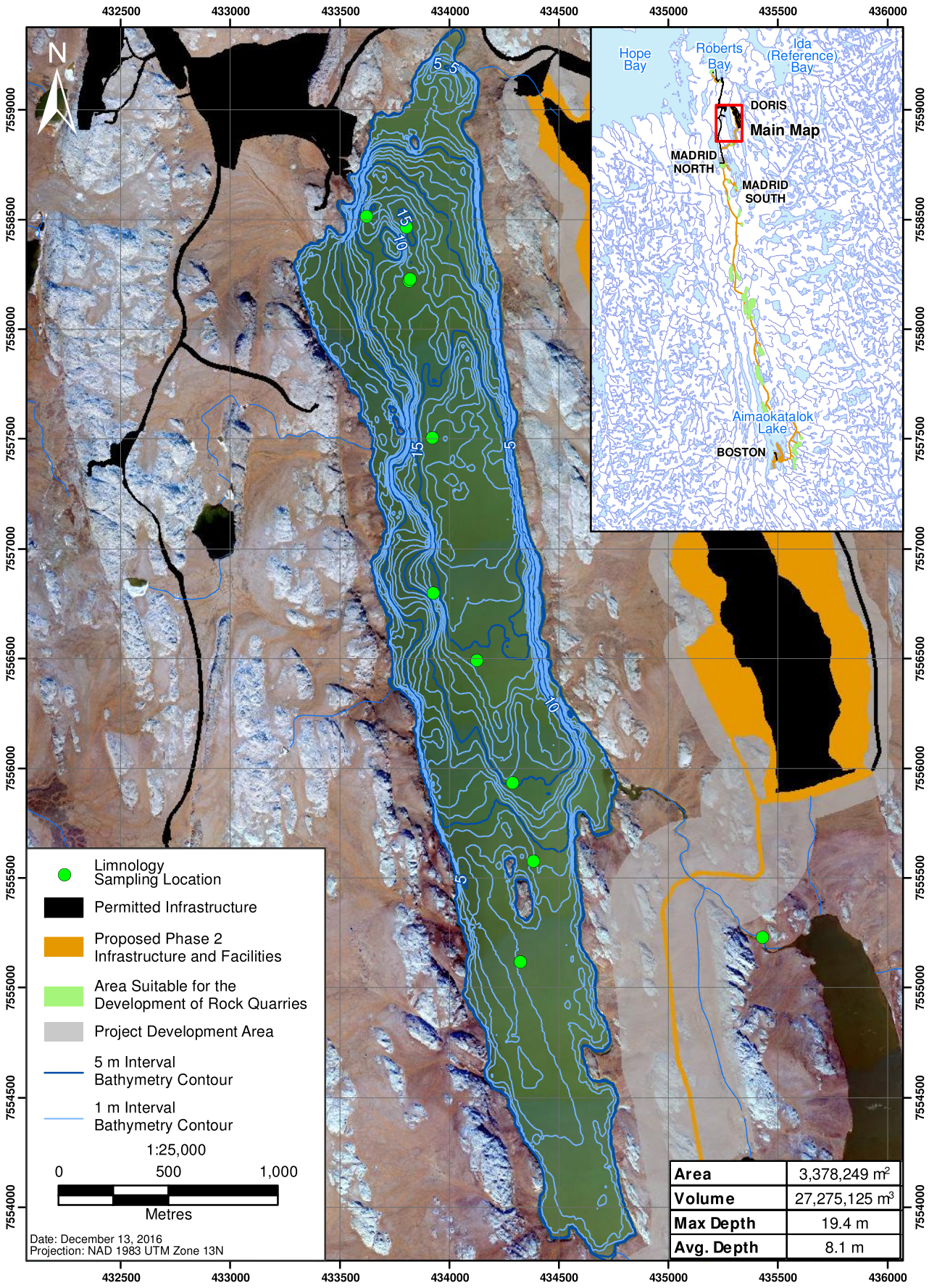


Figure V5-3C-2
Ogama Lake

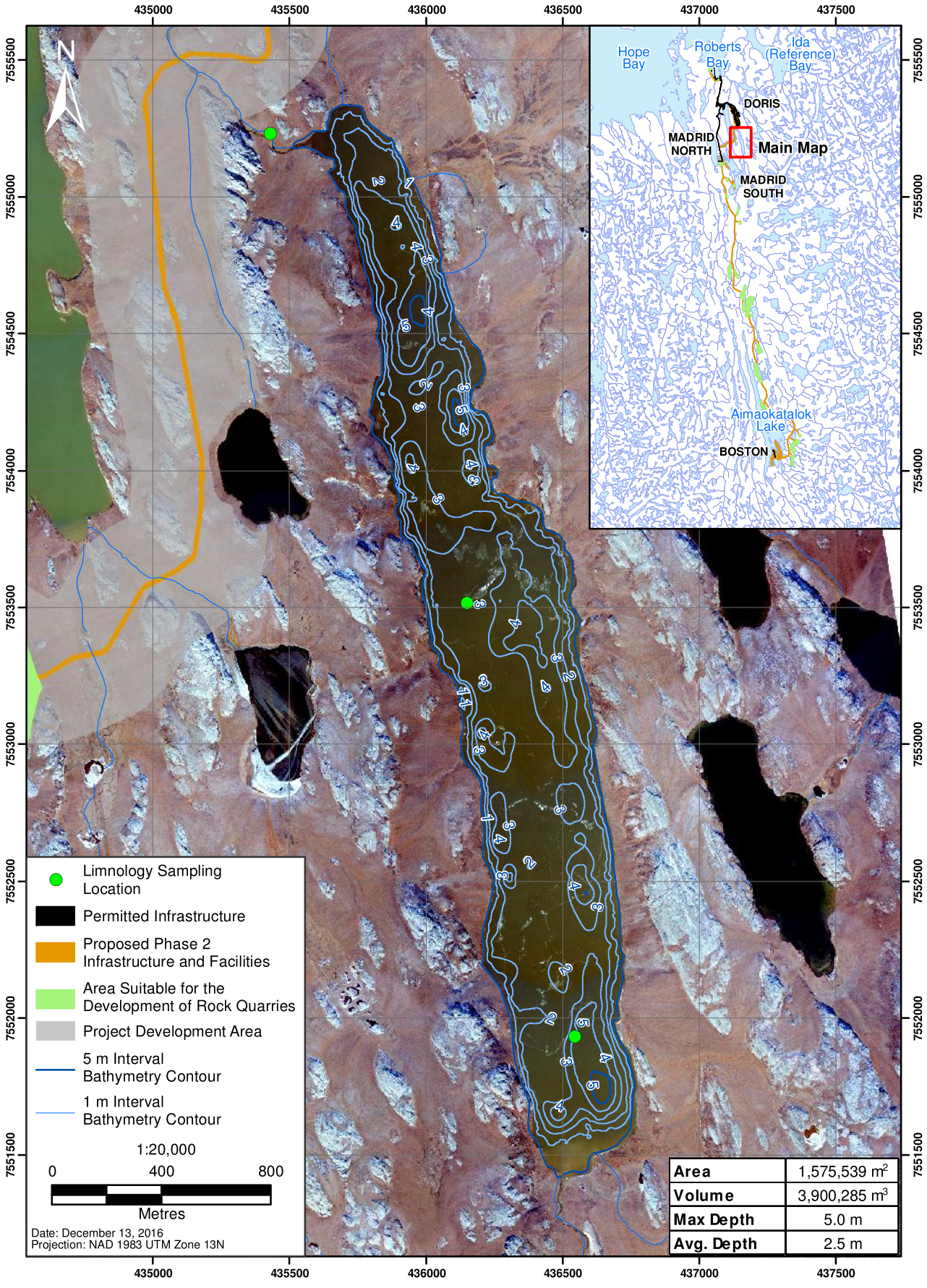


Figure V5-3C-3
Patch Lake

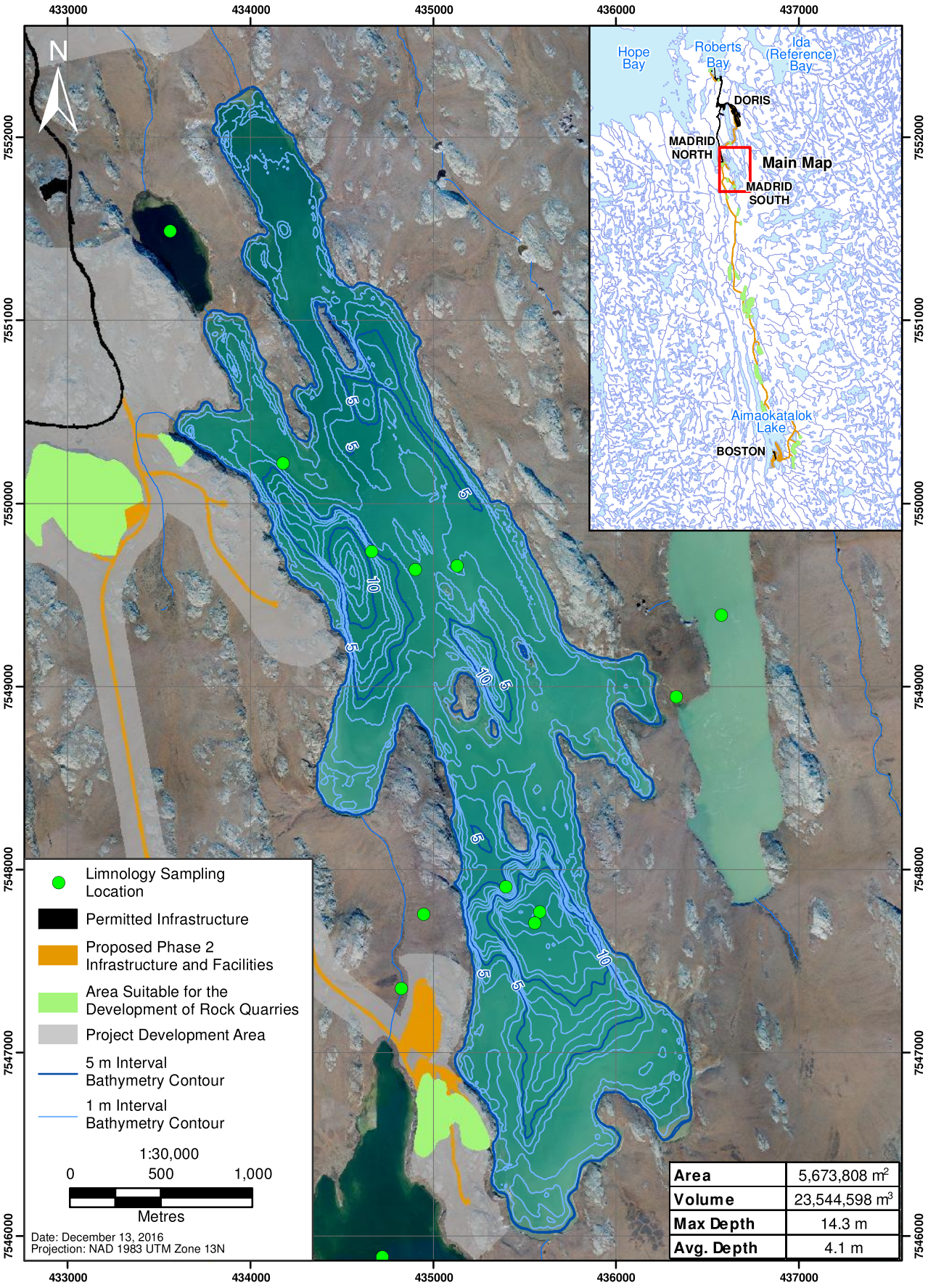


Figure V5-3C-4
Wolverine Lake

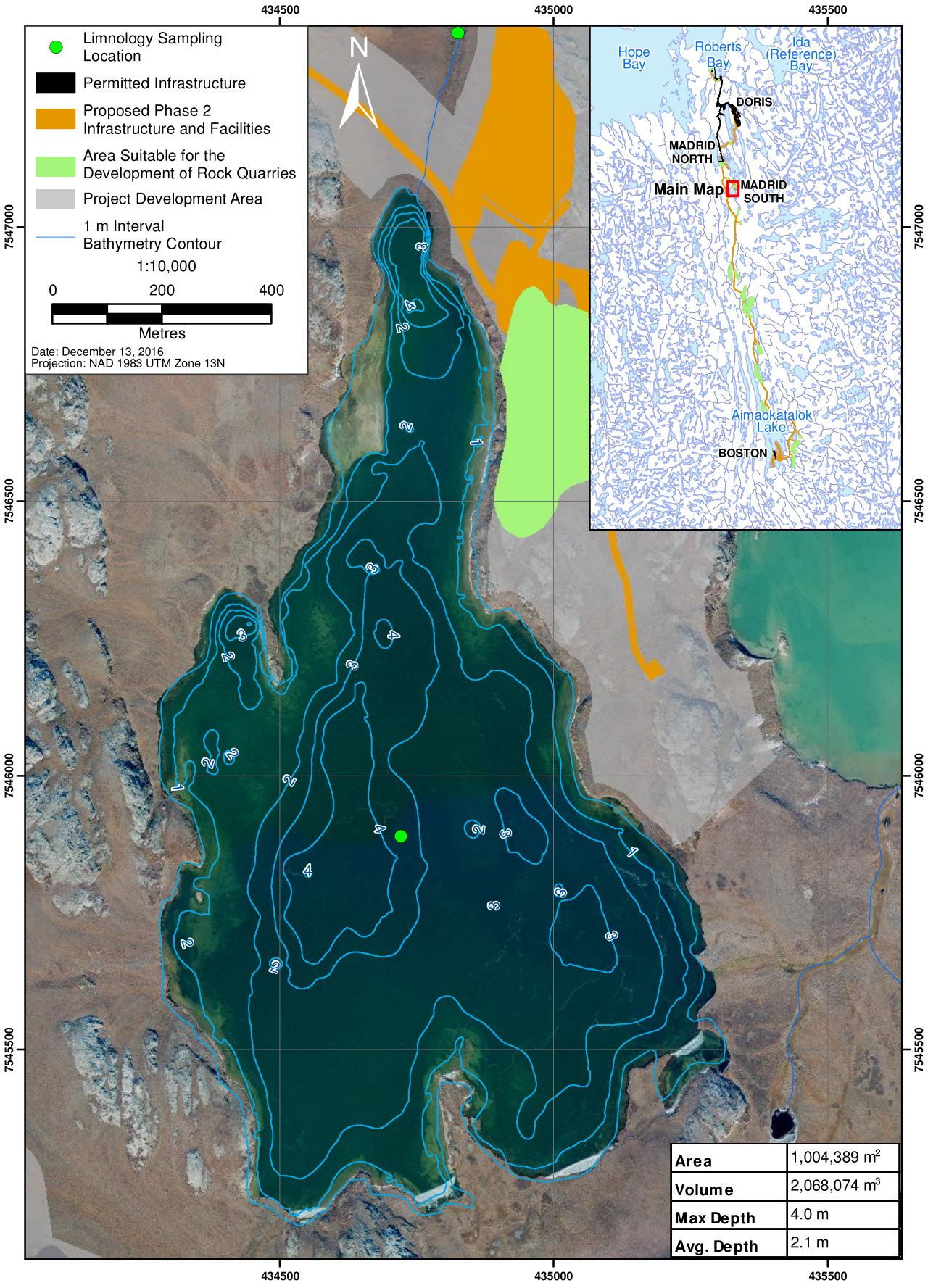


Figure V5-3C-5
Little Roberts Lake

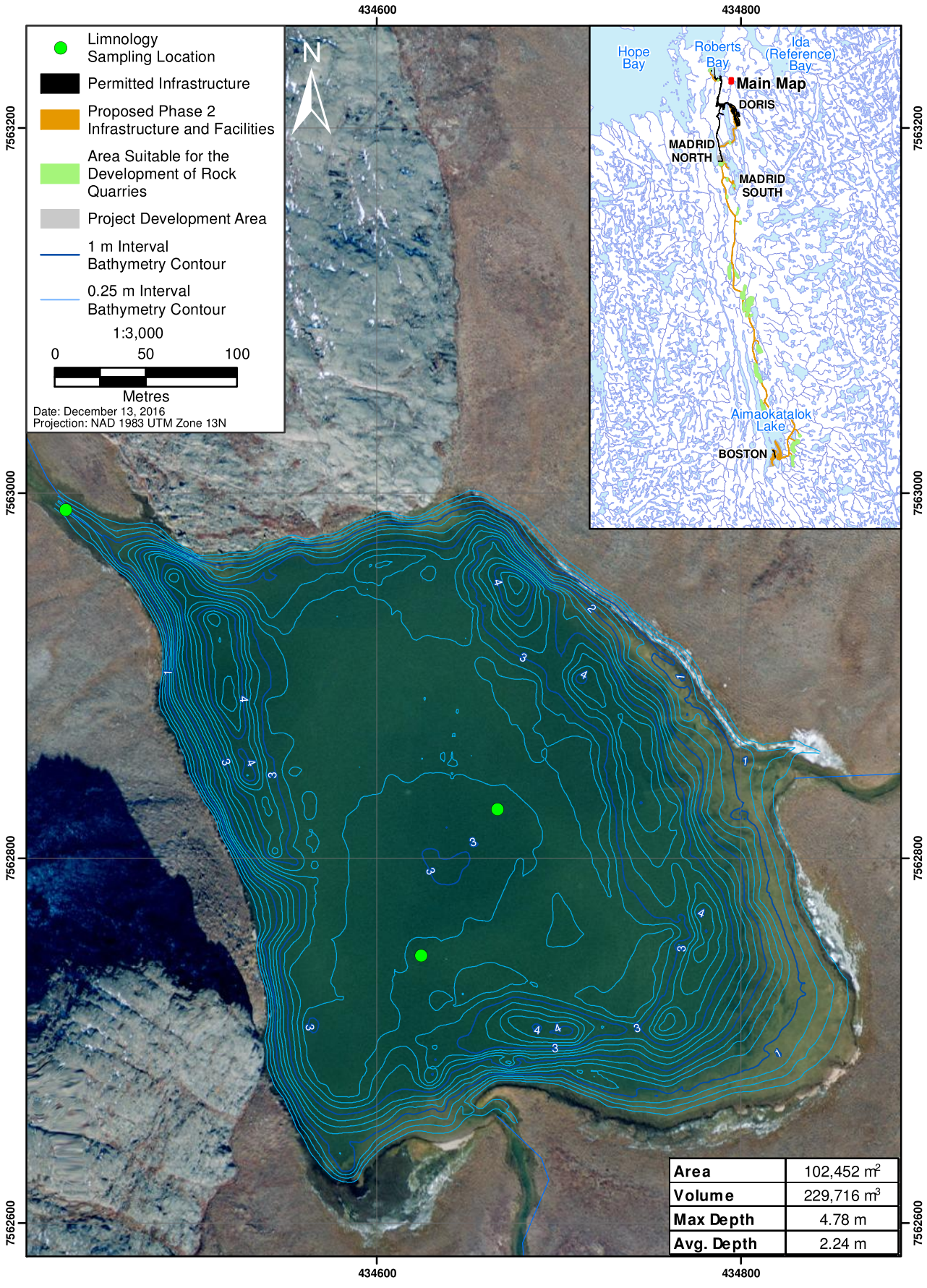


Figure V5-3C-6
Imniagut Lake

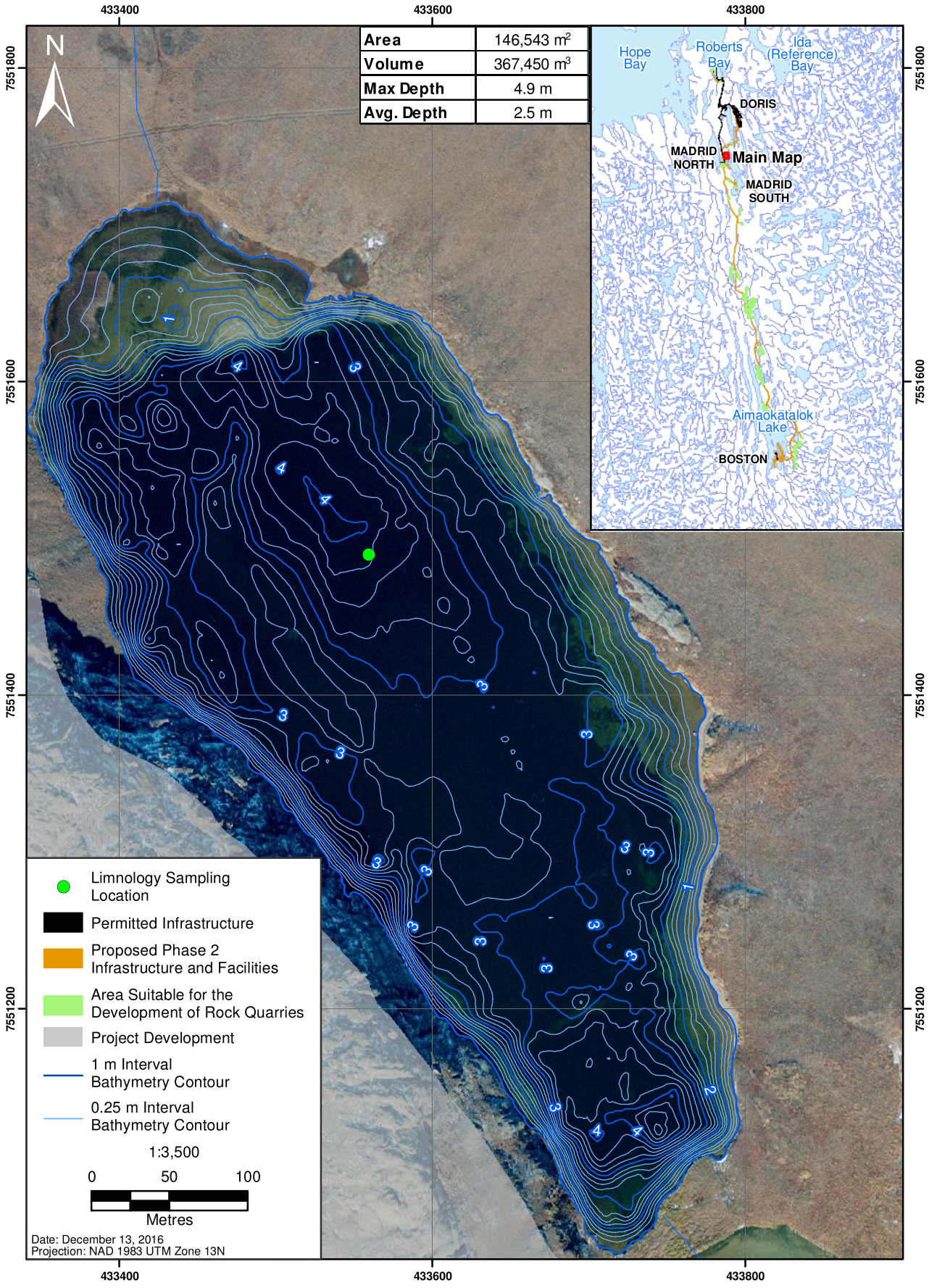


Figure V5-3C-7
P.O. Lake

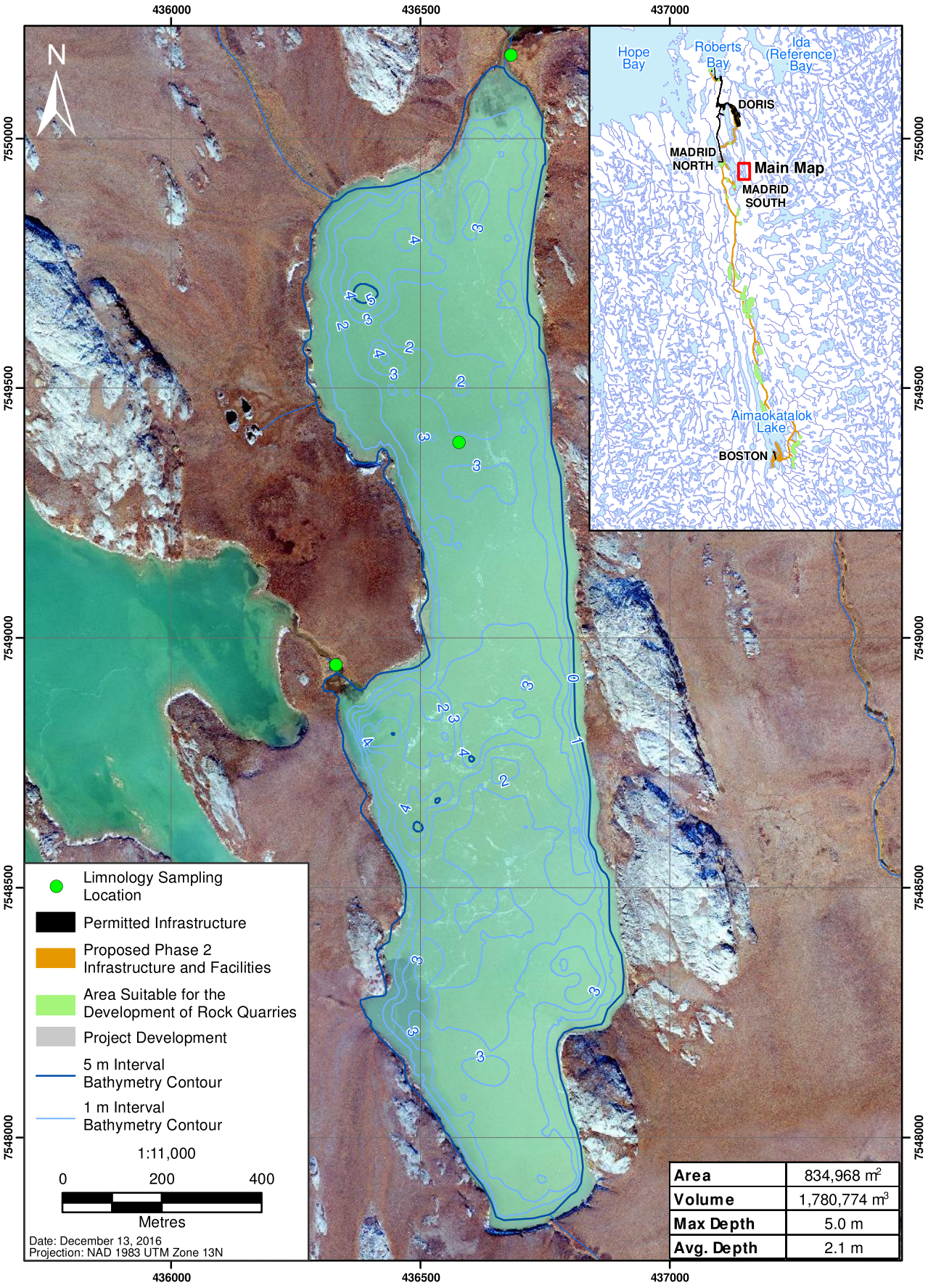


Figure V5-3C-8
Windy Lake

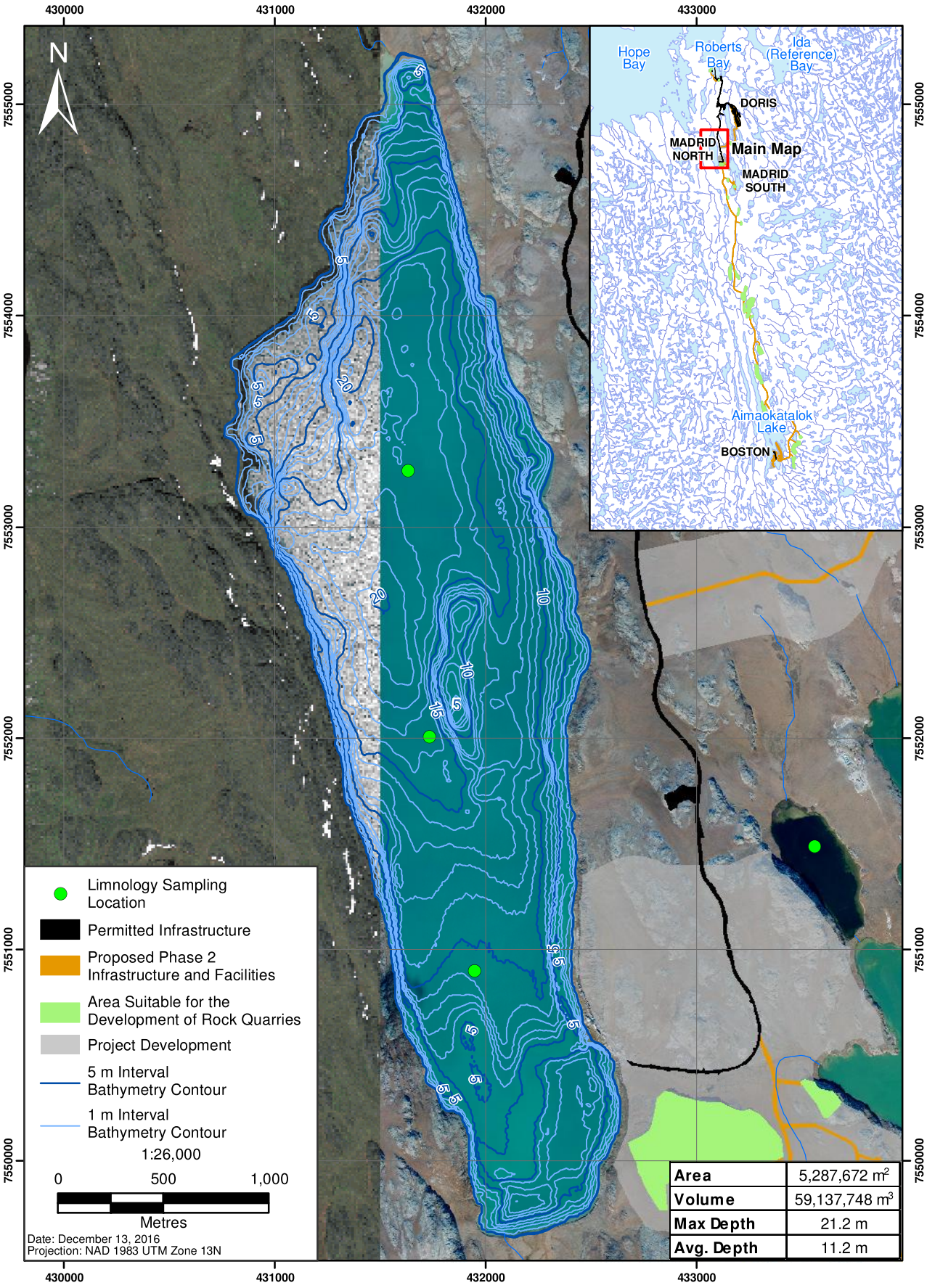


Figure V5-3C-9
Aimaokatalok Lake

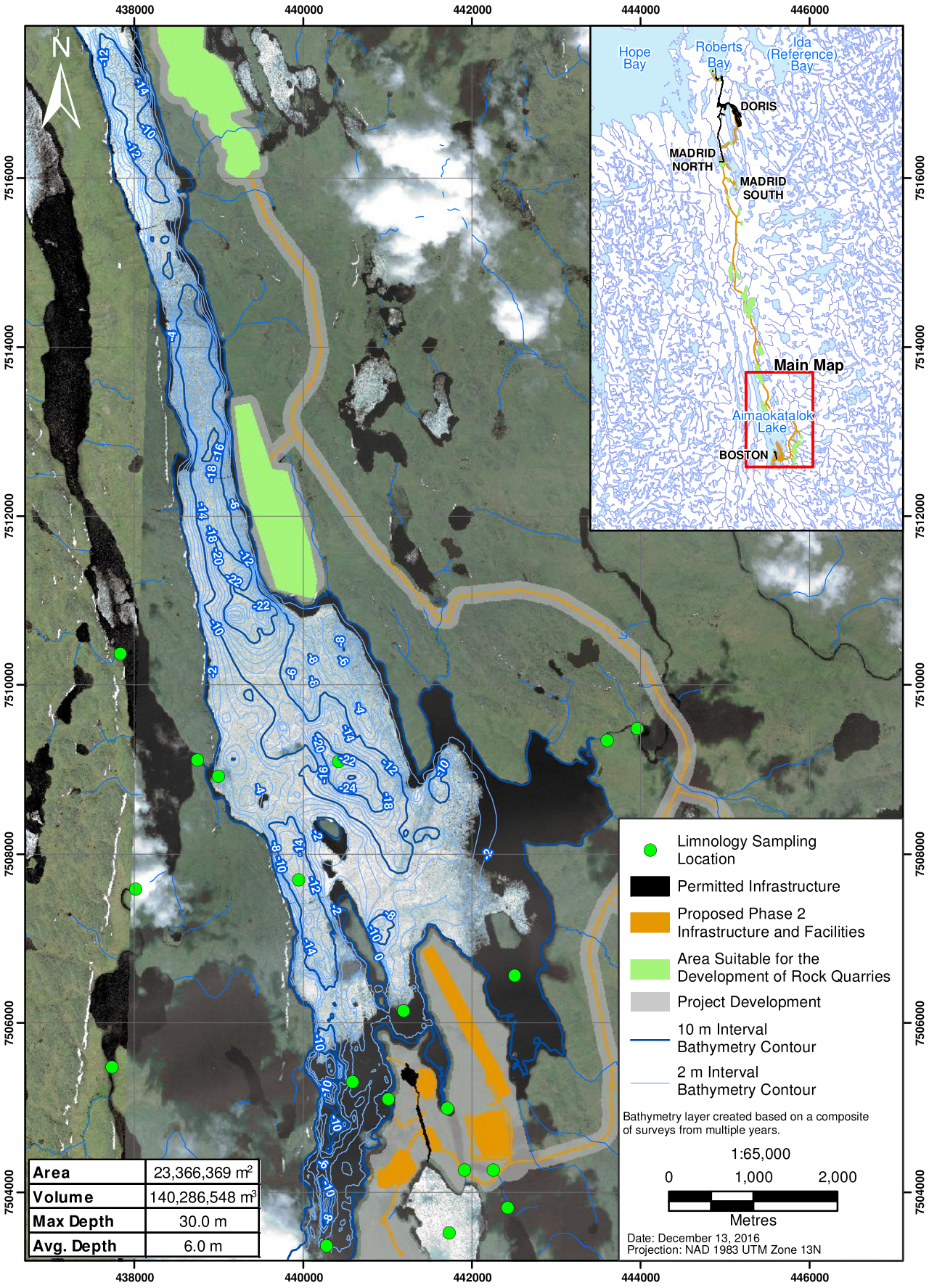


Figure V5-3C-10
Stickleback Lake

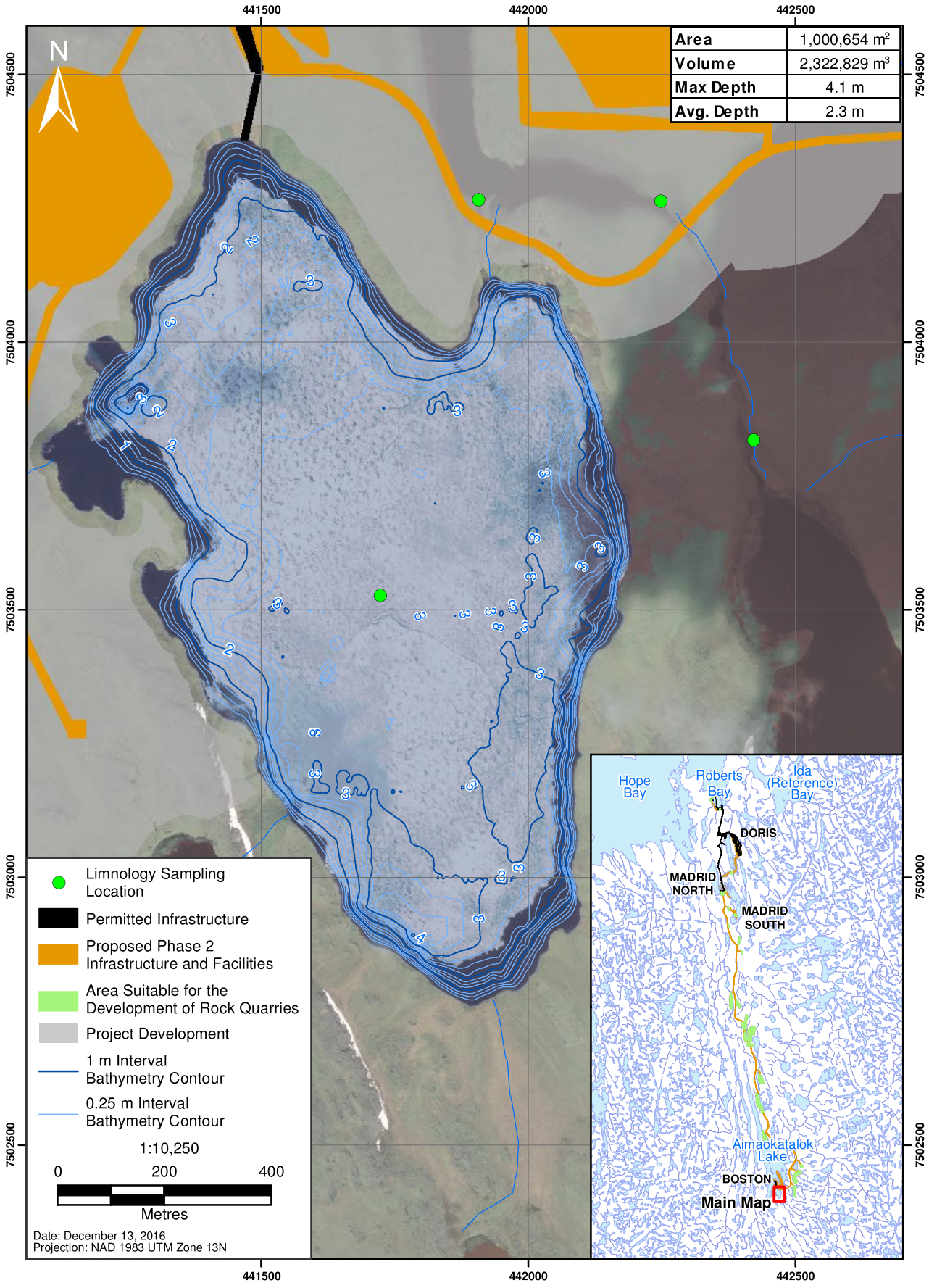


Figure V5-3C-11
Trout Lake

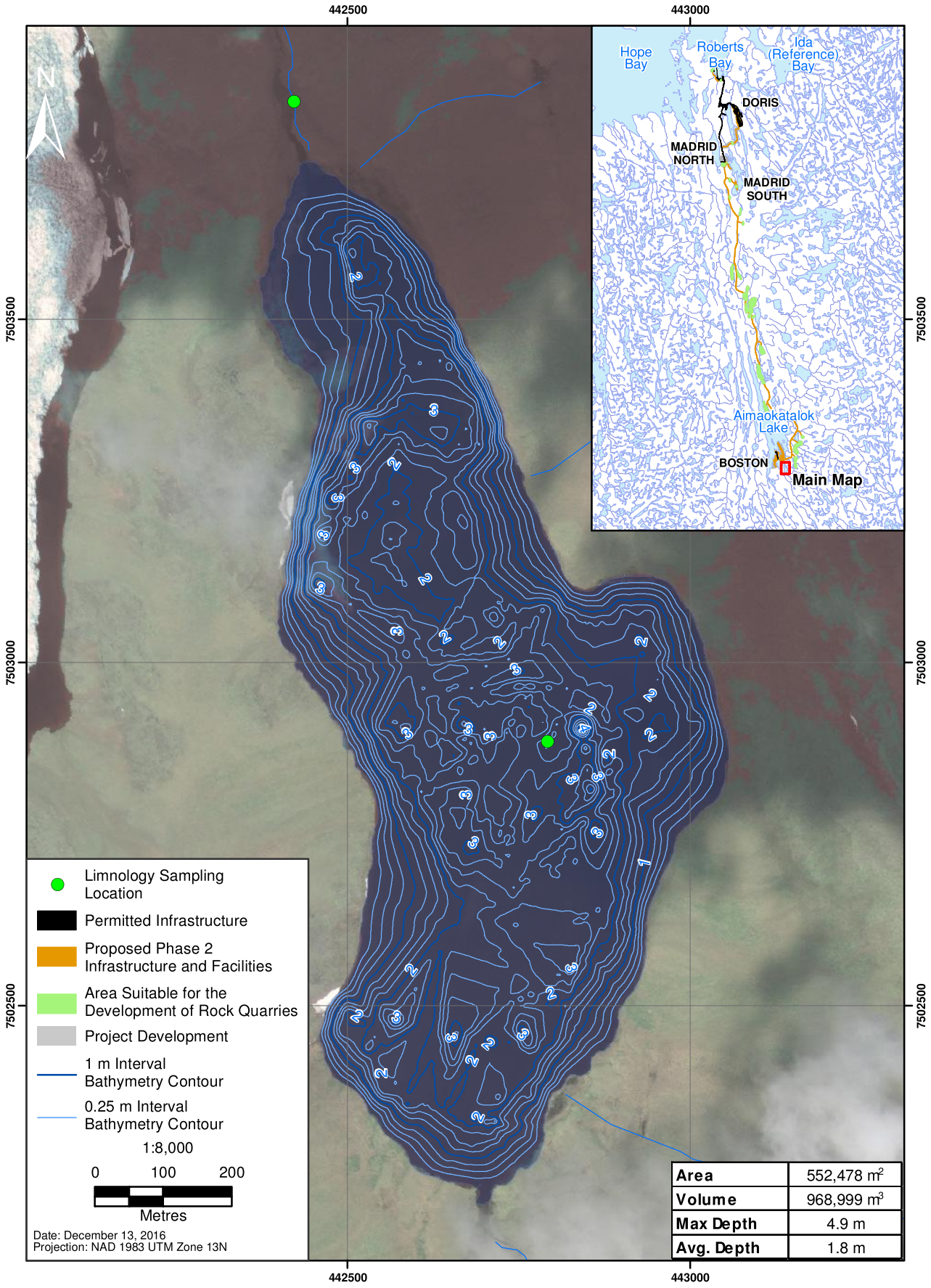
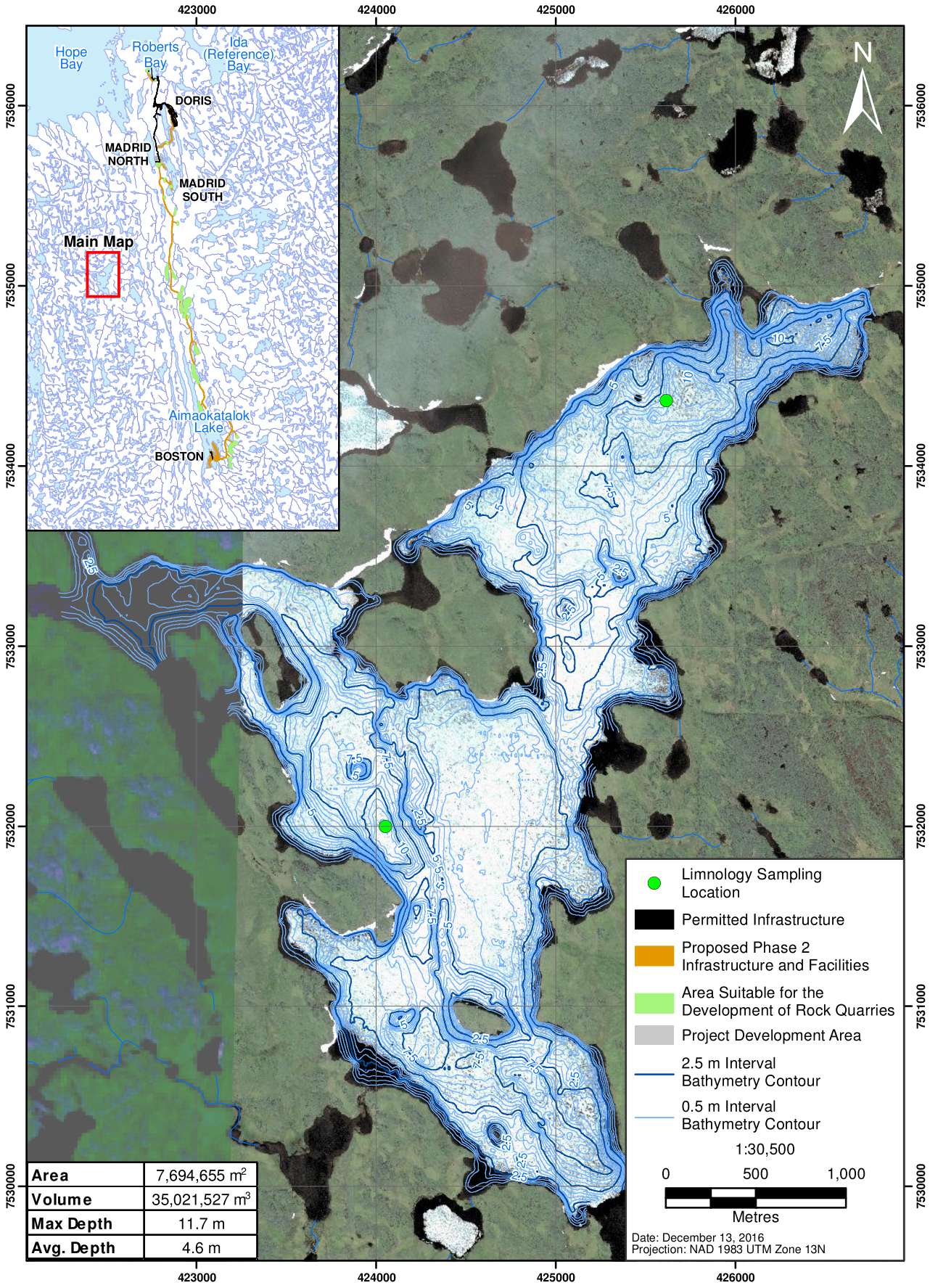


Figure V5-3C-12
Reference Lake B



Appendix B – Overburden Data

Table 1: Drillhole Summary for Onshore Overburden Drill Holes

Hole ID	Interval (m)	Description
SRK-07-34	0.0 – 0.03	Frozen Muskeg
	0.03 – 0.5	Brown sandy silt with rootlets
	0.5 – 1.4	Brown silty clay; Vs with occasional thick ice layers
	1.4 – 14.5	Consolidated grey clay; Vx, Vs and occasional thick ice layers
	14.5 – 14.8	Well graded till
	14.8 – 19.7	Competent bedrock to EOH
SRK-07-35	0 – 0.1	Frozen Muskeg
	0.1 – 1.7	Dark brown sandy silt; Vs
	1.7 – 14.0	Dark grey silty fine sand; Vx, Vs, and Vr (ice content 10 - 50%) with massive ice lenses 0.9 – 1.2 m thick
	14.0 – 15.6	Fine sand, Nbn
	15.6 – 16.2	Till
	16.2 – 19.2	Bedrock to EOH
SRK-07-36	0 – 0.03	Frozen Muskeg
	0.03 – 0.4	Brown Sandy Silt
	0.4 – 3.3	Silty Sand; Vs with massive ice
	3.3 – 7.9	Dark grey silty fine sand; Vx, Vs, and Vr (ice content 10 - 15%) with massive ice lenses 0.9 – 1.2 m thick
	7.9 – 8.5	Till
	8.5 – 9.7	Intensely fractured bedrock
	9.7 – 12.5	Competent bedrock to EOH
SRK-07-37	0 – 0.2	Frozen Muskeg
	0.2 – 0.6	Dry light tan silt with rootlets
	0.6 – 1.9	Silty clay; Vx and Vs = 35%
	1.9 – 3.4	Grey consolidated glacial clay Vs = 10 – 15%
	3.4 – 5.3	Consolidated grey/brown silty clay; Vs with occasional massive ice lenses
	5.3 – 7.2	Consolidated glacial clay grading to sand with depth; Vx with occasional massive ice layers
	7.2 – 11.6	Bedrock to EOH

Vx – Individual ice inclusion
Vs – Stratified or distinctly oriented ice formations
Vr – Random or irregularly oriented ice formations
EOH – End of Hole

Table 2: Drillhole Summary for Holes Below Patch Lake at a Proposed Dewatering Dike Alignment Location

Hole ID	Interval (m)	Description
SRK-07-27	0.0 – 3.0	Ice (2 m) & water
	3.0 – 6.0	Lacustrine sediments / Unconsolidated glacial clay
	6.0 – 24.3	Consolidated glacial clay; granular ice crystals at ~11 m
	24.3 – 27.5	Well graded till with boulders
	27.5 – 36.7	Highly fractured bedrock
	36.7 – 40.0	Competent bedrock to EOH
SRK-07-28	0.0 – 3.0	Ice (2 m) & water
	3.0 – 9.0	Lacustrine sediments
	9.0 – 20.0	Glacial clay; ice lenses present
	20.0 – 20.3	Till (upper zone mainly sand; bottom contains boulders)
	20.3 – 25.0	Competent bedrock to EOH
SRK-07-29	0 – 1.9	Ice
	1.0 – 11.9	Unconsolidated soupy glacial clay
	11.9 – 19.3	Consolidated glacial clay; no ice present
	19.3 – 27.4	Sandy till; occasional pebbles, cobbles and boulders
	27.4 – 33.0	Fractured bedrock; fracture density decreases with depth
	33.0 – 37.4	Competent bedrock to EOH
SRK-07-30	0.0 – 3.0	Ice (2.1 m) & water
	3.0 – 8.0	Lacustrine deposits / Unconsolidated glacial clay; visible Ice lenses
	8.0 – 16.0	Consolidated glacial clay; Vs present in upper zone
	16.0 –17.0	Sand
	17.0 – 32.0	Consolidated glacial clay
	32.0 – 37.3	Bedrock to EOH

Vx – Individual ice inclusion
Vs – Stratified or distinctly oriented ice formations
Vr – Random or irregularly oriented ice formations
EOH – End of Hole

Table 3: Drillhole Summary for Holes Below Patch Lake in the Vicinity of the Proposed Suluk and Rand Open Pits

Hole ID	Interval (m)	Description
SRK-07-38	0.0 – 2.3	Ice (0.2 m) & water
	2.3 – 6.1	Very loose lacustrine and glacial clay
	6.1 – 21.3	Grey unconsolidated glacial clay, black mottled texture
	21.3 – 22.9	Sandy silty clay. Sand fraction is coarse
	22.9 – 25.9	Grey unconsolidated glacial clay with black mottling
	25.9 – 29.0	Sand
	29.0 – 31.4	Well graded Till
	31.4 – 35.1	Unconsolidated glacial clay
	35.1 – 38.1	Well graded Till
	38.1 – 45.7	Bedrock to EOH
SRK-07-39	0.0 – 2.3	Ice (1.8 m) & water
	2.3 – 3.8	Light grey unconsolidated glacial clay; Vx
	3.8 – 6.7	Dark grey consolidated glacial clay (one ice lens at 4 m)
	6.7 – 7.1	Sand
	7.1 – 11.9	Competent bedrock to EOH
SRK-07-40	0.0 – 12.8	Ice (1.8 m) & water
	12.8 – 30.6	Consolidated Glacial Clay; 0.04 m ice lens at top
	30.6 – 36.6	Highly fractured bedrock
	36.6 – 39.6	Competent bedrock to EOH
SRK-07-40A	0.0 – 7.0	Ice (1.8 m) & water
	7.0 – 7.6	Unconsolidated Glacial Clay; Vx, 0.05 m massive ice at top
	7.6 – 11.6	No recovery (drill rods met no resistance)
	11.6 – 15.6	Well graded sand, clay to coarse sand; 0.08 m ice lens at 11.6 m
	15.6 – 19.8	Competent bedrock to EOH
SRK-07-41	0 – 1.8	Ice
	1.8 – 12.2	Water / Unconsolidated Sediments
	12.2 – 13.7	Unconsolidated Glacial Clay; 0.05 m ice lenses throughout
	13.7 – 15.2	Unconsolidated Glacial Clay
	15.2 – 18.9	Consolidated Glacial Clay
	18.9 – 30.5	Well graded Till
	30.5 – 36.6	Competent bedrock to EOH

Vx – Individual ice inclusion
Vs – Stratified or distinctly oriented ice formations
Vr – Random or irregularly oriented ice formations
EOH – End of Hole

Table 4: Pore Pressure Dissipation Test Results under Doris Lake

Hole	Duration (s)	Test Depth Below Ground Level (m)	Equilibrium Pore Pressure (m)	Inferred Soil Type (CPT Log)
SRK CPT08-06	2,000	10.00	10.1	Clayey Silt
	700	11.95	11.8	Silty Sand/Sand
SRK CPT08-07	2,000	5.00	Not Achieved	Sensitive Fines
	600	7.78	Not Achieved	Silty Sand/Sand
SRK CPT08-08	1,600	15.00	Not Achieved	Sensitive Fines
	3,600	20.60	Not Achieved	Silty Sand/Sand

Table 5: Pore Pressure Dissipation Test Results under Patch Lake

Hole	Duration (s)	Test Depth Below Ground Level (m)	Equilibrium Pore Pressure (m)	Inferred Soil Type
SRK CPT08-14	650	10.00	Not Achieved	Sensitive Fines
	2,200	10.50	Not Achieved	Sensitive Fines
	2,000	16.80	16.9	Silty Sand/Sand
SRK CPT08-15	1,200	10.00	Not Achieved	Sensitive Fines
SRK CPT08-16	1,800	10.00	Not Achieved	Sensitive Fines
	200	15.73	15.7	Silty Sand/Sand
SRK CPT08-17	2,000	8.53	Not Achieved	Sensitive Fines
	900	25.33	Not Achieved	Sandy Silt
SRK CPT08-19	2,000	10.00	Not Achieved	Clayey Silt
	600	14.43	14.3	Sandy Silt
SRK CPT08-20	6,000	15.33	Not Achieved	Sensitive Fines
	2,905	25.08	Not Achieved	Clayey Silt
	1,200	33.90	35.2	Sandy Silt
SRK CPT08-21	3,600	10.00	Not Achieved	Sensitive Fines
	2,500	20.00	Not Achieved	Sensitive Fines
	1,200	30.00	Not Achieved	Silt
SRK CPT08-23[1]	200	3.75	3.6	Data point does not exist
SRK CPT08-23	2,400	10.00	Not Achieved	Sensitive Fines
	2,700	20.00	Not Achieved	Sensitive Fines
	3,000	28.48	28.4	Silty Sand/Sand

1. At a depth of 3.75 m in SRK CPT08-23 there is lake water. This data point is therefore erroneous.

Table 6: Pore Pressure Dissipation Test Results under Spyder Lake

Hole	Duration (s)	Test Depth Below Ground Level (m)	Equilibrium Pore Pressure (m)	Inferred Soil Type
SRK CPT08-29	13,755	5.00	Not Achieved	Sensitive Fines
SRK CPT08-31	5,000	5.00	Not Achieved	Sensitive Fines
	200	9.03	9.2	Sand

Table 7: Summary of Typical Overburden Characteristics

Area	Element	Value/Comment
Thermal Properties	Permafrost Zone	Continuous
	Permafrost Temperature	-8°C to -11°C
	Thermal Gradient	11.4°C/km at Doris and 18°C/km at Boston
	Permafrost Depth	About 550 m at Doris and 560 m at Boston
	Active Layer Thickness	0.5 to 1.0 m
	Depth of Zero Annual Amplitude	10 m
	Pore Water Salinity	Variable, but typically between 34 and 45 ppm
	Recommended Design Freezing Point	-2°C
	Talik Conditions	Assume open talik under Doris, Patch and Spyder Lakes with vertical transition at the shoreline. Assume closed talik under Tail Lake.

Area	Element	Value/Comment
Indicator Properties	Natural Moisture Content	Variable, but typically greater than 40%
	Plastic Limit	38 to 58
	Liquid Limit	22 to 35
	Plasticity Index	16 to 19
	Clay Fraction	31 to 52%
	Clay Mineralogy	Illite, chlorite, albite, kaolin, quartz, plagioclase
	Primary Soil Type	Clay (CL)
	Specific Gravity	2.7
	Bulk Density	1.55 to 1.93 kg/m^3
	Shrinkage Limit	17 to 23
	Shrinkage Ratio	1.5 to 1.8
Engineering Properties	Volumetric Fraction of Unfrozen Water at -5ºC	0.3 to 0.6
	Peak Undrained Shear Strength	11 to 25 kPa
	Remoulded Shear Strength	0 to 4 kPa
	Clay Sensitivity	4 to 22
	Total Strength, cohesion	3 to 10 kPa
	Total Strength, friction angle	12 to 15º
	Effective Strength, cohesion	5 to 8 kPa
	Effective Strength, friction angle	26 to 31º
	Coefficient of Consolidation	0.59 to 1.03 m^2/yr
	Saturated Hydraulic Conductivity	3.55 to 4.61 x 10^{-10} m/sec

Appendix C – Hydraulic Conductivity Data

Test Information										Test Interval along hole (mah)		
ID1	Area	Sub-Area	Test Number	Date	Time test started	Time not drilled (hours)	QA/QC	Last checked by	Date checked	Top	Bottom	Interval length
08TDD628	Doris	Central	1	27-May-08	11:02	2:47	SRK	JA	Jul-2011	52.2	141.0	88.8
08TDD630	Doris	Central	1	29-May-08	9:20	1:58	SRK	JA	Jul-2011	32.2	62.0	29.8
08TDD630	Doris	Central	2	30-May-08	9:00	4:00	SRK	JA	Jul-2011	99.2	134.0	34.8
08TDD630	Doris	Central	3	31-May-08	15:30	1:00	SRK	JA	Jul-2011	138.2	164.0	25.8
08TDD630	Doris	Central	4	1-Jun-08	12:30	1:10	SRK	JA	Jul-2011	166.2	195.0	28.8
08TDD630	Doris	Central	5	3-Jun-08	14:30	2:20	SRK	JA	Jul-2011	201.2	263.0	61.8
08TDD631	Doris	Central	1	1-Jun-08	9:00	3:00	SRK	JA	Jul-2011	39.2	65.0	25.8
08TDD631	Doris	Central	2	3-Jun-08	17:30	5:30	SRK	JA	Jul-2011	96.2	122.0	25.8
08TDD632	Doris	North	1	8-Jun-08	10:30	2:00	SRK	JA	Jul-2011	48.2	122.0	73.8
08TDD632	Doris	North	2	11-Jun-08	8:20	3:20	SRK	JA	Jul-2011	174.2	245.0	70.8
08TDD632	Doris	North	3	13-Jun-08	13:30	3:00	SRK	JA	Jul-2011	264.2	338.0	73.8
08TDD632	Doris	North	4	14-Jun-08	23:55	2:35	SRK	JA	Jul-2011	339.2	401.0	61.8
08TDD633	Doris	Central	1	8-Jun-08	12:00	4:15	SRK	JA	Jul-2011	15.2	50.0	34.8
08TDD633	Doris	Central	2	11-Jun-08	11:30	2:00	SRK	JA	Jul-2011	156.2	218.0	61.8
08TDD633	Doris	Central	3	13-Jun-08	8:30	3:00	SRK	JA	Jul-2011	279.2	341.0	61.8
08TDD633	Doris	Central	4	15-Jun-08	4:00	2:30	SRK	JA	Jul-2011	357.2	401.0	43.8
08TDD634	Doris	North	1	#N/A	#N/A	#N/A	SRK	JA	Jul-2011	43.3	140.3	97.1
10WBW001	Doris	Central	1	17-Apr-10	14:45	2:45	SRK	JA	Jul-2011	25.0	63.0	38.0
10WBW001	Doris	Central	2	18-Apr-10	15:15	1:30	SRK	JA	Jul-2011	64.0	102.0	38.0
10WBW001	Doris	Central	3	19-Apr-10	14:00	1:00	SRK	JA	Jul-2011	121.5	144.5	23.0
10WBW001	Doris	Central	4	19-Apr-10	15:00	1:15	SRK	JA	Jul-2011	103.0	144.5	41.5
10WBW001	Doris	Central	5	20-Apr-10	13:15	1:55	SRK	JA	Jul-2011	154.0	204.8	50.8
10WBW001	Doris	Central	6	20-Apr-10	15:10	1:35	SRK	JA	Jul-2011	103.0	154.0	51.0

Test Information										Test Interval along hole (mah)		
ID1	Area	Sub-Area	Test Number	Date	Time test started	Time not drilled (hours)	QA/QC	Last checked by	Date checked	Top	Bottom	Interval length
10WBW001	Doris	Central	7	21-Apr-10	15:00	2:10	SRK	JA	Jul-2011	203.0	252.0	49.0
10WBW001	Doris	Central	8	22-Apr-10	12:45	1:20	SRK	JA	Jul-2011	252.0	279.0	27.0
10WBW001	Doris	Central	9	22-Apr-10	12:45	1:20	SRK	JA	Jul-2011	279.0	297.0	18.0
10WBW001	Doris	Central	10	23-Apr-10	14:15	1:50	SRK	JA	Jul-2011	297.0	345.0	48.0
10WBW001	Doris	Central	11	24-Apr-10	12:50	1:50	SRK	JA	Jul-2011	345.0	387.0	42.0
10WBW001	Doris	Central	12	25-Apr-10	15:05	2:25	SRK	JA	Jul-2011	387.0	422.5	35.5
10WBW001	Doris	Central	13	26-Apr-10	15:50	1:25	SRK	JA	Jul-2011	423.0	471.0	48.0
10WBW001	Doris	Central	14	28-Apr-10	16:05	1:25	SRK	JA	Jul-2011	471.0	564.0	93.0
10WBW001	Doris	Central	14a	28-Apr-10	16:05	1:25	SRK	JA	Jul-2011	548.0	564.0	16.1
10WBW001	Doris	Central	6a	20-Apr-10	15:10	1:35	SRK	JA	Jul-2011	103.0	204.8	101.8
10WBW001	Doris	Central	8a	22-Apr-10	12:45	1:20	SRK	JA	Jul-2011	252.0	297.0	45.0
10WBW002	Doris	North	1	21-Jun-10	11:00	2:30	SRK	JA	Jul-2011	402.3	482	79.7

Test Information										Test Interval along hole (mah)		
ID1	Area	Sub-Area	Test Number	Date	Time test started	Time not drilled (hours)	QA/QC	Last checked by	Date checked	Top	Bottom	Interval length
10WBW002	Doris	North	2	21-Jun-10	14:00	1:30	SRK	JA	Jul-2011	447.3	482	34.7
10WBW002	Doris	North	3	22-Jun-10	14:30	2:00	SRK	JA	Jul-2011	483.3	518	34.7
10WBW002	Doris	North	4	23-Jun-10	16:45	1:30	SRK	JA	Jul-2011	519.3	569	49.7
10WBW002	Doris	North	5	24-Jun-10	13:00	15:30	SRK	JA	Jul-2011	570.3	602	31.7
11TDD763	Doris	Central	1	11-Mar-11	12:30	2:10	SRK	JA	Jul-2011	52.3	207.0	154.7
11TDD764	Doris	Und Con	1	14-Mar-11	12:00	1:35	SRK	JA	Jul-2011	41.4	131.1	89.7
11TDD764	Doris	Und Con	2	19-Mar-11	14:30	3:30	SRK	JA	Jul-2011	264.3	341.1	76.8
11TDD765	Doris	Near Mine	1	23-Mar-11	16:30	2:00	SRK	JA	Jul-2011	310.3	322.0	11.7
11TDD765	Doris	Near Mine	2	26-Mar-11	15:30	1:30	SRK	JA	Jul-2011	398.1	437.2	39.1
11TDD766	Doris	Central	1	22-Mar-11	14:00	2:00	SRK	JA	Jul-2011	28.75	51.2	22.4
11TDD766	Doris	Central	2	23-Mar-11	14:45	1:15	SRK	JA	Jul-2011	101.75	130.5	28.7
11TDD766	Doris	Central	3	25-Mar-11	11:00	2:00	SRK	JA	Jul-2011	198.85	240.3	41.4
11TDD768	Doris	Central	1	30-Mar-11	13:15	1:15	SRK	JA	Jul-2011	69.4	104.2	34.8
11TDD768	Doris	Central	2	31-Mar-11	9:15	1:30	SRK	JA	Jul-2011	111.4	152.2	40.8
11TDD768	Doris	Central	3	2-Apr-11	18:30	2:15	SRK	JA	Jul-2011	225.4	242.2	16.8
11TDD768	Doris	Central	4	3-Apr-11	11:30	1:15	SRK	JA	Jul-2011	225.4	269.2	43.8
11TDD768	Doris	Central	5	3-Apr-11	13:10	1:20	SRK	JA	Jul-2011	234.4	269.2	34.8
11TDD768	Doris	Central	6	4-Apr-11	20:00	3:00	SRK	JA	Jul-2011	267.43	299.2	31.8
11TDD769	Doris	Central	1	7-Apr-11	17:00	5:30	SRK	JA	Jul-2011	30.4	38.2	7.8
11TDD769	Doris	Central	2	9-Apr-11	15:50	2:40	SRK	JA	Jul-2011	129.4	143.2	13.8
11TDD769	Doris	Central	3	10-Apr-11	14:00	2:00	SRK	JA	Jul-2011	189.4	200.2	10.8
11TDD769	Doris	Central	4	13-Apr-11	23:30	2:00	SRK	JA	Jul-2011	299.3	309	9.7

Test Information										Test Interval along hole (mah)		
ID1	Area	Sub-Area	Test Number	Date	Time test started	Time not drilled (hours)	QA/QC	Last checked by	Date checked	Top	Bottom	Interval length
11TDD769	Doris	Central	1ss	12-Apr-11	12:30	1:45	SRK	JA	Jul-2011	129.1	290	160.9
11TDD769	Doris	Central	2ss	12-Apr-11	14:00	9:30	SRK	JA	Jul-2011	153.1	290	136.9
11TDD771	Doris	Central	1	21-Apr-11	17:00	1:45	SRK	JA	Jul-2011	48.6	74.25	25.7
11TDD771	Doris	Central	2	24-Apr-11	15:15	2:15	SRK	JA	Jul-2011	112.3	135	22.7
11TDD771	Doris	Central	3	26-Apr-11	9:45	1:30	SRK	JA	Jul-2011	118.3	162	43.7
11TDD771	Doris	Central	4	27-Apr-11	8:30	1:30	SRK	JA	Jul-2011	151.3	198	46.7
11TDD771	Doris	Central	5	27-Apr-11	10:00	1:15	SRK	JA	Jul-2011	181.3	198	16.7
11TDD771	Doris	Central	6	1-May-11	10:00	1:30	SRK	JA	Jul-2011	232.1	294	61.9
11TDD772	Doris	Central	1	4-May-11	13:40	1:30	SRK	JA	Jul-2011	55.3	87.2	31.9
11TDD772	Doris	Central	2	6-May-11	11:00	1:05	SRK	JA	Jul-2011	88.3	147.2	58.9
11TDD772	Doris	Central	3	8-May-11	8:20	1:00	SRK	JA	Jul-2011	145.3	228.2	82.9
11TDD772	Doris	Central	4	11-May-11	1:20	0:45	SRK	JA	Jul-2011	283.3	321.2	37.9
11TDD772	Doris	Central	5	11-May-11	2:10	1:00	SRK	JA	Jul-2011	289.3	321.2	31.9
DCN-20-52118	Doris	-	-	-	-	-	HR	GF	Apr-2022	0	123.5	123.5
DCN-20-52119	Doris	-	-	-	-	-	HR	GF	Apr-2022	0	102.02	102.0
DCN-20-52123	Doris	-	-	-	-	-	HR	GF	Apr-2022	0	114	114.0

Test Information										Test Interval along hole (mah)		
ID1	Area	Sub-Area	Test Number	Date	Time test started	Time not drilled (hours)	QA/QC	Last checked by	Date checked	Top	Bottom	Interval length
DCN-20-52125	Doris	-	-	-	-	-	HR	GF	Apr-2022	0	174	174.0
DCN-20-52126	Doris	-	-	-	-	-	HR	GF	Apr-2022	0	170	170.0
DCN-20-52127	Doris	-	-	-	-	-	HR	GF	Apr-2022	0	177	177.0
DCN-20-52127	Doris	-	-	-	-	-	HR	GF	Apr-2022	0	177	177.0
DCN-20-52128	Doris	-	-	-	-	-	HR	GF	Apr-2022	0	174.02	174.0
DCN-20-52128	Doris	-	-	-	-	-	HR	GF	Apr-2022	0	174.02	174.0
DCN-20-52221	Doris	-	-	-	-	-	HR	GF	Apr-2022	0	128.67	128.7
DCN-20-52222	Doris	-	-	-	-	-	HR	GF	Apr-2022	0	130.22	130.2
DCN-20-52223	Doris	-	-	-	-	-	HR	GF	Apr-2022	0	145.1	145.1
DCN-20-52225	Doris	-	-	-	-	-	HR	GF	Apr-2022	0	377.02	377.0
DCN-20-52228	Doris	-	-	-	-	-	HR	GF	Apr-2022	0	140.22	140.2
DCN-20-52229	Doris	-	-	-	-	-	HR	GF	Apr-2022	0	110.42	110.4
DCN-20-52230	Doris	-	-	-	-	-	HR	GF	Apr-2022	0	170.7	170.7
DCN-20-52230	Doris	-	-	-	-	-	HR	GF	Apr-2022	0	170.7	170.7

Test Information										Test Interval along hole (mah)		
ID1	Area	Sub-Area	Test Number	Date	Time test started	Time not drilled (hours)	QA/QC	Last checked by	Date checked	Top	Bottom	Interval length
DCN-20-52231	Doris	-	-	-	-	-	HR	GF	Apr-2022	0	130	130.0
DCN-20-52232	Doris	-	-	-	-	-	HR	GF	Apr-2022	0	125.3	125.3
DCN-20-52232	Doris	-	-	-	-	-	HR	GF	Apr-2022	0	125.3	125.3
DCN-20-52234	Doris	-	-	-	-	-	HR	GF	Apr-2022	0	143	143.0
DCN-20-52235	Doris	-	-	-	-	-	HR	GF	Apr-2022	0	100	100.0
DCN-20-52236	Doris	-	-	-	-	-	HR	GF	Apr-2022	0	338.7	338.7
DCN-20-52237	Doris	-	-	-	-	-	HR	GF	Apr-2022	0	127.02	127.0
DCN-20-52238	Doris	-	-	-	-	-	HR	GF	Apr-2022	0	129.5	129.5
DCN-20-52241	Doris	-	-	-	-	-	HR	GF	Apr-2022	0	209.62	209.6
DCN-21-50206	Doris	-	-	-	-	-	HR	GF	Apr-2022	0	89.72	89.7
DCN-21-50207	Doris	-	-	-	-	-	HR	GF	Apr-2022	0	104.97	105.0
DCN-21-50211	Doris	-	-	-	-	-	HR	GF	Apr-2022	0	111.7	111.7
DCN-21-50219	Doris	-	-	-	-	-	HR	GF	Apr-2022	0	110.62	110.6
DCN-21-50221	Doris	-	-	-	-	-	HR	GF	Apr-2022	0	102.52	102.5
DCN-21-50222	Doris	-	-	-	-	-	HR	GF	Apr-2022	0	128.42	128.4

Test Information										Test Interval along hole (mah)		
ID1	Area	Sub-Area	Test Number	Date	Time test started	Time not drilled (hours)	QA/QC	Last checked by	Date checked	Top	Bottom	Interval length
DCN-21-50228	Doris	-	-	-	-	-	HR	GF	Apr-2022	0	122	122.0
DCN-21-50240	Doris	-	-	-	-	-	HR	GF	Apr-2022	0	133.32	133.3
DCN-21-50242	Doris	-	-	-	-	-	HR	GF	Apr-2022	0	137.32	137.3
DCN-21-50246	Doris	-	-	-	-	-	HR	GF	Apr-2022	0	167.42	167.4
DCN-21-50247	Doris	-	-	-	-	-	HR	GF	Apr-2022	0	99	99.0
DCN-21-50248	Doris	-	-	-	-	-	HR	GF	Apr-2022	0	217	217.0
DCN-21-50249	Doris	-	-	-	-	-	HR	GF	Apr-2022	0	187.02	187.0
DCN-21-50250	Doris	-	-	-	-	-	HR	GF	Apr-2022	0	107.8	107.8
DCN-21-50252	Doris	-	-	-	-	-	HR	GF	Apr-2022	0	89	89.0
DCN-21-50264	Doris	-	-	-	-	-	HR	GF	Apr-2022	0	104.02	104.0
DCN-21-50267	Doris	-	-	-	-	-	HR	GF	Apr-2022	0	139.02	139.0
DCN-21-52246	Doris	-	-	-	-	-	HR	GF	Apr-2022	0	115.32	115.3
DCN-21-52247	Doris	-	-	-	-	-	HR	GF	Apr-2022	0	119.62	119.6
HB-BCO-22-150	Doris	-	12	20-Nov-22	-	-	Lorax	GF	Oct-2024	22.3	378	355.7
HB-BCO-22-150	Doris	-	23	30-Nov-22	-	-	Lorax	GF	Oct-2024	376.3	699	322.7
HB-BCO-22-150	Doris	-	24	1-Dec-22	-	-	Lorax	GF	Oct-2024	22.3	699	676.7

Test Information				Test Interval - Vertical depth (mbgs)					Hydraulic Conductivity K (m/s)				Test Description			
ID1	Area	Sub-Area	Test Number	Hole Dip (degrees)	Top	Bottom	Interval length	Mid point	Max	Geomean	Min	Valid K (excl. poor or in prmfst)	Geol. Type	Test Zone Lithology	Test Quality	Subprmf, talik/ Frozen
08TDD628	Doris	Central	1	62.3	46.2	124.8	78.6	85.5	2.8E-08	2.0E-08	1.2E-08	**2.0E-08**	BDR	Deformation zone with basalts and foliation	G	-
08TDD630	Doris	Central	1	65.0	29.2	56.2	27.0	42.7	1.5E-07	1.2E-07	9.7E-08	**1.2E-07**	BDR	Basalt	G	-
08TDD630	Doris	Central	2	65.0	89.9	121.4	31.5	105.7	3.1E-07	2.4E-07	2.1E-07	**2.4E-07**	BDR	Foliated Basalt	G	-
08TDD630	Doris	Central	3	65.0	125.3	148.6	23.4	136.9	1.4E-08	1.3E-08	1.2E-08	**1.3E-08**	BDR	Foliated Basalt	G	-
08TDD630	Doris	Central	4	65.0	150.6	176.7	26.1	163.7	2.4E-08	2.2E-08	2.1E-08	**2.2E-08**	BDR	Basalt and diabase contact	G	-
08TDD630	Doris	Central	5	65.0	182.3	238.4	56.0	210.4	7.5E-08	6.6E-08	6.1E-08	**6.6E-08**	BDR	Basalt-diabase-gabbro; quartz veining	G	-
08TDD631	Doris	Central	1	80.0	38.6	64.0	25.4	51.3	4.6E-08	3.5E-08	2.1E-08	**3.5E-08**	BDR	Foliated Basalt w calcite and dolomite veining	G	-
08TDD631	Doris	Central	2	80.0	94.7	120.1	25.4	107.4	1.0E-08	3.5E-09	1.4E-09	**3.5E-09**	BDR	Basalt	G	-
08TDD632	Doris	North	1	61.0	42.2	106.7	64.5	74.4	5.0E-10	3.0E-10	1.7E-10	**#N/A**	BDR	Foliated Basalt	G	Frozen
08TDD632	Doris	North	2	61.0	152.4	214.3	61.9	183.3	2.4E-10	1.4E-10	5.5E-11	**#N/A**	BDR	Foliated to Massive Basalt; diabase contact; structure 178.7-180.2m - fault and gouge	G	Frozen
08TDD632	Doris	North	3	61.0	231.1	295.6	64.5	263.3	1.7E-10	1.2E-10	9.4E-11	**#N/A**	BDR	Foliated Basalt and Diabase	OK	Frozen
08TDD632	Doris	North	4	61.0	296.7	350.7	54.1	323.7	2.2E-10	9.6E-11	4.7E-11	**#N/A**	BDR	pillow basalt below flow basalts	OK	Frozen
08TDD633	Doris	Central	1	55.0	12.5	41.0	28.5	26.7	1.1E-09	3.6E-10	3.9E-10	**#N/A**	BDR	Foliated Basalt	G	Frozen
08TDD633	Doris	Central	2	55.0	128.0	178.6	50.6	153.3	2.6E-10	6.3E-11	#N/A	**#N/A**	BDR	Foliated Basalt	G	Frozen
08TDD633	Doris	Central	3	55.0	228.7	279.3	50.6	254.0	4.3E-09	3.4E-09	2.5E-09	**#N/A**	BDR	Foliated Basalt	G	Partially frozen
08TDD633	Doris	Central	4	55.0	292.6	328.5	35.9	310.5	2.1E-10	4.8E-11	2.2E-10	**4.8E-11**	BDR	Diabase/foliated basalt contact - mostly in diabase; RZ at 357m along upper contact	G	-
08TDD634	Doris	North	1	60.0	37.5	121.5	84.0	79.5	#N/A	3.0E-10	#N/A	**#N/A**	BDR	Basalt, basalt-dibase contact at 116 m	na	Frozen
10WBW001	Doris	Central	1	62.3	22.1	55.8	33.6	39.0	2.4E-06	1.4E-06	1.0E-06	**1.4E-06**	BDR	Fractured basalt. Loss of circulation during drilling in this zone.	G	-
10WBW001	Doris	Central	2	62.3	56.7	90.3	33.6	73.5	5.6E-07	4.7E-07	3.7E-07	**4.7E-07**	BDR	Fractured basalt with foliation. Jointed diabase in test zone, contact also jointed.	G	-
10WBW001	Doris	Central	3	62.3	107.6	127.9	20.4	117.8	6.5E-07	3.8E-07	2.2E-07	**#N/A**	BDR	[packer bybass ignore results]	P	-
10WBW001	Doris	Central	4	62.3	91.2	127.9	36.7	109.6	3.8E-07	2.8E-07	1.8E-07	**#N/A**	BDR	[packer bybass ignore results]	P	-
10WBW001	Doris	Central	5	62.3	136.4	181.3	45.0	158.8	3.3E-09	2.6E-09	2.1E-09	**2.6E-09**	BDR	Altered and foliated basalt, some heavy foliation but low joint frequency.	G	-
10WBW001	Doris	Central	6	62.3	91.2	136.4	45.2	113.8	6.7E-08	5.2E-08	4.1E-08	**5.2E-08**	BDR	Same as test 6a and 5.	G	-

Test Information				Test Interval - Vertical depth (mbgs)					Hydraulic Conductivity K (m/s)				Test Description			
ID1	Area	Sub-Area	Test Number	Hole Dip (degrees)	Top	Bottom	Interval length	Mid point	Max	Geomean	Min	Valid K (excl. poor or in prmfst)	Geol. Type	Test Zone Lithology	Test Quality	Subprmf, talik/ Frozen
10WBW001	Doris	Central	7	62.3	179.7	223.1	43.4	201.4	1.2E-07	9.4E-08	7.0E-08	9.4E-08	BDR	Basalt with quartz veins and two small dykes. Higher FF/m around dykes. Slow artesian flow from rods before test, shut in pressure low, artesian head ~ 3m above Doris Lk level estimate. Formation could be pressurized from other drills.	G	-
10WBW001	Doris	Central	8	62.3	223.1	247.0	23.9	235.1	2.0E-06	1.5E-06	1.3E-06	1.5E-06	BDR	Basalt, quartz and dolomite veins (2m) with fractures (no recovery). Main ore body. Loss of pressue during drilling, artesian flow source, and also reach limit of injection rate.	G	-
10WBW001	Doris	Central	9	62.3	247.0	263.0	15.9	255.0	1.2E-08	9.6E-09	7.7E-09	9.6E-09	BDR	Basalt, a few rubble zones or small faults between the altered baslat zones.	G	-
10WBW001	Doris	Central	10	62.3	263.0	305.5	42.5	284.2	8.5E-09	7.2E-09	5.8E-09	7.2E-09	BDR	Altered foliated basalt, intermediate dyke with broken contact, unaltered basalt.	G	-
10WBW001	Doris	Central	11	62.3	305.5	342.6	37.2	324.1	3.3E-08	2.7E-08	2.3E-08	2.7E-08	BDR	Basalt. Major diabase upper contact with only minor jointing.	G	-
10WBW001	Doris	Central	12	62.3	342.6	374.1	31.4	358.4	2.9E-11	1.4E-11	#N/A	1.4E-11	BDR	Diabase, very low FF/m.	G	-
10WBW001	Doris	Central	13	62.3	374.5	417.0	42.5	395.8	2.2E-11	1.4E-11	#N/A	1.4E-11	BDR	Diabase, very low FF/m.	G	-
10WBW001	Doris	Central	14	62.3	417.0	499.4	82.3	458.2	6.4E-09	5.1E-09	4.1E-09	5.1E-09	BDR	Major diabase lower contact, then fractured foliated vuggy basalt below. 83% of test zone is low FF/m diabase.	G	-
10WBW001	Doris	Central	14a	62.3	485.2	499.4	14.2	492.3	3.7E-08	2.9E-08	2.4E-08	2.9E-08	BDR	The result from test 14 if flow only came from the vuggy basalt below the diabase.	G	-
10WBW001	Doris	Central	6a	62.3	91.2	181.3	90.1	136.3	3.4E-08	2.7E-08	2.1E-08	2.7E-08	BDR	Competent basalt, small shears possible including alpha fault?, foliation. Test result determined by subtracting result from test 6a from test 5.	G	-
10WBW001	Doris	Central	8a	62.3	223.1	263.0	39.8	243.0	1.2E-06	9.2E-07	7.6E-07	9.2E-07	BDR	Same as test 8 and 9.	G	-
10WBW002	Doris	North	1	75.4	389.3	466.4	77.1	427.9	5.8E-10	2.6E-10	9.9E-11	2.6E-10	BDR	Basalt, foliated and unfoliated. Small diabase dyke. Very low fracture frequency. Possibly in permafrost	G	-

Test Information				Test Interval - Vertical depth (mbgs)					Hydraulic Conductivity K (m/s)				Test Description			
ID1	Area	Sub-Area	Test Number	Hole Dip (degrees)	Top	Bottom	Interval length	Mid point	Max	Geomean	Min	Valid K (excl. poor or in prmfst)	Geol. Type	Test Zone Lithology	Test Quality	Subprmf, talik/ Frozen
10WBW002	Doris	North	2	75.4	432.9	466.4	33.6	449.6	3.2E-09	9.6E-10	3.7E-10	**9.6E-10**	BDR	Unfoliated basalt. Small diabase dyke. Very low fracture frequency. Possibly in permafrost.	G	-
10WBW002	Doris	North	3	75.4	467.7	501.3	33.6	484.5	2.5E-10	7.3E-11	#N/A	**7.3E-11**	BDR	Basalt with small diabase dykes. Possibly in permafrost	G	-
10WBW002	Doris	North	4	75.4	502.5	550.6	48.1	526.6	3.9E-09	7.5E-10	1.2E-10	**7.5E-10**	BDR	Basalt, unfoliated. Low fracture frequency.	G	-
10WBW002	Doris	North	5	75.4	551.9	582.6	30.7	567.2	4.5E-09	1.6E-10	1.3E-10	**1.6E-10**	BDR	Basalt, unfoliated. Low fracture frequency.	G	-
11TDD763	Doris	Central	1	57.0	43.9	173.6	129.7	108.7	8.0E-08	7.3E-08	6.7E-08	**7.3E-08**	BDR	Mafic volcanic flow w 5m ore zone and 5m dyke	G	-
11TDD764	Doris	Und Con	1	59.0	35.5	112.4	76.9	73.9	2.3E-07	2.0E-07	1.8E-07	**2.0E-07**	BDR	Mafic volcanic pillow w Gabbro intrusion (95-114m), occasional mafic dyke	G	-
11TDD764	Doris	Und Con	2	53.0	211.1	272.4	61.3	241.7	5.2E-09	4.2E-09	2.8E-09	**4.2E-09**	BDR	Mafic volcanic pillow w ore zones (275-276m, 293-296m).	G	-
11TDD765	Doris	Near Mine	1	45.0	219.4	227.7	8.3	223.6	7.2E-09	4.4E-09	2.5E-09	**#N/A**	BDR	Diabase/basalt contact @ 318.5m	G	Frozen
11TDD765	Doris	Near Mine	2	44.0	276.5	303.7	27.2	290.1	5.7E-10	3.9E-10	1.0E-10	**#N/A**	BDR	Deep basalt	G	Frozen
11TDD766	Doris	Central	1	60.0	24.9	44.3	19.4	34.6	2.6E-06	1.8E-06	1.4E-06	**#N/A**	BDR	Mafic volcanic flow w felsic dyke (28-34m)	P	-
11TDD766	Doris	Central	2	60.0	88.1	113.0	24.9	100.5	1.7E-09	8.9E-10	8.5E-10	**8.9E-10**	BDR	Mafic volcanic pillow	G	-
11TDD766	Doris	Central	3	60.0	172.2	208.1	35.9	190.1	5.5E-08	4.2E-08	3.3E-08	**#N/A**	BDR	Mafic volcanic flow	P	-
11TDD768	Doris	Central	1	61.0	60.7	91.1	30.4	75.9	3.4E-07	1.3E-07	6.6E-08	**1.3E-07**	BDR	Mafic volcanic pillow foliated basalt w volcanic flow feldspar (82-86m)	OK	-
11TDD768	Doris	Central	2	61.0	97.4	133.1	35.7	115.3	6.9E-09	3.4E-09	1.2E-09	**3.4E-09**	BDR	Mafic volcanic pillow (foliated basalt) w ore zone (122-131m)	G	-
11TDD768	Doris	Central	3	61.0	197.1	211.8	14.7	204.5	#N/A	#N/A	#N/A	**#N/A**	BDR	mafic volcanic pillow	P	-
11TDD768	Doris	Central	4	58.0	191.2	228.3	37.1	209.7	2.3E-08	1.8E-08	1.5E-08	**1.8E-08**	BDR	Mafic volcanic pillow (foliated basalt) w ore zone (231-247m)	G	-
11TDD768	Doris	Central	5	57.0	196.6	225.8	29.2	211.2	1.9E-08	1.7E-08	1.5E-08	**1.7E-08**	BDR	Mafic volcanic pillow (foliated basalt) w ore zone (231-247m)	G	-
11TDD768	Doris	Central	6	57.0	224.3	250.9	26.6	237.6	6.2E-07	5.9E-07	5.7E-07	**5.9E-07**	BDR	Mafic volcanic pillow (foliated basalt)	G	-
11TDD769	Doris	Central	1	67.0	28.0	35.2	7.2	31.6	7.3E-07	5.9E-07	4.3E-07	**5.9E-07**	BDR	Mafic volcanic pillow (foliated basalt); major structure (20cm) shear zone	G	-
11TDD769	Doris	Central	2	65.0	117.3	129.8	12.5	123.5	3.3E-06	2.9E-06	2.5E-06	**2.9E-06**	BDR	Mafic volcanic pillow (foliated basalt); major joints with gouge present	G	-
11TDD769	Doris	Central	3	64.0	170.2	179.9	9.7	175.1	8.8E-07	7.5E-07	6.8E-07	**7.5E-07**	BDR	Mafic volcanic pillow (foliated basalt); natural rubble zone present	G	-
11TDD769	Doris	Central	4	65.0	271.3	280.0	8.8	275.7	#N/A	#N/A	#N/A	**#N/A**	BDR	Diabase/basalt contact	P	-

Test Information				Test Interval - Vertical depth (mbgs)					Hydraulic Conductivity K (m/s)				Test Description			
ID1	Area	Sub-Area	Test Number	Hole Dip (degrees)	Top	Bottom	Interval length	Mid point	Max	Geomean	Min	Valid K (excl. poor or in prmfst)	Geol. Type	Test Zone Lithology	Test Quality	Subprmf, talik/ Frozen
11TDD769	Doris	Central	1ss	66.0	117.9	264.9	147.0	191.4	2.8E-07	3.2E-08	#N/A	3.2E-08	BDR	Primarily Mafic volcanic pillow, w 3m gabbro and 5m diabase intrusion, + ore zone.	OK	-
11TDD769	Doris	Central	2ss	66.0	139.9	264.9	125.1	202.4	1.7E-07	1.0E-07	7.5E-08	1.0E-07	BDR	Primarily Mafic volcanic pillow, w 3m gabbro and 5m diabase intrusion, + ore zone.	G	-
11TDD771	Doris	Central	1	80.0	47.9	73.1	25.3	60.5	4.7E-08	3.4E-08	2.5E-08	3.4E-08	BDR	Mafic volcanic pillow (foliated basalt)	G	-
11TDD771	Doris	Central	2	79.0	110.2	132.5	22.3	121.4	2.6E-08	1.7E-08	1.2E-08	1.7E-08	BDR	Primarily quartz (ore zone) w mafic volcanic pillow (112-118m)	G	-
11TDD771	Doris	Central	3	78.0	115.7	158.5	42.7	137.1	1.7E-09	5.3E-10	5.2E-10	5.3E-10	BDR	Primarily quartz (discontinuous) w mafic volcanic pillow (153-162m); small structure	G	-
11TDD771	Doris	Central	4	78	148.0	193.7	45.7	170.8	3.0E-06	7.1E-08	2.8E-08	7.1E-08	BDR	Primarily volcanic pillow w quartz (ore zone, 166-171m); structure at ore zone contact	G	-
11TDD771	Doris	Central	5	78	177.3	193.7	16.3	185.5	4.5E-06	1.9E-07	7.3E-08	1.9E-07	BDR	Primarily quartz (discontinuous) w mafic volcanic pillow (181-186m); structure at contact with ore	G	-
11TDD771	Doris	Central	6	77	226.2	286.5	60.3	256.3	1.4E-07	9.5E-08	6.9E-08	9.5E-08	BDR	Mafic volcanic pillow (foliated basalt) to 286, above diabase; contact	G	-
11TDD772	Doris	Central	1	65	50.1	79.0	28.9	64.6	3.6E-08	3.3E-08	3.0E-08	3.3E-08	BDR	Mafic volcanic pillow w quartz (ore zone, 57-59m); fault C3PO, NW6	G	-
11TDD772	Doris	Central	2	65	80.0	133.4	53.4	106.7	1.9E-08	1.6E-08	1.2E-08	1.6E-08	BDR	Mafic volcanic pillow (foliated basalt)	G	-
11TDD772	Doris	Central	3	65	131.7	206.8	75.1	169.3	1.9E-08	1.7E-08	1.5E-08	1.7E-08	BDR	Mafic volcanic pillow (foliated basalt) w felsic dyke (200-202m)	G	-
11TDD772	Doris	Central	4	65	256.8	291.1	34.3	273.9	7.4E-08	6.0E-08	4.6E-08	6.0E-08	BDR	Mafic volcanic pillow (foliated basalt) w quartz (ore zone); fault Force 1	G	-
11TDD772	Doris	Central	5	65	262.2	291.1	28.9	276.7	5.8E-08	4.9E-08	4.1E-08	4.9E-08	BDR	Mafic volcanic pillow (foliated basalt) w quartz (ore zone)	G	-
DCN-20-52118	Doris	-	-	see survey and HR compil	#N/A	#N/A	0.8	73.0	-	1.0E-06	-	1.0E-06	BDR	Bedrock	na	-
DCN-20-52119	Doris	-	-	see survey and HR compil	#N/A	#N/A	19.8	97.4	-	1.0E-06	-	1.0E-06	BDR	Bedrock	na	-
DCN-20-52123	Doris	-	-	see survey and HR compil	#N/A	#N/A	42.0	118.9	-	4.0E-08	-	4.0E-08	BDR	Bedrock	na	-

Test Information				Test Interval - Vertical depth (mbgs)					Hydraulic Conductivity K (m/s)				Test Description			
ID1	Area	Sub-Area	Test Number	Hole Dip (degrees)	Top	Bottom	Interval length	Mid point	Max	Geomean	Min	Valid K (excl. poor or in prmfst)	Geol. Type	Test Zone Lithology	Test Quality	Subprmf, talik/ Frozen
DCN-20-52125	Doris	-	-	see survey and HR compil	#N/A	#N/A	32.7	102.7	-	2.0E-07	-	**2.0E-07**	BDR	Bedrock	na	-
DCN-20-52126	Doris	-	-	see survey and HR compil	#N/A	#N/A	63.1	136.0	-	4.0E-06	-	**4.0E-06**	BDR	Bedrock	na	-
DCN-20-52127	Doris	-	-	see survey and HR compil	#N/A	#N/A	2.8	73.1	-	8.0E-07	-	**8.0E-07**	BDR	Bedrock	na	-
DCN-20-52127	Doris	-	-	see survey and HR compil	#N/A	#N/A	2.8	73.1	-	4.0E-07	-	**4.0E-07**	BDR	Bedrock	na	-
DCN-20-52128	Doris	-	-	see survey and HR compil	#N/A	#N/A	32.7	107.4	-	5.0E-07	-	**5.0E-07**	BDR	Bedrock	na	-
DCN-20-52128	Doris	-	-	see survey and HR compil	#N/A	#N/A	32.7	107.4	-	2.0E-07	-	**2.0E-07**	BDR	Bedrock	na	-
DCN-20-52221	Doris	-	-	see survey and HR compil	#N/A	#N/A	0.5	72.2	-	3.0E-07	-	**3.0E-07**	BDR	Bedrock	na	-
DCN-20-52222	Doris	-	-	see survey and HR compil	#N/A	#N/A	40.4	116.6	-	4.0E-08	-	**4.0E-08**	BDR	Bedrock	na	-
DCN-20-52223	Doris	-	-	see survey and HR compil	#N/A	#N/A	69.8	146.5	-	6.0E-07	-	**6.0E-07**	BDR	Bedrock	na	-
DCN-20-52225	Doris	-	-	see survey and HR compil	#N/A	#N/A	66.4	141.1	-	1.0E-07	-	**1.0E-07**	BDR	Bedrock	na	-
DCN-20-52228	Doris	-	-	see survey and HR compil	#N/A	#N/A	0.5	70.2	-	3.0E-07	-	**3.0E-07**	BDR	Bedrock	na	-
DCN-20-52229	Doris	-	-	see survey and HR compil	#N/A	#N/A	22.7	90.9	-	2.0E-09	-	**2.0E-09**	BDR	Bedrock	na	-
DCN-20-52230	Doris	-	-	see survey and HR compil	#N/A	#N/A	22.7	90.9	-	3.0E-08	-	**3.0E-08**	BDR	Bedrock	na	-
DCN-20-52230	Doris	-	-	see survey and HR compil	#N/A	#N/A	36.2	110.9	-	1.0E-07	-	**1.0E-07**	BDR	Bedrock	na	-

Test Information				Test Interval - Vertical depth (mbgs)					Hydraulic Conductivity K (m/s)				Test Description			
ID1	Area	Sub-Area	Test Number	Hole Dip (degrees)	Top	Bottom	Interval length	Mid point	Max	Geomean	Min	Valid K (excl. poor or in prmfst)	Geol. Type	Test Zone Lithology	Test Quality	Subprmf, talik/ Frozen
DCN-20-52231	Doris	-	-	see survey and HR compil	#N/A	#N/A	49.2	125.9	-	1.0E-07	-	1.0E-07	BDR	Bedrock	na	-
DCN-20-52232	Doris	-	-	see survey and HR compil	#N/A	#N/A	49.2	125.9	-	5.0E-08	-	5.0E-08	BDR	Bedrock	na	-
DCN-20-52232	Doris	-	-	see survey and HR compil	#N/A	#N/A	2.8	69.5	-	4.0E-08	-	4.0E-08	BDR	Bedrock	na	-
DCN-20-52234	Doris	-	-	see survey and HR compil	#N/A	#N/A	17.6	93.6	-	1.0E-08	-	1.0E-08	BDR	Bedrock	na	-
DCN-20-52235	Doris	-	-	see survey and HR compil	#N/A	#N/A	104.3	177.6	-	3.0E-08	-	3.0E-08	BDR	Bedrock	na	-
DCN-20-52236	Doris	-	-	see survey and HR compil	#N/A	#N/A	52.8	132.2	-	9.0E-07	-	9.0E-07	BDR	Bedrock	na	-
DCN-20-52237	Doris	-	-	see survey and HR compil	#N/A	#N/A	59.6	142.8	-	1.0E-08	-	1.0E-08	BDR	Bedrock	na	-
DCN-20-52238	Doris	-	-	see survey and HR compil	#N/A	#N/A	68.2	144.3	-	1.0E-06	-	1.0E-06	BDR	Bedrock	na	-
DCN-20-52241	Doris	-	-	see survey and HR compil	#N/A	#N/A	8.6	84.9	-	3.0E-07	-	3.0E-07	BDR	Bedrock	na	-
DCN-21-50206	Doris	-	-	see survey and HR compil	#N/A	#N/A	29.6	108.2	-	2.0E-07	-	2.0E-07	BDR	Bedrock	na	-
DCN-21-50207	Doris	-	-	see survey and HR compil	#N/A	#N/A	11.0	85.1	-	4.0E-07	-	4.0E-07	BDR	Bedrock	na	-
DCN-21-50211	Doris	-	-	see survey and HR compil	#N/A	#N/A	22.7	93.6	-	5.0E-07	-	5.0E-07	BDR	Bedrock	na	-
DCN-21-50219	Doris	-	-	see survey and HR compil	#N/A	#N/A	12.2	82.4	-	1.0E-07	-	1.0E-07	BDR	Bedrock	na	-
DCN-21-50221	Doris	-	-	see survey and HR compil	#N/A	#N/A	36.5	108.7	-	2.0E-07	-	2.0E-07	BDR	Bedrock	na	-
DCN-21-50222	Doris	-	-	see survey and HR compil	#N/A	#N/A	30.4	258.5	-	1.0E-07	-	1.0E-07	BDR	Bedrock	na	-

Test Information				Test Interval - Vertical depth (mbgs)					Hydraulic Conductivity K (m/s)				Test Description			
ID1	Area	Sub-Area	Test Number	Hole Dip (degrees)	Top	Bottom	Interval length	Mid point	Max	Geomean	Min	Valid K (excl. poor or in prmfst)	Geol. Type	Test Zone Lithology	Test Quality	Subprmf, talik/ Frozen
DCN-21-50228	Doris	-	-	see survey and HR compil	#N/A	#N/A	53.5	133.9	-	5.0E-07	-	**5.0E-07**	BDR	Bedrock	na	-
DCN-21-50240	Doris	-	-	see survey and HR compil	#N/A	#N/A	54.7	135.9	-	1.0E-07	-	**1.0E-07**	BDR	Bedrock	na	-
DCN-21-50242	Doris	-	-	see survey and HR compil	#N/A	#N/A	73.0	165.0	-	7.0E-08	-	**7.0E-08**	BDR	Bedrock	na	-
DCN-21-50246	Doris	-	-	see survey and HR compil	#N/A	#N/A	24.5	115.4	-	2.0E-07	-	**2.0E-07**	BDR	Bedrock	na	-
DCN-21-50247	Doris	-	-	see survey and HR compil	#N/A	#N/A	71.8	164.6	-	3.0E-07	-	**3.0E-07**	BDR	Bedrock	na	-
DCN-21-50248	Doris	-	-	see survey and HR compil	#N/A	#N/A	70.4	163.0	-	3.0E-07	-	**3.0E-07**	BDR	Bedrock	na	-
DCN-21-50249	Doris	-	-	see survey and HR compil	#N/A	#N/A	25.6	117.1	-	6.0E-07	-	**6.0E-07**	BDR	Bedrock	na	-
DCN-21-50250	Doris	-	-	see survey and HR compil	#N/A	#N/A	38.7	202.1	-	1.0E-06	-	**1.0E-06**	BDR	Bedrock	na	-
DCN-21-50252	Doris	-	-	see survey and HR compil	#N/A	#N/A	25.8	253.8	-	9.0E-07	-	**9.0E-07**	BDR	Bedrock	na	-
DCN-21-50264	Doris	-	-	see survey and HR compil	#N/A	#N/A	8.9	216.4	-	4.0E-07	-	**4.0E-07**	BDR	Bedrock	na	-
DCN-21-50267	Doris	-	-	see survey and HR compil	#N/A	#N/A	34.0	108.2	-	9.0E-10	-	**9.0E-10**	BDR	Bedrock	na	-
DCN-21-52246	Doris	-	-	see survey and HR compil	#N/A	#N/A	46.1	120.9	-	2.0E-07	-	**2.0E-07**	BDR	Bedrock	na	-
DCN-21-52247	Doris	-	-	see survey and HR compil	#N/A	#N/A	79.4	151.6	-	1.0E-07	-	**1.0E-07**	BDR	Bedrock	na	-
HB-BCO-22-150	Doris	-	12	see survey and Lorax 2024	21.4	346.5	325.1	162.6	-	1.0E-10	-	**#N/A**	BDR	Bedrock	G	Frozen
HB-BCO-22-150	Doris	-	23	see survey and Lorax 2024	345.0	608.3	263.3	131.7	-	3.0E-10	-	**#N/A**	BDR	Bedrock	G	Frozen
HB-BCO-22-150	Doris	-	24	see survey and Lorax 2024	21.4	608.3	586.9	293.5	-	7.0E-10	-	**#N/A**	BDR	Bedrock	G	Frozen

Test Information										Test Interval along hole (mah)		
ID1	Area	Sub-Area	Test Number	Date	Time test started	Time not drilled (hh:mm)	QA/QC'ed by	Last checked by	Date checked	Top	Bottom	Interval length
10WBW003	Madrid South	Patch 14	1	1-Jul-10	17:15	2:45	SRK	JA	Jul-2011	96.4	173.2	76.8
10WBW003	Madrid South	Patch 14	2	2-Jul-10	17:30	2:12	SRK	JA	Jul-2011	171.4	248.2	76.8
10WBW003	Madrid South	Patch 14	3	3-Jul-10	12:39	2:46	SRK	JA	Jul-2011	246.4	293.2	46.8
10WBW003	Madrid South	Patch 14	4	5-Jul-10	10:00	2:26	SRK	JA	Jul-2011	291.4	392.2	100.8
10WBW003	Madrid South	Patch 14	5	6-Jul-10	16:00	2:00	SRK	JA	Jul-2011	393.4	458.2	64.8
10WBW003	Madrid South	Patch 14	6	7-Jul-10	16:00	2:10	SRK	JA	Jul-2011	456.4	500.2	43.8
10WBW003	Madrid South	Patch 14	7	9-Jul-10	10:00	1:45	SRK	JA	Jul-2011	498.4	548.2	49.8
11PSD259	Madrid South	Patch 14	1	9-Mar-11	13:30	2:00	SRK	JA	Jul-2011	53.3	161.0	107.7
11PSD260	Madrid South	Patch 14	1	10-Mar-11	14:00	1:03	SRK	JA	Jul-2011	51.3	183.0	131.7
11PSD260	Madrid South	Patch 14	2	18-Mar-11	12:40	1:18	SRK	JA	Jul-2011	553.3	618.0	64.7
11PSD260	Madrid South	Patch 14	3	18-Mar-11	14:30	1:25	SRK	JA	Jul-2011	493.3	618.0	124.7
11PSD261	Madrid South	Patch 14	1	15-Mar-11	14:40	1:35	SRK	JA	Jul-2011	126.3	212.0	85.7
11PSD261	Madrid South	Patch 14	2	19-Mar-11	11:20	1:15	SRK	JA	Jul-2011	357.2	431.0	73.8
11PSD263	Madrid South	Patch 14	1	21-Mar-11	13:30	1:30	SRK	JA	Jul-2011	96.3	125.0	28.7
11PSD267	Madrid South	Patch 14	1	25-Mar-11	15:00	1:40	SRK	JA	Jul-2011	101.0	152.0	51.0
11PSD267	Madrid South	Patch 14	2	28-Mar-11	12:30	1:30	SRK	JA	Jul-2011	270.3	350.0	79.7

Test Information										Test Interval along hole (mah)		
ID1	Area	Sub-Area	Test Number	Date	Time test started	Time not drilled (hh:mm)	QA/QC'ed by	Last checked by	Date checked	Top	Bottom	Interval length
11PSD267	Madrid South	Patch 14	3	28-Mar-11	14:00	1:00	SRK	JA	Jul-2011	309.3	350.0	40.7
11PSD269	Madrid South	Patch 14	1	31-Mar-11	14:45	0:45	SRK	JA	Jul-2011	117.3	191.0	73.7
11PSD269	Madrid South	Patch 14	2	31-Mar-11	15:30	1:45	SRK	JA	Jul-2011	168.3	191.0	22.7
11PSD270	Madrid South	Patch 14	1	8-Apr-11	17:10	2:00	SRK	JA	Jul-2011	450.2	524.0	73.8
11PSD271	Madrid South	Wolverine	1	1-Apr-11	16:50	2:00	SRK	JA	Jul-2011	127.2	201.0	73.8
11PSD275	Madrid South	Patch 14	1	14-Apr-11	12:20	1:10	SRK	JA	Jul-2011	82.3	129.0	46.7
11PSD275A	Madrid South	Patch 14	1	17-Apr-11	15:50	1:25	SRK	JA	Jul-2011	90.3	130.0	39.7
11PSD275A	Madrid South	Patch 14	2	18-Apr-11	16:00	2:00	SRK	JA	Jul-2011	167.3	217.0	49.7
11PSD275A	Madrid South	Patch 14	3	20-Apr-11	15:00	1:30	SRK	JA	Jul-2011	311.3	358.0	46.7
11PSD276	Madrid South	Patch 14	1	14-Apr-11	14:15	1:45	SRK	JA	Jul-2011	73.8	103.0	29.2
11PSD276A	Madrid South	Patch 14	1	16-Apr-11	13:00	2:30	SRK	JA	Jul-2011	101.3	124.4	23.1
11PSD276A	Madrid South	Patch 14	2	18-Apr-11	13:30	1:00	SRK	JA	Jul-2011	180.5	209.7	29.2
11PSD276A	Madrid South	Patch 14	3	18-Apr-11	14:30	1:30	SRK	JA	Jul-2011	134.8	209.7	74.9
11PSD276A	Madrid South	Patch 14	5	22-Apr-11	13:00	3:00	SRK	JA	Jul-2011	363.4	395.6	32.2
11PSD276A	Madrid South	Patch 14	4si	19-Apr-11	10:00	2:45	SRK	JA	Jul-2011	40.1	306.2	266.1
11PSD279	Madrid South	Patch 14	1	25-Apr-11	14:00	1:30	SRK	JA	Jul-2011	70.8	112.2	41.4
11PSD279	Madrid South	Patch 14	2	25-Apr-11	15:30	1:30	SRK	JA	Jul-2011	97.2	112.2	15.0
11PSD279	Madrid South	Patch 14	3	27-Apr-11	14:00	2:00	SRK	JA	Jul-2011	204.9	231.0	26.1
11PSD279	Madrid South	Patch 14	4	30-Apr-11	10:20	2:00	SRK	JA	Jul-2011	284.0	359.0	75.0
11PSD279	Madrid South	Patch 14	5	2-May-11	10:30	6:30	SRK	JA	Jul-2011	357.1	444.4	87.3
11PSD284	Madrid South	Patch 14	1	4-May-11	9:00	2:00	SRK	JA	Jul-2011	52.3	103.0	50.7
11PSD284	Madrid South	Patch 14	2	4-May-11	11:15	1:00	SRK	JA	Jul-2011	77.7	103.0	25.3
HBM-23-085	Madrid South	-	1	24-Mar-23	-	-	Lorax	GF	Apr-2022	51.2	86.0	34.8
HBM-23-085	Madrid South	-	2	26-Mar-23	-	-	Lorax	GF	Apr-2022	84.2	128.0	43.8

Test Information										Test Interval along hole (mah)		
ID1	Area	Sub-Area	Test Number	Date	Time test started	Time not drilled (hh:mm)	QA/QC'ed by	Last checked by	Date checked	Top	Bottom	Interval length
HBM-23-085	Madrid South	-	3	27-Mar-23	-	-	Lorax	GF	Apr-2022	126.2	170.0	43.8
HBM-23-085	Madrid South	-	4	28-Mar-23	-	-	Lorax	GF	Apr-2022	168.2	251.0	82.8
HBM-23-085	Madrid South	-	5	29-Mar-23	-	-	Lorax	GF	Apr-2022	249.2	257.0	7.8
HBM-23-085	Madrid South	-	5	29-Mar-23	-	-	Lorax	GF	Apr-2022	258.2	323.0	64.8
HBM-23-085	Madrid South	-	6	30-Mar-23	-	-	Lorax	GF	Apr-2022	384.2	477.2	93.0
HBM-23-085	Madrid South	-	8	31-Mar-23	-	-	Lorax	GF	Apr-2022	384.2	497.0	112.8
HBM-23-085	Madrid South	-	9	2-Apr-23	-	-	Lorax	GF	Apr-2022	477.2	497.0	19.8
HBM-23-085	Madrid South	-	10	2-Apr-23	-	-	Lorax	GF	Apr-2022	495.2	587.0	91.8
08PMD668	Madrid North	Naartok	1	4-Apr-23	#N/A	#N/A	Test sheet not found	JA	Jul-2011	165.3	176.0	10.8
08PMD669	Madrid North	Naartok	1	28-Jun-08	14:10	2:50	SRK	JA	Jul-2011	318.3	368.0	49.8
08PMD669	Madrid North	Naartok	2	30-Jun-08	10:45	4:15	SRK	JA	Jul-2011	369.3	428.0	58.8
08PMD669	Madrid North	Naartok	3	4-Jul-08	2:17	1:32	SRK	JA	Jul-2011	468.3	530.0	61.8
08PMD671	Madrid North	Naartok	1	#N/A	#N/A	#N/A	Test sheet not found	JA	Jul-2011	160.3	275.0	114.7
08PMD650	Madrid North	Suluk	1	1-May-08	9:45	1:45	SRK	JA	Jul-2011	32.0	36.0	4.0
08PMD650	Madrid North	Suluk	2	4-May-08	8:45	1:45	SRK	JA	Jul-2011	99.0	111.0	12.0
08PMD650	Madrid North	Suluk	3	5-May-08	12:00	4:00	SRK	JA	Jul-2011	133.0	156.0	23.0
08PMD650	Madrid North	Suluk	4	6-May-08	14:00	2:00	SRK	JA	Jul-2011	161.7	196.5	34.8

Test Information										Test Interval along hole (mah)		
ID1	Area	Sub-Area	Test Number	Date	Time test started	Time not drilled (hh:mm)	QA/QC'ed by	Last checked by	Date checked	Top	Bottom	Interval length
08PMD657a	Madrid North	Suluk	1	19-May-08	8:30	1:45	SRK	JA	Jul-2011	92.2	131.0	38.8
08PMD657a	Madrid North	Suluk	2	19-May-08	19:30	3:15	SRK	JA	Jul-2011	123.2	179.0	55.8
08PMD657a	Madrid North	Suluk	3	20-May-08	16:00	1:00	SRK	JA	Jul-2011	179.2	241.0	61.8
08PMD657a	Madrid North	Suluk	4	#N/A	#N/A	#N/A	SRK	JA	Jul-2011	294.0	300.0	6.0
08PSD142	Madrid North	Suluk	1	6-May-08	9:00	1:30	SRK	JA	Jul-2011	60.2	86.0	25.8
08PSD142	Madrid North	Suluk	2	7-May-08	20:30	1:50	SRK	JA	Jul-2011	156.0	182.0	26.0
08PSD142	Madrid North	Suluk	3	8-May-08	19:00	2:30	SRK	JA	Jul-2011	191.3	227.0	35.7
08PSD142	Madrid North	Suluk	4	8-May-08	16:40	1:20	SRK	JA	Jul-2011	248.2	284.0	35.8
08PSD142	Madrid North	Suluk	5	11-May-08	11:00	0:45	SRK	JA	Jul-2011	318.2	356.0	37.8
08PSD143B	Madrid North	Suluk	1	25-May-08	8:00	7:00	SRK	JA	Jul-2011	240.2	293.0	52.8
08PSD143B	Madrid North	Suluk	2	#N/A	#N/A	#N/A	SRK	JA	Jul-2011	#N/A	#N/A	#N/A
08PSD144	Madrid North	Suluk	1	#N/A	#N/A	#N/A	SRK	JA	Jul-2011	246.8	350.0	103.2
HBM-22-059	Madrid North	Naartok	1	2-Nov-22	-	-	Lorax	GF	Apr-2022	333.4	362.2	28.8
HBM-22-059	Madrid North	Naartok	2	3-Nov-22	-	-	Lorax	GF	Apr-2022	362.2	395.2	33.0
HBM-22-059	Madrid North	Naartok	3	4-Nov-22	-	-	Lorax	GF	Apr-2022	393.4	428.2	34.8
HBM-22-059	Madrid North	Naartok	4	5-Nov-22	-	-	Lorax	GF	Apr-2022	426.2	464.2	38.0
HBM-22-059	Madrid North	Naartok	5	7-Nov-22	-	-	Lorax	GF	Apr-2022	465.0	508.8	43.8
HBM-22-059	Madrid North	Naartok	6	8-Nov-22	-	-	Lorax	GF	Apr-2022	507.0	559.8	52.8
HBM-22-059	Madrid North	Naartok	7	10-Nov-22	-	-	Lorax	GF	Apr-2022	558.0	625.8	67.8
HBM-22-059	Madrid North	Naartok	8	12-Nov-22	-	-	Lorax	GF	Apr-2022	624.0	700.8	76.8
HBM-22-059	Madrid North	Naartok	9	12-Nov-22	-	-	Lorax	GF	Apr-2022	501.0	700.8	199.8

Test Information				Test Interval - Vertical depth (mbgs)					Hydraulic Conductivity K (m/s)				Test description	
ID1	Area	Sub-Area	Test Number	Hole Dip (degrees)	Top	Bottom	Interval length	Mid point	Max	Geomean	Min	Valid K (excl. poor or in prmfst)	Geol. type	Test Zone Lithology
10WBW003	Madrid South	Patch 14	1	67.3	88.9	159.8	70.9	124.4	5.5E-09	4.4E-09	3.2E-09	#N/A	BDR	Unstrained volcanics. Permafrost at top of interval.
10WBW003	Madrid South	Patch 14	2	67.3	158.1	229.0	70.9	193.5	6.3E-09	5.4E-09	4.6E-09	5.4E-09	BDR	Weakly strained, complex metavolcanics. Overall competent rock.
10WBW003	Madrid South	Patch 14	3	67.3	227.3	270.5	43.2	248.9	4.5E-11	2.3E-11	1.1E-11	2.3E-11	BDR	Widely intercalated felsic and mafic metavolcanics. Increasing strain. Very low / no flow despite broken zones and faults. Pre-plug blowout flows exceeded injection test flows.
10WBW003	Madrid South	Patch 14	4	67.3	268.8	361.8	93.0	315.3	7.3E-11	5.8E-11	4.5E-11	5.8E-11	BDR	Widely intercalated highly strained felsic and mafic metavolcanics. Some qtz/carbonate veining, some veins brecciated. Increasing strain. Otherwise competent rock Pre-plug blowout flows exceeded injection test flows.
10WBW003	Madrid South	Patch 14	5	67.3	362.9	422.7	59.8	392.8	3.6E-09	2.5E-09	1.8E-09	2.5E-09	BDR	Widely intercalated highly strained felsic and mafic metavolcanics. Permeability consistent with observations.
10WBW003	Madrid South	Patch 14	6	67.3	421.0	461.5	40.4	441.2	8.3E-10	7.4E-10	6.3E-10	7.4E-10	BDR	Continuation of metavolcanics. Permeability could be significantly less than shown. Pre-test leakage exceeded injection test flows.
10WBW003	Madrid South	Patch 14	7	67.3	459.8	505.7	45.9	482.8	1.5E-09	1.1E-09	8.7E-10	1.1E-09	BDR	Mafic metavolcancis and carbonate/qtz veinings. Low fracture count. Pre-plug blowout flows exceeded injection test fows.
11PSD259	Madrid South	Patch 14	1	54.5	43.4	131.1	87.7	87.2	3.6E-09	3.0E-09	2.5E-09	3.0E-09	BDR	Primarily mafic volcanic undifferentiated, w occasional felsic, dolomite and quartz zones
11PSD260	Madrid South	Patch 14	1	67.5	47.4	169.1	121.7	108.2	1.1E-10	8.3E-11	2.1E-11	8.3E-11	BDR	Mafic volcanic pillow and felsic volcanic flow w 3 ore zones
11PSD260	Madrid South	Patch 14	2	64.0	497.3	555.5	58.2	526.4	1.0E-09	7.1E-10	5.0E-10	7.1E-10	BDR	Felsic volcanic flow w ore zone (discontinuous, 554-580m)
11PSD260	Madrid South	Patch 14	3	63.0	439.5	550.6	111.1	495.1	4.7E-10	3.7E-10	3.1E-10	3.7E-10	BDR	Felsic volcanic flow w ore zone (discontinuous, 554-580m)
11PSD261	Madrid South	Patch 14	1	50.0	96.8	162.4	65.7	129.6	1.2E-08	9.8E-09	7.5E-09	9.8E-09	BDR	Mafic volcanic pillow (foliated basalt) w minor felsic volcanic and argillite, and quartz (175-177m)
11PSD261	Madrid South	Patch 14	2	45.0	252.6	304.8	52.2	278.7	1.8E-10	1.1E-10	6.8E-11	1.1E-10	BDR	Mafic volcanic pillow and felsic volcanic flow w quartz (discontinuous, 362-368m)
11PSD263	Madrid South	Patch 14	1	53.0	76.9	99.8	22.9	88.4	1.2E-07	9.5E-08	7.4E-08	9.5E-08	BDR	Mafic volcanic flow (to 112m) above felsic volcanic flow
11PSD267	Madrid South	Patch 14	1	48.0	75.1	113.0	37.9	94.0	4.6E-09	2.2E-09	7.2E-10	2.2E-09	BDR	Mafic volcanic and felsic flows w quartz (discontinuous ore zone 112-118m)
11PSD267	Madrid South	Patch 14	2	48.0	200.9	260.1	59.2	230.5	5.0E-09	2.6E-09	1.5E-09	2.6E-09	BDR	Mafic volcanic flow w quartz (discontinuous ore zone, 271-288m)

Test Information				Test Interval - Vertical depth (mbgs)					Hydraulic Conductivity K (m/s)				Test description	
ID1	Area	Sub-Area	Test Number	Hole Dip (degrees)	Top	Bottom	Interval length	Mid point	Max	Geomean	Min	Valid K (excl. poor or in prmfst)	Geol. type	Test Zone Lithology
11PSD267	Madrid South	Patch 14	3	48.0	229.9	260.1	30.2	245.0	9.8E-09	4.7E-09	2.1E-09	**4.7E-09**	BDR	Mafic volcanic flow
11PSD269	Madrid South	Patch 14	1	64.0	105.4	171.7	66.2	138.5	1.5E-06	5.9E-07	3.4E-07	**5.9E-07**	BDR	Mafic volcanic flow w quartz (3 discontinuous ore zone)
11PSD269	Madrid South	Patch 14	2	64.0	151.3	171.7	20.4	161.5	1.7E-08	1.2E-08	7.9E-09	**1.2E-08**	BDR	Mafic volcanic flow w quartz (discontinuous ore zone, 171-175m)
11PSD270	Madrid South	Patch 14	1	58.0	381.8	444.4	62.6	413.1	2.0E-10	7.4E-11	##N/A	**#N/A**	BDR	Mafic voclanic flow w quartz (2 ore zones, 451-452m, 482-483m)
11PSD271	Madrid South	Wolverine	1	69.0	118.8	187.6	68.9	153.2	2.0E-09	9.7E-10	5.7E-10	**9.7E-10**	BDR	Primarily felsic volcanic pillow
11PSD275	Madrid South	Patch 14	1	66.0	75.2	117.8	42.7	96.5	1.3E-07	1.1E-08	4.6E-09	**1.1E-08**	BDR	Felsic volcanic pillow w intervleaved quartz (ore zone)
11PSD275A	Madrid South	Patch 14	1	65.0	81.8	117.8	36.0	99.8	7.9E-09	5.3E-09	3.2E-09	**5.3E-09**	BDR	Felsic volcanic flow w quartz (ore zone 111-118m)
11PSD275A	Madrid South	Patch 14	2	62.0	147.7	191.6	43.9	169.7	5.1E-10	3.6E-10	1.6E-10	**3.6E-10**	BDR	Felsic volcanic flow above mafic volcanic flow (213-217m)
11PSD275A	Madrid South	Patch 14	3	59.0	266.8	306.9	40.0	286.9	4.3E-10	1.4E-10	#N/A	**1.4E-10**	BDR	Mafic volcanic flow w quartz (discontinuous ore zone, 311-323m, 257-158m)
11PSD276	Madrid South	Patch 14	1	57.0	61.9	86.4	24.5	74.1	2.4E-06	9.0E-07	5.2E-07	**9.0E-07**	BDR	Mafic volcanic (undifferentiated) w quartz (ore zone, 101-103m) based on 11PSD276A
11PSD276A	Madrid South	Patch 14	1	59.0	86.8	106.6	19.8	96.7	3.3E-08	2.1E-08	1.4E-08	**2.1E-08**	BDR	Mafic volcanic (undifferentiated) w quartz (101-103m, 120-124m)
11PSD276A	Madrid South	Patch 14	2	57.5	152.2	176.9	24.6	164.5	5.2E-09	4.4E-09	3.3E-09	**4.4E-09**	BDR	Felsic volcanic
11PSD276A	Madrid South	Patch 14	3	57.5	113.7	176.9	63.2	145.3	4.2E-08	3.4E-08	2.8E-08	**3.4E-08**	BDR	Felsic volcanic and quartz (ore zone, discontinuous, 139-175m)
11PSD276A	Madrid South	Patch 14	5	56.0	301.3	328.0	26.7	314.6	#N/A	#N/A	#N/A	**#N/A**	BDR	Primarliy mafic volcanic w quartz (ore zone, discontinuous, 333-348m)
11PSD276A	Madrid South	Patch 14	4si	57.0	33.6	256.8	223.2	145.2	#N/A	#N/A	#N/A	**#N/A**	BDR	Primarily mafic volcanic w quartz and felsic volcanic
11PSD279	Madrid South	Patch 14	1	60.0	61.3	97.2	35.9	79.2	1.7E-08	1.2E-08	7.7E-09	**1.2E-08**	BDR	Mafic volcanic pillow w quartz (ore zone, 102-108m)
11PSD279	Madrid South	Patch 14	2	60.0	84.2	97.2	13.0	90.7	#N/A	#N/A	#N/A	**#N/A**	BDR	Mafic volcanic pillow w quartz (ore zone, 102-108m)
11PSD279	Madrid South	Patch 14	3	56.0	169.9	191.5	21.6	180.7	2.3E-08	1.2E-08	6.5E-09	**1.2E-08**	BDR	Felisc volcanic flow (to 206m) over Mafic volcanic pillow
11PSD279	Madrid South	Patch 14	4	56.0	235.4	297.6	62.2	266.5	2.4E-09	2.1E-09	1.8E-09	**2.1E-09**	BDR	Felsic and mafic volcanic flows w quartz (discontinuous ore zone 348-258m)
11PSD279	Madrid South	Patch 14	5	53.0	285.2	354.9	69.7	320.1	#N/A	#N/A	#N/A	**#N/A**	BDR	Mafic volcanic pillow w quartz (discontinuous ore zones 373-382m, 243-432m)
11PSD284	Madrid South	Patch 14	1	67.0	48.1	94.8	46.7	71.5	1.7E-07	1.5E-07	1.2E-07	**1.5E-07**	BDR	Mafic volcanic undifferentiated (to 98m) overlying felsic volcanic flow w quartz (52-56m, 97-98m)
11PSD284	Madrid South	Patch 14	2	67.0	71.5	94.8	23.3	83.2	3.4E-07	3.2E-07	2.8E-07	**3.2E-07**	BDR	Mafic volcanic undifferentiated (to 98m) overlying felsic volcanic flow w quartz (97-98m)
HBM-23-085	Madrid South	-	1	See survey and Lorax 2023a	48.3	80.9	32.6	16.3	#N/A	3.0E-08	#N/A	**3.0E-08**	BDR	Mafic Volcanic
HBM-23-085	Madrid South	-	2	See survey and Lorax 2023a	79.2	119.9	40.7	20.4	#N/A	1.0E-08	#N/A	**1.0E-08**	BDR	Mafic Volcanic

Test Information				Test Interval - Vertical depth (mbgs)					Hydraulic Conductivity K (m/s)				Test description	
ID1	Area	Sub-Area	Test Number	Hole Dip (degrees)	Top	Bottom	Interval length	Mid point	Max	Geomean	Min	Valid K (excl. poor or in prmfst)	Geol. type	Test Zone Lithology
HBM-23-085	Madrid South	-	3	See survey and Lorax 2023a	118.2	158.3	40.1	20.1	#N/A	2.0E-10	#N/A	**2.0E-10**	BDR	Mafic Volcanic
HBM-23-085	Madrid South	-	4	See survey and Lorax 2023a	156.6	231.3	74.7	37.4	#N/A	6.0E-11	#N/A	**6.0E-11**	BDR	Mafic Volcanic / Argillite
HBM-23-085	Madrid South	-	5	See survey and Lorax 2023a	229.7	236.6	6.9	3.5	#N/A	1.0E-06	#N/A	**1.0E-06**	BDR	Argillite / Mafic Volcanic
HBM-23-085	Madrid South	-	5	See survey and Lorax 2023a	237.7	294.8	57.1	28.6	#N/A	5.0E-10	#N/A	**5.0E-10**	BDR	Mafic Volcanic
HBM-23-085	Madrid South	-	6	See survey and Lorax 2023a	347.9	426.7	78.8	39.4	#N/A	5.0E-10	#N/A	**5.0E-10**	BDR	Mafic Volcanic / Ultramafic Volcanic
HBM-23-085	Madrid South	-	8	See survey and Lorax 2023a	347.9	443.3	95.4	47.7	#N/A	6.0E-10	#N/A	**6.0E-10**	BDR	Mafic Volcanic / Ultramafic Volcanic / Argillite
HBM-23-085	Madrid South	-	9	See survey and Lorax 2023a	426.7	443.3	16.6	8.3	#N/A	1.0E-09	#N/A	**1.0E-09**	BDR	Ultramafic Volcanic / Argillite / Mafic Volcanic
HBM-23-085	Madrid South	-	10	See survey and Lorax 2023a	441.8	516.4	74.6	37.3	#N/A	2.0E-10	#N/A	**2.0E-10**	BDR	Mafic Volcanic / Ultramafic Volcanic
08PMD668	Madrid North	Naartok	1	55.0	135.4	144.2	8.8	139.8	#N/A	1.0E-09	#N/A	**#N/A**	BDR	Fault/Deformation zone; Lithologoical change with breccia at top
08PMD669	Madrid North	Naartok	1	65.0	288.4	333.5	45.1	311.0	5.2E-10	3.7E-10	2.3E-10	**#N/A**	BDR	PGP Basalt
08PMD669	Madrid North	Naartok	2	63.0	329.0	381.4	52.3	355.2	1.8E-09	1.5E-09	1.2E-09	**#N/A**	BDR	Flow basalt
08PMD669	Madrid North	Naartok	3	62.5	415.3	470.1	54.8	442.7	1.3E-09	1.1E-09	1.0E-09	**#N/A**	BDR	Flow basalt, ore
08PMD671	Madrid North	Naartok	1	60.0	138.8	238.2	99.3	188.5	#N/A	1.0E-10	#N/A	**#N/A**	BDR	altered basalts with joints and rubble zones between ~175-195m, and ~212-227m
08PMD650	Madrid North	Suluk	1	60.0	27.7	31.2	3.5	29.4	2.3E-09	5.6E-10	2.5E-10	**5.6E-10**	BDR	PGP Basalt; shattered structure (possibly mechanical); graphite and sediments present
08PMD650	Madrid North	Suluk	2	60.0	85.7	96.1	10.4	90.9	7.7E-09	5.6E-09	4.5E-09	**5.6E-09**	BDR	PGP Basalt; 4cm fault zone (no gouge)
08PMD650	Madrid North	Suluk	3	60.0	115.2	135.1	19.9	125.1	5.0E-09	4.0E-09	3.1E-09	**4.0E-09**	BDR	PGP Basalt
08PMD650	Madrid North	Suluk	4	60.0	140.0	170.2	30.1	155.1	#N/A	#N/A	#N/A	**#N/A**	BDR	PGP basalt

Test Information				Test Interval - Vertical depth (mbgs)					Hydraulic Conductivity K (m/s)				Test description	
ID1	Area	Sub-Area	Test Number	Hole Dip (degrees)	Top	Bottom	Interval length	Mid point	Max	Geomean	Min	Valid K (excl. poor or in prmfst)	Geol. type	Test Zone Lithology
08PMD657a	Madrid North	Suluk	1	55.0	75.5	107.3	31.8	91.4	9.2E-10	6.9E-10	4.7E-10	**6.9E-10**	BDR	Deformation Zone (Foliated basalt with med-strong sericitic ateration)
08PMD657a	Madrid North	Suluk	2	55.0	100.9	146.6	45.7	123.8	6.7E-10	5.1E-10	3.2E-10	**5.1E-10**	BDR	Deformation Zone (Foliated basalt with med-strong sericitic ateration)
08PMD657a	Madrid North	Suluk	3	55.0	146.8	197.4	50.6	172.1	4.9E-10	3.9E-10	3.3E-10	**3.9E-10**	BDR	Deformation Zone (Foliated basalt with med-strong sericitic ateration)
08PMD657a	Madrid North	Suluk	4	55.0	240.8	245.7	4.9	243.3	#N/A	#N/A	#N/A	**#N/A**	BDR	#N/A
08PSD142	Madrid North	Suluk	1	55.0	49.3	70.4	21.1	59.9	7.0E-09	5.5E-09	4.1E-09	**5.5E-09**	BDR	PGP Basalt
08PSD142	Madrid North	Suluk	2	55.0	127.8	149.1	21.3	138.4	1.0E-07	7.7E-08	6.5E-08	**7.7E-08**	BDR	Basalt, transition to PGP; set of joints with calcite crystals formed inside
08PSD142	Madrid North	Suluk	3	55.0	156.7	185.9	29.2	171.3	1.2E-08	9.0E-09	5.0E-09	**9.0E-09**	BDR	PGP Basalt with calcite veining
08PSD142	Madrid North	Suluk	4	55.0	203.3	232.6	29.3	218.0	1.0E-09	6.3E-10	4.5E-10	**6.3E-10**	BDR	PGP Basalt
08PSD142	Madrid North	Suluk	5	55.0	260.7	291.6	31.0	276.1	7.6E-10	6.0E-10	4.0E-10	**6.0E-10**	BDR	PGP Basalt & Deformation Zone
08PSD143B	Madrid North	Suluk	1	55.0	196.8	240.0	43.3	218.4	9.5E-10	8.0E-10	6.8E-10	**8.0E-10**	BDR	Deformation zone with basalts
08PSD143B	Madrid North	Suluk	2	#N/A	#N/A	#N/A	#N/A	#N/A	#N/A	#N/A	#N/A	**#N/A**	BDR	#N/A
08PSD144	Madrid North	Suluk	1	53.0	197.1	279.5	82.4	238.3	#N/A	#N/A	#N/A	**#N/A**	BDR	#N/A
HBM-22-059	Madrid North	Naartok	1	66.0	313.1	339.6	26.4	13.2	#N/A	< 1E-10	#N/A	**#N/A**	BDR	Deformation zone
HBM-22-059	Madrid North	Naartok	2	66.0	339.6	369.8	30.1	15.1	#N/A	< 1E-10	#N/A	**#N/A**	BDR	Deformation zone
HBM-22-059	Madrid North	Naartok	3	66.0	368.2	399.6	31.4	15.7	#N/A	< 1E-10	#N/A	**#N/A**	BDR	Deformation zone
HBM-22-059	Madrid North	Naartok	4	66.0	397.8	431.4	33.7	16.8	#N/A	< 1E-10	#N/A	**#N/A**	BDR	Deformation zone
HBM-22-059	Madrid North	Naartok	5	66.0	432.2	470.4	38.2	19.1	#N/A	< 1E-10	#N/A	**#N/A**	BDR	Fresh rock
HBM-22-059	Madrid North	Naartok	6	66.0	468.9	514.5	45.6	22.8	#N/A	< 1E-10	#N/A	**#N/A**	BDR	Fresh rock
HBM-22-059	Madrid North	Naartok	7	66.0	513.0	571.0	58.0	29.0	#N/A	< 1E-10	#N/A	**#N/A**	BDR	Fresh rock
HBM-22-059	Madrid North	Naartok	8	66.0	569.5	634.5	65.1	32.5	#N/A	< 1E-10	#N/A	**#N/A**	BDR	Fresh rock -
HBM-22-059	Madrid North	Naartok	9	66.0	463.7	634.5	170.9	85.4	#N/A	< 1E-10	#N/A	**#N/A**	BDR	Fresh rock

Appendix D – CPT Data

Table 1: Pore Pressure Dissipation Test Results under Doris Lake

Hole	Duration (s)	Test Depth Below Ground Level (m)	Equilibrium Pore Pressure (m)	Inferred Soil Type (CPT Log)
SRK CPT08-06	2,000	10.00	10.1	Clayey Silt
	700	11.95	11.8	Silty Sand/Sand
SRK CPT08-07	2,000	5.00	Not Achieved	Sensitive Fines
	600	7.78	Not Achieved	Silty Sand/Sand
SRK CPT08-08	1,600	15.00	Not Achieved	Sensitive Fines
	3,600	20.60	Not Achieved	Silty Sand/Sand

Table 2: Pore Pressure Dissipation Test Results under Patch Lake

Hole	Duration (s)	Test Depth Below Ground Level (m)	Equilibrium Pore Pressure (m)	Inferred Soil Type
SRK CPT08-14	650	10.00	Not Achieved	Sensitive Fines
	2,200	10.50	Not Achieved	Sensitive Fines
	2,000	16.80	16.9	Silty Sand/Sand
SRK CPT08-15	1,200	10.00	Not Achieved	Sensitive Fines
SRK CPT08-16	1,800	10.00	Not Achieved	Sensitive Fines
	200	15.73	15.7	Silty Sand/Sand
SRK CPT08-17	2,000	8.53	Not Achieved	Sensitive Fines
	900	25.33	Not Achieved	Sandy Silt
SRK CPT08-19	2,000	10.00	Not Achieved	Clayey Silt
	600	14.43	14.3	Sandy Silt
SRK CPT08-20	6,000	15.33	Not Achieved	Sensitive Fines
	2,905	25.08	Not Achieved	Clayey Silt
	1,200	33.90	35.2	Sandy Silt
SRK CPT08-21	3,600	10.00	Not Achieved	Sensitive Fines
	2,500	20.00	Not Achieved	Sensitive Fines
	1,200	30.00	Not Achieved	Silt
SRK CPT08-23[1]	200	3.75	3.6	Data point does not exist
SRK CPT08-23	2,400	10.00	Not Achieved	Sensitive Fines
	2,700	20.00	Not Achieved	Sensitive Fines
	3,000	28.48	28.4	Silty Sand/Sand

1. At a depth of 3.75 m in SRK CPT08-23 there is lake water. This data point is therefore erroneous.

Table 3: Pore Pressure Dissipation Test Results under Spyder Lake

Hole	Duration (s)	Test Depth Below Ground Level (m)	Equilibrium Pore Pressure (m)	Inferred Soil Type
SRK CPT08-29	13,755	5.00	Not Achieved	Sensitive Fines
SRK CPT08-31	5,000	5.00	Not Achieved	Sensitive Fines
	200	9.03	9.2	Sand

Appendix E – Groundwater Quality Data

Field Sample ID	Deposit	Sample Location	Sample Zone	Location of port in zone	Zone port drillhole depth	Zone port vertical depth	Field Data	Field pH	Field Electrical Conductivity	Field Turbidity	Field DO	Field Temperature	Field Salinity	Field TDS	Field ORP	ALS DATA	ALS File No.	ALS Date Sampled	ALS Time Sampled	ALS Lab Reference	Physical Tests	Conductivity (EC)	Density	Hardness (as CaCO3)	pH	Salinity (EC)	Total Dissolved Solids	
					m	m		pH Units	mS/cm	NTU	mg/L	°C	%	g/L	mV							uS/cm	kg/m3	mg/L	pH	g/L	mg/L	
10WBW004-123	Boston	10WBW004	6	Meas Port Upper	295.7	271.54		6.26	37.2	6.9	13.54	5.5	2.3	23	163		L957001	18-NOV-10	18:00	L957001-1		30200	1.02	13900	7.05	-	28500	
10WBW004-124	Boston	10WBW004	6	Meas Port Upper	295.7	271.54		5.43	39	0.05	19.97	6.37	2.4	23.5	263		L960194	25-NOV-10	18:00	L960194-1		30900	1.00	12900	6.66	-	32000	
10WBW004-125	Boston	10WBW004	6	Meas Port Upper	295.7	271.54		5.43	39	0.05	19.97	6.37	2.4	23.5	263		L960194	25-NOV-10	18:00	L960194-2		30700	1.02	12700	6.68	-	30800	
10WBW004-126	Boston	10WBW004	6	Meas Port Lower	304.8	379.6		6.83	40.4	40.0	19.08	10.52	2.5	25.0	161		L960194	26-NOV-10	19:00	L960194-3		33800	1.02	12100	6.81	-	33500	
10WBW004-128	Boston	10WBW004	6	Meas Port Upper	295.7	271.54		6.38	44.0	0.0	>20	3.68	2.7	27	199		L960194	27-NOV-10	16:00	L960194-4		31400	1.02	12100	6.96	-	31700	
10WBW004-129	Boston	10WBW004	6	Meas Port Lower	304.8	379.6		6.64	40.3	0.0	15.85	15.13	2.6	25	251		L960194	28-NOV-10	10:30	L960194-5		33000	1.02	12600	7.02	-	33900	
10WBW004-130	Boston	10WBW004	6	Meas Port Lower	304.8	379.6		6.80	40.0	0.0	19.37	9.23	2.5	24	164		L960194	29-NOV-10	11:00	L960194-6		33000	1.02	13300	7.09	21.0	33300	
10WBW004-131	Boston	10WBW004	6	Meas Port Upper	295.7	271.54		6.30	39.1	0.2	14.71	6.88	2.4	24	195		L960194	30-NOV-10	09:00	L960194-7		31800	1.01	11800	7.03	20.2	32300	
10WBW004-Z6-312	Boston	10WBW004	6	Meas Port Upper	295.7	271.54		6.61	35.2	25.2	9.4	18.9	2.3	21.7	-28.7		L998529	21-APR-11	16:00	L998529-3		30800	1.02	14300	6.63	-	24200	
10WBW004-Z6-313	Boston	10WBW004	6	Meas Port Upper	295.7	271.54		6.61	35.2	25.2	9.4	18.9	2.3	21.7	-28.7		L998529	21-APR-11	16:00	L998529-4		30700	1.02	12900	6.59	-	25000	
10WBW004-Z6-314	Boston	10WBW004	6	Meas Port Lower	304.8	379.6		6.51	41.3	38.35	7.75	16.65	2.65	25	-17.5		L998529	22-APR-11	08:00	L998529-5		41000	1.02	14800	6.41	-	33500	
10WBW004-Z6-315	Boston	10WBW004	6	Meas Port Upper	295.7	271.54		7.04	36	7.6	8.8	15.21	2.3	22	-67		L998529	22-APR-11	15:40	L998529-6		31200	-	13800	6.94	-	25100	
10WBW004-Z6-316	Boston	10WBW004	6	Meas Port Lower	304.8	379.6		-	-	-	-	-	-	-	-		L998529	23-APR-11	09:00	L998529-7		34200	-	14400	6.91	-	27500	
10WBW004-Z6-317	Boston	10WBW004	6	Meas Port Upper	295.7	271.54		7.13	36	36.7	7.86	17.2	2.3	22	-80		L998529	23-APR-11	15:00	L998529-8		31400	1.02	12900	7.00	-	25300	
10WBW004-Z6-318	Boston	10WBW004	6	Meas Port Lower	304.8	379.6		-	-	-	-	-	-	-	-		L998529	23-APR-11	16:30	L998529-9		34400	1.02	13700	6.98	-	27700	
10WBW004-Z6-404	Boston	10WBW004	6	Bottom	305	279.60		6.63	33.1	244	13.58	7.87	2	20	36		-	23-JUN-11	12:00	L1023975-1		36500	1.02	11900	6.67	-	38800	
10WBW004-Z6-405	Boston	10WBW004	6	Bottom	305	279.60		6.63	33.1	244	13.58	7.87	2	20	36		-	23-JUN-11	12:00	L1023975-2		36600	1.02	11900	6.72	-	39000	
10WBW004-Z6-406	Boston	10WBW004	6	Top	296	271.54		7.12	30.5	86.6	13.02	11.45	1.9	19	-17		-	23-JUN-11	16:00	L1023975-3		32100	1.02	11400	7	-	35300	
10WBW004-Z6-508	Boston	10WBW004	6	Bottom	305	279.60		7.12	36.07	5.1	11.04	6.28	22.47	23.44	-63		-	15-SEP-11	09:00	L1060807-1		37400	1	14300	6.66	-	28200	
10WBW004-Z6-509	Boston	10WBW004	6	Top	296	271.54		7.04	31.27	0.5	9.57	8.86	19.34	20.31	-35.7		-	15-SEP-11	12:00	L1060807-2		31500	1.02	13000	6.74	-	21900	
10WBW001-02b	Doris Central	10WBW001	6	Meas Port Upper	246.0	221.1		6.975	>20	-	-	-	-	-	-		L909782	09-JUL-10	14:00	L909782-2		52800	1.02	9980	6.90	-	36900	
10WBW001-03b	Doris Central	10WBW001	10	Meas Port Upper	63.5	57.4		7.765	>20	-	-	-	-	-	-		L909782	09-JUL-10	14:00	L909782-3		27600	1.00	4960	7.37	-	18700	
10WBW001-04b	Doris Central	10WBW001	10	Meas Port Upper	63.5	57.4		7.8	>20	-	-	-	-	-	-		L909782	09-JUL-10	14:00	L909782-4		27500	1.01	5060	7.42	-	18500	
10WBW001-12	Doris Central	10WBW001	10	Pump Port Lower	107.50	97		7.5	>20	-	-	4.5	-	-	-		L911681	20-JUL-01	09:49	L911681-3		41400	1.01	7150	7.38	-	27700	
10WBW001-14	Doris Central	10WBW001	10	Pump Port Lower	107.50	97		7.56	>20	-	-	4.6	-	-	-		L911681	20-JUL-01	16:30	L911681-5		45700	1.02	7750	7.34	-	31000	
10WBW001-15	Doris Central	10WBW001	10	Pump Port Lower	107.50	97		7.39	>20	-	-	8	-	-	-		L915201	21-JUL-10	16:28	L915201-1		46500	-	8360	7.35	-	32200	
10WBW001-16	Doris Central	10WBW001	10	Pump Port Lower	107.50	97		7.39	>20	-	-	8	-	-	-		L915201	21-JUL-10	17:28	L915201-2		46600	-	9250	7.39	-	32700	
10WBW001-28	Doris Central	10WBW001	6	Pump Port Lower	274.00	246		8.04	>20	-	-	2.8	-	-	-		L915201	26-JUL-10	16:23	L915201-16		41600	-	7280	7.58	-	29000	
10WBW001-31	Doris Central	10WBW001	6	Pump Port Lower	274.00	246		7.78	>20	-	-	2.6	-	-	-		L915201	27-JUL-10	10:35	L915201-19		42900	-	8550	7.51	-	30000	
10WBW001-33	Doris Central	10WBW001	6	Pump Port Lower	274.00	246		7.52	>20	-	-	3.1	-	-	-		L915201	27-JUL-10	15:21	L915201-21		44400	-	8870	7.43	-	30400	
10WBW001-36	Doris Central	10WBW001	6	Meas Port Upper	246.0	221.1		8.27	>20	-	-	9.6	-	-	-		L917645	05-AUG-10	09:00	L917645-2		24600	-	4760	7.83	-	19600	
10WBW001-37	Doris Central	10WBW001	10	Meas Port Upper	63.5	57.4		7.86	>20	-	-	8.3	-	-	-		L917645	05-AUG-10	11:40	L917645-3		30300	-	6030	7.47	-	23100	
10WBW001-101	Doris Central	10WBW001	6	Meas Port Upper	246.0	221.1		7.91	40.3	118	12.23	7.44	2.5	25	10		L946743	19-OCT-10	15:00	L946743-2		34900	1.01	6720	7.79	22.10	28900	
10WBW001-102	Doris Central	10WBW001	10	Meas Port Upper	63.5	57.4		7.55	40.60	39.35	6.44	5.09	2.45	24.50	-151.50		L946743	20-OCT-10	11:00	L946743-3		33800	1.01	6360	7.46	-	28300	
10WBW001-103	Doris Central	10WBW001	6	Pump Port Lower	274.00	246		5.59	60.13	7.30	11.52	2.66	3.77	36.00	-115.00		L948685	25-OCT-10	00:00	L948685-2		48500		10000	7.04	32.4	35400	
10WBW001-105	Doris Central	10WBW001	10	Meas Port Upper	63.5	57.4		7.50	50.20	36.85	10.44	6.19	3.20	30.00	-117.00		L949713	29-OCT-10	15:00	L949713-1		43300	1.01	8900	7.44	28.5	34500	
10WBW001-107	Doris Central	10WBW001	6	Pump Port Lower	274.00	246		6.35	62.75	6.20	12.33	1.73	3.90	37.50	-110.00		L949713	30-OCT-10	14:00	L949713-4		48800	1.03	9760	7.46	32.6	39000	
10WBW001-108	Doris Central	10WBW001	6	Meas Port Upper	246.0	221.1		7.29	44.10	38.90	8.26	6.47	2.75	27.00	-55.00		L951724	01-NOV-10	15:00	L951724-2		37000	1.03	7340	7.59	23.5	25500	
10WBW001-Z1-300	Doris Central	10WBW001	1	Meas Port Upper	548.0	484.8		7.79	>40	-	-	11.7	-	-	-		L994212	06-APR-11	09:00	L994212-1		46700	1.03	12200	7.09	-	41200	
10WBW001-Z6-301	Doris Central	10WBW001	6	Meas Port Upper	246.0	221.1		7.71	>20	-	-	8.5	-	-	-		L994212	06-APR-11	14:00	L994212-2		45500	1.03	8720	7.67	-	36100	
10WBW001-Z10-302	Doris Central	10WBW001	10	Meas Port Upper	63.5	57.4		7.32	>20	-	-	9.3	-	-	-		L994212	06-APR-11	09:00	L994212-3		47000	1.03	8810	7.59	-	37800	
10WBW001-Z10-303	Doris Central	10WBW001	10	Meas Port Lower	105.0	94.8		7.22	>20	-	-	8.2	-	-	-		L994212	07-APR-11	11:00	L994212-4		51800	1.03	11000	7.56	-	40800	
10WBW001-Z6-304	Doris Central	10WBW001	6	Meas Port Lower	271.0	243.2		7.07	>20	-	-	11.7	-	-	-		L994212	08-APR-11	16:00	L994212-5		57300	1.03	11800	7.37	-	48300	
10WBW001-Z10-500	Doris Central	10WBW001	10	Top	63.00	57.43		6.43	36.26	99.1	9.75	11.46	31.86	31.8	227.5		-	11-SEP-11	15:00	L1060818-1		47600	1.02	9000	7.68	-	32400	
10WBW001-Z1-501	Doris Central	10WBW001	1	Bottom	548.00	484.82		6.93	48.32	-1.1	9.24	6.04	30.8	31.29	199.7		-	12-SEP-11	07:00	L1060818-2		48500	1.02	12300	7.21	-	36500	
10WBW001-Z6-502	Doris Central	10WBW001	6	Top	246.00	221.06		6.91	50.02	12.3	9.35	5.65	32.12	32.43	-66.7		-	12-SEP-11	10:30	L1060818-3		49300	1.02	9220	7.63	-	34600	
10WBW001-Z6-503	Doris Central	10WBW001	6	Top	246.00	221.06		6.91	50.02	12.3	9.35	5.65	32.12	32.43	-66.7		-	12-SEP-11	10:30	L1060818-4		47000	1.02	9270	7.35	-	33500	
10WBW001-Z6-504	Doris Central	10WBW001	6	Bottom	271.00	243.15		7.07	62.28	1.8	11.37	3.3	40.54	40.45	-70.4		-	12-SEP-11	02:00	L1060818-5		56800	1	12200	7.09	-	40200	
10WBW001-Z10-505	Doris Central	10WBW001	10	Bottom	105.0	94.8		7.11	56.38	0.9	9.55	3.3	36.29	36.63	20.5		-	12-SEP-11	07:00	L1060818-6		51300	1.03	10300	7.23	-	41400	
10WBW001-Z10	Doris Central	10WBW001	10	Top	63.5	57.43		6.73	41.8	0	5.39	11.9	2.63	25.5	-55		L1193743	6-Aug-12	14:00	L1193743-1		44200	1.02	8150	7.61	-	32200	
10WBW001-Z01	Doris Central	10WBW001	1	Top	548	484.82		6.54	44.2	40.8	8.71	13.75	2.81	26.9	36		L1193743	6-Aug-12	0:00	L1193743-2		45700	1.02	11300	7.36	-	44400	
10WBW001-Z6	Doris Central	10WBW001	6	Top	246	221.06		6.68	48.9	6.5	6.68	13.04	3.14	29.8	-58		L1193743	7-Aug-12	8:45	L1193743-4		51800	1.02	9650	7.49	-	40800	
10WBW001-01-2022	Doris Central	10WBW001	1	Top	548	484.8		6.91	over range	-	-	3.8	over range	over range	95		YL2201796	4-Oct-22	16:00	YL2201796-003		47200	-	11200	6.7	-	38100	
10WBW001-01-2023	Doris Central	10WBW001	1	Top	548	484.8		7.24	45.479	-	10.27	11.6	2.929	over range	80.4		EO2306938	31-Jul-23	14:00	EO2306938-004		23700	-	12100	6.78	-	29600	
10WBW001-01-2024	Doris Central	10WBW001	1	Top	548	484.8		7.2	43.383	-	N/A	4.1	2.753	over range	48		EO2405676	4-Jul-24	13:00	EO2405676-001		N/A	-	12200	N/A	-	31400	
10WBW001-06-2022	Doris Central	10WBW001	6	Top	246	221.1		7.43	17.38	-	-	3.5	over range	-	135		YL2201796	4-Oct-22	14:25	YL2201796-002		17300	-	2140	8.22	-	13400	
10WBW001-06-2023	Doris Central	10WBW001	6	Top	246	221.1		7.6	17.89	-	-	12.5	1.01	-	8.1		EO2306938	31-Jul-23	11:00	EO2306938-003		11900	-	2450	7.75	-	10300	
10WBW001-06-2024	Doris Central	10WBW001	6	Top	246	221.1		7.5	16.32	-	-	7.97	0.945	-	-77		EO2405676	4-Jul-24	9:50	EO2405676-003		N/A	-	2060	-	-	10200	
10WBW001-10-2022	Doris Central	10WBW001	10	Top	63.5	57.43		8.18	0.00315	-	-	3	-	3.1	136		YL2201796	4-Oct-22	12:20	YL2201796-001		-	-	206	-	-	-	
10WBW001-10-2023	Doris Central	10WBW001	10	Top	63.5	57.43		8.15	0.00333	-	8.46	10.6	0.176	0.00265	90.9		EO2306938	31-Jul-23	8:30	EO2306938-001		3430	-	215	8.23	-	1910	
10WBW001-10-2024	Doris Central	10WBW001	10	Top	63.5	57.43		8.21	3.512	-	8.79	3.7	0.182	-	79		EO2405676	4-Jul-24	15:30	EO2405676-005		N/A	-	222	N/A	-	1920	
10WBW001-01b	Doris Lower	10WBW001	1	Meas Port Upper	548.0	484.8		8.03	>20	-	-	-	-	-	-		L909782	08-JUL-10	15:00	L909782-1		47600	1.02	11700	7.67	-	33100	
10WBW001-17	Doris Lower	10WBW001	1	Meas Port Upper	548.0	484.8		8	>20	-	-	14.4	-	-	-		L915201	25-JUL-10	11:25	L915201-3		47400	-	11500	7.91	-	32400	
10WBW001-20	Doris Lower	10WBW001	1	Pump Port Middle	554.0	490.8		8.19	>20	-	-	3.9	-	-	-		L915201	25-JUL-10	17:11	L915201-6		47500	-	10900	7.83	-	33200	
10WBW001-25	Doris Lower	10WBW001	1	Pump Port Middle	554.0	490.8		8.24	>20	-	-	-	-	-	-		L915201	25-JUL-10	12:37	L915201-13		47600	-	11500	7.65	-	33300	
10WBW001-26	Doris Lower	10WBW001	1	Pump Port Middle	554.0	490.8		8.24	>20	-	-	-	-	-	-		L915201	25-JUL-10	12:37	L915201-14		47600	-	11100	7.72	-	32400	
10WBW001-35	Doris Lower	10WBW001	1	Meas Port Upper	548.0	484.8		8.44	>20	-	-	-	-	-	-		L917645	04-AUG-10	13:42	L917645-1		46600	-	12700	7.43	-	47800	
10WBW001-100	Doris Lower	10WBW001	1	Meas Port Upper	548.0	484.8		7.73	52	72.85	11.2	11.79	3.5	32.5	39.5		L946743	19-OCT-10	12:00	L946743-1		46700	1.01	12600	7.38	30.50	42300	
10WBW001-106	Doris Lower	10WBW001	1	Meas Port Upper	548.0	484.8		6.00	52.65	211.00	11.43	4.51	3.50	32.00	15.00		L949713	30-OCT-10	13:00	L949713-3		46900	1.03	12100	7.69	31.2	47500	
10WBW002-01	Doris North	10WBW002	1	Meas Port Upper	594.4	575.06		-	-	-	-	-	-	-	-		L909782	03-JUL-10	14:00	L909782-5		160000	1.13	180000	-	-	250000	
10WBW002-02	Doris North	10WBW002	1	Meas Port Upper	594.4	575.06		-	-	-	-	-	-	-	-		L909782	04-JUL-10	14:00	L909782-6		182000	1.14	200000	-	-	225000	
10WBW002-109a	Doris North	10WBW002	1	Meas Port Upper	594.4	575.06		6.02	> 99.9	409	12.35	0.69	> 4.0	> 99	146		L956881	07-NOV-10	17:00	L956881-1		-	-	187000	-	-	-	
10WBW002-109b	Doris North	10WBW002	1	Meas Port Upper	594.4	575.06		6.02	> 99.9	409	12.35	0.69	> 4.0	> 99	146		L956881	08-NOV-10	11:00	L956881-2			-	189000	-	-	-	
10WBW002-121	Doris North	10WBW002	1	Meas Port Upper	594.4	575.06		6.13	99.9	-5.0	14.15	4.33	4.0	99.0	106		L956881	13-NOV-10	11:00	L956881-4		182000	1.17	183000	8.51	-	223000	
10WBW002-Z1-305	Doris North	10WBW002	1	Meas Port Upper	594.40	575.06		-	-	-	-	-	-	-	-		L996991	16-APR-11	15:18	L996991-1		182000	1.16	-	7.22	-	207000	
10WBW002-Z1-306	Doris North	10WBW002	1	Meas Port Upper	594.40	575.06		8.85	>99.9	515	15.73	4.85	>4	>99	272		L996991	16-APR-11	17:18	L996991-2		-	-	172000	-	-	-	
10WBW002-Z1-307	Doris North	10WBW002	1	Meas Port Upper	594.40	575.06		8.21 to 8.66	>99.9	443 to 395	10.08 to 8.64	4.6 to 1.51	>4	>99	288 to 201		L996991	17-APR-11	14:00	L996991-3		183000	1.16	178000	8.10	-	202000	
10WBW002-Z3-308	Doris North	10WBW002	3	Meas Port Upper	498.40	481.78		8.43	>99.9	31	13.12	1.25	>4	>99	138		L996991	17-APR-11	18:10	L996991-4		176000	1.15	164000	7.95	-	205000	
10WBW002-Z2-309	Doris North	10WBW002	2	Meas Port Upper	506.00	489.16		7.46	43	94.4	12.44	0.92	2.5	26	73		L996991	18-APR-11	13:30	L996991-5		39400	1.07	57600	7.50	-	97600	
10WBW002-Z1-400	Doris North	10WBW002	1	Top	594.4	575.06		8.41	>99.9	262	19.38	-2.25	>4.0%	>99	230		-	20-JUN-11	11:00	L1021760-1		181000	1.16	208000	7.57	-	-	
10WBW002-Z1-401	Doris North	10WBW002	1	Top	594.4	575.06		9.17	>99.9	112	19.69	-1.49	>4.0%	>99	181		-	20-JUN-11	15:00	L1021760-2		182000	1.16	187000	8.12	-	193000	
10WBW002-Z3-403	Doris North	10WBW002	3	Top	498.4	481.78		6.87	>99.9	164	17.15	-2.13	>4.0%	>99	301		-	21-JUN-11	11:00	L1021760-4		159000	-	158000	7.03	-	169000	
10WBW002-Z1-510	Doris North	10WBW002	1	Top	594.4	575.06		7.21	176.8	-0.3	4.88	4.83	140.9	114.8	349.7		-	15-SEP-11	08:00	L1060807-3		189000	1.1	179000	7.16	-	205000	
10WBW002-Z1-511	Doris North	10WBW002	1	Top	594.4	575.06		8.03	175.1	20.4	6.26	7.53	141.3	113.7	231.8		-	15-SEP-11	10:30	L1060807-4		189000	1.11	200000	7.72	-	204000	
10WBW002-Z3-512	Doris North	10WBW002	3	Top	498.4	481.78		-	-	-	-	-	-	-	-		-	15-SEP-11	13:30	L1060807-5		155000	1.1	161000	7.41	-	171000	

Field Sample ID	Anions and Nutrients	Alkalinity, Bicarbonate (as CaCO3)	Alkalinity, Carbonate (as CaCO3)	Alkalinity, Hydroxide (as CaCO3)	Alkalinity, Total (as CaCO3)	Ammonia as N	Bromide (Br)	Chloride (Cl)	Fluoride (F)	Nitrate (as N)	Nitrite (as N)	Ortho Phosphate as P	Total Phosphate as P	Silicate (as SIO2)	Sulfate (SO4)	Additional Anions and Nutrients
		mg/L	mg/L	mg/L	mg/L	mg/L	mg/L	mg/L	mg/L	mg/L	mg/L	mg/L	mg/L	mg/L	mg/L	
10WBW004-123		35.8	<1	<1	35.8	2.33	6.3	12100	0.78	<0.5	<0.1	<0.005	0.123	<10	244	
10WBW004-124		35.5	<1.0	<1.0	35.5	-	6.4	12400	0.669	<0.50	<0.10	-	-	-	264	
10WBW004-125		35.3	<1.0	<1.0	35.3	-	6.5	12400	0.677	<0.50	<0.10	-	-	-	260	
10WBW004-126		40.0	<1.0	<1.0	40.0	-	9.2	13700	0.983	<0.50	<0.10	-	-	-	336	
10WBW004-128		48.7	<1.0	<1.0	48.7	-	8.2	12600	0.645	0.53	<0.10	-	-	-	322	
10WBW004-129		50.5	<1.0	<1.0	50.5	-	9.9	13400	0.716	<0.50	<0.10	-	-	-	349	
10WBW004-130		53.0	<1.0	<1.0	53.0	1.96	9.3	13400	0.689	<0.50	<0.10	<0.0010	0.148	8.2	347	
10WBW004-131		53.5	<1.0	<1.0	53.5	1.95	9.0	12800	0.642	<0.50	<0.10	<0.0010	0.155	6.5	330	
10WBW004-Z6-312		24.5	<2.0	<2.0	24.5	2.38	5.1	12100	0.76	<0.50	<0.10	<0.0010	0.190	<10	271	
10WBW004-Z6-313		25.3	<2.0	<2.0	25.3	2.37	7.3	12700	0.78	<0.50	<0.10	<0.0010	0.189	<10	285	
10WBW004-Z6-314		11.6	<2.0	<2.0	11.6	-	7.3	17400	1.48	<0.50	<0.10	-	-	-	300	
10WBW004-Z6-315		34.9	<2.0	<2.0	34.9	-	6.8	12300	0.83	<0.50	<0.10	-	-	-	278	
10WBW004-Z6-316		33.0	<2.0	<2.0	33.0	-	8.0	13500	0.94	<0.50	<0.10	-	-	-	330	
10WBW004-Z6-317		35.4	<2.0	<2.0	35.4	2.38	7.3	13000	0.83	<0.50	<0.10	<0.0010	0.196	<10	295	
10WBW004-Z6-318		34.0	<2.0	<2.0	34.0	-	9.4	14600	0.95	<0.50	<0.10	-	-	-	360	
10WBW004-Z6-404		32.5	<1.0	<1.0	32.5	2.38	12.1	14700	0.749	<0.50	<0.10	-	0.0787	<10	385	
10WBW004-Z6-405		34.7	<1.0	<1.0	34.7	2.44	14.2	14900	0.727	<0.50	<0.10	-	0.0897	<10	405	
10WBW004-Z6-406		45.6	<1.0	<1.0	45.6	2.45	11	12400	0.587	<0.50	<0.10	-	0.11	<10	325	
10WBW004-Z6-508		17.4	<2.0	<2.0	17.4	2.28	18.2	13800	0.618	0.88	<0.10	<0.0010	0.145	<10	405	
10WBW004-Z6-509		23.3	<2.0	<2.0	23.3	2.48	16.6	13000	0.528	0.84	<0.10	<0.0010	0.0918	<10	361	
10WBW001-02b		-	-	-	87.3	-	-	20100	<5	<5	<5	-	-	-	2090	
10WBW001-03b		-	-	-	66.3	-	-	9650	<5	<5	<5	-	-	-	995	
10WBW001-04b		-	-	-	64.8	-	-	9610	<5	<5	<5	-	-	-	991	
10WBW001-12		-	-	-	90.6	-	-	15200	<2.5	<2.5	<2.5	-	-	-	1490	
10WBW001-14		-	-	-	83.3	-	-	17100	<2.5	<2.5	<2.5	-	-	-	1700	
10WBW001-15		-	-	-	82.3	-	-	17700	<1	<1	<1	-	-	-	1750	
10WBW001-16		-	-	-	81.7	-	-	18200	<1	<1	<1	-	-	-	1790	
10WBW001-28		-	-	-	63.4	-	-	15900	<1	<1	<1	-	-	-	1690	
10WBW001-31		-	-	-	67.7	-	-	16500	<1	<1	<1	-	-	-	1760	
10WBW001-33		-	-	-	70.8	-	-	17100	<1	<1	<1	-	-	-	1820	
10WBW001-36		-	-	-	44.2	-	21.2	09130	<0.75	<0.5	<0.1	-	-	-	0940	
10WBW001-37		-	-	-	49.7	-	27.6	11500	<0.75	<0.5	<0.1	-	-	-	1160	
10WBW001-101		44.2	<2	<2	44.2	-	38.1	13400	<0.75	<0.5	<0.1	0.0017	-	5.0	1390	
10WBW001-102		77.3	<1	<1	77.3	-	36.4	13100	<0.75	<0.5	<0.1	<0.001	-	3.8	1230	
10WBW001-103		-	-	-	72.4	3.14	49.1	19000	0.091	<0.5	<0.1	-	0.0262	6.1	2020	
10WBW001-105		106	<2	<2	106	3.46	41	16500	<0.75	<1	<0.2	<0.001	0.0389	7.5	1580	
10WBW001-107		76.5	<1	<1	76.5	3.37	52	19100	<0.75	<1	<0.2	<0.001	0.0124	9.7	2000	
10WBW001-108		43.7	<2	<2	43.7	2.32	41.3	14200	<0.75	<0.5	<0.1	<0.001	0.0162	5.8	1500	
10WBW001-Z1-300		2.7	<2.0	<2.0	2.7	0.0619	100	19000	<0.75	<0.50	<0.10	<0.0010	0.0094	<10	944	
10WBW001-Z6-301		49.8	<2.0	<2.0	49.8	2.90	67	18300	<0.75	<1.0	<0.20	0.0012	0.0314	9.0	1780	
10WBW001-Z10-302		119	<2.0	<2.0	119	3.54	63	18800	<0.75	<1.0	<0.20	<0.0010	0.0644	5.7	1730	
10WBW001-Z10-303		115	<2.0	<2.0	115	4.05	77	21100	<0.75	<1.0	<0.20	<0.0010	0.0150	8.8	2040	
10WBW001-Z6-304		102	<2.0	<2.0	102	3.65	84	24000	<0.75	<1.0	<0.20	<0.0010	0.0145	9.1	2450	
10WBW001-Z10-500		115	<2.0	<2.0	115	3.29	63.5	18100	0.094	0.72	<0.10	<0.0010	0.0433	11.3	1720	
10WBW001-Z1-501		<2.0	<2.0	<2.0	<2.0	0.0538	122	18600	0.057	<0.50	<0.10	0.0031	0.0194	5.3	972	
10WBW001-Z6-502		44.1	<2.0	<2.0	44.1	3.22	67.3	18800	0.087	0.53	<0.10	<0.0010	0.0316	9.9	2000	
10WBW001-Z6-503		44.7	<2.0	<2.0	44.7	3.16	68	19000	0.083	0.6	<0.10	<0.0010	0.0306	8.2	2030	
10WBW001-Z6-504		47.4	<2.0	<2.0	47.4	3.87	83.6	23600	0.075	0.61	<0.10	<0.0010	0.0137	12.2	2510	
10WBW001-Z10-505		97.7	<2.0	<2.0	97.7	4.2	75.3	21000	0.097	0.64	<0.10	<0.0010	0.018	18.1	2150	
10WBW001-Z10		116	<2.0	<2.0	116	2.94	74.8	18700	<0.75	<0.50	<0.10	<0.0010	0.0649	1.94	1900	
10WBW001-Z01		<2.0	<2.0	<2.0	<2.0	0.0492	131	18100	<0.75	<0.50	<0.10	<0.0010	0.0073	6.7	940	
10WBW001-Z6		47	<2.0	<2.0	47	2.98	78.8	20600	<0.75	<0.50	<0.10	<0.0010	0.022	6	2110	
10WBW001-01-2022		14.4	<1	<1	14.4	0.0138	129	19700	<2	<0.5	<0.10	0.01	-	6.38	964	
10WBW001-01-2023		15	<1	<1	15	<0.005	21.6	19800	<2	0.879	<0.10	<0.10	-	9.52	476	
10WBW001-01-2024		16.5	<1	<1	16.5	N/A	114	18300	<2	<0.5	<0.10	0.001	-	8.67	922	
10WBW001-06-2022		260	<1	<1	260	1.99	21.8	6060	<2	<0.5	<0.10	0.11	-	11	403	
10WBW001-06-2023		289	<1	<1	289	3.23	20.6	6020	<0.2	0.093	0.0159	0.16	-	11.2	440	
10WBW001-06-2024		316	<1	<1	316	N/A	18.4	5440	0.4	0.1	0.2	0.206	-	11.9	405	
10WBW001-10-2022		-	-	-	-	0.61	-	-	-	-	-	-	-	11.6	-	
10WBW001-10-2023		229	<1	<1	229	0.731	3.4	992	<0.7	<0.025	<0.10	<0.55	-	11.7	85.9	
10WBW001-10-2024		256	1.8	<1	258	N/A	3.28	1000	0.846	<0.025	0.005	0.652	-	11.9	92.9	
10WBW001-01b		8.4	-	-	-	-	-	18200	<5	<5	<5	-	-	-	1020	
10WBW001-17		9.7	-	-	-	-	-	19100	<1	<1	<1	-	-	-	1010	
10WBW001-20		9.3	-	-	-	-	-	19000	<1	<1	<1	-	-	-	0997	
10WBW001-25		8.2	-	-	-	-	-	18700	<1	<1	<1	-	-	-	0960	
10WBW001-26		7.9	-	-	-	-	-	18800	<1	<1	<1	-	-	-	0964	
10WBW001-35		<2	-	-	-	-	100	19000	<0.75	<0.5	<0.1	-	-	-	0981	
10WBW001-100		<2	<2	<2	<2	-	101	19000	<0.75	0.96	<0.1	0.0264	-	7.8	980	
10WBW001-106		<2	<2	<2	<2	0.0631	101	18400	<0.75	<0.5	<0.1	0.0086	0.0163	<10	935	
10WBW002-01		-	-	-	56.0	-	-	114000	16	<10	<10	-	-	-	<100	
10WBW002-02		-	-	-	59.5	-	-	123000	20	<10	<10	-	-	-	<100	
10WBW002-109a		-	-	-	-	4.55	-	-	-	-	-	-	-	-	-	
10WBW002-109b		-	-	-	-	-	-	-	-	-	-	-	-	-	-	
10WBW002-121		57.4	1.6	<1	59.0	4.58	<250	133000	<100	<25	<5	<0.1	1.01	<100	<2500	
10WBW002-Z1-305		220	<1.0	<1.0	220	-	10.6	138000	<30	<0.50	<0.10	0.53	0.62	-	<50	
10WBW002-Z1-306		-	-	-	-	-	-	-	-	-	-	-	-	-	-	
10WBW002-Z1-307		160	<1.0	<1.0	160	6.4	58.9	138000	<30	<0.50	<0.10	0.41	0.81	<100	70	
10WBW002-Z3-308		145	<1.0	<1.0	145	6.3	<5.0	129000	<30	<0.50	<0.10	0.57	0.57	<100	78	
10WBW002-Z2-309		97.7	<2.0	<2.0	97.7	-	<5.0	43600	<30	<0.50	<0.10	-	-	-	<50	
10WBW002-Z1-400		-	-	-	-	-	-	-	-	-	-	-	-	-	-	
10WBW002-Z1-401		49.8	<1.0	<1.0	49.8	8.3	-	128000	-	-	-	-	0.58	-	51	
10WBW002-Z3-403		-	-	-	-	-	-	104000	-	-	-	-	-	-	146	
10WBW002-Z1-510		40.2	<1.0	<1.0	40.2	-	30.9	126000	2.31	1.75	<0.10	-	-	-	55	
10WBW002-Z1-511		44.9	<1.0	<1.0	44.9	7.22	30.5	125000	2.31	0.91	<0.10	0.021	0.336	386	55	
10WBW002-Z3-512		47.3	<1.0	<1.0	47.3	-	28.8	99200	2.65	1.62	<0.10	-	-	-	170	

Field Sample ID	Bicarbonate (HCO3)	Carbonate (CO3)	Hydroxide (OH)	Nitrate and Nitrite as N	TDS (Calculated)	Total Metals	Aluminum (Al)-Total	Antimony (Sb)-Total	Arsenic (As)-Total	Barium (Ba)-Total	Beryllium (Be)-Total	Bismuth (Bi)-Total	Boron (B)-Total	Cadmium (Cd)-Total	Calcium (Ca)-Total
	mg/L	mg/L	mg/L	mg/L	mg/L		mg/L	mg/L	mg/L	mg/L	mg/L	mg/L	mg/L	mg/L	mg/L
10WBW004-123	-	-	-	-	-		0.0469	0.0184	<0.002	0.530	<0.0005	<0.0005	0.79	<0.0001	4700
10WBW004-124	-	-	-	-	-		0.0114	0.0180	<0.0020	0.567	<0.00050	<0.00050	0.87	<0.00010	4460
10WBW004-125	-	-	-	-	-		0.0133	0.0180	<0.0020	0.557	<0.00050	<0.00050	0.87	<0.00010	4510
10WBW004-126	-	-	-	-	-		0.0152	0.0176	<0.0030	0.554	<0.00050	<0.00050	1.00	<0.00010	4730
10WBW004-128	-	-	-	-	-		0.0189	0.0199	<0.0020	0.570	<0.00050	<0.00050	0.92	<0.00010	4180
10WBW004-129	-	-	-	-	-		0.0110	0.0199	<0.0030	0.562	<0.00050	<0.00050	0.96	<0.00010	4330
10WBW004-130	-	-	-	-	-		0.0167	0.0214	<0.0030	0.596	<0.00050	<0.00050	0.99	<0.00010	4380
10WBW004-131	-	-	-	-	-		0.0087	0.0203	<0.0030	0.564	<0.00050	<0.00050	0.96	<0.00010	4110
10WBW004-Z6-312	-	-	-	-	-		0.0123	0.0179	<0.0020	0.553	<0.00050	<0.00050	0.90	<0.00010	4730
10WBW004-Z6-313	-	-	-	-	-		0.0069	0.0163	<0.0020	0.500	<0.00050	<0.00050	0.84	<0.00010	4560
10WBW004-Z6-314	-	-	-	-	-		0.0118	0.0139	<0.0020	0.532	<0.00050	<0.00050	0.92	<0.00010	5360
10WBW004-Z6-315	-	-	-	-	-		-	-	-	-	-	-	-	-	4830
10WBW004-Z6-316	-	-	-	-	-		-	-	-	-	-	-	-	-	4960
10WBW004-Z6-317	-	-	-	-	-		<0.0050	0.0204	<0.0020	0.577	<0.00050	<0.00050	0.89	<0.00010	4590
10WBW004-Z6-318	-	-	-	-	-		0.0071	0.0178	0.0021	0.479	<0.00050	<0.00050	0.88	<0.00010	4710
10WBW004-Z6-404	-	-	-	-	-		0.0105	0.0134	<0.0020	0.467	<0.00050	<0.00050	0.87	<0.000050	4510
10WBW004-Z6-405	-	-	-	-	-		0.039	0.0139	<0.0020	0.494	<0.00050	<0.00050	0.88	<0.000050	4530
10WBW004-Z6-406	-	-	-	-	-		0.0068	0.0161	<0.0020	0.528	<0.00050	<0.00050	0.77	<0.000050	4630
10WBW004-Z6-508	-	-	-	-	-		0.02	0.0167	<0.0050	0.466	<0.00050	<0.00050	0.83	<0.000050	5490
10WBW004-Z6-509	-	-	-	-	-		0.0078	0.0136	<0.0080	0.537	<0.00050	<0.00050	0.89	<0.000050	4580
10WBW001-02b	106.0	<5	<5	<7.1	34600		<0.2	<0.008	<0.08	0.072	<0.02	-	2.88	<0.001	1750
10WBW001-03b	80.9	<5	<5	<7.1	16800		<0.2	<0.008	<0.08	0.187	<0.02	-	1.34	<0.001	851
10WBW001-04b	79.0	<5	<5	<7.1	16900		<0.2	<0.008	<0.08	0.185	<0.02	-	1.37	<0.001	867
10WBW001-12	111	<5	<5	<3.5	26300		<2	<0.08	<0.08	0.125	<0.2	-	1.91	<0.01	1120
10WBW001-14	102	<5	<5	<3.5	29300		<2	<0.08	0.098	0.136	<0.2	-	2.22	<0.01	1290
10WBW001-15	100	<5	<5	<1.4	30300		<2	<0.08	0.083	0.102	<0.2	-	2.32	<0.01	1590
10WBW001-16	99.6	<5	<5	<1.4	32600		<2	<0.08	0.090	0.113	<0.2	-	2.31	<0.01	1580
10WBW001-28	77.3	<5	<5	<1.4	26500		<2	<0.08	0.085	0.139	<0.2	-	1.54	<0.01	1190
10WBW001-31	083	<5	<5	<1.4	29000		<2	<0.08	0.095	0.125	<0.2	-	1.64	<0.01	1370
10WBW001-33	086	<5	<5	<1.4	30000		<2	<0.08	0.121	0.107	<0.2	-	1.91	<0.01	1280
10WBW001-36	-	-	-	-	-		0.0281	0.00745	0.003	0.130	<0.0005	<0.0005	1.04	<0.00012	0805
10WBW001-37	-	-	-	-	-		0.0146	0.00349	<0.002	0.179	<0.0005	<0.0005	1.51	<0.00012	1020
10WBW001-101	-	-	-	-	-		0.0052	0.005	<0.002	0.175	<0.0005	<0.0005	1.38	<0.00005	1140
10WBW001-102	-	-	-	-	-		<0.005	0.00099	<0.002	0.177	<0.0005	<0.0005	1.53	<0.00005	1080
10WBW001-103	-	-	-	-	-		0.0318	0.00127	0.007	0.117	<0.0005	<0.0005	2.65	<0.00005	1600
10WBW001-105	-	-	-	-	-		<0.005	0.00054	<0.002	0.129	<0.0005	<0.0005	2.8	<0.00005	1540
10WBW001-107	-	-	-	-	-		0.0053	0.00115	0.0068	0.112	<0.0005	<0.0005	2.66	<0.00005	1570
10WBW001-108	-	-	-	-	-		0.0059	0.00461	<0.002	0.169	<0.0005	<0.0005	1.50	<0.00005	1170
10WBW001-Z1-300	-	-	-	-	-		0.0109	0.00081	<0.0020	0.0539	<0.00050	<0.00050	3.05	<0.000050	4930
10WBW001-Z6-301	-	-	-	-	-		0.0058	<0.00050	<0.0020	0.181	<0.00050	<0.00050	1.79	<0.000050	1420
10WBW001-Z10-302	-	-	-	-	-		0.0242	0.00131	<0.0020	0.105	<0.00050	<0.00050	2.72	0.000411	1630
10WBW001-Z10-303	-	-	-	-	-		0.0740	<0.00050	<0.0020	0.0680	<0.00050	<0.00050	2.81	0.000095	2130
10WBW001-Z6-304	-	-	-	-	-		0.168	<0.00050	<0.0020	0.0615	<0.00050	<0.00050	3.33	0.000130	2140
10WBW001-Z10-500	-	-	-	-	-		<0.0050	<0.00050	<0.0050	0.111	<0.00050	<0.00050	1.92	<0.000050	1580
10WBW001-Z1-501	-	-	-	-	-		0.0089	0.00063	<0.0050	0.0477	<0.00050	<0.00050	2.48	0.00012	5010
10WBW001-Z6-502	-	-	-	-	-		0.0102	0.00067	<0.020	0.131	<0.00050	<0.00050	1.74	0.000076	1490
10WBW001-Z6-503	-	-	-	-	-		<0.0050	0.00058	<0.0030	0.135	<0.00050	<0.00050	1.9	0.000112	1490
10WBW001-Z6-504	-	-	-	-	-		0.015	0.00069	<0.010	0.0589	<0.00050	<0.00050	2.72	0.000087	1990
10WBW001-Z10-505	-	-	-	-	-		0.0537	<0.00050	<0.0040	0.0647	<0.00050	<0.00050	2.56	0.000163	1880
10WBW001-Z10	-	-	-	-	-		0.0224	<0.00050	<0.0040	0.102	<0.00050	<0.00050	2.66	0.000088	1460
10WBW001-Z01	-	-	-	-	-		0.0327	0.00069	<0.040	0.0681	<0.00050	<0.00050	6.75	0.000145	4800
10WBW001-Z6	-	-	-	-	-		0.0102	<0.00050	<0.0020	0.123	<0.00050	<0.00050	2.78	0.000096	1570
10WBW001-01-2022	-	-	-	-	-		<0.06	<0.0020	<0.0020	0.0585	<0.0004	<0.001	2.55	<0.0001	4730
10WBW001-01-2023	-	-	-	-	-		<0.15	<0.005	<0.005	0.0617	<0.001	<0.0025	2.86	<0.00025	4800
10WBW001-01-2024	-	-	-	-	-		<0.15	0.005	<0.005	0.0577	<0.001	<0.0025	3.27	0.00025	4660
10WBW001-06-2022	-	-	-	-	-		<0.06	<0.0020	<0.0020	0.0508	<0.0004	<0.001	1.72	<0.0001	323
10WBW001-06-2023	-	-	-	-	-		<0.03	<0.001	<0.001	0.0616	<0.0002	<0.0005	2.14	<0.00005	348
10WBW001-06-2024	-	-	-	-	-		<0.03	0.001	0.00148	0.0538	0.0002	<0.0005	2.31	0.00005	304
10WBW001-10-2022	-	-	-	-	-		0.018	0.0005	0.00066	0.046	<0.0001	<0.00025	1.24	-	31
10WBW001-10-2023	-	-	-	-	-		0.0212	<0.0020	0.00109	0.0481	<0.00004	<0.0001	1.19	0.0000138	28.3
10WBW001-10-2024	-	-	-	-	-		0.0132	<0.0020	0.00088	0.0551	<0.00004	<0.0001	1.46	0.00001	29.7
10WBW001-01b	10.2	<5	<5	<7.1	30700		0.42	<0.008	<0.08	0.059	<0.02	-	3.11	<0.001	4650
10WBW001-17	11.9	<5	<5	<1.4	31500		<2	<0.08	0.113	0.046	<0.2	-	2.38	<0.01	4100
10WBW001-20	011	<5	<5	<1.4	30800		<2	<0.08	0.114	0.054	<0.2	-	2.59	<0.01	4430
10WBW001-25	010	<5	<5	<1.4	31000		<2	<0.08	0.296	0.054	<0.2	-	2.56	<0.01	4430
10WBW001-26	010	<5	<5	<1.4	30500		<2	<0.08	0.101	0.059	<0.2	-	2.50	<0.01	4380
10WBW001-35	-	-	-	-	-		0.0992	<0.0005	<0.002	0.051	<0.0005	<0.0005	2.93	<0.00012	5070
10WBW001-100	-	-	-	-	-		0.0136	<0.0005	<0.002	0.053	<0.0005	<0.0005	2.89	0.000066	4960
10WBW001-106	-	-	-	-	-		0.0086	<0.0005	<0.002	0.0521	<0.0005	<0.0005	3.25	0.000085	4700
10WBW002-01	68.3	<5	<5	<14	187000		30.5	<0.08	0.218	0.719	<0.2	-	0.95	<0.01	78500
10WBW002-02	11.9	29.9	<5	<14	203000		9.7	<0.08	0.507	0.736	<0.2	-	0.99	<0.01	96200
10WBW002-109a	-	-	-	-	-		0.161	0.0104	<0.02	0.860	<0.005	<0.005	<1	<0.0005	77400
10WBW002-109b	-	-	-	-	-		9.40	0.0107	<0.02	0.827	<0.005	<0.005	<1	<0.0005	75500
10WBW002-121	-	-	-	-	-		9.94	0.0117	<0.02	0.832	<0.005	<0.005	<1	<0.0005	78800
10WBW002-Z1-305	-	-	-	-	-		-	-	-	-	-	-	-	-	-
10WBW002-Z1-306	-	-	-	-	-		6.24	0.0110	<0.020	0.808	<0.0050	<0.0050	1.0	<0.00050	68800
10WBW002-Z1-307	-	-	-	-	-		7.04	0.0109	<0.020	0.845	<0.0050	<0.0050	<1.0	<0.00060	70800
10WBW002-Z3-308	-	-	-	-	-		0.254	0.0085	<0.020	0.964	<0.0050	<0.0050	<1.0	<0.00050	65900
10WBW002-Z2-309	-	-	-	-	-		0.256	0.0065	0.038	0.276	<0.0025	<0.0025	<0.50	0.00115	22600
10WBW002-Z1-400	-	-	-	-	-		-	-	-	-	-	-	-	-	-
10WBW002-Z1-401	-	-	-	-	-		-	-	-	-	-	-	-	-	-
10WBW002-Z3-403	-	-	-	-	-		0.172	0.0068	<0.020	0.715	<0.0025	<0.0025	0.91	<0.00050	57600
10WBW002-Z1-510	-	-	-	-	-		-	-	-	-	-	-	-	-	-
10WBW002-Z1-511	-	-	-	-	-		0.308	0.0091	<0.050	0.741	<0.0050	<0.0050	<1.0	<0.00050	76500
10WBW002-Z3-512	-	-	-	-	-		-	-	-	-	-	-	-	-	-

Field Sample ID	Cesium (Cs)-Total	Chromium (Cr)-Total	Cobalt (Co)-Total	Copper (Cu)-Total	Gallium (Ga)-Total	Iron (Fe)-Total	Lead (Pb)-Total	Lithium (Li)-Total	Magnesium (Mg)-Total	Manganese (Mn)-Total	Mercury (Hg)-Total	Molybdenum (Mo)-Total	Nickel (Ni)-Total	Phosphorus (P)-Total	Potassium (K)-Total
	mg/L	mg/L	mg/L	mg/L	mg/L	mg/L	mg/L	mg/L	mg/L	mg/L	mg/L	mg/L	mg/L	mg/L	mg/L
10WBW004-123	0.00485	0.00776	0.00717	0.00083	<0.0005	8.23	0.00602	0.049	287	0.965	<0.00001	0.0837	0.0343	<1	44
10WBW004-124	0.00531	<0.0020	0.00712	<0.00050	<0.00050	7.74	<0.00050	0.052	305	0.936	-	0.0879	0.0309	<1.0	46
10WBW004-125	0.00519	<0.0030	0.00699	<0.00050	<0.00050	7.62	<0.00050	0.051	306	0.926	-	0.0853	0.0305	<1.0	47
10WBW004-126	0.00665	<0.0040	0.00562	<0.00050	<0.00050	8.25	<0.00050	0.059	413	0.909	-	0.118	0.0220	<1.0	50
10WBW004-128	0.00600	<0.0020	0.00585	<0.00050	<0.00050	5.83	<0.00050	0.054	370	0.903	-	0.0937	0.0239	<1.0	48
10WBW004-129	0.00659	<0.0030	0.00537	<0.00050	<0.00050	5.68	<0.00050	0.055	414	0.888	-	0.101	0.0216	<1.0	50
10WBW004-130	0.00671	<0.0030	0.00612	<0.00050	<0.00050	5.21	<0.00050	0.057	411	0.953	<0.000050	0.108	0.0228	<1.0	50
10WBW004-131	0.00644	<0.0030	0.00556	<0.00050	<0.00050	4.89	<0.00050	0.053	394	0.887	<0.000050	0.0942	0.0223	<1.0	49
10WBW004-Z6-312	0.00619	0.00106	0.00352	0.00592	<0.00050	12.1	0.00067	0.046	415	0.890	<0.000010	0.0975	0.0130	<1.0	52
10WBW004-Z6-313	0.00565	<0.00070	0.00313	0.00286	<0.00050	10.8	<0.00030	0.047	408	0.814	<0.000010	0.0914	0.0123	<1.0	51
10WBW004-Z6-314	0.00809	<0.00050	0.00482	<0.00050	<0.00050	15.7	<0.00030	0.053	447	0.989	-	0.110	0.0121	<1.0	51
10WBW004-Z6-315	-	-	-	-	-	-	-	-	422	-	-	-	-	-	54
10WBW004-Z6-316	-	-	-	-	-	-	-	-	481	-	-	-	-	-	53
10WBW004-Z6-317	0.00622	0.00155	0.00509	<0.00050	<0.00050	4.74	<0.00030	0.048	411	0.847	<0.000010	0.0968	0.0180	<1.0	52
10WBW004-Z6-318	0.00674	0.00213	0.00339	<0.00050	<0.00050	5.05	0.00802	0.047	494	0.826	-	0.0966	0.0143	<1.0	53
10WBW004-Z6-404	0.00806	0.00251	0.00295	<0.00050	<0.00050	13.3	0.00045	0.043	476	0.847	<0.000050	0.0968	0.0109	<1.0	48
10WBW004-Z6-405	0.00821	0.00834	0.00306	<0.00050	<0.00050	13.4	0.00046	0.044	475	0.864	<0.000050	0.1	0.0147	<1.0	48
10WBW004-Z6-406	0.00589	0.00591	0.00477	<0.00050	<0.00050	6.7	<0.00030	0.04	417	0.841	<0.000050	0.0908	0.0187	<1.0	51
10WBW004-Z6-508	0.00815	0.00903	0.00298	<0.00050	<0.00050	10.5	0.00071	0.045	519	0.841	<0.000050	0.101	0.0165	<1.0	52
10WBW004-Z6-509	0.00682	0.00521	0.00341	<0.00050	<0.00050	10.4	0.0004	0.043	452	0.855	<0.000050	0.101	0.015	<1.0	52
10WBW001-02b	-	0.033	<0.004	<0.02	-	12.00	0.002	0.37	1540	2.62	<0.0001	0.0059	0.0335	-	268
10WBW001-03b	-	<0.016	<0.004	<0.02	-	3.53	<0.002	0.13	726	1.04	<0.0001	0.0244	0.0138	-	114
10WBW001-04b	-	0.024	<0.004	<0.02	-	3.65	<0.002	0.14	736	1.06	<0.0001	0.0237	0.0144	-	116
10WBW001-12	-	<0.16	<0.04	<0.2	-	7.51	<0.02	<1.2	914	1.23	<0.0001	<0.02	<0.04	-	211
10WBW001-14	-	0.55	<0.04	<0.2	-	5.08	<0.02	<1.2	1020	1.40	<0.0001	<0.02	<0.04	-	223
10WBW001-15	-	0.61	<0.04	<0.2	-	7.15	<0.02	<1.2	1290	1.73	<0.0001	<0.02	<0.04	-	294
10WBW001-16	-	0.66	<0.04	<0.2	-	7.14	<0.02	<1.2	1290	1.76	<0.0001	<0.02	<0.04	-	292
10WBW001-28	-	0.660	<0.04	<0.2	-	4.74	<0.02	<1.2	1120	1.27	<0.0001	0.0250	<0.04	-	185
10WBW001-31	-	0.72	<0.04	<0.2	-	3.33	<0.02	<1.2	1290	1.73	<0.0001	0.02	<0.04	-	227
10WBW001-33	-	0.86	<0.04	<0.2	-	3.54	<0.02	<1.2	1210	1.81	<0.0001	<0.02	<0.04	-	203
10WBW001-36	0000	0.00	<0.0005	<0.001	<0.0005	1.60	<0.001	0.093	0739	0.56	-	0.0403	0.00159	<1	125
10WBW001-37	0.00097	0.0030	<0.0005	<0.001	<0.0005	3.95	<0.001	0.128	867	1.09	-	0.0225	0.00237	<1	166
10WBW001-101	0000	0.00	0.000092	<0.0005	<0.0005	2.94	0.00035	0.117	1010	0.95	<0.00001	0.037	0.00059	<1	171
10WBW001-102	0.001	0.00011	0.000084	<0.0005	<0.0005	4.31	<0.0003	0.128	797	1.15	<0.00001	0.0244	<0.0005	<1	166
10WBW001-103	0.00155	<0.0005	0.000381	<0.0005	<0.0005	4.53	<0.0003	0.228	1510	2.08	<0.00005	0.0140	0.00095	<1	240
10WBW001-105	0.00151	0.00016	0.000132	<0.0005	<0.0005	11	<0.0003	0.2	1230	1.73	<0.00001	0.0072	<0.0005	<1	262
10WBW001-107	0.00155	<0.0001	0.000356	<0.0005	<0.0005	4.56	<0.0003	0.217	1480	2.13	<0.00001	0.012	0.00098	<1	233
10WBW001-108	0.00095	<0.0005	0.000103	0.00061	<0.0005	2.28	<0.0003	0.131	1080	0.892	-	0.0361	0.00120	<1	172
10WBW001-Z1-300	0.00101	0.0139	0.000241	0.00354	<0.00050	0.256	0.00061	0.375	74.9	0.750	<0.000010	0.0145	0.00733	<1.0	41
10WBW001-Z6-301	0.00114	0.00163	0.000078	0.00065	<0.00050	4.41	0.00044	0.167	1280	1.25	<0.000010	0.0292	0.00169	<1.0	210
10WBW001-Z10-302	0.00120	0.00132	0.000159	0.00122	<0.00050	9.52	0.00051	0.194	1250	1.29	<0.000010	0.0056	0.00230	<1.0	261
10WBW001-Z10-303	0.00085	0.00294	0.000171	<0.00050	<0.00050	1.45	0.00083	0.192	1480	2.04	<0.000010	<0.0020	0.00185	<1.0	282
10WBW001-Z6-304	0.00203	0.00321	0.000535	0.00181	<0.00050	10.3	0.00111	0.470	1760	2.45	<0.000010	0.0051	0.00192	<1.0	286
10WBW001-Z10-500	0.00105	0.00364	0.000235	0.00346	<0.00050	6.7	<0.00030	0.143	1230	1.3	<0.000050	0.0062	0.00363	<1.0	243
10WBW001-Z1-501	0.00095	0.00481	0.000322	0.00064	<0.00050	0.274	<0.00030	0.301	71.4	0.69	<0.000050	0.0107	0.00346	<1.0	39
10WBW001-Z6-502	0.00127	0.00471	0.00019	0.00061	<0.00050	7.08	0.00051	0.158	1340	1.63	<0.000050	0.0211	0.00343	<1.0	213
10WBW001-Z6-503	0.00134	0.00697	0.000224	0.00057	<0.00050	7.29	<0.00030	0.171	1360	1.65	<0.000050	0.0225	0.00486	<1.0	218
10WBW001-Z6-504	0.00194	0.004	0.00018	0.00061	<0.00050	9.46	0.00054	0.368	1670	2.4	<0.000050	0.0052	0.0029	<1.0	277
10WBW001-Z10-505	0.00102	0.00307	0.000209	0.0007	<0.00050	4.03	0.00103	0.169	1360	2.07	<0.000050	<0.0020	0.00201	<1.0	262
10WBW001-Z10	0.00123	0.0185	0.000709	0.00171	<0.00050	8.72	0.00038	0.208	1150	1.14	<0.000010	0.0102	0.0163	<1.0	249
10WBW001-Z01	0.00122	0.0098	0.000447	0.00184	<0.00050	0.554	0.00037	0.561	69.9	0.706	<0.000010	0.0217	0.0117	<1.0	39
10WBW001-Z6	0.00154	0.0151	0.000269	0.00145	<0.00050	11.5	<0.00030	0.278	1420	1.83	<0.000010	0.0158	0.00675	<1.0	244
10WBW001-01-2022	0.00104	-	<0.002	<0.01	-	2.58	<0.001	0.362	68.3	0.887	<0.000005	0.0124	<0.01	<1	40.5
10WBW001-01-2023	0.00106	<0.025	<0.005	<0.025	-	2.92	<0.0025	0.321	64.4	0.902	<0.000005	0.012	<0.025	<2.5	41.1
10WBW001-01-2024	0.00108	<0.025	<0.005	<0.025	-	2.27	<0.0025	0.355	63.7	0.85	<0.000005	0.0104	<0.025	<2.5	40.2
10WBW001-06-2022	0.00062	-	<0.002	<0.01	-	<0.2	<0.001	0.0675	332	0.293	<0.000005	<0.001	<0.01	<1	94.9
10WBW001-06-2023	0.000694	0.00567	<0.001	<0.005	-	0.12	<0.0005	0.0639	390	0.333	0.0000062	0.000601	<0.005	<0.5	107
10WBW001-06-2024	0.000633	0.0112	<0.001	<0.005	-	0.196	<0.0005	0.0648	326	0.28	<0.000005	0.0015	0.00512	<0.5	92.7
10WBW001-10-2022	0.000175	-	<0.0005	<0.0025	-	0.283	<0.00025	0.0176	36	0.0395	<0.000005	0.0024	<0.0025	0.7	30.8
10WBW001-10-2023	0.000161	0.00216	0.0002	0.00112	-	0.298	0.000135	0.0157	34.5	0.0378	<0.000005	0.003	0.0014	0.79	29.8
10WBW001-10-2024	0.000161	0.002	0.0035	0.00123	-	0.267	0.000114	0.0168	38	0.0407	<0.000005	0.00472	0.00109	0.842	30.6
10WBW001-01b	-	0.036	0.0046	<0.02	-	2.27	0.0021	0.37	181	1.44	<0.0001	0.0411	0.0774	-	057
10WBW001-17	-	0.960	<0.04	<0.2	-	0.51	<0.02	<1.2	076	0.77	<0.0001	0.0200	0.0740	-	036
10WBW001-20	-	0.95	<0.04	<0.2	-	0.68	<0.02	<1.2	066	0.71	<0.0001	<0.02	0.071	-	035
10WBW001-25	-	0.62	<0.04	<0.2	-	0.15	<0.02	<1.2	0051	0.62	<0.0001	<0.02	0.068	-	044
10WBW001-26	-	0.74	<0.04	<0.2	-	0.16	<0.02	<1.2	0053	0.64	<0.0001	<0.02	0.074	-	045
10WBW001-35	0000	0.01	<0.0005	0.0018	<0.0005	0.46	0.0013	0.37	0071	0.72	-	0.0136	0.00437	<1	040
10WBW001-100	0.00102	0.0006	0.000073	0.00059	<0.0005	0.24	<0.0003	0.346	064	0.72	<0.00001	0.0089	0.00075	<1	040
10WBW001-106	0.0011	0.0002	0.000051	0.00102	<0.0005	0.197	<0.0003	0.381	67.8	0.712	<0.00001	0.0088	0.00265	<1	39
10WBW002-01	-	0.63	0.094	<0.2	-	133	0.113	<1.2	132	2.68	<0.0001	0.222	1.40	-	36
10WBW002-02	-	0.48	0.088	<0.2	-	34.4	0.030	<1.2	114	0.47	<0.0001	0.223	1.82	-	35
10WBW002-109a	0.0057	0.0062	<0.0005	0.0242	<0.005	0.51	0.0039	<0.2	113	0.0233	<0.00001	0.178	0.0076	<10	<200
10WBW002-109b	0.0061	0.107	0.00841	0.0467	<0.005	38.6	0.0438	0.44	129	1.05	<0.00001	0.178	0.0359	<10	<200
10WBW002-121	0.0063	0.120	0.00949	0.0585	<0.005	54.6	0.0663	<0.2	135	1.15	0.000014	0.193	0.0402	<10	<200
10WBW002-Z1-305	-	-	-	-	-	-	-	-	-	-	-	-	-	-	-
10WBW002-Z1-306	0.0064	0.0707	0.00610	0.0409	<0.0050	27.0	0.0403	1.01	101	0.642	-	0.166	0.0321	<10	<200
10WBW002-Z1-307	0.0066	0.0783	0.00725	0.0406	<0.0050	28.4	0.0336	0.51	110	0.759	<0.000010	0.165	0.0299	<10	<200
10WBW002-Z3-308	<0.0050	0.0178	<0.00050	0.0127	<0.0050	0.94	<0.0030	0.21	103	0.0460	<0.000010	0.221	0.0220	<10	<200
10WBW002-Z2-309	<0.0025	0.00534	0.00071	0.0174	<0.0025	1.30	0.0154	<0.10	41.8	0.150	-	0.049	0.0145	<5.0	<100
10WBW002-Z1-400	-	-	-	-	-	-	-	-	-	-	-	-	-	-	-
10WBW002-Z1-401	-	-	-	-	-	-	-	-	-	-	-	-	-	-	-
10WBW002-Z3-403	0.0045	<0.0090	0.00063	0.0231	<0.0025	0.734	0.0041	0.33	102	0.181	<0.000050	0.19	0.0231	<5.0	<200
10WBW002-Z1-510	-	-	-	-	-	-	-	-	-	-	-	-	-	-	-
10WBW002-Z1-511	0.0055	0.0111	0.00055	0.0135	<0.0050	1.19	<0.0030	<0.20	111	0.0347	<0.000050	0.177	0.0133	<10	<200
10WBW002-Z3-512	-	-	-	-	-	-	-	-	-	-	-	-	-	-	-

Field Sample ID	Rhenium (Re)-Total	Rubidium (Rb)-Total	Selenium (Se)-Total	Silicon (Si)-Total	Silver (Ag)-Total	Sodium (Na)-Total	Strontium (Sr)-Total	Tellurium (Te)-Total	Thallium (Tl)-Total	Thorium (Th)-Total	Tin (Sn)-Total	Titanium (Ti)-Total	Tungsten (W)-Total	Uranium (U)-Total	Vanadium (V)-Total
	mg/L	mg/L	mg/L	mg/L	mg/L	mg/L	mg/L	mg/L	mg/L	mg/L	mg/L	mg/L	mg/L	mg/L	mg/L
10WBW004-123	<0.0005	0.0533	<0.002	1.61	<0.0001	1680	17.2	<0.0005	<0.00005	<0.0005	<0.001	<0.005	<0.001	0.00503	<0.0005
10WBW004-124	<0.00050	0.0568	<0.0020	1.62	<0.00010	1760	19.9	<0.00050	<0.000050	<0.00050	<0.0010	<0.0050	<0.0010	0.00517	<0.00050
10WBW004-125	<0.00050	0.0555	<0.0020	1.68	<0.00010	1780	19.8	<0.00050	<0.000050	<0.00050	<0.0010	<0.0050	<0.0010	0.00501	<0.00050
10WBW004-126	<0.00050	0.0556	<0.0020	1.67	<0.00010	2500	26.1	<0.00050	<0.000050	<0.00050	<0.0010	<0.0050	0.0014	0.00636	<0.00050
10WBW004-128	<0.00050	0.0544	<0.0020	1.76	<0.00010	2190	23.0	<0.00050	<0.000050	<0.00050	<0.0010	<0.0050	0.0015	0.00733	<0.00050
10WBW004-129	<0.00050	0.0536	<0.0020	1.77	<0.00010	2480	26.0	<0.00050	<0.000050	<0.00050	<0.0010	<0.0050	0.0029	0.00840	<0.00050
10WBW004-130	<0.00050	0.0554	<0.0020	1.80	<0.00010	2460	26.5	<0.00050	<0.000050	<0.00050	<0.0010	<0.0050	0.0053	0.0101	<0.00050
10WBW004-131	<0.00050	0.0544	<0.0020	1.81	<0.00010	2360	24.8	<0.00050	<0.000050	<0.00050	<0.0010	<0.0050	0.0015	0.00864	<0.00050
10WBW004-Z6-312	<0.00050	0.0540	<0.0020	1.81	<0.00010	2450	24.7	<0.00050	0.000055	<0.00050	<0.0010	<0.0050	<0.0010	0.00395	<0.00050
10WBW004-Z6-313	<0.00050	0.0502	<0.0020	1.76	<0.00010	2430	26.6	<0.00050	<0.000050	<0.00050	<0.0010	<0.0050	<0.0010	0.00389	<0.00050
10WBW004-Z6-314	<0.00050	0.0523	<0.0020	1.47	<0.00010	2600	28.4	<0.00050	<0.000050	<0.00050	<0.0010	<0.0050	<0.0010	0.00299	<0.00050
10WBW004-Z6-315	-	-	-	-	-	2500	-	-	-	-	-	-	-	-	-
10WBW004-Z6-316	-	-	-	-	-	2830	-	-	-	-	-	-	-	-	-
10WBW004-Z6-317	<0.00050	0.0529	<0.0020	1.88	<0.00010	2440	26.4	<0.00050	<0.000050	<0.00050	<0.0010	<0.0050	<0.0010	0.00822	<0.00050
10WBW004-Z6-318	<0.00050	0.0496	<0.0020	1.92	<0.00010	2900	30.2	<0.00050	<0.000050	<0.00050	<0.0010	<0.0050	0.0066	0.00783	<0.00050
10WBW004-Z6-404	<0.00050	0.0473	<0.0020	1.54	<0.00010	2840	25.3	<0.00050	<0.000050	<0.00050	<0.0010	<0.0050	<0.0010	0.00398	<0.00050
10WBW004-Z6-405	<0.00050	0.0484	<0.0020	1.62	<0.00010	2850	26.3	<0.00050	<0.000050	<0.00050	<0.0010	<0.0050	0.0012	0.00435	<0.00050
10WBW004-Z6-406	<0.00050	0.0476	<0.0020	1.92	<0.00010	2370	21.6	<0.00050	<0.000050	<0.00050	<0.0010	<0.0050	<0.0010	0.00799	<0.00050
10WBW004-Z6-508	<0.00050	0.0481	<0.0080	1.88	<0.00010	3110	27.1	<0.00050	<0.000050	<0.00050	<0.0010	<0.0050	0.001	0.0047	<0.00050
10WBW004-Z6-509	<0.00050	0.0526	<0.020	1.88	<0.00010	2770	25.4	<0.00050	<0.000050	<0.00050	<0.0010	<0.0050	<0.0010	0.00604	<0.00050
10WBW001-02b	-	-	<0.4	-	<0.002	9750	-	-	<0.002	-	<0.05	<0.012	-	<0.002	0.17
10WBW001-03b	-	-	<0.4	-	<0.002	4860	-	-	<0.002	-	<0.05	<0.012	-	<0.002	<0.1
10WBW001-04b	-	-	<0.4	-	<0.002	4930	-	-	<0.002	-	<0.05	<0.012	-	<0.002	<0.1
10WBW001-12	-	-	0.106	-	<0.02	6640	-	-	<0.02	-	<0.08	<0.12	-	<0.02	<0.1
10WBW001-14	-	-	0.147	-	<0.02	7150	-	-	<0.02	-	<0.08	<0.12	-	<0.02	0.18
10WBW001-15	-	-	<0.4	-	<0.02	9260	-	-	<0.02	-	<0.08	<0.12	-	<0.02	0.20
10WBW001-16	-	-	<0.4	-	<0.02	9580	-	-	<0.02	-	<0.08	<0.12	-	<0.02	0.22
10WBW001-28	-	-	<0.4	-	<0.02	6830	-	-	<0.02	-	<0.08	<0.12	-	<0.02	0.22
10WBW001-31	-	-	<0.4	-	<0.02	8290	-	-	<0.02	-	<0.08	<0.12	-	<0.02	0.25
10WBW001-33	-	-	<0.4	-	<0.02	7450	-	-	<0.02	-	<0.08	<0.12	-	<0.02	0.27
10WBW001-36	<0.0005	000	<0.002	2.88	<0.0002	4460	0010	<0.0005	<0.0005	<0.0005	<0.001	<0.005	0.0334	<0.0005	<0.0005
10WBW001-37	<0.0005	0.0816	<0.002	2.12	<0.0002	5590	11.7	<0.0005	<0.0005	<0.0005	<0.001	<0.005	0.0067	<0.0005	<0.0005
10WBW001-101	<0.0005	000	<0.002	3.5	<0.0001	6410	0014	<0.0005	<0.00005	<0.0005	<0.001	<0.005	0.0247	<0.00005	<0.0005
10WBW001-102	<0.0005	0.0842	<0.002	2.42	<0.0001	5530	11.1	<0.0005	<0.00005	<0.0005	<0.001	<0.005	0.0051	0.000057	<0.0005
10WBW001-103	<0.0005	0.1420	<0.002	3.68	<0.0001	9350	21.2	<0.0005	<0.00005	<0.0005	<0.001	<0.005	0.0056	0.00023	0.00054
10WBW001-105	<0.0005	0.104	<0.002	3.51	<0.0001	8990	16.4	<0.0005	<0.00005	<0.0005	<0.001	<0.005	0.0059	<0.00005	<0.0005
10WBW001-107	<0.0005	0.141	<0.002	3.48	<0.0001	9170	19.9	<0.0005	<0.00005	<0.0005	<0.001	<0.005	0.0049	0.000228	<0.0005
10WBW001-108	<0.0005	0.102	<0.002	3.82	0.00018	6790	14.6	<0.0005	<0.00005	<0.0005	<0.001	<0.005	0.0227	0.000059	<0.0005
10WBW001-Z1-300	<0.00050	0.0546	<0.0020	2.51	<0.00010	7290	57.7	<0.00050	<0.000050	<0.00050	<0.0010	<0.0050	0.0018	<0.000050	<0.00050
10WBW001-Z6-301	<0.00050	0.133	<0.0020	3.36	<0.00010	8390	18.4	<0.00050	<0.000050	<0.00050	<0.0010	<0.0050	0.0163	<0.000050	<0.00050
10WBW001-Z10-302	<0.00050	0.114	<0.0020	3.22	<0.00010	9090	17.7	<0.00050	<0.000050	<0.00050	<0.0010	<0.0050	0.0088	<0.000050	<0.00050
10WBW001-Z10-303	<0.00050	0.115	<0.0020	3.6	<0.00010	10200	22.7	<0.00050	<0.000050	<0.00050	<0.0010	<0.0050	0.0021	<0.000050	0.00087
10WBW001-Z6-304	<0.00050	0.193	<0.0020	4.1	<0.00010	11300	29.4	<0.00050	<0.000050	<0.00050	<0.0010	0.0303	0.0026	<0.000050	0.00157
10WBW001-Z10-500	<0.00050	0.0949	<0.030	3.38	<0.00010	8680	15.6	<0.00050	<0.000050	<0.00050	<0.0010	<0.0050	0.0085	<0.000050	<0.00050
10WBW001-Z1-501	<0.00050	0.0481	<0.030	2.55	<0.00010	7130	52.9	<0.00050	<0.000050	<0.00050	<0.0010	<0.0050	0.0018	<0.000050	0.00138
10WBW001-Z6-502	<0.00050	0.128	<0.050	3.08	<0.00010	8560	18	<0.00050	<0.000050	<0.00050	<0.0010	<0.0050	0.0096	<0.000050	<0.00050
10WBW001-Z6-503	<0.00050	0.141	<0.030	3.11	<0.00010	8720	18.7	<0.00050	<0.000050	<0.00050	<0.0010	<0.0050	0.0096	<0.000050	<0.00050
10WBW001-Z6-504	<0.00050	0.178	<0.050	3.6	<0.00010	10700	27.2	<0.00050	<0.000050	<0.00050	<0.0010	<0.0050	0.0025	<0.000050	<0.00050
10WBW001-Z10-505	<0.00050	0.115	<0.030	3.03	<0.00010	9440	20.8	<0.00050	<0.000050	<0.00050	<0.0010	<0.0050	0.0027	0.000201	<0.00050
10WBW001-Z10	<0.00050	0.111	<0.0020	3.04	0.00101	8710	16.4	<0.00050	<0.000050	<0.00050	<0.0010	<0.0050	0.0084	0.00008	<0.00050
10WBW001-Z01	<0.00050	0.135	<0.0020	2.39	0.00015	7310	58.1	<0.00050	<0.000050	<0.00050	<0.0010	<0.0050	0.0019	0.00165	0.00076
10WBW001-Z6	<0.00050	0.155	<0.0020	2.9	<0.00010	9470	21.5	<0.00050	<0.000050	<0.00050	<0.0010	<0.0050	0.0098	<0.000050	<0.00050
10WBW001-01-2022	-	0.0493	0.00213	3.1	<0.0002	6720	60.3	0.00443	<0.0002	<0.002	<0.002	<0.006	<0.002	<0.0002	<0.01
10WBW001-01-2023	-	0.0495	<0.0025	<5	<0.0005	6720	55.4	<0.01	<0.0005	<0.005	<0.005	<0.015	<0.005	<0.0005	<0.025
10WBW001-01-2024	-	0.047	<0.0025	<5	<0.0005	6890	55.7	<0.01	<0.0005	<0.005	<0.005	<0.015	<0.005	<0.0005	<0.025
10WBW001-06-2022	-	0.0514	<0.001	5.14	<0.0002	2980	4.34	<0.004	<0.0002	<0.002	<0.002	<0.006	0.0026	<0.0002	<0.01
10WBW001-06-2023	-	0.056	<0.0005	6.39	<0.0001	3380	4.27	<0.002	<0.0001	<0.001	<0.001	<0.003	0.0022	0.00022	<0.01
10WBW001-06-2024	-	0.0491	<0.0005	6.09	0.0001	2980	3.8	<0.004	<0.0002	<0.002	<0.002	0.00116	0.00142	0.000237	0.00207
10WBW001-10-2022	-	0.0117	0.00101	5.54	<0.00005	715	0.382	<0.001	<0.00005	<0.0005	<0.0005	<0.0015	0.0014	0.000261	<0.0025
10WBW001-10-2023	-	0.0115	0.000168	5.84	<0.00002	656	0.311	<0.0004	<0.00002	<0.0002	<0.0002	0.00104	0.0013	0.000219	0.00229
10WBW001-10-2024	-	0.0118	0.000137	6.35	0.00002	696	0.334	<0.0004	<0.00002	<0.0002	<0.0002	0.00116	0.00142	0.000237	0.00207
10WBW001-01b	-	-	<0.4	-	<0.002	7390	-	-	<0.002	-	<0.05	0.052	-	<0.002	<0.1
10WBW001-17	-	-	<0.4	-	<0.02	6290	-	-	<0.02	-	<0.08	<0.12	-	<0.02	0.31
10WBW001-20	-	-	<0.4	-	<0.02	6580	-	-	<0.02	-	<0.08	<0.12	-	<0.02	0.33
10WBW001-25	-	-	<0.4	-	<0.02	7420	-	-	<0.02	-	<0.08	<0.12	-	<0.02	0.21
10WBW001-26	-	-	<0.4	-	<0.02	7870	-	-	<0.02	-	<0.08	<0.12	-	<0.02	0.23
10WBW001-35	<0.0005	000	<0.002	2.61	<0.0002	7470	0060	<0.0005	<0.0005	<0.0005	<0.001	0.0082	<0.001	<0.0005	0.00
10WBW001-100	<0.0005	0.0526	<0.002	2.79	<0.0001	7200	57.2	<0.0005	<0.00005	<0.0005	<0.001	<0.005	0.0014	<0.00005	<0.0005
10WBW001-106	<0.0005	0.0531	<0.002	2.47	<0.0001	6850	54.6	<0.0005	<0.00005	<0.0005	<0.001	<0.005	0.0016	<0.00005	<0.0005
10WBW002-01	-	-	<0.4	-	<0.02	580	-	-	<0.02	-	<0.08	2.97	-	<0.02	0.98
10WBW002-02	-	-	<0.4	-	<0.02	240	-	-	<0.02	-	<0.08	0.81	-	<0.02	1.34
10WBW002-109a	<0.005	0.051	<0.02	<5	<0.001	280	33.1	<0.005	0.00054	<0.005	<0.01	<0.05	0.028	<0.0005	<0.005
10WBW002-109b	<0.005	0.053	<0.02	25.4	0.0018	1770	59.0	<0.005	0.00052	<0.005	<0.01	0.366	0.028	<0.0005	0.0279
10WBW002-121	<0.005	<0.05	<0.02	27.8	0.0022	450	37.3	<0.005	<0.0005	<0.005	<0.01	0.378	0.030	<0.0005	0.0282
10WBW002-Z1-305	-	-	-	-	-	-	-	-	-	-	-	-	-	-	-
10WBW002-Z1-306	<0.0050	0.070	<0.020	9.8	0.0016	4070	94.3	<0.0050	0.00056	<0.0050	<0.010	0.315	0.030	<0.00050	0.0223
10WBW002-Z1-307	<0.0050	0.060	<0.020	11.2	0.0016	1930	60.3	<0.0050	0.00057	<0.0050	<0.010	0.386	0.028	<0.00050	0.0243
10WBW002-Z3-308	<0.0050	0.054	<0.020	<5.0	<0.0010	880	33.7	<0.0050	<0.00050	<0.0050	<0.010	<0.050	0.018	<0.00050	<0.0050
10WBW002-Z2-309	<0.0025	<0.025	<0.10	<2.5	<0.00050	<100	9.76	<0.0025	<0.00025	<0.0025	<0.0050	<0.025	<0.0050	<0.00025	<0.0025
10WBW002-Z1-400	-	-	-	-	-	-	-	-	-	-	-	-	-	-	-
10WBW002-Z1-401	-	-	-	-	-	-	-	-	-	-	-	-	-	-	-
10WBW002-Z3-403	<0.0025	0.05	<0.030	<5.0	0.0018	1530	31.9	<0.0025	<0.00025	<0.0025	0.0052	<0.025	0.0121	<0.00025	<0.0025
10WBW002-Z1-510	-	-	-	-	-	-	-	-	-	-	-	-	-	-	-
10WBW002-Z1-511	<0.0050	0.05	<0.020	<5.0	<0.0010	810	35.5	<0.0050	<0.00050	<0.0050	<0.010	<0.050	0.023	<0.00050	<0.0050
10WBW002-Z3-512	-	-	-	-	-	-	-	-	-	-	-	-	-	-	-

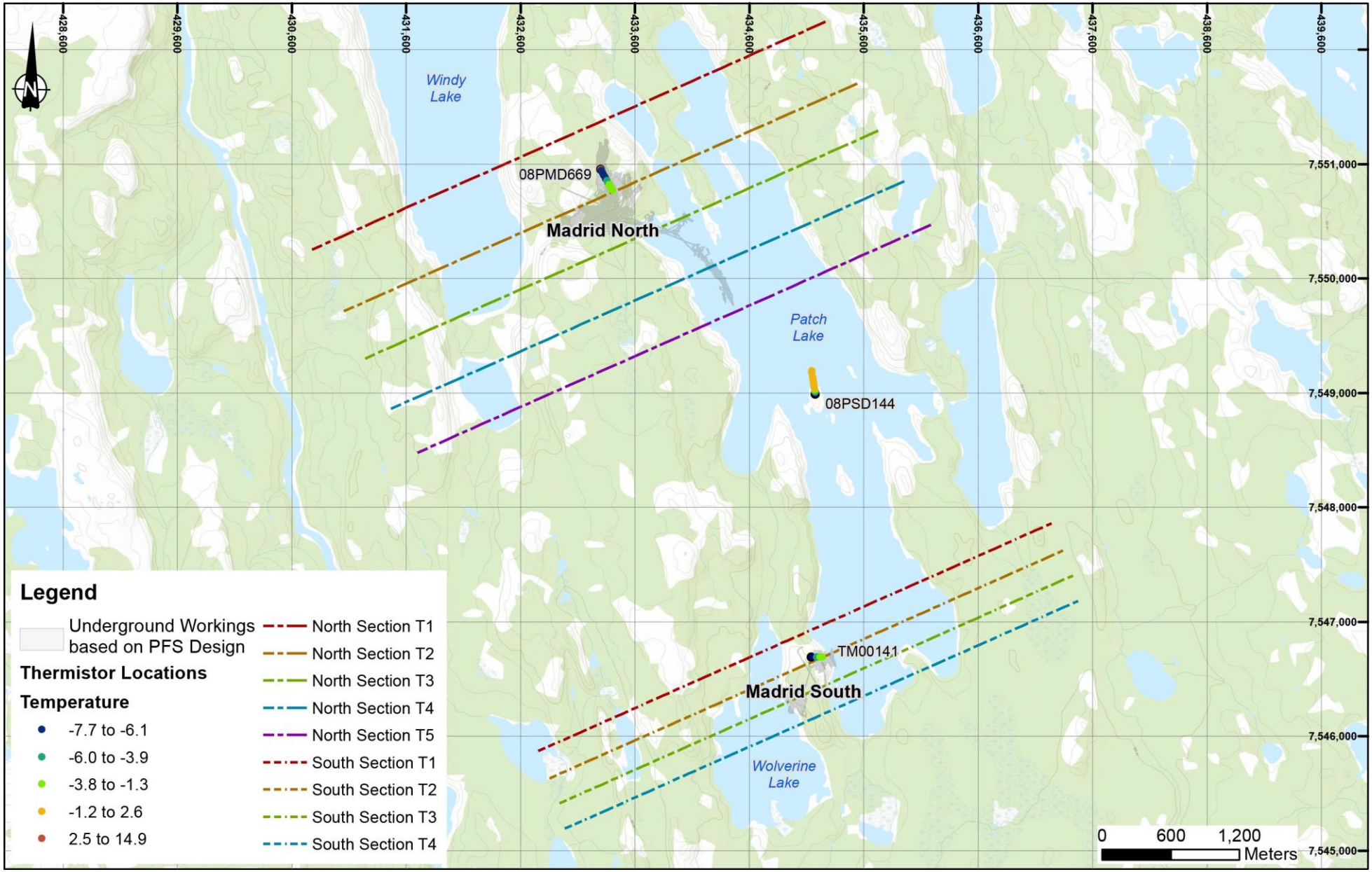
Field Sample ID	Yttrium (Y)-Total	Zinc (Zn)-Total	Zirconium (Zr)-Total	Dissolved Metals	Aluminum (Al)-Dissolved	Antimony (Sb)-Dissolved	Arsenic (As)-Dissolved	Barium (Ba)-Dissolved	Beryllium (Be)-Dissolved	Bismuth (Bi)-Dissolved	Boron (B)-Dissolved	Cadmium (Cd)-Dissolved	Calcium (Ca)-Dissolved	Cesium (Cs)-Dissolved	Chromium (Cr)-Dissolved
	mg/L	mg/L	mg/L		mg/L	mg/L	mg/L	mg/L	mg/L	mg/L	mg/L	mg/L	mg/L	mg/L	mg/L
10WBW004-123	<0.0005	0.392	<0.0005		<0.005	0.0182	<0.002	0.594	<0.0005	<0.0005	0.84	<0.0001	5050	0.00540	<0.0001
10WBW004-124	<0.00050	0.188	<0.00050		<0.0050	0.0178	<0.0020	0.586	<0.00050	<0.00050	0.93	<0.00010	4630	0.00553	<0.00050
10WBW004-125	<0.00050	0.206	<0.00050		<0.0050	0.0182	<0.0020	0.570	<0.00050	<0.00050	0.90	<0.00010	4580	0.00537	<0.00050
10WBW004-126	<0.00050	0.204	<0.00050		<0.0050	0.0178	<0.0020	0.533	<0.00050	<0.00050	0.97	<0.00010	4180	0.00648	<0.00050
10WBW004-128	<0.00050	0.148	<0.00050		<0.0050	0.0194	<0.0020	0.563	<0.00050	<0.00050	0.92	<0.00010	4230	0.00595	<0.00050
10WBW004-129	<0.00050	0.196	<0.00050		<0.0050	0.0211	<0.0020	0.582	<0.00050	<0.00050	1.01	<0.00010	4350	0.00683	<0.00050
10WBW004-130	<0.00050	0.217	<0.00050		<0.0050	0.0207	<0.0020	0.575	<0.00050	<0.00050	0.96	<0.00010	4620	0.00651	<0.00050
10WBW004-131	<0.00050	0.193	<0.00050		<0.0050	0.0192	<0.0020	0.555	<0.00050	<0.00050	0.95	<0.00010	4080	0.00621	<0.00050
10WBW004-Z6-312	<0.00050	0.156	<0.00050		<0.0050	0.0156	<0.0020	0.544	<0.00050	<0.00050	0.86	<0.00010	5040	0.00605	<0.00010
10WBW004-Z6-313	<0.00050	0.145	<0.00050		<0.0050	0.0160	<0.0020	0.554	<0.00050	<0.00050	0.91	<0.00010	4490	0.00612	<0.00010
10WBW004-Z6-314	<0.00050	0.139	<0.00050		<0.0050	0.0118	<0.0020	0.491	<0.00050	<0.00050	0.83	<0.00010	5200	0.00737	<0.00010
10WBW004-Z6-315	-	-	-		-	-	-	-	-	-	-	-	-	-	-
10WBW004-Z6-316	-	-	-		-	-	-	-	-	-	-	-	-	-	-
10WBW004-Z6-317	<0.00050	0.180	<0.00050		<0.0050	0.0180	<0.0020	0.564	<0.00050	<0.00050	0.88	<0.00010	4500	0.00618	<0.00010
10WBW004-Z6-318	<0.00050	0.265	<0.00050		<0.0050	0.0176	<0.0020	0.499	<0.00050	<0.00050	0.88	<0.00010	4690	0.00693	<0.00010
10WBW004-Z6-404	<0.00050	0.125	<0.02		<0.0050	0.0152	<0.0020	0.496	<0.00050	<0.00050	0.9	<0.000050	4700	0.00786	<0.00050
10WBW004-Z6-405	<0.00050	0.867	<0.00050		<0.0050	0.0153	<0.0020	0.528	<0.00050	<0.00050	0.9	<0.000050	4530	0.00852	<0.00050
10WBW004-Z6-406	<0.00050	0.133	<0.00050		<0.0050	0.0157	<0.0030	0.541	<0.00050	<0.00050	0.81	<0.000050	4530	0.00618	<0.00050
10WBW004-Z6-508	<0.00050	0.881	<0.00050		<0.0050	0.0151	<0.0050	0.496	<0.00050	<0.00050	0.94	<0.00010	4860	0.00874	<0.00050
10WBW004-Z6-509	<0.00050	0.377	<0.00050		<0.0050	0.0122	<0.0030	0.533	<0.00050	<0.00050	0.85	<0.000050	4490	0.00658	<0.00050
10WBW001-02b	-	0.088	-		<0.1	<0.008	<0.08	0.062	<0.01	-	2.44	<0.001	1640	-	0.0385
10WBW001-03b	-	<0.08	-		0.13	<0.008	<0.08	0.186	<0.01	-	1.31	<0.001	822	-	0.0178
10WBW001-04b	-	<0.08	-		<0.1	<0.008	<0.08	0.188	<0.01	-	1.38	<0.001	837	-	0.0264
10WBW001-12	-	<0.8	-		<1	<0.08	0.100	0.135	<0.1	-	2.06	<0.01	1230	-	<0.8
10WBW001-14	-	<0.8	-		<1	<0.08	0.116	0.105	<0.1	-	2.43	<0.01	1340	-	0.739
10WBW001-15	-	<0.8	-		<1	<0.08	0.091	0.100	<0.1	-	2.23	<0.01	1420	-	0.747
10WBW001-16	-	<0.8	-		<1	<0.08	0.097	0.097	<0.1	-	2.32	<0.01	1560	-	0.874
10WBW001-28	-	<0.8	-		<1	<0.08	<0.08	0.143	<0.1	-	1.64	<0.01	1150	-	0.3130
10WBW001-31	-	<0.8	-		<1	<0.08	<0.08	0.115	<0.1	-	2.03	<0.01	1330	-	0.451
10WBW001-33	-	<0.8	-		<1	<0.08	0.102	0.120	<0.1	-	1.97	<0.01	1390	-	0.682
10WBW001-36	<0.0005	0.195	<0.0005		<0.005	0.00703	<0.002	0.120	<0.0005	<0.0005	0.94	<0.00012	0749	0000	<0.001
10WBW001-37	<0.0005	0.261	<0.0005		<0.005	0.00306	<0.002	0.169	<0.0005	<0.0005	1.42	<0.00012	1010	0.00092	<0.001
10WBW001-101	<0.0005	0.236	<0.0005		<0.005	0.0048	<0.002	0.178	<0.0005	<0.0005	1.38	<0.00005	1100	0000	<0.0001
10WBW001-102	<0.0005	0.173	<0.0005		<0.005	0.00097	<0.002	0.178	<0.0005	<0.0005	1.54	<0.00005	1110	0.00104	<0.0001
10WBW001-103	<0.0005	0.046	<0.0005		<0.005	0.00121	0.0066	0.113	<0.0005	<0.0005	2.64	<0.00005	1550	0.00154	<0.0005
10WBW001-105	<0.0005	0.107	<0.0005		<0.005	0.00053	<0.002	0.122	<0.0005	<0.0005	2.86	<0.00005	1560	0.00148	<0.0001
10WBW001-107	<0.0005	0.0241	<0.0005		<0.005	0.00116	0.0069	0.115	<0.0005	<0.0005	2.61	<0.00005	1520	0.00159	<0.0001
10WBW001-108	<0.0005	0.115	<0.0005		<0.005	0.00393	<0.002	0.169	<0.0005	<0.0005	1.48	<0.00005	1160	0.00097	<0.0005
10WBW001-Z1-300	<0.00050	0.150	<0.00050		<0.0050	<0.00050	<0.0020	0.0522	<0.00050	<0.00050	3.05	<0.000050	4770	0.00103	<0.00050
10WBW001-Z6-301	<0.00050	0.335	<0.00050		<0.0050	<0.00050	<0.0020	0.182	<0.00050	<0.00050	1.86	<0.000050	1400	0.00119	<0.00050
10WBW001-Z10-302	<0.00050	0.278	<0.00050		<0.0050	<0.00050	<0.0020	0.0973	<0.00050	<0.00050	2.67	0.000138	1560	0.00116	<0.00050
10WBW001-Z10-303	<0.00050	0.212	<0.00050		<0.0050	<0.00050	<0.0020	0.0651	<0.00050	<0.00050	2.75	0.000082	2050	0.00081	<0.00050
10WBW001-Z6-304	<0.00050	0.217	<0.00050		<0.0050	<0.00050	<0.0020	0.0576	<0.00050	<0.00050	3.05	0.000100	2010	0.00180	<0.00050
10WBW001-Z10-500	<0.00050	0.259	<0.00050		<0.0050	<0.00050	<0.0040	0.0986	<0.00050	<0.00050	2.13	<0.000050	1590	0.00114	<0.00050
10WBW001-Z1-501	<0.00050	0.279	<0.00050		<0.0050	<0.00050	<0.0020	0.051	<0.00050	<0.00050	2.54	0.000195	4820	0.00103	<0.00050
10WBW001-Z6-502	<0.00050	1.82	<0.00050		<0.0050	<0.00050	<0.0020	0.129	<0.00050	<0.00050	1.86	<0.000050	1480	0.00132	<0.00050
10WBW001-Z6-503	<0.00050	0.376	<0.00050		<0.0050	<0.00050	<0.0020	0.125	<0.00050	<0.00050	1.98	<0.000050	1490	0.00132	<0.00050
10WBW001-Z6-504	<0.00050	1.71	<0.00050		<0.0050	<0.00050	<0.0050	0.0568	<0.00050	<0.00050	2.83	0.000083	2030	0.00193	<0.00050
10WBW001-Z10-505	<0.00050	0.761	<0.00050		<0.0050	<0.00050	<0.0080	0.0621	<0.00050	<0.00050	2.52	0.000108	1870	0.00102	<0.00050
10WBW001-Z10	<0.00050	1.35	<0.00050		0.0056	0.0008	<0.11	0.102	<0.00050	<0.00050	2.66	0.000414	1430	0.00119	<0.00050
10WBW001-Z01	<0.00050	1.27	<0.00050		<0.0050	<0.00050	<0.020	0.0509	<0.00050	<0.00050	3.9	0.00013	4430	0.00102	<0.00050
10WBW001-Z6	<0.00050	0.488	<0.00050		<0.0050	<0.00050	<0.020	0.119	<0.00050	<0.00050	2.89	0.000158	1560	0.00152	<0.00050
10WBW001-01-2022	-	0.683	<0.004		<0.05	<0.005	<0.005	0.0642	<0.001	<0.0025	2.38	<0.00025	4400	0.00111	-
10WBW001-01-2023	-	0.685	<0.01		0.0861	<0.005	<0.005	0.0639	<0.001	<0.0025	3.14	<0.00025	4750	0.00103	<0.025
10WBW001-01-2024	-	1.52	<0.01		0.05	<0.005	<0.005	0.0627	<0.001	<0.0025	3.39	<0.00025	4730	0.00115	<0.025
10WBW001-06-2022	-	0.197	<0.004		0.0204	<0.002	<0.002	0.0506	<0.0004	<0.001	1.73	<0.0001	298	0.000572	-
10WBW001-06-2023	-	0.0913	<0.002		0.0188	<0.001	<0.001	0.0629	<0.0002	<0.0005	2.32	<0.00005	335	0.000704	<0.005
10WBW001-06-2024	-	0.198	<0.004		0.01	<0.001	<0.001	0.0525	<0.0002	<0.0005	2.5	<0.00005	295	0.00065	<0.005
10WBW001-10-2022	-	0.241	<0.001		0.015	<0.0005	0.00074	0.0438	<0.0001	<0.00025	1.1	-	26.9	0.000153	-
10WBW001-10-2023	-	0.248	<0.0004		0.0064	<0.0002	0.00055	0.0504	<0.00004	<0.0001	1.35	<0.00001	26.7	0.00017	<0.001
10WBW001-10-2024	-	0.198	<0.0004		0.0041	<0.0002	0.00058	0.053	<0.00004	<0.0001	1.53	<0.00001	31.2	0.00016	<0.001
10WBW001-01b	-	<0.08	-		0.12	<0.008	<0.08	0.057	<0.01	-	3.19	<0.001	4390	-	0.0444
10WBW001-17	-	<0.8	-		<1	<0.08	0.103	0.052	<0.1	-	2.64	<0.01	4480	-	0.8840
10WBW001-20	-	<0.8	-		<1	<0.08	0.103	0.048	<0.1	-	2.62	<0.01	4260	-	0.899
10WBW001-25	-	<0.8	-		<1	<0.08	<0.08	0.051	<0.1	-	2.87	<0.01	4520	-	0.351
10WBW001-26	-	<0.8	-		<1	<0.08	0.090	0.052	<0.1	-	2.74	<0.01	4360	-	0.532
10WBW001-35	<0.0005	0.503	<0.0005		<0.005	<0.0005	<0.002	0.052	<0.0005	<0.0005	2.99	<0.00012	4960	0000	<0.001
10WBW001-100	0.00052	0.279	<0.0005		<0.005	<0.0005	<0.002	0.053	<0.0005	<0.0005	2.92	0.000083	4920	0.00102	<0.0001
10WBW001-106	0.00057	0.285	<0.0005		0.005	<0.0005	<0.002	0.0526	<0.0005	<0.0005	3.3	0.000097	4730	0.0011	<0.0001
10WBW002-01	-	<0.8	-		<1	<0.08	0.266	0.683	<0.1	-	0.86	<0.01	72100	-	0.371
10WBW002-02	-	<0.8	-		<1	<0.08	0.421	0.770	<0.1	-	0.99	<0.01	79800	-	0.328
10WBW002-109a	<0.005	0.595	<0.005		<0.05	0.0093	<0.02	0.833	<0.005	<0.005	<1	<0.0005	74700	0.0063	0.0079
10WBW002-109b	<0.005	0.373	<0.005		-	-	-	-	-	-	-	-	-	-	-
10WBW002-121	<0.005	0.557	<0.005		<0.05	0.0094	<0.02	0.817	<0.005	<0.005	<1	<0.0005	73100	0.0062	<0.001
10WBW002-Z1-305	-	-	-		-	-	-	-	-	-	-	-	-	-	-
10WBW002-Z1-306	<0.0050	2.51	<0.0050		-	-	-	-	-	-	-	-	-	-	-
10WBW002-Z1-307	<0.0050	1.91	<0.0050		<0.050	0.0087	<0.020	0.815	<0.0050	<0.0050	<1.0	<0.00050	71100	0.0065	<0.0020
10WBW002-Z3-308	<0.0050	0.703	<0.0050		0.052	0.0082	<0.020	0.986	<0.0050	<0.0050	<1.0	<0.00050	65300	0.0052	<0.0010
10WBW002-Z2-309	<0.0025	76.7	<0.0025		<0.025	0.0044	0.029	0.265	<0.0025	<0.0025	<0.50	0.00094	23000	<0.0025	<0.00050
10WBW002-Z1-400	-	-	-		0.04	0.0087	<0.020	0.829	<0.0025	<0.0025	1.48	<0.00050	83000	0.0057	<0.0020
10WBW002-Z1-401	-	-	-		0.042	0.0085	<0.010	0.818	<0.0025	<0.0025	1.03	<0.00050	74600	0.0061	<0.00050
10WBW002-Z3-403	<0.0025	1.71	<0.0025		<0.025	0.0075	<0.020	0.795	<0.0025	<0.0025	0.9	<0.00050	63100	0.005	<0.00050
10WBW002-Z1-510	-	-	-		<0.050	0.0095	<0.20	0.82	<0.0050	<0.0050	<1.0	<0.00050	71600	0.0061	<0.0050
10WBW002-Z1-511	<0.0050	0.658	<0.0050		<0.050	0.0092	<0.20	0.851	<0.0050	<0.0050	<1.0	<0.00050	80000	0.0063	<0.0050
10WBW002-Z3-512	-	-	-		<0.050	0.0088	<0.20	0.728	<0.0050	<0.0050	<1.0	0.00059	64300	0.0052	<0.0050

Field Sample ID	Cobalt (Co)-Dissolved	Copper (Cu)-Dissolved	Gallium (Ga)-Dissolved	Iron (Fe)-Dissolved	Lead (Pb)-Dissolved	Lithium (Li)-Dissolved	Magnesium (Mg)-Dissolved	Manganese (Mn)-Dissolved	Mercury (Hg)-Dissolved	Molybdenum (Mo)-Dissolved	Nickel (Ni)-Dissolved	Phosphorus (P)-Dissolved	Potassium (K)-Dissolved	Rhenium (Re)-Dissolved	Rubidium (Rb)-Dissolved
	mg/L	mg/L	mg/L	mg/L	mg/L	mg/L	mg/L	mg/L	mg/L	mg/L	mg/L	mg/L	mg/L	mg/L	mg/L
10WBW004-123	0.00779	<0.0005	<0.0005	8.05	<0.0003	0.054	311	1.01	<0.00001	0.0902	0.0320	<1	47	<0.0005	0.0601
10WBW004-124	0.00736	<0.00050	<0.00050	7.38	<0.00050	0.055	312	0.989	-	0.0866	0.0313	<1.0	47	<0.00050	0.0587
10WBW004-125	0.00708	<0.00050	<0.00050	7.06	<0.00050	0.055	309	0.950	-	0.0860	0.0301	<1.0	47	<0.00050	0.0576
10WBW004-126	0.00526	<0.00050	<0.00050	6.43	<0.00050	0.055	404	0.888	-	0.0990	0.0199	<1.0	48	<0.00050	0.0530
10WBW004-128	0.00575	<0.00050	<0.00050	5.06	<0.00050	0.055	365	0.899	-	0.0931	0.0229	<1.0	48	<0.00050	0.0551
10WBW004-129	0.00529	<0.00050	<0.00050	4.34	<0.00050	0.057	425	0.911	-	0.100	0.0203	<1.0	50	<0.00050	0.0564
10WBW004-130	0.00566	<0.00050	<0.00050	4.45	<0.00050	0.055	432	0.904	<0.000050	0.101	0.0201	<1.0	53	<0.00050	0.0541
10WBW004-131	0.00529	<0.00050	<0.00050	4.45	<0.00050	0.054	387	0.870	<0.000050	0.0967	0.0208	<1.0	49	<0.00050	0.0539
10WBW004-Z6-312	0.00452	<0.00050	<0.00050	3.50	<0.00030	0.044	425	0.859	<0.000010	0.0852	0.0157	<1.0	55	<0.00050	0.0531
10WBW004-Z6-313	0.00465	<0.00050	<0.00050	3.54	<0.00030	0.049	403	0.853	<0.000010	0.0868	0.0163	<1.0	51	<0.00050	0.0533
10WBW004-Z6-314	0.00434	<0.00050	<0.00050	11.8	<0.00030	0.048	435	0.889	-	0.0956	0.0110	<1.0	51	<0.00050	0.0483
10WBW004-Z6-315	-	-	-	-	-	-	-	-	-	-	-	-	-	-	-
10WBW004-Z6-316	-	-	-	-	-	-	-	-	-	-	-	-	-	-	-
10WBW004-Z6-317	0.00504	<0.00050	<0.00050	0.233	<0.00030	0.048	404	0.840	<0.000010	0.0878	0.0167	<1.0	51	<0.00050	0.0533
10WBW004-Z6-318	0.00327	<0.00050	<0.00050	3.48	<0.00030	0.047	492	0.836	-	0.0970	0.0138	<1.0	52	<0.00050	0.0499
10WBW004-Z6-404	0.00323	<0.00050	<0.00050	8.51	<0.00030	0.045	496	0.891	<0.000050	0.1	0.0122	<1.0	50	<0.00050	0.0494
10WBW004-Z6-405	0.00346	<0.00050	<0.00050	10	<0.00030	0.047	473	0.97	<0.000050	0.104	0.0129	<1.0	49	<0.00050	0.0525
10WBW004-Z6-406	0.00314	<0.00050	<0.00050	10.3	<0.00030	0.042	425	0.881	<0.000050	0.095	0.0115	<1.0	51	<0.00050	0.0503
10WBW004-Z6-508	0.00275	<0.00050	<0.00050	10.9	<0.00030	0.048	525	0.88	<0.000050	0.11	0.00999	<1.0	53	<0.00050	0.052
10WBW004-Z6-509	0.00374	0.00187	<0.00050	8.68	<0.00030	0.043	441	0.849	<0.000050	0.0988	0.0131	<1.0	51	<0.00050	0.051
10WBW001-02b	<0.002	<0.012	-	9.26	<0.002	0.297	1430	2.48	<0.0001	<0.005	0.0289	-	251	-	-
10WBW001-03b	<0.002	<0.012	-	1.88	<0.002	0.128	707	1.01	<0.0001	0.0240	0.0146	-	129	-	-
10WBW001-04b	<0.002	<0.012	-	1.63	<0.002	0.136	721	1.01	<0.0001	0.0239	0.0159	-	131	-	-
10WBW001-12	<0.02	0.13	-	-	<0.02	<0.6	990	-	<0.0001	<0.02	0.032	-	225	-	-
10WBW001-14	<0.02	<0.12	-	-	<0.02	<0.6	1070	-	<0.0001	<0.02	0.043	-	245	-	-
10WBW001-15	<0.02	0.19	-	5.77	<0.02	<0.6	1170	1.56	<0.0001	<0.02	<0.02	-	206	-	-
10WBW001-16	<0.02	<0.12	-	6.25	<0.02	<0.6	1300	1.72	<0.0001	<0.02	<0.02	-	294	-	-
10WBW001-28	<0.02	<0.12	-	1.54	<0.02	<0.6	1070	1.17	<0.0001	0.0280	<0.02	-	170	-	-
10WBW001-31	<0.02	<0.12	-	2.87	<0.02	<0.6	1270	1.7	<0.0001	0.023	<0.02	-	186	-	-
10WBW001-33	<0.02	<0.12	-	3.32	<0.02	<0.6	1310	1.96	<0.0001	<0.02	<0.02	-	194	-	-
10WBW001-36	<0.0005	<0.001	<0.0005	0.06	<0.001	0.087	0702	0.53	-	0.0379	0.00076	<1	117	<0.0005	000
10WBW001-37	<0.0005	<0.001	<0.0005	2.68	<0.001	0.121	849	1.04	-	0.0211	<0.0005	<1	160	<0.0005	0.0766
10WBW001-101	0.000087	<0.0005	<0.0005	0.13	<0.0003	0.12	0964	0.94	<0.00001	0.037	<0.0005	<1	160	<0.0005	000
10WBW001-102	0.000102	<0.0005	<0.0005	3.15	<0.0003	0.13	869	1.17	<0.00001	0.0259	<0.0005	<1	173	<0.0005	0.085
10WBW001-103	0.000315	<0.0005	<0.0005	4.31	<0.003	0.223	1490	2.03	<0.00005	0.0138	0.00101	<1	233	<0.0005	0.1400
10WBW001-105	0.000187	0.00296	<0.0005	8.94	<0.0003	0.201	1250	1.69	<0.00001	0.0044	0.0006	<1	249	<0.0005	0.107
10WBW001-107	0.000312	<0.0005	<0.0005	4.55	<0.0003	0.223	1450	2.11	<0.00001	0.0122	0.00094	<1	229	<0.0005	0.139
10WBW001-108	0.000091	<0.0005	<0.0005	0.503	<0.0003	0.127	1080	0.888	-	0.0345	0.00158	<1	172	<0.0005	0.106
10WBW001-Z1-300	0.000059	0.00083	<0.00050	0.034	<0.00030	0.371	71.2	0.731	<0.000010	0.0112	0.00163	<1.0	39	<0.00050	0.0529
10WBW001-Z6-301	<0.000050	<0.00050	<0.00050	0.624	<0.00030	0.175	1270	1.22	<0.000010	0.0311	0.00100	<1.0	208	<0.00050	0.140
10WBW001-Z10-302	<0.000050	<0.00050	<0.00050	5.83	<0.00030	0.190	1200	1.20	<0.000010	0.0038	0.00073	<1.0	251	<0.00050	0.109
10WBW001-Z10-303	<0.000050	<0.00050	<0.00050	0.881	<0.00030	0.189	1420	2.01	<0.000010	<0.0020	<0.00050	<1.0	270	<0.00050	0.112
10WBW001-Z6-304	0.000153	<0.00050	<0.00050	7.28	<0.00030	0.428	1640	2.15	<0.000010	0.0054	0.00140	<1.0	268	<0.00050	0.172
10WBW001-Z10-500	0.00012	<0.00050	<0.00050	6.72	<0.00030	0.156	1220	1.36	<0.000050	0.0052	0.00102	<1.0	244	<0.00050	0.101
10WBW001-Z1-501	<0.000050	<0.00050	<0.00050	0.02	<0.00030	0.309	67.9	0.736	<0.000050	0.0102	0.0005	<1.0	38	<0.00050	0.0502
10WBW001-Z6-502	0.000067	<0.00050	<0.00050	3.81	<0.00030	0.165	1340	1.7	<0.000050	0.0181	0.00063	<1.0	217	<0.00050	0.136
10WBW001-Z6-503	0.000075	<0.00050	<0.00050	3.96	<0.00030	0.173	1350	1.75	<0.000050	0.0187	0.00066	<1.0	218	<0.00050	0.141
10WBW001-Z6-504	0.000093	0.00054	<0.00050	8.91	<0.00030	0.379	1720	2.48	<0.000050	0.0044	0.00057	<1.0	282	<0.00050	0.182
10WBW001-Z10-505	0.000067	<0.00050	<0.00050	3.87	<0.00030	0.166	1370	2.09	<0.000050	<0.0020	0.00053	<1.0	264	<0.00050	0.115
10WBW001-Z10	0.00127	0.00064	<0.00050	5.78	<0.00030	0.213	1110	1.2	<0.000010	0.0116	0.0263	<1.0	245	<0.00050	0.112
10WBW001-Z01	0.000188	<0.00050	<0.00050	0.08	<0.00030	0.476	65.8	0.701	<0.000010	0.0129	0.00466	<1.0	40	<0.00050	0.0547
10WBW001-Z6	0.000127	<0.00050	<0.00050	4.81	<0.00030	0.275	1400	1.71	<0.000010	0.0143	0.00179	<1.0	242	<0.00050	0.158
10WBW001-01-2022	<0.005	<0.01	-	3.18	<0.0025	0.308	64	0.89	<0.000005	0.0116	0.128	<2.5	38.2	-	0.0471
10WBW001-01-2023	<0.005	<0.01	-	2.66	<0.0025	0.337	66.5	0.905	<0.000005	0.0101	<0.025	<2.5	41.2	-	0.0506
10WBW001-01-2024	<0.005	<0.01	-	2.09	<0.0025	0.366	63.4	0.85	<0.000005	0.00896	<0.025	<2.5	39.7	-	0.0473
10WBW001-06-2022	<0.002	<0.004	-	<0.2	<0.001	0.06	340	0.302	<0.000005	<0.001	<0.01	<1	94.7	-	0.0534
10WBW001-06-2023	<0.001	<0.002	-	<0.1	<0.0005	0.0672	393	0.316	<0.000005	<0.0005	<0.005	<0.5	103	-	0.056
10WBW001-06-2024	<0.001	<0.002	-	<0.1	<0.0005	0.064	321	0.275	<0.000005	<0.0005	<0.005	<0.5	208	-	0.0478
10WBW001-10-2022	<0.0005	0.00129	-	0.226	0.000298	0.0155	33.7	0.0359	<0.000005	0.00196	<0.0025	0.7	29.9	-	0.0118
10WBW001-10-2023	<0.0002	<0.0004	-	0.163	<0.0001	0.0167	36	0.0353	<0.000005	0.00225	<0.001	0.78	29.7	-	0.0117
10WBW001-10-2024	<0.0002	0.00043	-	0.136	<0.0001	0.0182	37.5	0.0397	<0.000005	0.00305	<0.001	0.818	30.5	-	0.0116
10WBW001-01b	0.0043	0.014	-	0.22	<0.002	0.370	172	1.34	<0.0001	0.0411	0.0817	-	054	-	-
10WBW001-17	<0.02	<0.12	-	<0.15	<0.02	<0.6	080	0.81	<0.0001	0.0200	0.0640	-	043	-	-
10WBW001-20	<0.02	<0.12	-	<0.15	<0.02	<0.6	066	0.694	<0.0001	<0.02	0.055	-	039	-	-
10WBW001-25	<0.02	<0.12	-	<0.15	<0.02	<0.6	0046	0.544	<0.0001	<0.02	0.061	-	039	-	-
10WBW001-26	<0.02	<0.12	-	<0.15	<0.02	<0.6	0045	0.53	<0.0001	<0.02	0.066	-	037	-	-
10WBW001-35	<0.0005	<0.001	<0.0005	<0.05	<0.001	0.37	0070	0.69	-	0.0128	<0.0005	<1	039	<0.0005	000
10WBW001-100	<0.00005	<0.0005	<0.0005	0.06	<0.0003	0.350	064	0.71	<0.00001	0.0092	<0.0005	<1	039	<0.0005	0.0528
10WBW001-106	<0.00005	0.00067	<0.0005	0.075	<0.0003	0.39	68.1	0.725	<0.00001	0.009	0.00237	<1	40	<0.0005	0.0532
10WBW002-01	0.061	<0.12	-	<1.5	<0.02	<0.6	113	<0.25	<0.0001	0.222	1.43	-	39	-	-
10WBW002-02	0.074	<0.12	-	<1.5	<0.02	<0.6	124	<0.25	<0.0001	0.180	1.68	-	52	-	-
10WBW002-109a	<0.0005	0.0129	<0.005	0.12	0.0030	0.44	110	0.0196	<0.00001	0.163	<0.005	<10	<200	<0.005	0.053
10WBW002-109b	-	-	-	-	-	-	-	-	-	-	-	-	-	-	-
10WBW002-121	<0.0005	0.0158	<0.005	<0.1	<0.003	<0.2	113	0.0141	<0.00001	0.175	0.0072	<10	<200	<0.005	<0.05
10WBW002-Z1-305	-	-	-	-	-	-	-	-	-	-	-	-	-	-	-
10WBW002-Z1-306	-	-	-	-	-	-	-	-	-	-	-	-	-	-	-
10WBW002-Z1-307	<0.00050	0.0123	<0.0050	<0.10	<0.0030	0.50	102	0.0182	-	0.157	0.0059	<10	<200	<0.0050	0.059
10WBW002-Z3-308	<0.00050	0.0115	<0.0050	<0.10	<0.0030	0.22	102	0.0372	-	0.220	0.0098	<10	<200	<0.0050	0.057
10WBW002-Z2-309	0.00038	0.0094	<0.0025	<0.050	0.0024	<0.10	42.4	0.120	-	0.047	0.0103	<5.0	<100	<0.0025	<0.025
10WBW002-Z1-400	<0.00025	0.0155	<0.0025	<0.050	<0.0015	0.1	125	0.0088	-	0.189	0.0113	<5.0	<200	<0.0025	0.056
10WBW002-Z1-401	<0.00025	0.0134	<0.0025	0.058	<0.0015	0.29	111	0.0151	<0.000050	0.195	0.008	<5.0	<200	<0.0025	0.056
10WBW002-Z3-403	0.00039	0.0186	<0.0025	<0.050	<0.0015	0.37	111	0.185	<0.000050	0.199	0.0177	<5.0	<200	<0.0025	0.054
10WBW002-Z1-510	<0.00050	0.0129	<0.0050	<0.10	<0.0030	<0.20	108	0.0116	<0.000050	0.196	0.0069	<10	<200	<0.0050	0.052
10WBW002-Z1-511	<0.00050	0.0133	<0.0050	<0.10	<0.0030	<0.20	116	0.012	<0.000050	0.209	0.0082	<10	<200	<0.0050	0.053
10WBW002-Z3-512	<0.00050	0.0123	<0.0050	<0.10	<0.0030	0.39	112	0.252	<0.000050	0.21	0.0101	<10	<200	<0.0050	0.052

Field Sample ID	Selenium (Se)-Dissolved	Silicon (Si)-Dissolved	Silver (Ag)-Dissolved	Sodium (Na)-Dissolved	Strontium (Sr)-Dissolved	Tellurium (Te)-Dissolved	Thallium (Tl)-Dissolved	Thorium (Th)-Dissolved	Tin (Sn)-Dissolved	Titanium (Ti)-Dissolved	Tungsten (W)-Dissolved	Uranium (U)-Dissolved	Vanadium (V)-Dissolved	Yttrium (Y)-Dissolved	Zinc (Zn)-Dissolved
	mg/L	mg/L	mg/L	mg/L	mg/L	mg/L	mg/L	mg/L	mg/L	mg/L	mg/L	mg/L	mg/L	mg/L	mg/L
10WBW004-123	<0.002	1.57	<0.0001	1820	18.8	<0.0005	<0.00005	<0.0005	<0.001	<0.005	<0.001	0.00512	<0.0005	<0.0005	0.156
10WBW004-124	<0.0020	1.65	<0.00010	1820	21.3	<0.00050	<0.000050	<0.00050	<0.0010	<0.0050	<0.0010	0.00523	<0.00050	<0.00050	0.0944
10WBW004-125	<0.0020	1.63	<0.00010	1790	20.1	<0.00050	<0.000050	<0.00050	<0.0010	<0.0050	<0.0010	0.00521	<0.00050	<0.00050	0.0933
10WBW004-126	<0.0030	1.65	<0.00010	2410	25.3	<0.00050	<0.000050	<0.00050	<0.0010	<0.0050	0.0020	0.00730	<0.00050	<0.00050	0.136
10WBW004-128	<0.0020	1.72	<0.00010	2200	23.1	<0.00050	<0.000050	<0.00050	<0.0010	<0.0050	0.0013	0.00730	<0.00050	<0.00050	0.114
10WBW004-129	<0.0021	1.71	<0.00010	2510	27.0	<0.00050	<0.000050	<0.00050	<0.0010	<0.0050	0.0029	0.00909	<0.00050	<0.00050	0.0941
10WBW004-130	<0.0045	1.89	<0.00010	2600	26.3	<0.00050	<0.000050	<0.00050	<0.0010	<0.0050	0.0050	0.0100	<0.00050	<0.00050	0.137
10WBW004-131	<0.0020	1.78	<0.00010	2330	24.4	<0.00050	<0.000050	<0.00050	<0.0010	<0.0050	0.0014	0.00863	<0.00050	<0.00050	0.131
10WBW004-Z6-312	<0.0020	1.93	<0.00010	2600	26.3	<0.00050	<0.000050	<0.00050	<0.0010	<0.0050	<0.0010	0.00621	<0.00050	<0.00050	0.298
10WBW004-Z6-313	<0.0020	1.75	<0.00010	2390	26.2	<0.00050	<0.000050	<0.00050	<0.0010	<0.0050	<0.0010	0.00655	<0.00050	<0.00050	0.296
10WBW004-Z6-314	<0.0020	1.31	<0.00010	2540	27.5	<0.00050	<0.000050	<0.00050	<0.0010	<0.0050	<0.0010	0.00281	<0.00050	<0.00050	0.105
10WBW004-Z6-315	-	-	-	-	-	-	-	-	-	-	-	-	-	-	-
10WBW004-Z6-316	-	-	-	-	-	-	-	-	-	-	-	-	-	-	-
10WBW004-Z6-317	<0.0020	1.75	<0.00010	2400	26.0	<0.00050	<0.000050	<0.00050	<0.0010	<0.0050	<0.0010	0.00848	<0.00050	<0.00050	0.104
10WBW004-Z6-318	<0.0020	1.86	<0.00010	2890	30.1	<0.00050	<0.000050	<0.00050	<0.0010	<0.0050	0.0054	0.00823	<0.00050	<0.00050	0.194
10WBW004-Z6-404	<0.0020	1.67	<0.00010	2960	26.8	<0.00050	<0.000050	<0.00050	<0.0010	<0.0050	<0.0010	0.00617	<0.00050	<0.00050	0.153
10WBW004-Z6-405	<0.0020	1.6	<0.00010	2850	28	<0.00050	<0.000050	<0.00050	<0.0010	<0.0050	<0.0010	0.00599	<0.00050	<0.00050	0.125
10WBW004-Z6-406	<0.0030	1.79	<0.00010	2400	23.1	<0.00050	<0.000050	<0.00050	<0.0010	<0.0050	<0.0010	0.00508	<0.00050	<0.00050	0.0548
10WBW004-Z6-508	<0.020	1.83	<0.00010	3170	27.6	<0.00050	<0.000050	<0.00050	<0.0010	<0.0050	<0.0010	0.00469	<0.00050	<0.00050	0.456
10WBW004-Z6-509	<0.010	1.87	<0.00010	2670	24.7	<0.00050	<0.000050	<0.00050	<0.0010	<0.0050	<0.0010	0.0067	<0.00050	<0.00050	0.161
10WBW001-02b	<0.4	-	<0.002	9080	-	-	<0.001	-	<0.05	<0.006	-	<0.002	0.152	-	0.041
10WBW001-03b	<0.4	-	<0.002	4470	-	-	<0.001	-	<0.05	0.0135	-	<0.002	0.077	-	0.026
10WBW001-04b	<0.4	-	<0.002	4540	-	-	<0.001	-	<0.05	0.0081	-	<0.002	0.099	-	0.022
10WBW001-12	0.107	-	<0.02	7130	-	-	<0.01	-	<0.05	<0.06	-	<0.02	0.221	-	<0.2
10WBW001-14	0.139	-	<0.02	7840	-	-	<0.01	-	<0.05	<0.06	-	<0.02	0.214	-	<0.2
10WBW001-15	<0.4	-	<0.02	7970	-	-	<0.01	-	<0.05	<0.06	-	<0.02	0.259	-	0.22
10WBW001-16	<0.4	-	<0.02	9450	-	-	0.010	-	<0.05	<0.06	-	<0.02	0.292	-	<0.2
10WBW001-28	<0.4	-	<0.02	6450	-	-	<0.01	-	<0.05	<0.06	-	<0.02	0.128	-	<0.2
10WBW001-31	<0.4	-	<0.02	7910	-	-	<0.01	-	<0.05	<0.06	-	<0.02	0.176	-	<0.2
10WBW001-33	<0.4	-	<0.02	8160	-	-	<0.01	-	<0.05	<0.06	-	<0.02	0.229	-	<0.2
10WBW001-36	<0.002	2.48	<0.0002	4130	0009	<0.0005	<0.0005	<0.0005	<0.001	<0.005	0.0316	<0.0005	<0.0005	<0.0005	0.02
10WBW001-37	<0.002	1.99	<0.0002	5400	11.3	<0.0005	<0.0005	<0.0005	<0.001	<0.005	0.0059	<0.0005	<0.0005	<0.0005	0.0504
10WBW001-101	<0.002	2.88	<0.0001	6010	0013	<0.0005	<0.00005	<0.0005	<0.001	<0.005	0.0246	<0.00005	<0.0005	<0.0005	0.0705
10WBW001-102	<0.002	2.38	<0.0001	5780	11.7	<0.0005	<0.00005	<0.0005	<0.001	<0.005	0.005	0.000059	<0.0005	<0.0005	0.061
10WBW001-103	<0.002	3.49	<0.0001	9130	21.1	<0.0005	<0.00005	<0.0005	<0.001	<0.005	0.0053	0.000231	<0.0005	<0.0005	0.0384
10WBW001-105	<0.002	3.3	<0.0001	8700	16.8	<0.0005	<0.00005	<0.0005	<0.001	<0.005	0.006	<0.00005	<0.0005	<0.0005	0.0851
10WBW001-107	<0.002	3.38	<0.0001	8980	19.4	<0.0005	<0.00005	<0.0005	<0.001	<0.005	0.0048	0.000234	<0.0005	<0.0005	0.0243
10WBW001-108	<0.002	3.33	<0.0001	6810	14.6	<0.0005	<0.00005	<0.0005	<0.001	<0.005	0.0231	0.000058	<0.0005	<0.0005	0.0295
10WBW001-Z1-300	<0.0020	2.42	<0.00010	7020	55.8	<0.00050	<0.000050	<0.00050	<0.0010	<0.0050	0.0018	<0.000050	<0.00050	<0.00050	0.157
10WBW001-Z6-301	<0.0020	3.00	<0.00010	8270	18.1	<0.00050	<0.000050	<0.00050	<0.0010	<0.0050	0.0159	<0.000050	<0.00050	<0.00050	0.154
10WBW001-Z10-302	<0.0020	2.88	<0.00010	8700	17.0	<0.00050	<0.000050	<0.00050	<0.0010	<0.0050	0.0082	<0.000050	<0.00050	<0.00050	0.0708
10WBW001-Z10-303	<0.0020	3.2	<0.00010	9790	21.8	<0.00050	<0.000050	<0.00050	<0.0010	<0.0050	0.0020	<0.000050	0.00058	<0.00050	0.0049
10WBW001-Z6-304	<0.0020	3.4	<0.00010	10600	27.6	<0.00050	<0.000050	<0.00050	<0.0010	<0.0050	0.0021	0.000054	<0.00050	<0.00050	0.669
10WBW001-Z10-500	<0.040	2.91	<0.00010	8540	16.5	<0.00050	<0.000050	<0.00050	<0.0010	<0.0050	0.0072	<0.000050	<0.00050	<0.00050	0.0511
10WBW001-Z1-501	<0.0040	2.35	<0.00010	7030	54.1	<0.00050	<0.000050	<0.00050	<0.0010	<0.0050	0.0018	<0.000050	<0.00050	<0.00050	0.116
10WBW001-Z6-502	<0.010	3.24	<0.00010	8650	18.2	<0.00050	<0.000050	<0.00050	<0.0010	<0.0050	0.0086	<0.000050	<0.00050	<0.00050	0.252
10WBW001-Z6-503	<0.020	3.25	<0.00010	8670	18.8	<0.00050	<0.000050	<0.00050	<0.0010	<0.0050	0.0087	<0.000050	<0.00050	<0.00050	0.304
10WBW001-Z6-504	<0.030	3.6	<0.00010	10900	27.3	<0.00050	<0.000050	<0.00050	<0.0010	<0.0050	0.0026	<0.000050	<0.00050	<0.00050	0.114
10WBW001-Z10-505	<0.050	3	<0.00010	9500	19.9	<0.00050	<0.000050	<0.00050	<0.0010	<0.0050	0.0025	0.000194	<0.00050	<0.00050	0.0337
10WBW001-Z10	<0.0020	2.78	<0.00010	8460	16.4	<0.00050	<0.000050	<0.00050	<0.0010	<0.0050	0.007	0.000063	<0.00050	<0.00050	2.28
10WBW001-Z01	<0.0020	2.16	<0.00010	6450	53.7	<0.00050	<0.000050	<0.00050	<0.0010	<0.0050	0.002	<0.000050	<0.00050	<0.00050	0.333
10WBW001-Z6	<0.0020	2.39	<0.00010	9370	21.1	<0.00050	<0.000050	<0.00050	<0.0010	<0.0050	0.0078	<0.000050	<0.00050	<0.00050	0.751
10WBW001-01-2022	<0.0025	3.1	<0.0005	6600	58.3	<0.01	<0.0005	<0.005	<0.005	<0.015	<0.005	<0.0005	<0.025	-	0.766
10WBW001-01-2023	<0.0025	3.36	<0.0005	6830	58.6	<0.01	<0.0005	<0.005	<0.005	<0.015	<0.005	<0.0005	<0.025	-	0.542
10WBW001-01-2024	<0.0025	3.26	<0.0005	6700	57.3	<0.01	<0.0005	<0.005	<0.005	<0.015	<0.005	<0.0005	<0.025	-	1.51
10WBW001-06-2022	<0.001	5.53	<0.0002	2960	4.23	<0.004	<0.0002	<0.002	<0.002	<0.006	0.0025	<0.0002	<0.01	-	0.208
10WBW001-06-2023	<0.0005	6.26	<0.0001	3370	4.49	<0.002	<0.0001	<0.001	<0.001	<0.003	0.0023	0.00022	<0.005	-	<0.01
10WBW001-06-2024	<0.0005	6.17	<0.0001	2850	3.66	<0.002	<0.0001	<0.001	<0.001	<0.003	0.00202	0.000234	<0.005	-	<0.01
10WBW001-10-2022	0.000286	5.36	<0.00005	664	0.335	<0.001	<0.00005	<0.0005	<0.0005	<0.0015	0.00115	0.000221	<0.0025	-	0.232
10WBW001-10-2023	0.000166	5.92	<0.00002	693	0.313	<0.0004	<0.00002	<0.0002	<0.0002	0.00063	0.00123	0.000208	0.00145	-	0.005
10WBW001-10-2024	0.000132	6.22	<0.00002	683	0.348	<0.0004	<0.00002	<0.0002	<0.0002	0.00066	0.00134	0.000221	0.00154	-	0.0312
10WBW001-01b	<0.4	-	<0.002	6840	-	-	<0.001	-	<0.05	0.0124	-	<0.002	0.129	-	0.044
10WBW001-17	<0.4	-	<0.02	6810	-	-	0.01	-	<0.05	<0.06	-	<0.02	0.291	-	<0.2
10WBW001-20	<0.4	-	<0.02	6480	-	-	0.013	-	<0.05	<0.06	-	<0.02	0.302	-	0.31
10WBW001-25	<0.4	-	<0.02	6730	-	-	<0.01	-	<0.05	<0.06	-	<0.02	0.122	-	<0.2
10WBW001-26	<0.4	-	<0.02	6260	-	-	<0.01	-	<0.05	<0.06	-	<0.02	0.174	-	<0.2
10WBW001-35	<0.002	2.3	<0.0002	7290	0059	<0.0005	<0.0005	<0.0005	<0.001	<0.005	<0.001	<0.0005	<0.0005	<0.0005	0.0897
10WBW001-100	<0.002	2.42	<0.0001	7200	56.7	<0.0005	<0.00005	<0.0005	<0.001	<0.005	0.0014	<0.00005	<0.0005	0.00051	0.1130
10WBW001-106	<0.002	2.43	<0.0001	6910	55.1	<0.0005	<0.00005	<0.0005	<0.001	<0.005	0.0015	<0.00005	<0.0005	0.00054	0.137
10WBW002-01	<0.4	-	<0.02	655	-	-	<0.01	-	<0.05	<0.06	-	<0.02	0.863	-	<0.2
10WBW002-02	<0.4	-	<0.02	300	-	-	<0.01	-	<0.05	<0.06	-	<0.02	1.08	-	<0.2
10WBW002-109a	<0.02	<5	<0.001	1680	57.6	<0.005	0.00053	<0.005	<0.01	<0.05	0.026	<0.0005	<0.005	<0.005	<0.03
10WBW002-109b	-	-	-	-	-	-	-	-	-	-	-	-	-	-	-
10WBW002-121	<0.02	<5	<0.001	490	35.8	<0.005	<0.0005	<0.005	<0.01	<0.05	0.024	<0.0005	<0.005	<0.005	0.044
10WBW002-Z1-305	-	-	-	-	-	-	-	-	-	-	-	-	-	-	-
10WBW002-Z1-306	-	-	-	-	-	-	-	-	-	-	-	-	-	-	-
10WBW002-Z1-307	<0.020	<5.0	<0.0010	1830	58.6	<0.0050	0.00054	<0.0050	<0.010	<0.050	0.024	<0.00050	<0.0050	<0.0050	0.294
10WBW002-Z3-308	<0.020	<5.0	<0.0010	900	33.2	<0.0050	<0.00050	<0.0050	<0.010	<0.050	0.019	<0.00050	<0.0050	<0.0050	0.180
10WBW002-Z2-309	<0.10	<2.5	<0.00050	<100	9.98	<0.0025	<0.00025	<0.0025	<0.0050	<0.025	<0.0050	<0.00025	<0.0025	<0.0025	35.2
10WBW002-Z1-400	<0.010	<5.0	0.00086	470	37.5	<0.0025	<0.00025	<0.0025	<0.0050	<0.025	0.0233	<0.00025	<0.0025	<0.0025	0.052
10WBW002-Z1-401	<0.010	<5.0	0.00109	1160	46	<0.0025	<0.00025	<0.0025	0.0068	<0.025	0.0229	<0.00025	<0.0025	<0.0025	0.06
10WBW002-Z3-403	<0.050	<5.0	0.00179	1680	35.1	<0.0025	<0.00025	<0.0025	<0.0050	<0.025	0.0131	<0.00025	<0.0025	<0.0025	0.828
10WBW002-Z1-510	<0.030	<5.0	<0.0010	810	39.8	<0.0050	<0.00050	<0.0050	<0.010	<0.050	0.026	<0.00050	<0.0050	<0.0050	0.085
10WBW002-Z1-511	<0.040	<5.0	<0.0010	870	41.3	<0.0050	<0.00050	<0.0050	<0.010	<0.050	0.026	<0.00050	<0.0050	<0.0050	0.197
10WBW002-Z3-512	<0.050	<5.0	<0.0010	2170	34.2	<0.0050	<0.00050	<0.0050	<0.010	<0.050	0.013	<0.00050	<0.0050	<0.0050	0.084

Field Sample ID	Zirconium (Zr)-Dissolved
	mg/L
10WBW004-123	<0.0005
10WBW004-124	<0.00050
10WBW004-125	<0.00050
10WBW004-126	<0.00050
10WBW004-128	<0.00050
10WBW004-129	<0.00050
10WBW004-130	<0.00050
10WBW004-131	<0.00050
10WBW004-Z6-312	<0.00050
10WBW004-Z6-313	<0.00050
10WBW004-Z6-314	<0.00050
10WBW004-Z6-315	-
10WBW004-Z6-316	-
10WBW004-Z6-317	<0.00050
10WBW004-Z6-318	<0.00050
10WBW004-Z6-404	<0.0149
10WBW004-Z6-405	<0.01536
10WBW004-Z6-406	<0.00050
10WBW004-Z6-508	<0.00050
10WBW004-Z6-509	<0.00050
10WBW001-02b	-
10WBW001-03b	-
10WBW001-04b	-
10WBW001-12	-
10WBW001-14	-
10WBW001-15	-
10WBW001-16	-
10WBW001-28	-
10WBW001-31	-
10WBW001-33	-
10WBW001-36	<0.0005
10WBW001-37	<0.0005
10WBW001-101	<0.0005
10WBW001-102	<0.0005
10WBW001-103	<0.0005
10WBW001-105	<0.0005
10WBW001-107	<0.0005
10WBW001-108	<0.0005
10WBW001-Z1-300	<0.00050
10WBW001-Z6-301	<0.00050
10WBW001-Z10-302	<0.00050
10WBW001-Z10-303	<0.00050
10WBW001-Z6-304	<0.00050
10WBW001-Z10-500	<0.00050
10WBW001-Z1-501	<0.00050
10WBW001-Z6-502	<0.00050
10WBW001-Z6-503	<0.00050
10WBW001-Z6-504	<0.00050
10WBW001-Z10-505	<0.00050
10WBW001-Z10	<0.00050
10WBW001-Z01	<0.00050
10WBW001-Z6	<0.00050
10WBW001-01-2022	<0.01
10WBW001-01-2023	<0.015
10WBW001-01-2024	<0.015
10WBW001-06-2022	<0.004
10WBW001-06-2023	<0.003
10WBW001-06-2024	<0.003
10WBW001-10-2022	<0.001
10WBW001-10-2023	<0.0006
10WBW001-10-2024	<0.0006
10WBW001-01b	-
10WBW001-17	-
10WBW001-20	-
10WBW001-25	-
10WBW001-26	-
10WBW001-35	<0.0005
10WBW001-100	<0.0005
10WBW001-106	<0.0005
10WBW002-01	-
10WBW002-02	-
10WBW002-109a	<0.005
10WBW002-109b	-
10WBW002-121	<0.005
10WBW002-Z1-305	-
10WBW002-Z1-306	-
10WBW002-Z1-307	<0.0050
10WBW002-Z3-308	<0.0050
10WBW002-Z2-309	<0.0025
10WBW002-Z1-400	<0.0025
10WBW002-Z1-401	<0.0025
10WBW002-Z3-403	<0.0025
10WBW002-Z1-510	<0.0050
10WBW002-Z1-511	<0.0050
10WBW002-Z3-512	<0.0050

Appendix F – Ground Temperature Data



Notes:

1. Coordinate System: UTM NAD 83 Zone13
2. Basemap Credits: ERSI, DeLorme, TomTom, Intermap, NRCAN, GeoBase
3. Underground Workings based on PFS Design

srk consulting

Job No: 1CT022.004

Filename: BostonDeepGroundTemperatures.pptx

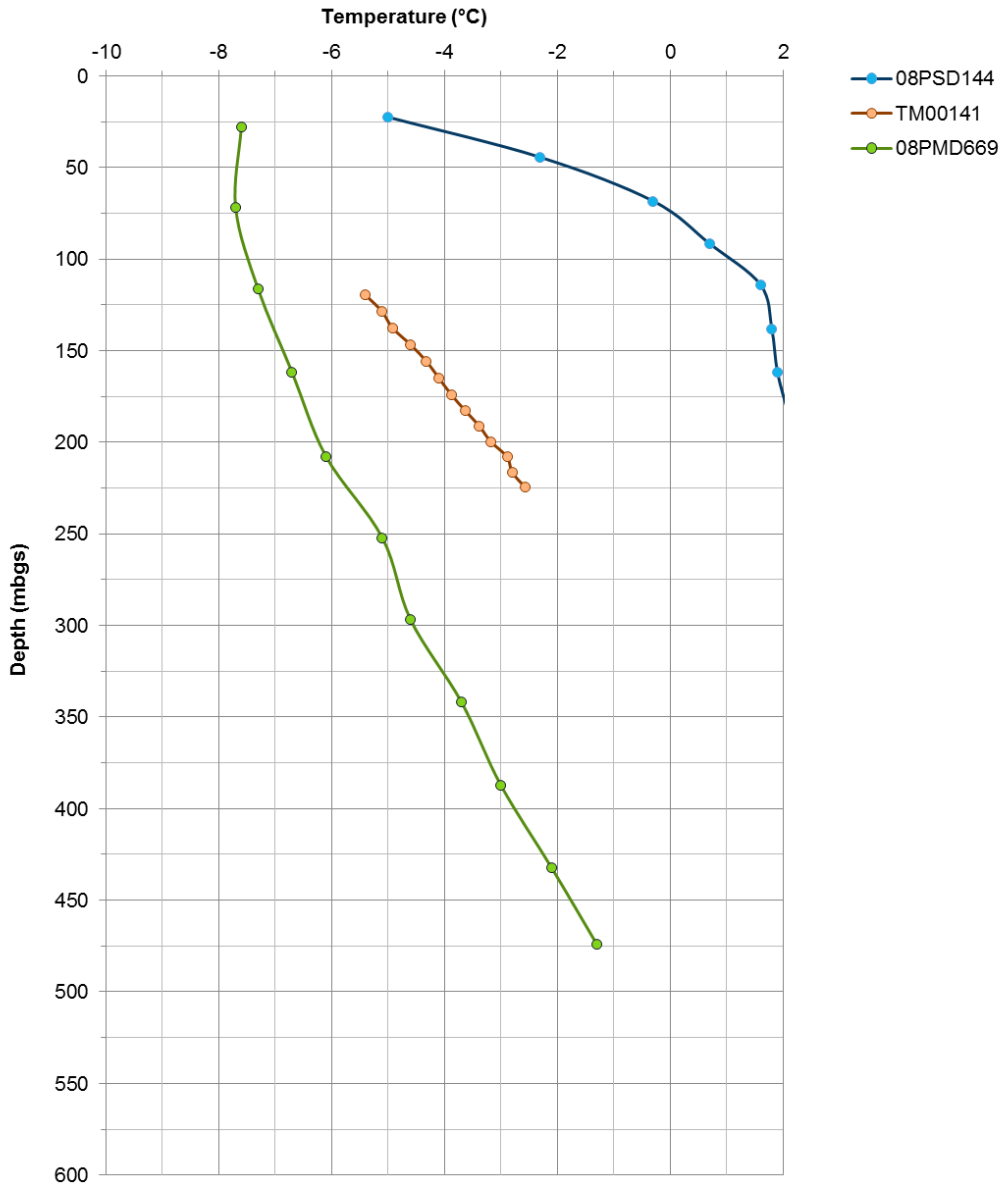
TMAC RESOURCES

HOPE BAY PROJECT

Lake Talik Configuration

Madrid North and South Mining Areas

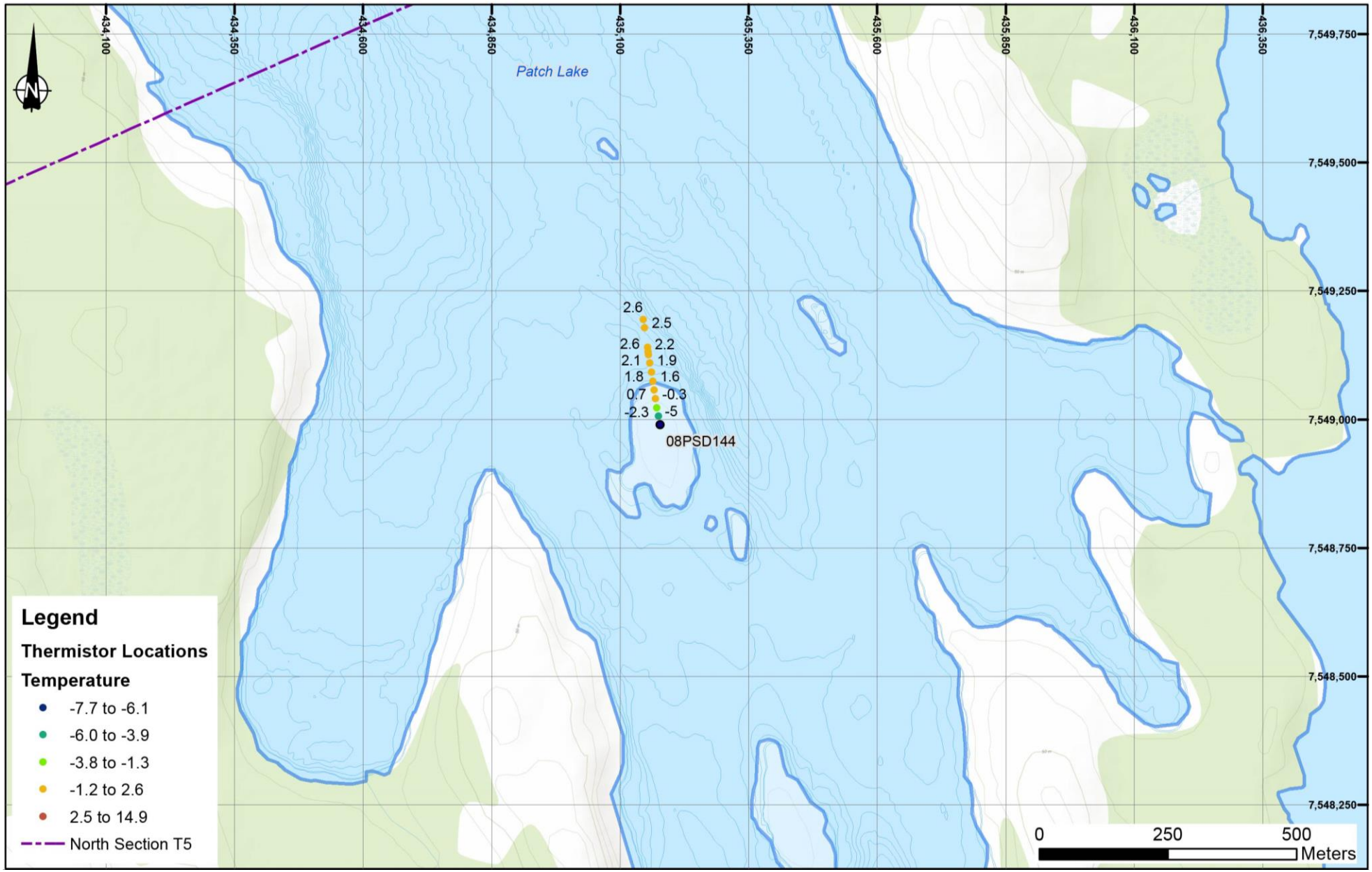
Date:	Approved:	Figure:
2/12/2016	cws	14



Notes:

1. Depth indicated as vertical metres below ground surface (mbgs)

srk consulting	TMAC RESOURCES	Lake Talik Configuration
Job No: 1CT022.004 Filename: BostonDeepGroundTemperatures.pptx	HOPE BAY PROJECT	**Deep Ground Temperatures – Madrid Mining Area**
		Date: 2/12/2016 | Approved: cws | Figure: **15**



Notes:

1. Coordinate System: UTM NAD 83 Zone13
2. Basemap Credits: ERSI, DeLorme, TomTom, Intermap, NRCAN, GeoBase
3. Underground Workings based on PFS Design

srk consulting

Job No: 1CT022.004

Filename: BostonDeepGroundTemperatures.pptx

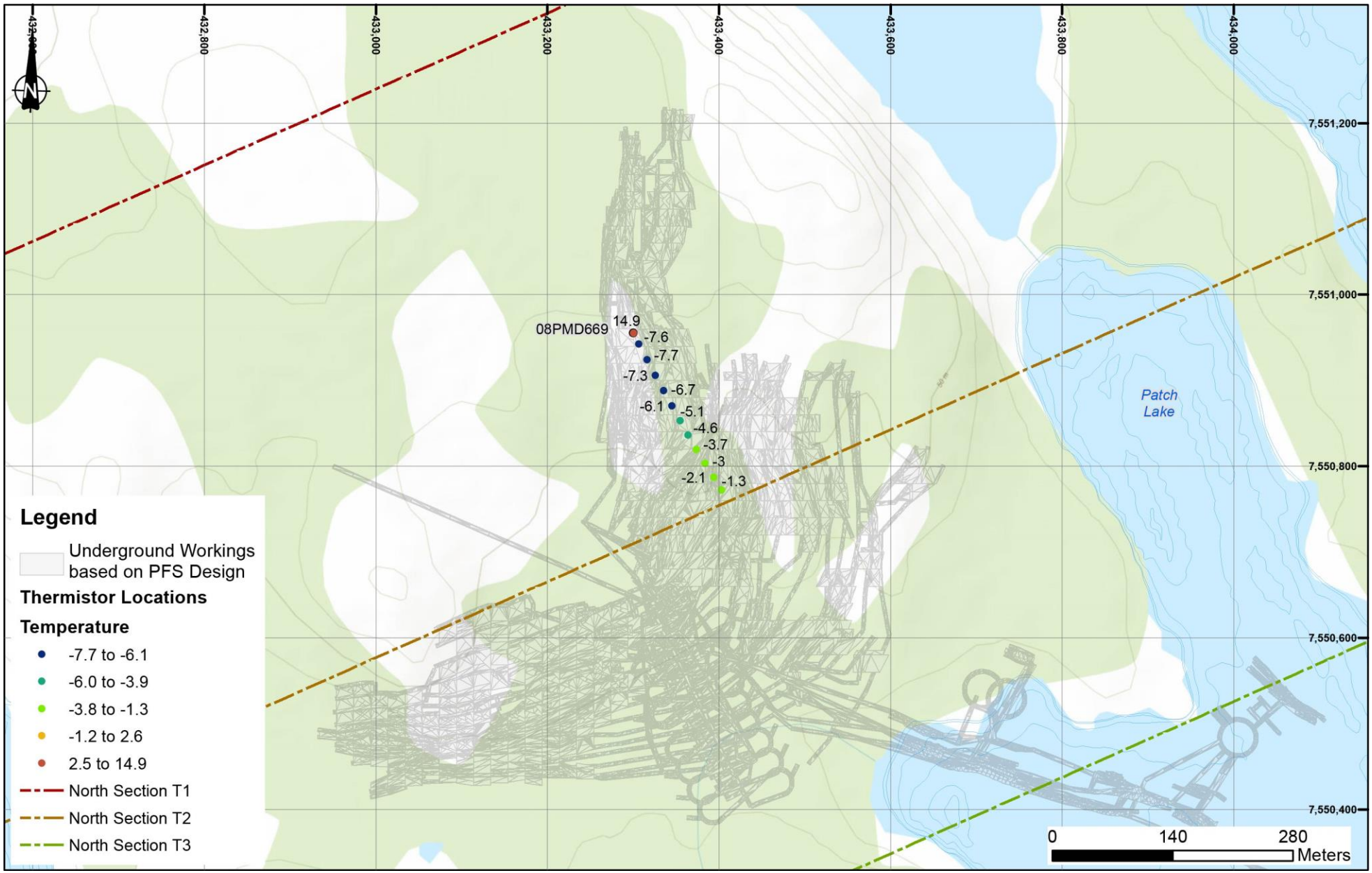
TMAC RESOURCES

HOPE BAY PROJECT

Lake Talik Configuration

Patch Island – Thermistor Site ID 08PSD144

Date:	Approved:	Figure:
2/12/2016	cws	**16**



Notes:

1. Coordinate System: UTM NAD 83 Zone13
2. Basemap Credits: ERSI, DeLorme, TomTom, Intermap, NRCAN, GeoBase
3. Underground Workings based on PFS Design

srk consulting

Job No: 1CT022.004

Filename: BostonDeepGroundTemperatures.pptx

TMAC RESOURCES

HOPE BAY PROJECT

Lake Talik Configuration

Madrid North Mining Area – Thermistor Site ID 08PMD669

Date:	Approved:	Figure:
2/12/2016	cws	17



Notes:

1. Coordinate System: UTM NAD 83 Zone13
2. Basemap Credits: ERSI, DeLorme, TomTom, Intermap, NRCAN, GeoBase
3. Underground Workings based on PFS Design

srk consulting

Job No: 1CT022.004

Filename: BostonDeepGroundTemperatures.pptx

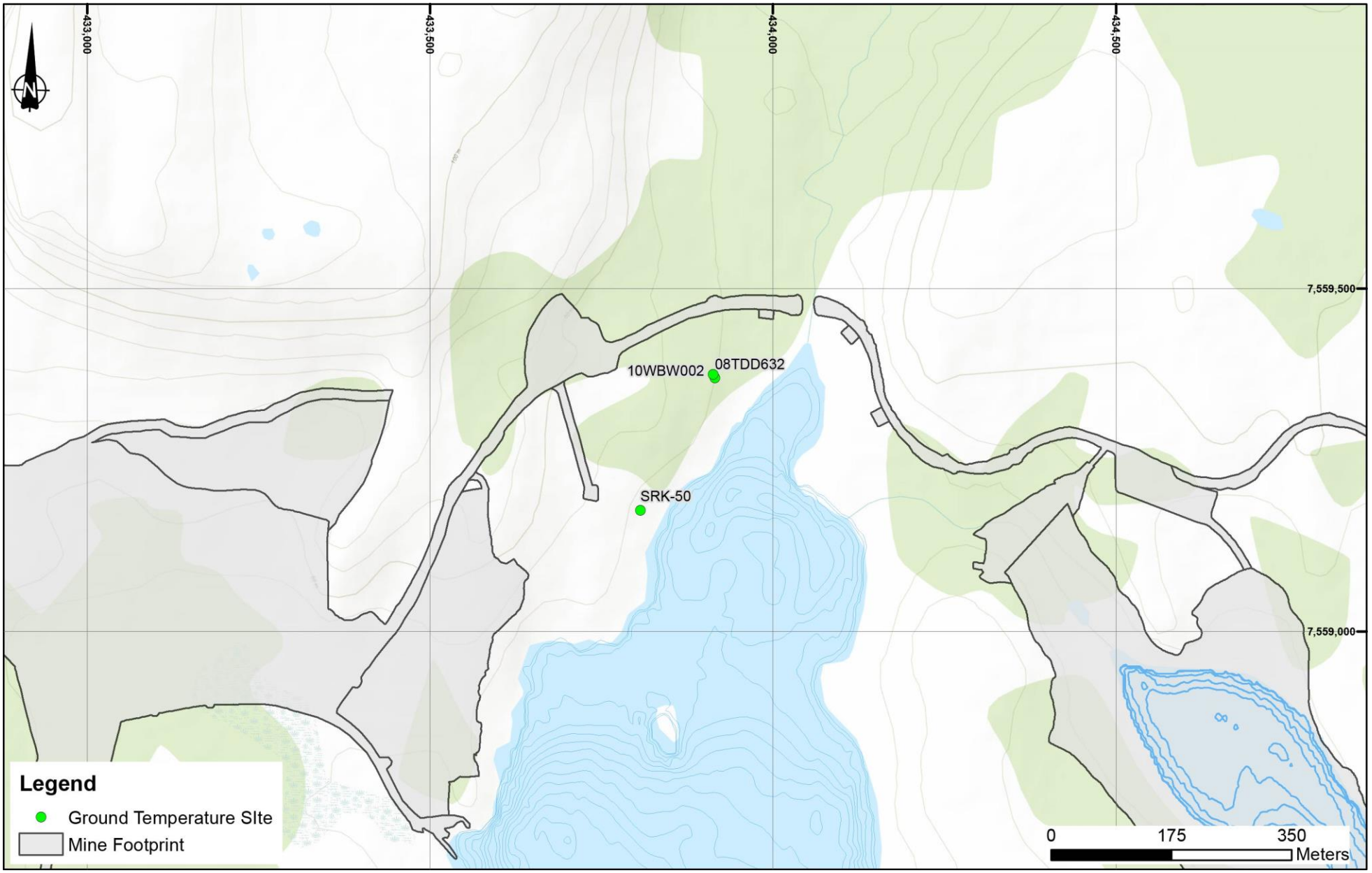
TMAC RESOURCES

HOPE BAY PROJECT

Lake Talik Configuration

Madrid South Mining Area – Thermistor Site ID TM00141

Date:	Approved:	Figure:
2/12/2016	cws	**18**



Notes:

1. Coordinate System: UTM NAD 83 Zone13
2. Basemap Credits: ERSI, DeLorme, TomTom, Intermap, NRCAN, GeoBase
3. Mine Footprint based on PFS Design

srk consulting

Job No: 1CT022.004

Filename: BostonDeepGroundTemperatures.pptx

TMAC RESOURCES

HOPE BAY PROJECT

Lake Talik Configuration

Madrid South Mining Area – Thermistor Site ID TM00141

Date:	Approved:	Figure:
2/12/2016	cws	**19**

4.3.2 VWP Data Summary

Multi-channel data logger collected readings from the VWP during grouting. The logger was removed once grout reached the surface so that the drillers could clean and push back the drill rig. All available readings collected were converted to pressure using the second order polynomial equation and are presented in Figure 4-2. Groundwater pressure at the elevation of the sensor was converted to a groundwater head by converting the recorded pressure from the VWP into a groundwater head reported in vertical meters below ground surface (m bgs). The water column above the pressure transducer was assumed to consist of fresh water with a density of 1000 kg/m^3, and VWP depth was estimated at 388.68 m bgs. However, it should be noted that these measurements are not representative of the piezometric conditions as the rock mass surrounding the borehole has not had time to stabilize following the grout injection.

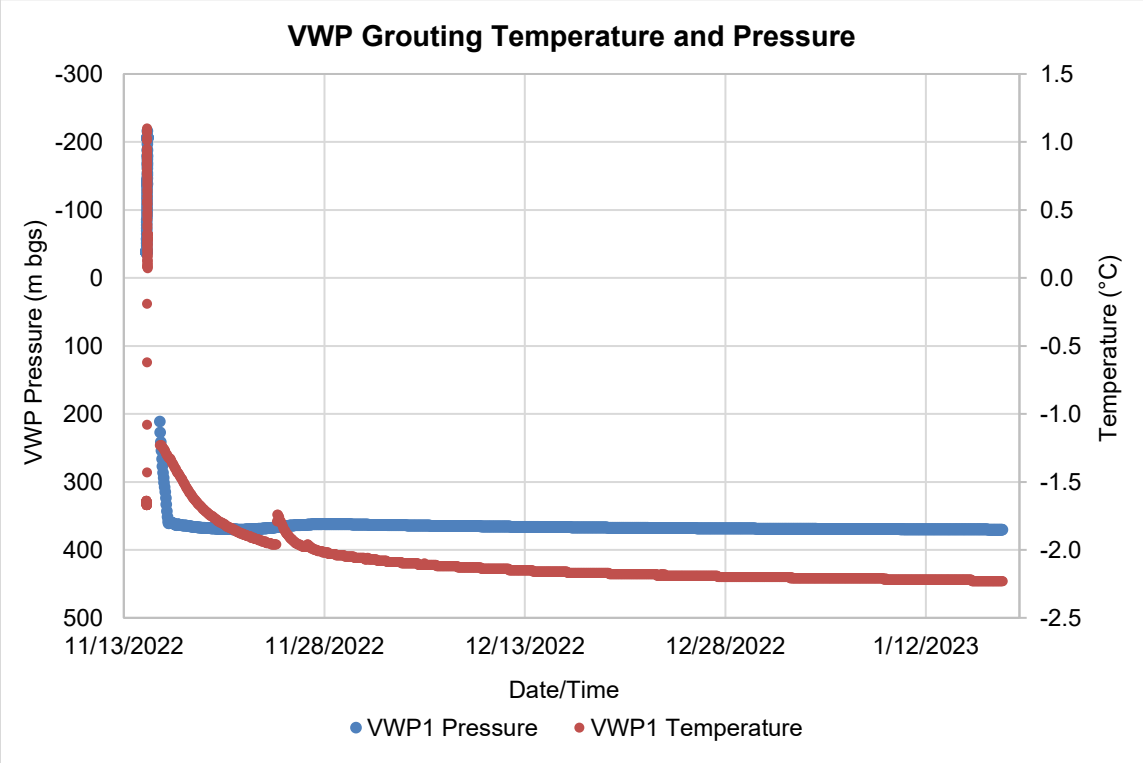


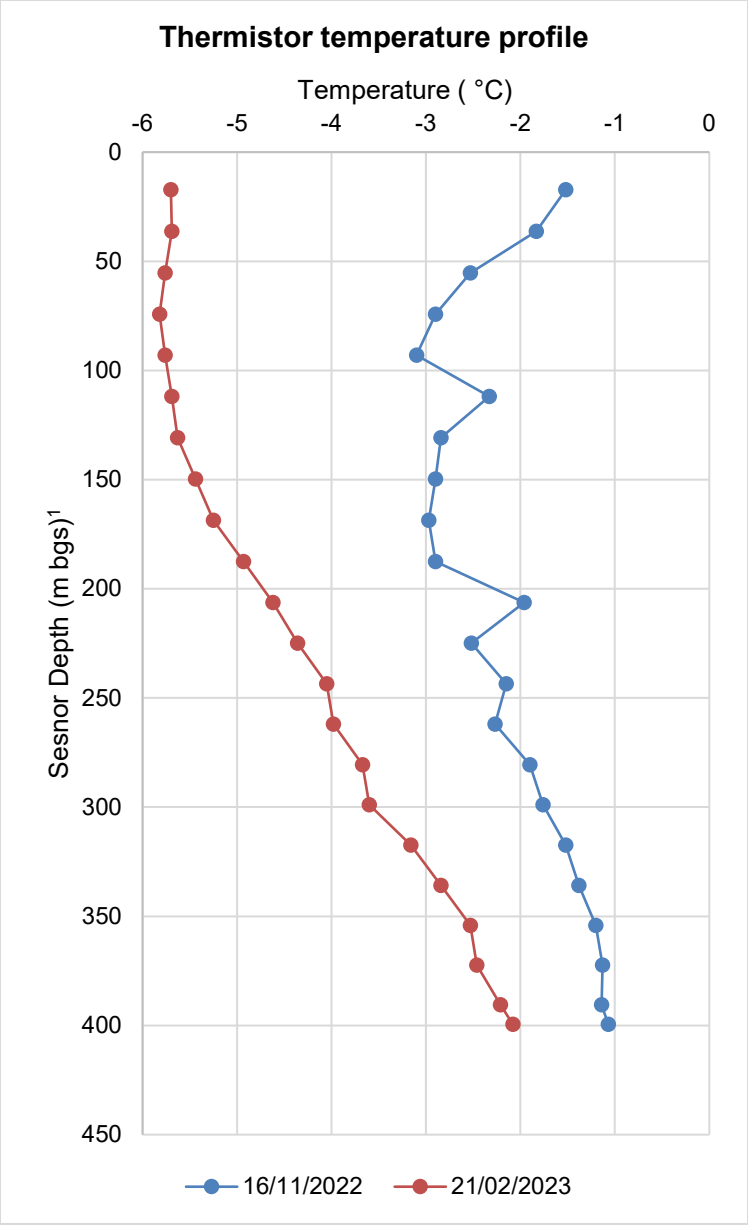
Figure 4-2 HBM-22-059 VWP Data

4.3.3 Thermistor

The thermistor installation was completed with a D605 data logger installed at surface for sensor data collection. The logger has an embedded two-way satellite transceiver and iridium antenna that allows for remote data collection and logger set-up. SRK plugged in the sensors and set the logger to be open for satellite transmission in the field and the manufacturer handled the remaining set-up remotely.

Thermistor temperature profiles from both 16th November 2022 and 21st February 2023 are presented below in Figure 4-3.The figure presents how the temperatures have altered since the installation was completed. The most recent profile might not be representative of the steady state temperature as based on similar installation (Mareschal et al. 2004) it could take up to one year for the temperature to return to the equilibrium following drilling and grouting.

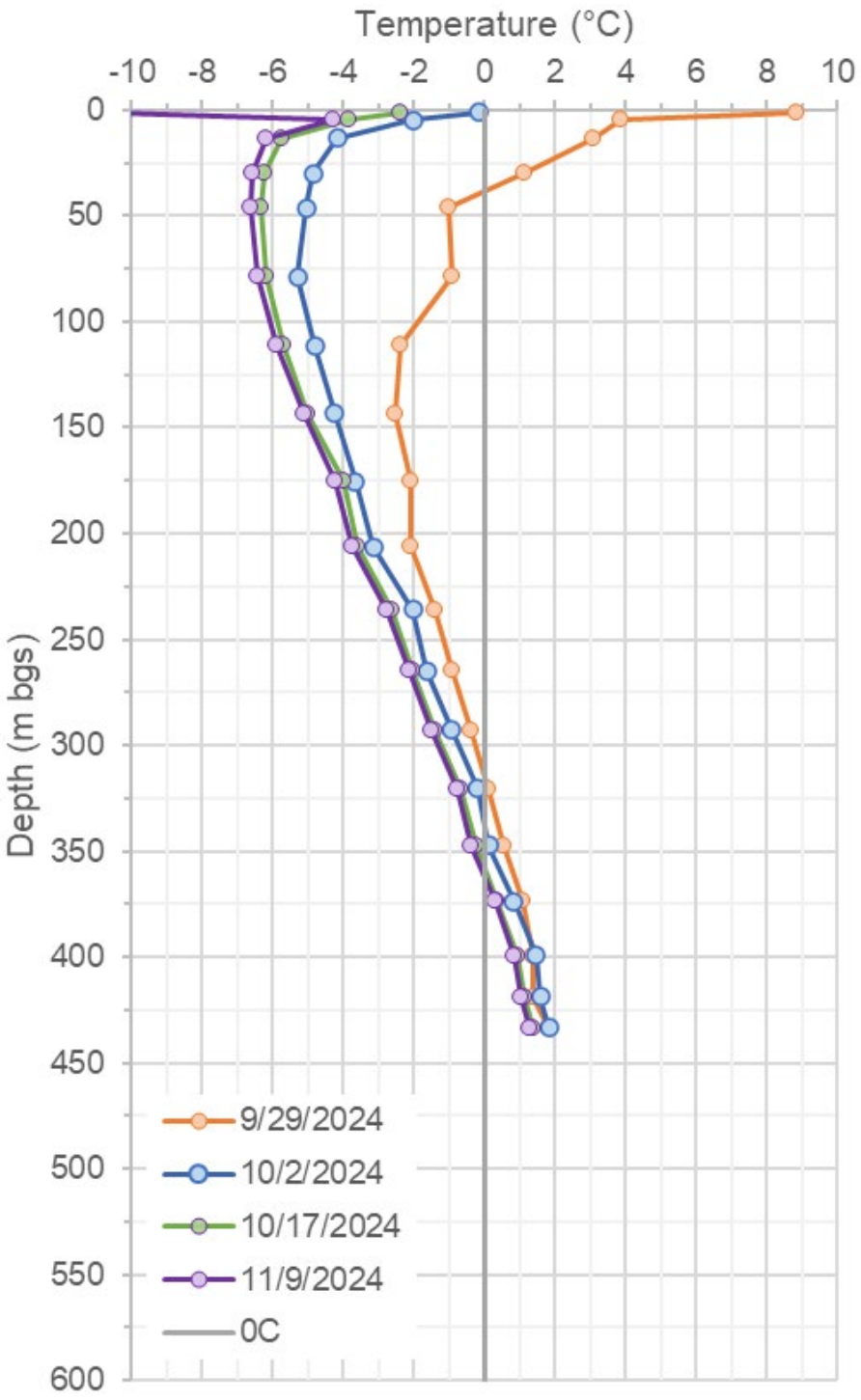
Based on geochemistry data reviewed by SRK as part of the Final Environmental Impact Assessment (SRK, 2017), the freeze point depression at the Hope Bay has been calculated at a temperature of -2°C. Therefore, the most recent ground temperature profile indicates that the base of permafrost is around 405 m bgs.



[1]. m bgs = vertical depth in meters below ground surface.

Figure 4-3 Thermistor temperature profiles

Figure 4-4: Ground temperature profiles from HBM-24-259



1. m bgs = vertical depth in meters below ground surface referenced to drillhole collar.

Appendix G – Thermal Models

SRK Consulting (US), Inc.
Suite E-12
4700 Business Park Blvd
Anchorage, Alaska 99503

T: +1 907 677 3520
F: +1 907 677 3620

anchorage@srk.com
www.srk.com

Memo

To:	John Roberts, PEng, Vice President Environment	**Client:**	TMAC Resources Inc.
From:	Christopher W. Stevens, PhD	**Project No:**	1CT022.013
Reviewed By:	Maritz Rykaart, PhD, PEng	**Date:**	November 30, 2017
Subject:	Hope Bay Project, Lake Talik Configuration		

Change Log

The following table provides an overview of material changes to this report from the previous version issued as Appendix V3-4B, Appendix A as part of the DEIS for Phase 2 of the Hope Bay Project dated December 2016.

Changes by Section

Information Request, Technical Comment, or Other Change	Section	Comments
NRCan-IR6	Section 5.2.1	Additional description of data added

1 Introduction

The Madrid-Boston Project (the Project) is a gold mining and milling undertaking of TMAC Resources Ltd (TMAC). The Project is located 705 km northeast of Yellowknife and 153 km southwest of Cambridge Bay in Nunavut Territory, and is situated east of Bathurst Inlet. The Project comprises three distinct areas of known mineralization plus extensive exploration potential and targets. The three areas that host mineral resources are Doris, Madrid, and Boston.

The Project consists of two phases; Phase 1 (Doris Project), which is currently being carried out under an existing Water Licence, and Phase 2 which is in the environmental assessment stage. Phase 1 includes mining and infrastructure at Doris only, while Phase 2 includes mining and infrastructure at Madrid and Boston located approximately 10 and 60 km due south from Doris respectively.

Although the Project is located in the continuous permafrost region of Canada, an evaluation is necessary to determine if the proposed underground mines will intercept talik zones. Where these talik zones are intercepted by the mine, groundwater inflow may be encountered, requiring appropriate management. Since the extent of these talik zones cannot be completely characterized through field verification, it is best practice to model the talik configuration. This memo provides a description of the modeling and presents the predicted talik configuration for use in subsequent mine inflow modeling.

2 Lake Taliks

2.1 Definition

A talik is defined as "*a layer or body of unfrozen ground occurring in a permafrost area due to local anomalies in thermal, hydrological, hydrogeological or hydrochemical conditions*" (van Everdingen 2005). In most cases, taliks are formed by lakes and other water bodies which cause a local departure in terrestrial ground temperature (Smith and Hwang 1973; Burn 2002).

In this memo, reference is made to both closed and open (or through) taliks. A closed talik is an unfrozen zone beneath a water body that is enclosed at the base and the surrounding sides by permafrost (Figure 1). An open talik is an unfrozen zone beneath a water body that penetrates the permafrost completely and may connect suprapermafrost (i.e. the layer of ground above permafrost) and subpermafrost (i.e. the unfrozen ground below the permafrost) groundwater.

2.2 Talik Configuration

Lake taliks are transient features in permafrost environments. Key factors influencing talik configuration include water bottom temperature, lake size (half width or radius), present and past ground thermal regime, and long-term changes to the landscape. Present-day water bathymetry can also effect talik configuration where shallow water allows for ice to seasonally freeze to the bottom (bottom-fast ice) and conduct heat from the ground (Burn 2002; 2005; Stevens *et al*. 2010a; 2010b).

The long-term thermal and physical evolution of the landscape is a factor in the present-day configuration of taliks that extend hundreds of metres below the surface. Lunardini (1995) showed temperature at depths up to 600 metres below ground surface (mbgs) can be influenced by surface temperatures as far back as 100,000 years.

Kerr (1994a) provides radiocarbon dating and stratigraphic interpretation of glacial and post-glacial deposits from Perry Peninsula and Queen Maud Gulf, and south of the Bathurst Inlet. His work suggests that deglaciation near the Madrid and Boston mining areas was between 9 ka and 8.7 ka (Kerr 1994a). Retreating ice may have been at or near the mining areas at around 9 ka, followed by a period of rapid ice retreat and ice-free conditions by 8.7 ka. Deglaciation was accompanied by synchronous marine incursion of the isostatically depressed terrain. Sea level curves constructed for the southern Bathurst Inlet suggest drainage of the marine water by at least 5 ka years BP (Kerr 1994b).

The sub-aerial exposure of land following drainage of marine water and cold air temperatures would have led to permafrost aggradation. Over time newly formed lakes and changes in water level of existing lakes due to changes in surface hydrology and climate would result in adjustment of lake taliks to a new equilibrium.

Open taliks are expected to be present beneath some lakes at the Property. Open taliks have been inferred from ground temperature measurements collected beneath Doris, Patch, and Aimaokatalok Lakes (SRK 2011a; Appendix A). Previous thermal modeling also supports the inference of open taliks beneath Doris and Tail Lakes, which are elongated lakes with a half-width of about 475 m and 390 m, respectively (SRK 2005a).

3 Ground Conditions

3.1 Permafrost

SRK (2017) provides detailed information on the baseline ground temperature and permafrost characteristics located in the Doris Mine, and the Madrid and Boston mining areas. The average present-day temperature of permafrost is -7.6°C at the Property, with a range from -5.6°C to -9.8°C (SRK 2017). The baseline ground temperature sites do not permit for separate assessment of permafrost temperatures at each of the three mining areas.

The base of permafrost has been estimated from ten sites to be 78 to 570 metres below ground surface(mbgs) based on the 0°C isotherm. Ground temperature sites removed from the thermal effects of nearby lakes indicate the base of permafrost extends to 570 mbgs (Site 08PMD669) at the Madrid mining area and 565 mbgs (Site 08SBD380) at the Boston mining area (Table 1). At Doris, the base of permafrost extent up to 511 mbgs at Site 10WB002. The geothermal gradient calculated from the deeper extent of permafrost averages 0.021°C m^{-1}, with a range of 0.014°C m^{-1} to 0.029°C m^{-1} (Table 1).

Table 1: Summary of Base of Permafrost and Geothermal Gradient

Thermistor Site ID	Northing	Easting	Location	Location Reference	Geothermal Gradient (°C/m)	Base of Permafrost (mbgs)
SRK-50	7,559,177	433,807	Doris Mining Area	Fig. 18	0.019	394
08TDD632	7,559,370	433,915	Doris Mining Area	Fig. 18	0.024	445
10WBW002	7,559,375	433,913	Doris Mining Area	Fig. 18	0.014	511
08PMD669	7,550,955	433,300	Madrid North Mining Area	Fig. 13+16	0.018	570
TM00141	7,546,691	435,141	Madrid South Mining Area	Fig. 13+17	0.023	346
08PSD144	7,548,990	435,178	Patch Lake Island	Fig. 13+15	-	78
08SBD380	7,504,780	441,080	Boston Mining Area	Fig. 5	0.017	565
08SBD381A	7,504,814	441,070	Boston Mining Area	Fig. 5	0.029	281
08SBD382	7,505,141	441,026	Boston Mining Area	Fig. 5	0.027	302
10WBW004	7,505,665	441,018	Boston Mining Area	Fig. 5	0.018	326
97NOD176	7,504,962	441,481	Boston Mining Area	Fig. 5	0.019	556
All Sites				**Average**	**0.021**	**398**
				Minimum	**0.014**	**78**
				Maximum	**0.029**	**570**
				Count	**10**	**11**

Water quality data collected from the Doris Central Westbay well (Site 10WBW001) indicates saline connate groundwater which is comparable to quality measurements observed at the Boston mining area. The lowest freezing point depression calculated from the concentration of dominate components of the groundwater was estimated to be -1.9°C (SRK 2011b). For the purpose of modeling talik extent, ground temperatures warmer than -2°C are expected to be unfrozen.

It should be recognized that the connection between surface water, mined structures, and subpermafrost groundwater is also a function of the hydraulic properties of the bedrock, the geological structures, and the hydraulic gradients that drive water movement; i.e. unfrozen ground does not necessarily constitute significant groundwater movement.

3.2 Lake Bottom Water Temperature

Table 2 shows average lake bottom water temperature (LbT) recorded during the month of April, July, August, and September for five lake locations over the period of 2010-2014 (ERM 2015; ERM 2014; Rescan 2012; Rescan 2011a). The lake bottom water temperatures are based on the deepest measurements collected at each site.

Table 2: Summary of Lake Bottom Water Temperatures

Location	Data Source (See notes)	Temperature (°C)					Ice Thickness (m)
		April	July	August	September	LbT	
Doris Lake North	1,3,4,5,6	1.5	7.8	11.0	6.2	4.7	1.8
Doris Lake South	1,3,4,5,6	1.0	9.0	10.7	5.7	4.2	1.9
Reference Lake A	1	1.6	-	4.3	-	2.5	1.8
Reference Lake B	1,3,4,5,6	2.6	9.1	11.1	3.9	5.5	1.7
Reference Lake C	2	2.0	-	8.3	-	4.1	1.9
Reference Lake D	1,3,4,5,6	0.8	11.4	12.1	2.5	4.6	1.9
Little Roberts Lake	1,3,4,5,6	0.7	10.6	10.9	3.4	4.1	1.9
Wolverine Lake	1	1.4	-	13.2	-	5.3	1.8
Patch Lake North	1	1.2	-	10.8	-	4.4	2.1
Patch Lake South	1	2.1	-	10.3	-	4.8	1.9
P.O. Lake	1	0.2	-	10.0	-	3.5	1.9
Ogama Lake	1	1.8	-	10.0	-	4.5	1.8
Doris Lake North	1	1.1	-	10.0	-	4.1	2.0
Doris Lake South	1	0.9	-	9.7	-	3.8	2.0
Naiqunnguut Lake	1	1.4	-	10.2	-	4.3	1.9
Nkhatok Lake	1	0.4	-	11.7	-	4.2	1.9
Glenn Lake	1	0.5	-	9.9	-	3.6	2.0
Imniagut Lake	1	-	-	12.2	-	-	2.0
Little Roberts Lake	1	1.3	-	10.0	-	4.2	2.1
Stickleback Lake	2	1.1	-	11.2	-	4.5	1.8
Trout Lake	2	0.8	-	12.6	-	4.7	1.8
Windy Lake	1,2	2.0	-	10.1	-	4.7	1.8
Aimaokatalok Lake: Station 2	2	-	-	11.6	-	-	-
Aimaokatalok Lake: Station 5	2	0.0	-	14.8	-	4.9	1.8
Aimaokatalok Lake: Station 6	2	2.3	-	12.1	-	5.6	1.6
Aimaokatalok Lake: Station 11	2	0.1	-	12.1	-	4.1	1.6
Aimaokatalok Lake: Station 13	2	-	-	13.9	-	-	-
All Sites					**Average**	**4.4**	**1.9**
					Minimum	**2.5**	**1.6**
					Maximum	**5.6**	**2.1**
					Count	**24**	**25**

Notes:

1. Average monthly temperature collected over the period of 2009- 2014 (see data source)
2. Annual lake bottom temperature (LbT) calculated using Equation 1
3. Ice thickness measured from ice auger hole drilled in April
4. Data source: 1 – Rescan (2010), 2 – Rescan (2011a), 3 – Rescan (2011b), 4 – Rescan (2012), 5 – ERM Rescan (2014), 6 – ERM (2015)

Mean annual lake bottom water temperature was calculated as a weighted mean of April and August temperatures:

$$LbT = 8LbTApr + 4LbTAug\ /P \quad \text{Eq. 1}$$

where:

LbT = mean annual lake bottom water temperature (°C)
$LbTApr$ = measured lake bottom water temperature in April (°C)
$LbTAug$ = measured lake bottom water temperature in August (°C)
P = is the period of time

Based on Equation 1, April water temperature is assumed to be representative of the period of ice cover (October to May). August water temperatures represent the warmest measurements and likely over-estimate water temperature throughout the ice-free period. Therefore, a conservative water temperature is computed using this approach, and allowed for in the thermal models.

The annual lake bottom water temperature is calculated to average of +4.4°C, with a range from +2.5°C to +5.6°C (Table 2). A value of +4.4°C is considered to be reasonable for base case conditions.

4 Regional Talik Model

4.1 Analytical Model

The critical lake dimension required for open (through) lake taliks was assessed using a one-dimensional (1D) steady state analytical model for lakes. The regional model was development to provide regional context for taliks in the area. The thermal models used for this assessment are presented by Mackay (1962), Smith (1976), and Burn (2002) for study sites in the Canadian Arctic, and have been used for talik characterization at other proposed mine projects located in the continuous permafrost region of mainland Nunavut, including the Back River Project (SRK 2015), Meliadine (Golder 2013), Kiggavik (Areva Resources Canada 2011), High Lake (Wolfden Resources Inc. 2006), Doris (SRK 2005b), and Meadowbank (Cumberland Resources Ltd. 2005) projects.

The temperature profile beneath the centre of a circular lake without terraces has been modeled by Mackay (1962) as:

$$T_z = T_g + \frac{z}{I} + (LbT - T_g)\left(1 - \frac{z}{\sqrt{z^2+R^2}}\right) \quad \text{Eq. 2.}$$

Where:
Tz = temperature at depth z (ºC)
LbT = Average annual lake bottom water temperature (°C)
Tg = average annual ground temperature (ºC)
I = inverse of the geothermal gradient (m ºC^{-1})
z = depth below bottom of lake (m)
R = radius of the lake (m)

The temperature profile beneath symmetrical elongated lakes without terraces has been modeled by Smith (1976) as:

$$T_z = T_g + \frac{z}{I} + \frac{LbT - T_g}{\pi}\left(2\tan^{-1}\frac{w}{z}\right) \quad \text{Eq. 3.}$$

Where:

Tz = Temperature at depth z (ºC)
LbT = Average annual lake bottom water temperature (°C)
Tg = Average annual ground temperature (ºC)
I= inverse of the geothermal gradient (m ºC^{-1})
z = depth below bottom of lake (m)
w = half-width of an elongated lake (m)

For conservatism, shallow-water terraces (lake terraces) which may be thermally influenced by bottom-fast ice were not considered in the analytical model. Table 3 shows the base case and sensitivity values using the in the 1D model. Base case values are representative of average measurements from the mining areas.

Table 3: Thermal Modeling Input Values for Analytical Talik Model

Parameter	Value (Base Case)	Value (Sensitivity Analysis)
Ground temperature (Tg)	-7.6°C	-5°C to -9°C
Mean annual lake-bottom temperature (LbT)	+4.4°C	+3°C to +6°C
Geothermal heat flux (G)	0.021°C m^{-1}	0.014 to 0.029°C m^{-1}

Notes:

1. Measured mean annual permafrost temperature is -7.6°C and mean annual lake bottom temperature is +4.4°C

2. Average geothermal gradient calculated from ground temperature measurements is 0.021°C m^{-1}

4.2 Model Assumptions

The modeling, as presented, is based on the following assumptions:

- Lake geometry is defined in the models as either circular or elongate, and does not account for actual lake geometries which can be quite complex.
- Modeling does not account for the thermal influence of adjacent lakes (lateral heat flow) and spatial variability in ground surface temperature. However, the sensitivity to lake-bottom temperature (LbT) and permafrost temperature are considered (Table 3).
- Water depth is assumed to be greater than the maximum thickness of seasonal ice, and the thermal influence of bottom-fast ice is not considered, making the results more conservative.
- Ground thermal properties and complex mechanisms for heat flow such as convection are not accounted for in the model.
- Geothermal heat flux is based on an average value calculated from ground temperature measurements with sensitivity around the range of values collected at the Property (Table 3).

- Steady-state models are used and therefore the transient effects, such as paleo-climate (i.e. long-term changes in ground surface and water temperature) are not considered.

Talik will naturally adjust to changes in climate and evolution of the landscape. Over the time scale of the Project, the most immediate effects would be an increase in extent of the talik beneath the shoreline, and possible subsidence and erosion of the shoreline at locations with ice-rich permafrost. A reduction in lake ice growth due to climate change would also be expected to widen and deepen existing taliks beneath shallow water bodies which rely on seasonal heat loss though the establishment of bottom-fast ice (Burn 2002; 2005; Stevens *et al*. 2010a; 2010b). The natural development of new ponds at the Property would also result in newly formed closed taliks. On the time scale of hundreds to thousands of years, open taliks may form as permafrost degrades beneath these recently formed water bodies. Natural lowering of lake water level or even complete drainage due to climate change may also result in permafrost aggradation beneath the former lake basin and long-term freezeback of taliks.

4.3 Model Results

The estimated critical dimensions for open (through) taliks beneath lakes at the Property are summarized in Table 4 and Table 5. The findings are based on a groundwater freezing point depression of -2°C and are graphically depicted in Figure 2 and Figure 3.

For the base case scenario, open taliks are estimated to occur beneath circular lakes with a diameter >224 m (i.e. lake radius of >112 m). For elongated lakes, the critical lake width is estimated to be >104 m wide (i.e. lake half-width >52 m).

Sensitivity of the critical lake dimension to change in the geothermal gradient is shown in Figure 4 and Figure 5.

Table 4: Circular Lake Critical Radius for Open (Through) Taliks Based on -2°C Isotherm

Permafrost Temperature	Annual Lake Bottom Temperature (LbT)				
	+3.0°C	+4.0°C	+4.4°C	+5.0°C	+6.0°C
-9.0°C	169 m	159 m	155 m	151 m	144 m
-8.0°C	138 m	129 m	126 m	122 m	117 m
-7.6°C	123 m	115 m	112 m	109 m	104 m
-7.0°C	108 m	101 m	98 m	95 m	91 m
-6.0°C	80 m	74 m	72 m	70 m	67 m
-5.0°C	54 m	50 m	49 m	47 m	44 m

Table 5: Elongated Lake Critical Half-width for Open (Through) Taliks Based on -2°C Isotherm

Permafrost Temperature	Annual Lake Bottom Temperature (LbT)				
	+3.0°C	+4.0°C	+4.4°C	+5.0°C	+6.0°C
-9.0°C	83 m	76 m	73 m	70 m	65 m
-8.0°C	66 m	60 m	58 m	55m	50 m
-7.6°C	60 m	54 m	52 m	49 m	45 m
-7.0°C	50 m	45 m	43 m	41 m	38 m
-6.0°C	36 m	32 m	30 m	28 m	26 m
-5.0°C	23 m	20 m	19 m	17 m	15 m

5 Site-specific Talik Model

5.1 Approach

Lake talik configuration adjacent to the Boston and Madrid mining areas was estimated using 2D thermal modeling. The model results were fitted to field observations of the -2°C isotherm, and therefore use calculated heat flow as a basis for estimating talik geometry. The modeling was carried out using a finite element code SVHeat developed by SoilVision Systems Ltd. with the FlexPDE solver.

5.1.1 Model Setup and Inputs

A long-term mean annual ground surface temperature was applied to the upper model boundary over areas of land. Long-term ground surface temperature was based on a projection of the thermal gradient from deep ground temperature measurements to the surface. The projected ground surface temperature reflects approximate paleo-surface temperature, which is typically colder than present day permafrost temperature calculated from the baseline ground temperature sites (SRK 2017). At the Madrid and Boston mining areas, the long-term ground surface temperature was estimated to be -9.6°C (Site 08PMD669) and -9.2°C (Site 08SBD380), respectively. A long-term ground surface temperature was used to more closely estimate talik configuration and the base of permafrost which result from paleo conditions. The geothermal gradient applied to the lower boundary of the model was based on Site 08PMD669 for Madrid Mining Area and Site 08SBD380 for the Boston mining area (Table 1).

A mean annual lake bottom water temperature of +4.4°C was applied to the upper boundary for lakes (Table 2). Lake width was based on current extent of water bodies at the underground mining areas. At Aimaokatalok Lake adjacent to the Boston mining area, an annual temperature of -2°C was also applied to lake areas with a water depth less than 1.3 m (i.e. water depth that is two-thirds of the mean annual ice thickness). A value of -2°C was applied to the shallow water lake terrace based on measured temperatures from similar environments (Burn 2002; 2005).The ice across these shallow water lake terraces freezes to the bottom with sufficient heat loss from the lake bottom to sustain permafrost beneath the shallow water terraces of Arctic lakes (Mackay 1992; Burn 2002). The thermal regime of shallow water was not considered at the Madrid underground mining areas due to the relatively rapid increase in water depth from shore.

Model simulations were based on a time step of one year. Table 5 summarises the thermal properties used in the transient lake talik model. The frozen and unfrozen thermal conductivity and heat capacity for bedrock (basalt) was based on previous thermal modeling at Hope Bay (SRK 2005; SRK 2011a).

Table 5: Bedrock Thermal Properties 2D Lake Talik Model

Material	Degree of Saturation (%)	Porosity	Thermal Conductivity (kJ m^{-1} day^{-1} $°C^{-1}$)		Volumetric Heat Capacity (kJ m^{-3} $°C^{-1}$)	
			Unfrozen	Frozen	Unfrozen	Frozen
Basalt Bedrock	100	0.05	260	260	2,380	2,133

5.1.2 Model Assumptions

The 2D thermal modeling, as presented, is based on the following assumptions:

- Lake geometry is defined by current lake extent and does not account for historic lake configuration which can be complex.
- Lake-bottom geometry is not directly considered in the model sections. The relatively shallow lake depths would have limited impact on talik configuration deep below the ground surface.
- Surface topography is not considered in the model sections due to low relatively relief across the Property and its limited influence on talik configuration.
- Long-term paleo ground surface temperatures are based on values projected from deep ground temperature measurements, and do not capture more recent variability in surface temperature.
- Ground thermal properties and complex mechanisms for heat flow such as convection are not accounted for in the model.

5.2 Boston Mine Area

The Boston underground mine will be located on the east side of Aimaokatalok Lake (Figure 6). A total of four sections were used to model the lake talik.

5.2.1 Ground Temperature Measurements

Deep ground temperature measurements have been collected from three deep inclined wells which extend beneath Aimaokatalok Lake; well 08SBD381A, 08SBD382, and 10WBW004 (Figure 7). Well 08SBD380 and 97NOD176 are two additional deep wells that have been drilled inland near the Boston mine workings.

Table 6 summarizes the position of the 0°C and -2°C isotherms for the Boston mining area. At 08SBD380 and 97NOD176, the ground temperature has been measured to a maximum depth of 241 mbgs and 247 mbgs, respectively. The base of permafrost is not directly incepted by these wells and the lowermost thermistors nodes indicate relatively cold permafrost temperatures (-5.1°C at 08SBD380 and -5.5°C at 97NOD176). The projected base of permafrost based on the

0°C isotherm is 565 mbgs at 08SBD380 and 556 mbgs at 97NOD176 (Table 6). The -2°C isotherm is projected to be 430 mbgs at 08SBD380 and 449 mbgs at 97NOD176. At site 08SBD380, the drill hole is orientated at an inclined angle toward Stickleback Lake. Based on the depth of the 0°C and -2°C isotherm and relatively cold temperatures measured from the lowermost thermistor node, it can be inferred that permafrost continues in the direction of Stickleback Lake and beyond the extent of the underground mine.

Ground temperatures measured at three sites beneath Aimaokatalok Lake provide information on the extent of the lake talik adjacent to the shoreline (Figure 6 and Figure 7). Figure 8 shows the depth of the -2°C isotherm and its distance from shore for these sites. The water bathymetry for the three areas with ground temperatures beneath the lake are shown in Figure 9. At site 08SBD382, the -2°C isotherm is up to 115 m from the lake shoreline and located at a depth of 224 mbgs. At site 08SBD381A and 10WBW004, the -2°C isotherm is 17 and 42 metres from shore and located between 202 and 209 mbgs (Table 6).

Table 6: Boston Mining Area Depth of 0°C and -2°C Isotherm from Ground Temperature Data

Site	Location	Maximum Instrumented Depth (mbgs)	-2°C Isotherm (mbgs)	0°C Isotherm (mbgs)
08SBD380	Near Underground Mine	241	430	565
97NOD176	Near Underground Mine	247	449	556
08SBD381A	Extends Beneath Lake	291	202	281
08SBD382	Extends Beneath Lake	313	224	302
10WBW004	Extends Beneath Lake	399	209	326

Notes:

1. Digital data not available for 97NOD176, depth and temperature determined from graphical form of data
2. Thermistor node depth corrected for vertical depth using downhole well survey and surface elevation
3. Depth shown as vertical metres below ground surface (mbgs)

For sites 08SBD381A and 08SBD382, the -2°C is located beneath water depths which are not expected to seasonally freeze to the bottom and therefore do not experience thermal conduction of heat through bottom-fast ice cover. The presence of floating ice at these locations implies that there is no significant means to vertically remove heat gained from the water and the lake bottom. At site 10WBW004, the -2°C isotherm is located beneath water depths that are about two-thirds the maximum ice thickness (i.e. an ice thickness of 1.3 m). It has been suggested that water depth less than two-thirds the maximum later winter ice thickness is required to sustain permafrost beneath shallow water margins of Arctic lakes impacted by bottom-fast ice (Mackay 1992; Burn 2002). This finding was also in agreement with shallow-water permafrost located within the nearshore zone of the Beaufort Sea (Stevens *et al*. 2010b).

Therefore, under present-day lake configuration the offshore position of the -2°C isotherm cannot be explained by heat loss from seasonal bottom-fast ice. Lateral heat flow from the adjacent land also does not explain the current talik extent beneath the lake. Significantly colder ground surface temperatures and lake bottom-temperatures would be required for the talik to extend beneath the Aimaokatalok Lake. Figure 8 shows the expected configuration of the Aimaokatalok Lake talik for

steady state compared to the position of the measured position of the -2°C isotherm. For steady state talik configuration to meet the field observations, the mean annual ground surface temperatures would need to be around -20°C.

We postulate that the lateral extent of permafrost beneath Aimaokatalok Lake is a direct physical consequence of the rise in lake level through time. Over time, permafrost formed through terrestrial exposure to cold air temperatures has been submerged with lake expansion. The talik is currently responding to the thermal forcing from the current lake and the talik will adjust to new conditions and evolve with the lake. The talik would be expected to adjust to equilibrium conditions on the time scale of hundreds to thousands of years.

5.2.2 Model Results

The 2D model sections were setup to simulate possible expansion of Aimaokatalok Lake and to allow for talik adjustment to meet ground temperature measured at the site. The model was run for 5,000 years which is estimated to be the approximate duration of time since drainage of the post-glacial marine incursion. The following major periods were included in the thermal model:

- From model year 0 to 4.5 ka, the lake was assumed to occupy a smaller area defined by current water depths greater than 5 m deep. This water depth represents the approximate transition from a relatively shallow to steep gradient in the water depth profile; i.e. the change in water depth verses distance (Figure 9). It was thus assumed that lake expansion would be most rapid across areas with a water depth less than 5 m deep where the gradient is shallow.
- From model year 4.5 to 5.0 ka, the lake was allowed to expand and flood the existing permafrost. This step was included in the model to allow for the interpreted adjustment of the talik over time. The position of the -2°C isotherm modeled was then selected to closely fit to the equivalent isotherm measured at sites 08SBD381A, 08SBD382, and 10WBW004.

Figures 10 to 13 show the model results for the Boston mining area. Table 7 shows a comparison between the model fit and the ground temperatures for the -2°C isotherm which represents the transition from frozen to unfrozen conditions at the three sites. In all cases, the model fit is conservative and underestimates the measured depth of the talik.

Table 7: Measured and Model Fit for Talik Surface

Model Section	Thermistor Site ID	Model (-2°C Isotherm)	Measured (-2°C Isotherm)
T1	10WBW004	192	209
T2	08SBD382	215	224
T3	08SBD381A	196	202

Notes:

1. Model position of the -2C isotherm based on manual fit to field data

5.3 Madrid Mining Area

The Madrid mining area consist of two distinct mines along the west side of Patch Lake. The northern mine (Madrid North) will be located between Windy Lake and Patch Lake, and the southern mine (Madrid South) will be located between Wolverine Lake and Patch Lake.

The 2D models included five sections for Madrid North and four sections for Madrid South (Figure 14). The model sections extend across the underground mining areas with an orientation that is approximately perpendicular to the long axis of the adjacent lakes. The modeled data was fit to the position of the -2°C isotherm measured at Madrid North. At Madrid South, the -2°C isotherm is located beyond the instrumented depth of the ground temperature cable. At this site, the modeled data was fit to the lowermost thermistor sensor (node).

5.3.1 Ground Temperature Measurements

Deep ground temperature measurements have been collected from three inclined wells; 08PMD669, 08PSD144, and TM00141 at the Madrid mining areas (Figure 14 and Figure 15).

Well 08PSD144 is located beneath an island centred within Patch Lake (Figure 16). Ground temperature measurements at the site indicate relatively shallow permafrost beneath the island (base of permafrost 78 mbgs) due to the surrounding heat from the lake.

Well 08PMD669 is located within the area of the Madrid North underground mine workings (Figure 17) and is instrumented to a maximum depth of 474 mbgs. The base of permafrost is 570 mbgs at this location.

Well TM00141 is located within the Madrid South underground mine between Wolverine Lake and Patch Lake (Figure 18). The well extends toward Patch Lake. Ground temperature measured from lowermost thermistors node is -2.6°C at 225 mbgs. The projected base of permafrost is 346 mbgs, intercepting the talik at the edge of the Patch Lake. The range in depth to the base of permafrost at Madrid North and Madrid South is similar to comparable measurements made at the Doris Mining Area (Table 1; Figure 19).

Table 8: Madrid Mining Area Depth of 0°C and -2°C Isotherm from Ground Temperature Data

Site ID	Location	Maximum Instrumented Depth (mbgs)	-2°C Isotherm (mbgs)	0°C Isotherm (mbgs)
08PMD669	Madrid North	474	438	570
08PSD144	Patch Lake Island	275	50	78
TM00141	Madrid South	225	303	346

Notes:

1. Thermistor node depth corrected for vertical depth using downhole well survey and surface elevation
2. Depth shown as vertical metres below ground surface (mbgs)

5.3.2 Model Results

Figures 20 to 24 show the model results for the Madrid North mining area. Lake expansion was not considered in the 2D thermal models since it is not supported by ground temperature data collected at the Madrid mining areas. Table 9 shows a comparison between site ground temperature measurements and the model fit. In all cases, the model fit is conservative and underestimates the depth of the talik

Table 9: Measured and Model Fit for Talik Surface

Model Section	Thermistor Site ID	Model (-2°C Isotherm)	Measured (-2°C Isotherm)
T2 (Madrid North)	08PMD669	412	438
T2* (Madrid South)	TM00141	258	303

Notes:

1. Asterisk indicates model fit with lowermost thermistor sensor.

At Madrid North, the model was fit to the -2°C isotherm at site 08PMD669. At this site, the lowermost sensor (node) measures -1.3°C at 474 mbgs. The equivalent isotherm estimated by the model is located at 453 mbgs or 21 m less than the measured depth.

Figures 25 to 28 show the model result for the Madrid South mining area. At Madrid South, the model was fit to the lowermost thermistor sensor (node) at site TM00141 which measures -2.6°C. The projected depth of the -2°C isotherm is 303 mbgs at the site. The equivalent isotherm estimated by the fitted model is located 258 mbgs. The model underestimates the position of the -2°C by 45 m.

Disclaimer—SRK Consulting (U.S.), Inc. has prepared this document for TMAC Resources Inc.. Any use or decisions by which a third party makes of this document are the responsibility of such third parties. In no circumstance does SRK accept any consequential liability arising from commercial decisions or actions resulting from the use of this document by a third party.

The opinions expressed in this document have been based on the information available to SRK at the time of preparation. SRK has exercised all due care in reviewing information supplied by others for use on this project. While SRK has compared key supplied data with expected values, the accuracy of the results and conclusions from the review are entirely reliant on the accuracy and completeness of the supplied data. SRK does not accept responsibility for any errors or omissions in the supplied information, except to the extent that SRK was hired to verify the data.

6 References

Areva Resources Canada Inc. 2011. Kiggavik Project Environmental Impact Statement Technical, Appendix 5B: Geology and Hydrogeology Baseline.

Burn CR. 2002. Tundra lakes and permafrost, Richards Island, western Arctic coast, Canada. Canadian Journal of Earth Sciences 39: 1281–1298.

Burn CR. 2005. Lake-bottom thermal regimes, western arctic coast, Canada. Permafrost and Periglacial Processes 16: 355–367.

Cumberland Resources Ltd. 2005. Meadow bank Gold Project: Final Environmental Impact Statement.

ERM Rescan. 2014. Doris North Project: 2013 Aquatic Effects Monitoring Program Report. Prepared for TMAC Resources Inc. by ERM Rescan: Yellowknife, Northwest Territories.

ERM. 2015. Doris North Project: 2014 Aquatic Effects Monitoring Program. Prepared for TMAC Resources Inc. by ERM Consultants Canada Ltd.: Yellowknife, Northwest Territories.

Golder Associates 2013. Meliadine. Draft Environmental Impact Statement - Volume 7 Freshwater Environment - Appendix 7.2-A Groundwater Quality Baseline Report.

Kerr, D.E. 1994a. Late Quaternary Stratigraphy and Depositional History of the Parry Peninsula-Perry River Area, District of Mackenzie, Northwest Territories. Geological Survey of Canada Bulletin 465. 34 p.

Kerr, D.E. 1994b. Late Quaternary History of the Parry Peninusula to Perry River Region, Northwest Territories. PhD. Dissertation. University of Alberta.

Lunardini V.J. 1995. Permafrost Formation Time. CRREL Report 95-8, US Army Corps of Engineers, Cold Regions Research & Engineering Laboratory, April 1995.

Mackay J.R. 1962. Pingos of the Pleistocene Mackenzie delta area. Geographical Bulletin, 18: 21-63.

Mackay, J.R. 1992. Lake stability in an ice-rich permafrost environment: examples from the western Arctic coast. In Aquatic ecosystems in semi-arid regions: implications for resource management. Edited by R.D. Robarts and M.L. Bothwell. National Hydrology Research Institute, Environment Canada, Saskatoon, Sask., Symposium Series 7, 1–26.

Rescan. 2010. 2009 Freshwater Baseline Report, Hope Bay Belt Project. Prepared for Hope Bay Mining Limited by Rescan Environmental Services Ltd.

Rescan. 2011a. Hope Bay Belt Project: 2010 Freshwater Baseline Report. Prepared for Hope Bay Mining Limited by Rescan Environmental Services Ltd.

Rescan. 2011b. Doris North Gold Mine Project: 2010 Aquatic Effects Monitoring Program Report. Prepared for Hope Bay Mining Limited by Rescan Environmental Services Ltd.: Vancouver, British Columbia.

Rescan. 2012. Doris North Gold Mine Project: 2011 Aquatic Effects Monitoring Program Report. Prepared for Hope Bay Mining Limited by Rescan Environmental Services Ltd.

Smith MW. and Hwang CT. 1973. Thermal disturbance due to channel shifting, Mackenzie Delta, N.W.T., Canada. Second International Conference on Permafrost. U.S.S.R., National Academy of Science, Washington, D.C., 51-60.

Smith M.W. 1976. Permafrost in the Mackenzie delta, Northwest Territories. Geological Survey of Canada. Paper 75-28.

SRK 2015a. Hope Bay Doris North Project Thermal Modelling – Permafrost between Doris and Tail Lakes.

SRK. 2005b. Groundwater Assessment, Doris North Project, Hope Bay, Nunavut.

SRK 2009. Hope Bay Gold Project: Stage 2 Overburden Characterization Report. Report submitted to Hope Bay Mining Ltd.

SRK 2011a. Hope Bay Project – Geotechnical Design Parameters. Report prepared for Hope Bay Mining Limited.

SRK 2011b. Stage 2 Geotechnical and Hydrogeological Assessment for Doris Central and Connector Underground Mines. Prepared for Hope Bay Mining Limited.

SRK 2015. Back River Project: Goose Property Talik Thermal Modeling. Prepared for Sabina Gold & Silver Corp.

SRK 2017. Hope Bay Project: Thermal Modelling to Support Run-of-Quarry Pad Design. Prepared for TMAC Resources Inc.

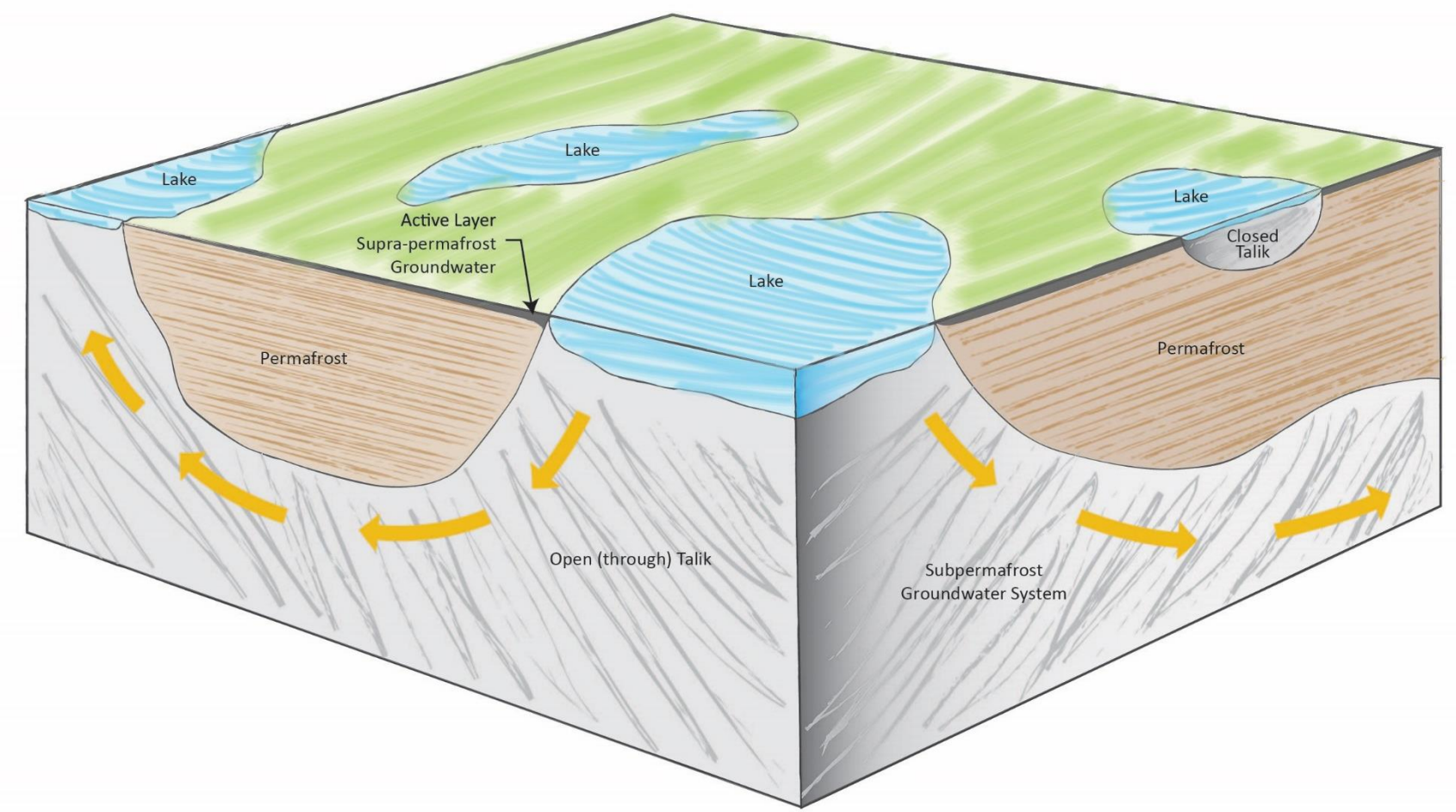
Stevens CW. 2010a. Interannual Changes in Seasonal Ground Freezing and Near-surface Heat Flow beneath Bottom-fast Ice in the Near-shore Zone, Mackenzie Delta, NWT, Canada. Permafrost and Periglacial Processes 21: 256-270.

Stevens CW. 2010b. Modeling Ground Thermal Conditions and the Limit of Permafrost within the Nearshore Zone of the Mackenzie Delta, Canada. Journal of Geophysical Research. 115: F04027.

van Everdingen, R. (ed.). 2005. Multi-language glossary of permafrost and related ground-ice terms. Boulder, CO: National Snow and Ice Data Center.

Wolfden Resources Inc. 2006. High Lake Project Environmental Impact Statement.

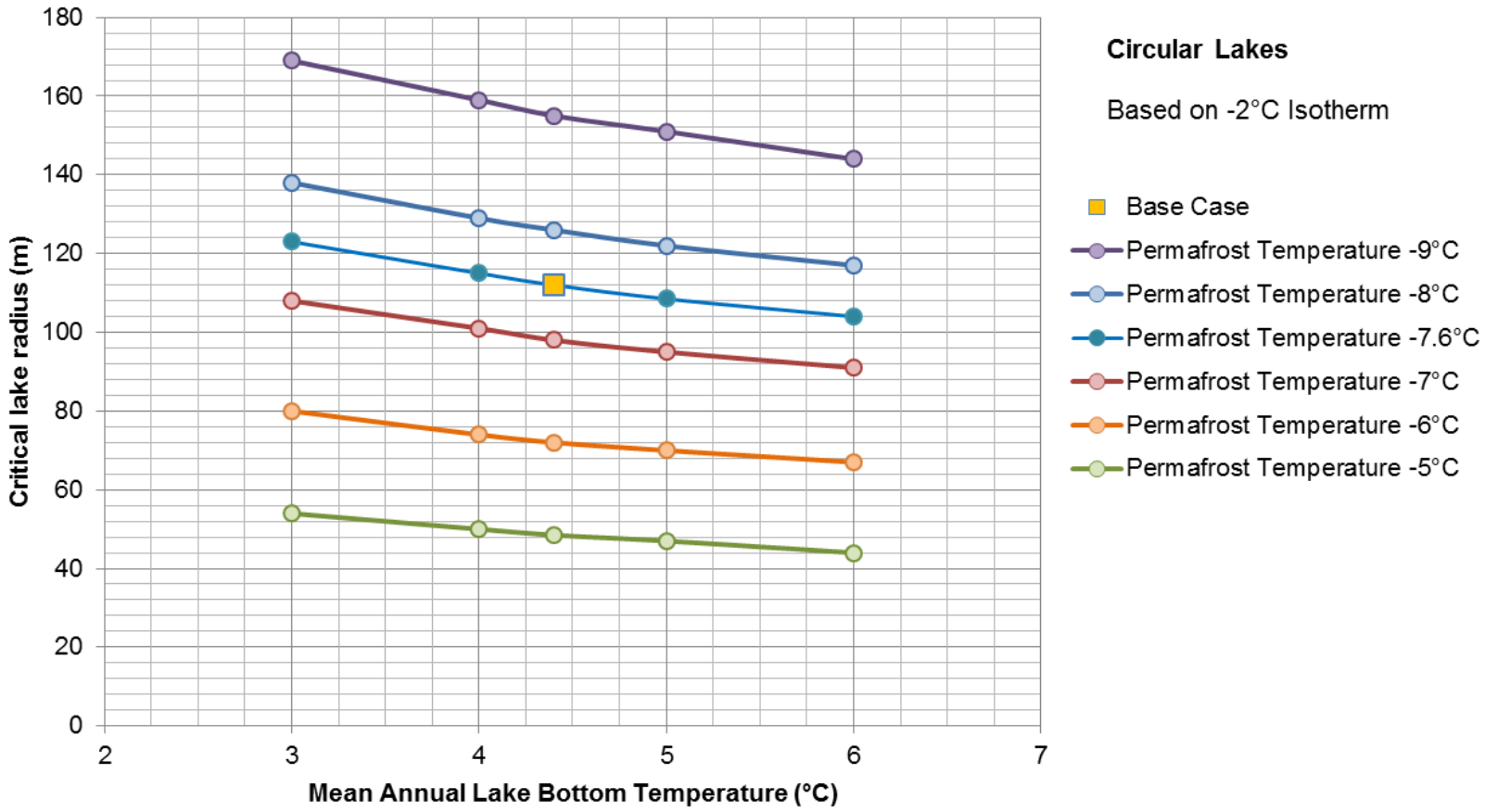
Figures



Notes:

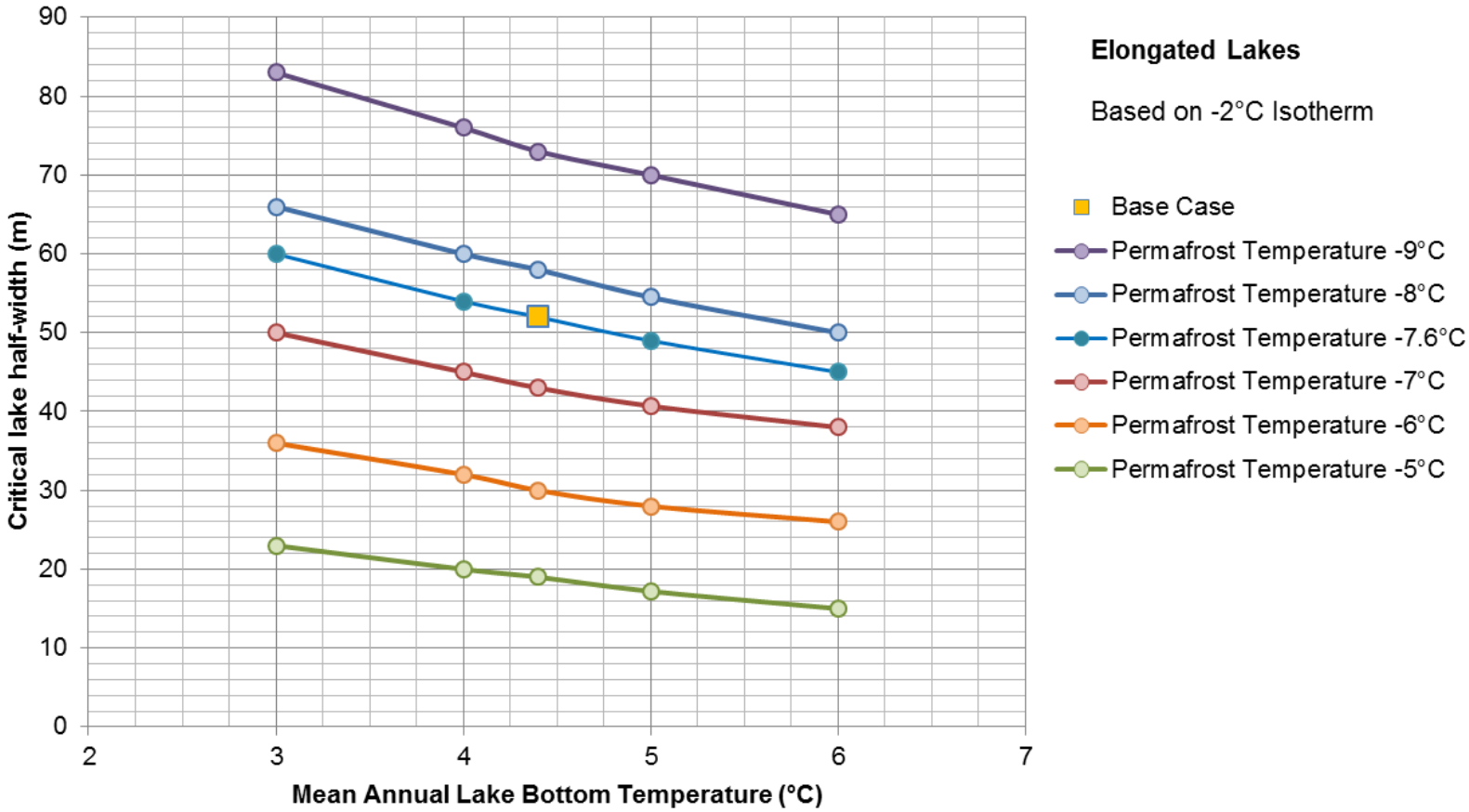
1. Orange arrows show potential direction of groundwater flow for illustrative purposes only

srk consulting	TMAC RESOURCES	Lake Talik Configuration
Job No: 1CT022.004 Filename: ElongatedLakesCriticalLakeHalf-Width.pptx	HOPE BAY PROJECT	**Conceptual Drawing – Open and Closed Lake Taliks**
		Date: 2/12/2016 | Approved: cws | Figure: **1**



Notes:
1. Open (through) taliks estimated for circular lakes with a dimensions greater than the critical radius
2. Permafrost temperature refers to mean annual ground temperature near the depth of zero annual amplitude
3. Results based on -2°C isotherm

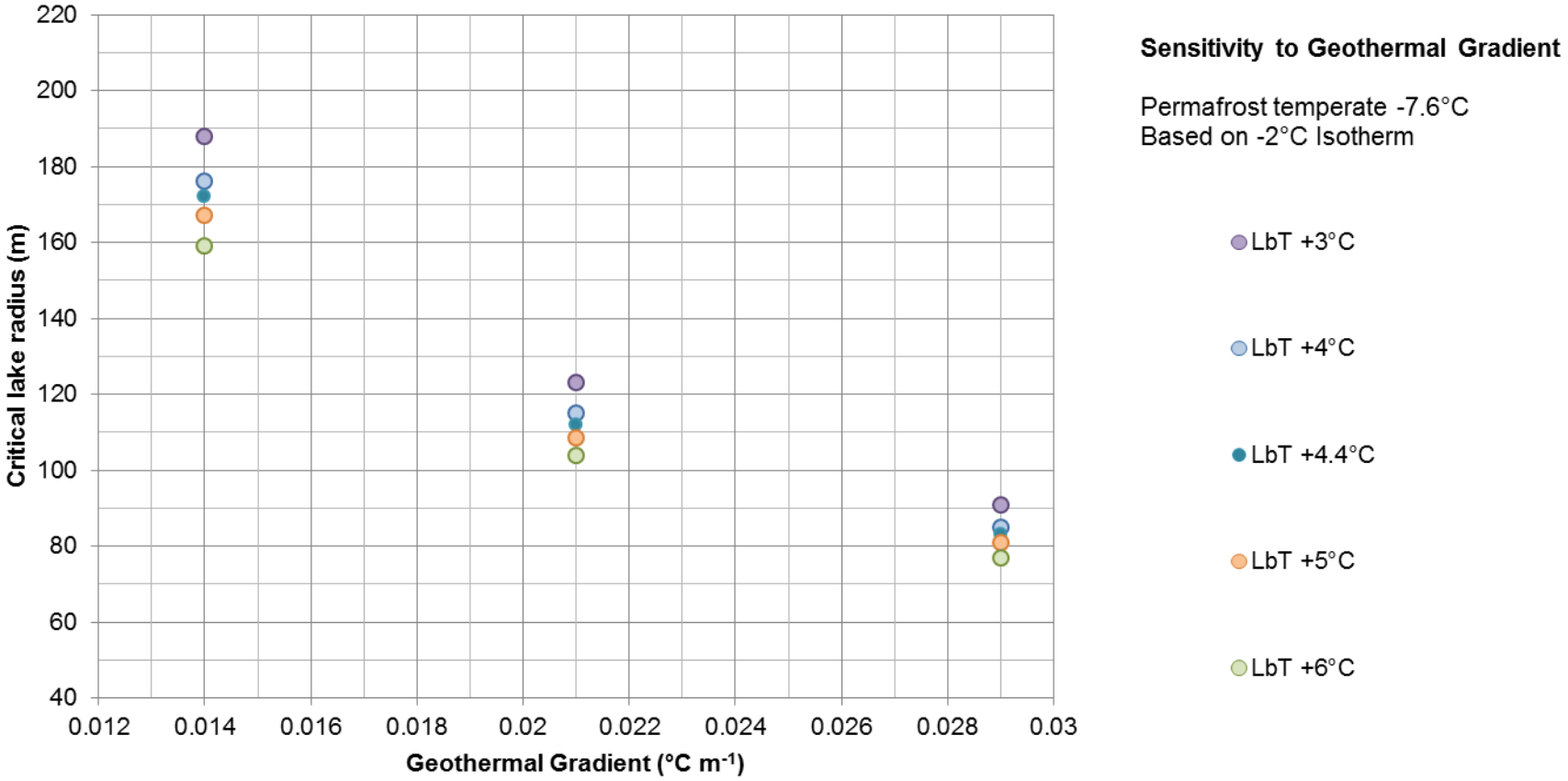
srk consulting	TMAC RESOURCES	Lake Talik Configuration
Job No: 1CT022.004 Filename: ElongatedLakesCriticalLakeHalf-Width.pptx	HOPE BAY PROJECT	**Circular Lakes - Critical Half-width for Open Taliks**
		Date: 2/12/2016 | Approved: cws | Figure: **2**



Notes:

1. Open (through) taliks estimated for circular lakes with a dimensions greater than the critical half-width
2. Permafrost temperature refers to mean annual ground temperature near the depth of zero annual amplitude
3. Results based on -2°C isotherm

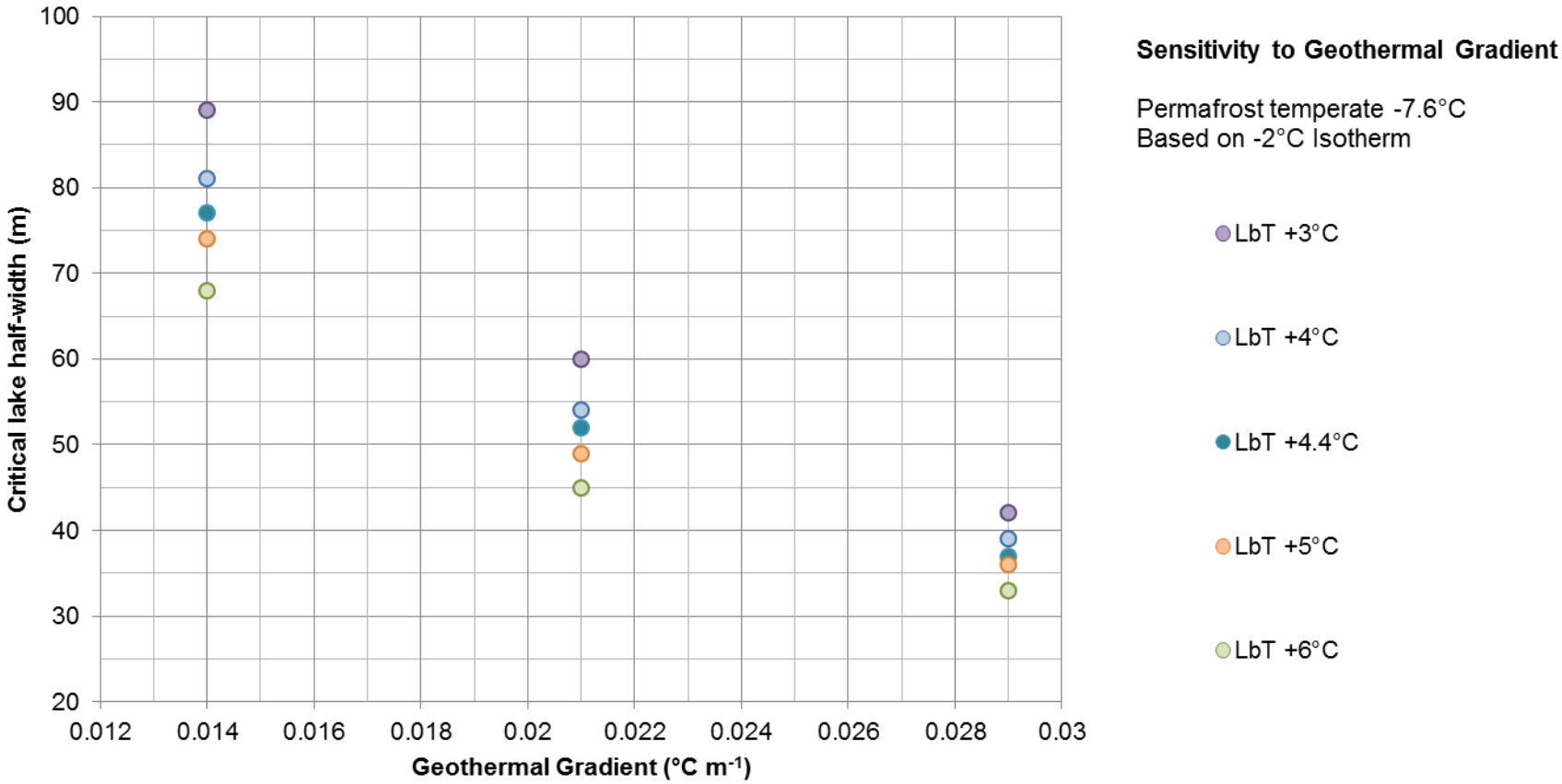
srk consulting	MAC RESOURCES	Lake Talik Configuration
Job No: 1CT022.004 Filename: ElongatedLakesCriticalLakeHalf-Width.pptx	HOPE BAY PROJECT	**Elongated Lakes - Critical Half-width for Open Taliks**
		Date: 2/12/2016 | Approved: cws | Figure: **3**



Notes:

1. Open (through) taliks estimated for circular lakes with a dimensions greater than the critical radius
2. Sensitivity of critical lake radius based on average geothermal gradient measured at the Doris, Madrid, and Boston mining areas
3. Permafrost temperature based on base case value of -7.6°C
4. LbT – Lake bottom temperature
5. Results based on -2°C isotherm

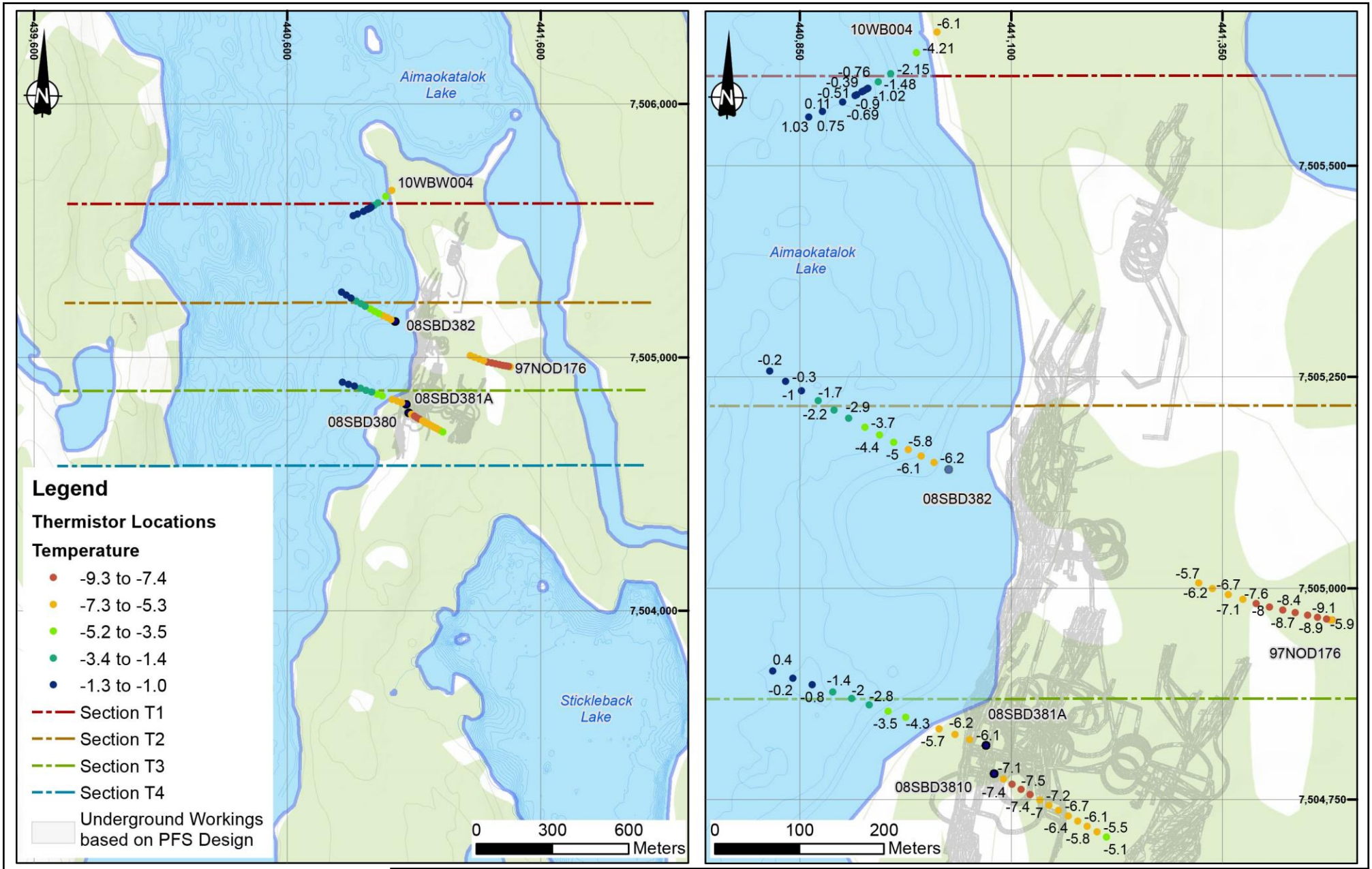
srk consulting	TMAC RESOURCES	Lake Talik Configuration		
		Circular Lakes – Sensitivity to Geothermal Gradient		
Job No: 1CT022.004 Filename: CircularLakesSensitivitytoGeothermalGradient.pptx	HOPE BAY PROJECT	Date: 2/12/2016	Approved: cws	Figure: 4



Notes:

1. Open (through) taliks estimated for circular lakes with a dimensions greater than the critical half-width
2. Sensitivity of critical lake half-width based on average geothermal gradient measured at the Doris, Madrid, and Boston mining areas
3. Permafrost temperature based on base case value of -7.6°C
4. LbT – Lake bottom temperature
5. Results based on -2°C isotherm

srk consulting	MAC RESOURCES	Lake Talik Configuration
Job No: 1CT022.004 Filename: ElongatedLakesSensitivitytoGeothermalGradient.pptx	HOPE BAY PROJECT	**Elongated Lakes – Sensitivity to Geothermal Gradient**
		Date: 2/12/2016 | Approved: cws | Figure: **5**



Notes:

1. Coordinate System: UTM NAD 83 Zone13
2. Basemap Credits: ERSI, DeLorme, TomTom, Intermap, NRCAN, GeoBase
3. Underground Workings based on PFS Design

srk consulting

Job No: 1CT022.004

Filename: BostonDeepGroundTemperatures.pptx

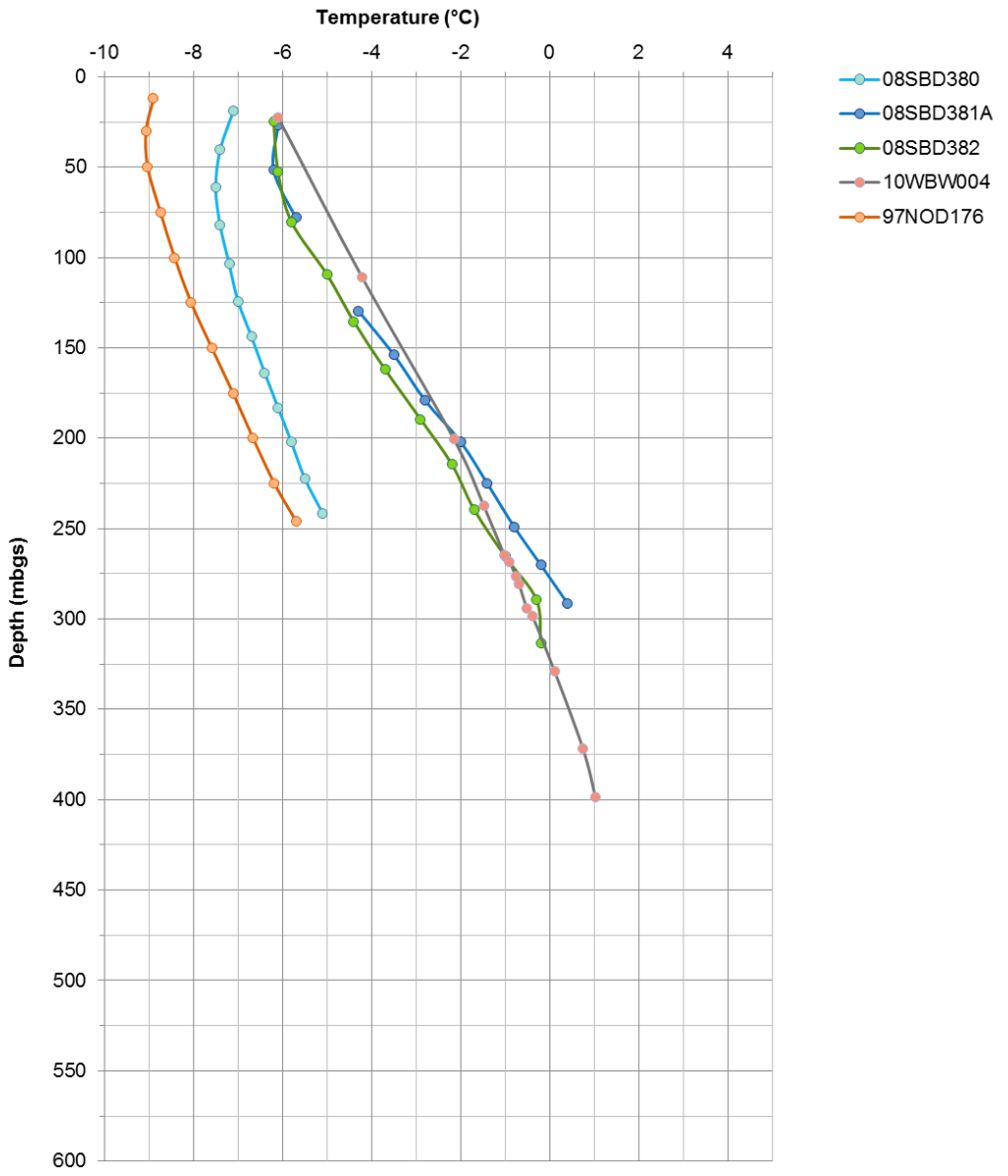
TMAC RESOURCES

HOPE BAY PROJECT

Lake Talik Configuration

Boston Mining Area

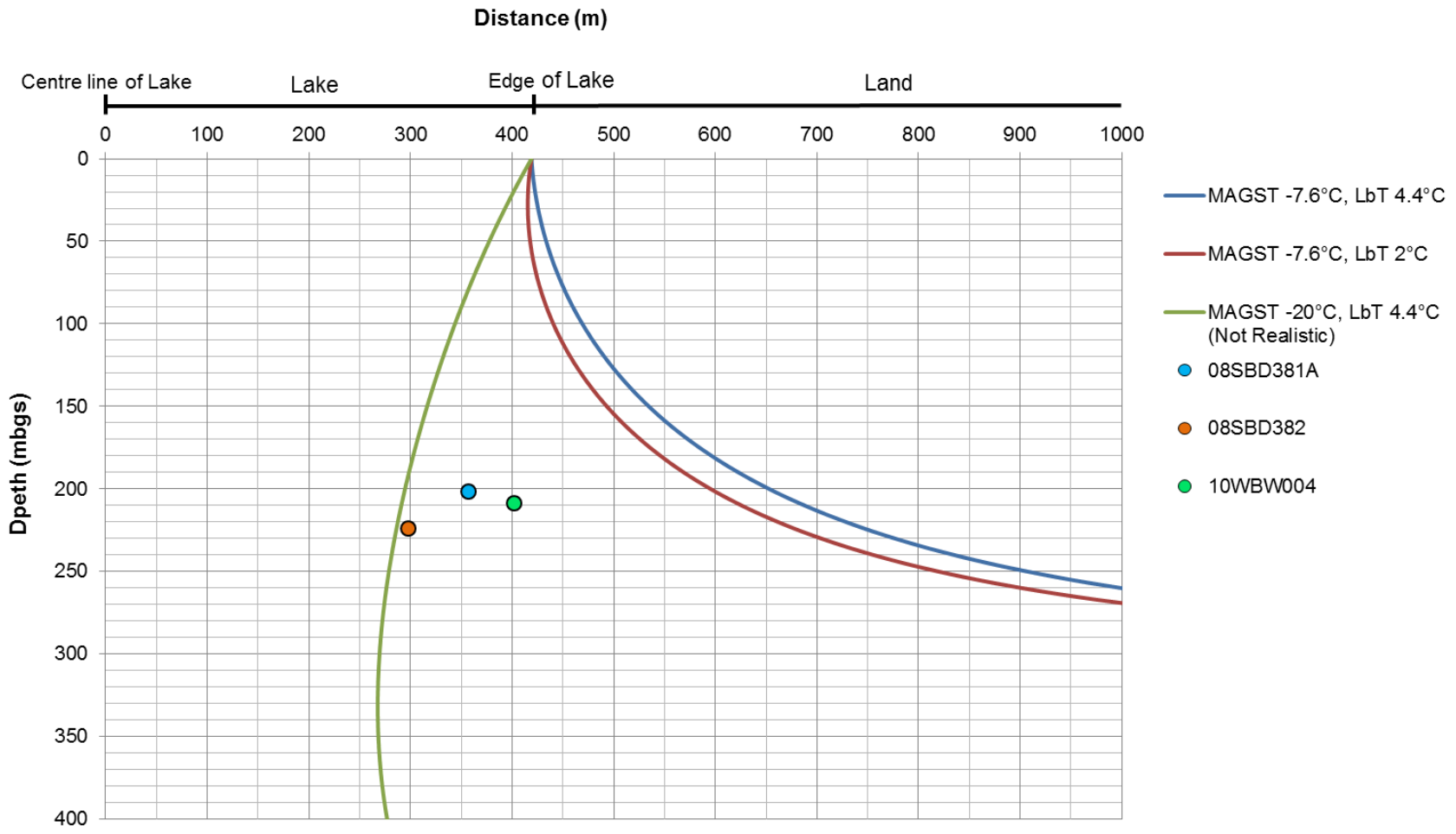
Date:	Approved:	Figure:
2/12/2016	cws	6



Notes:

1. Depth indicated as vertical metres below ground surface (mbgs)

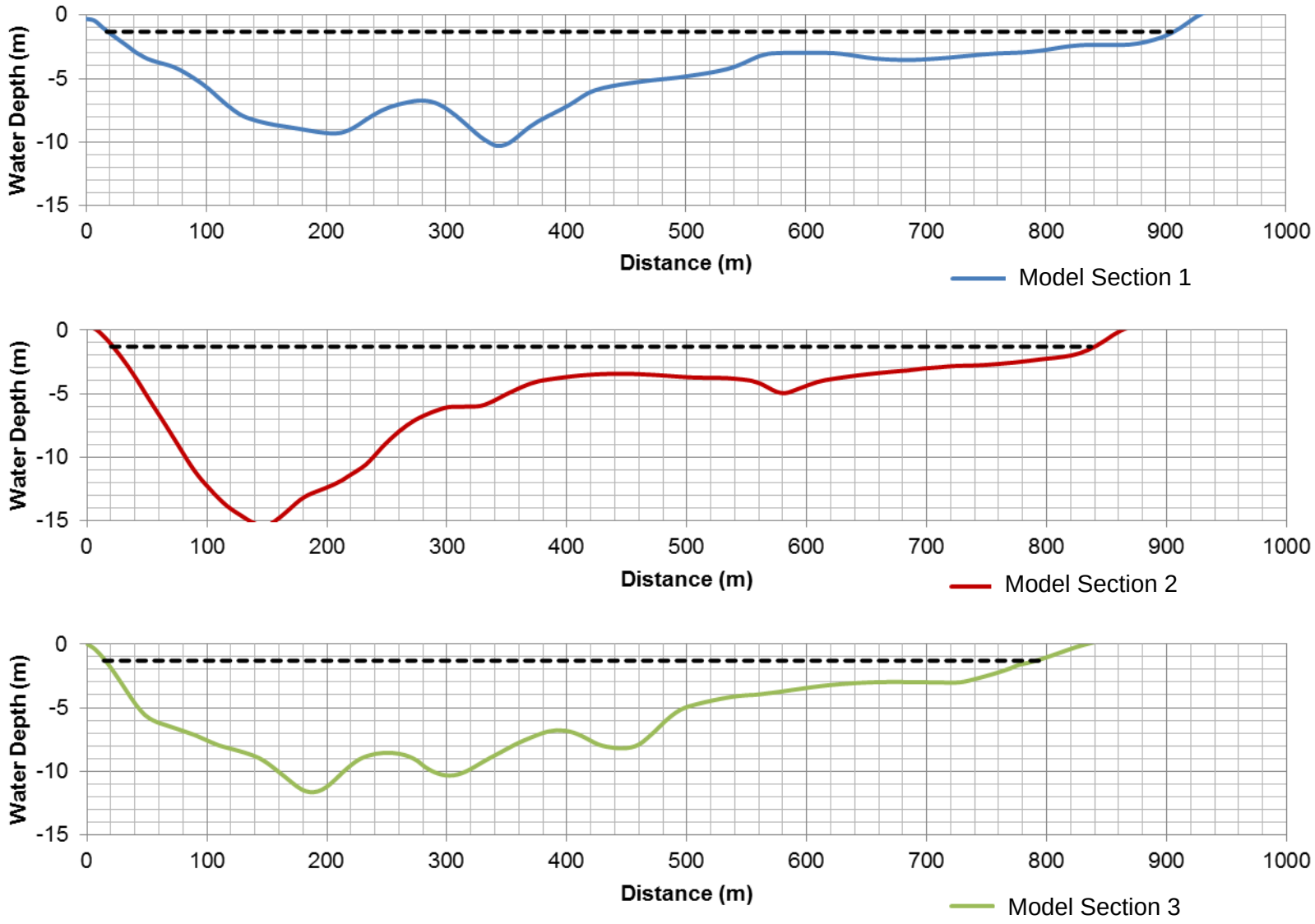
srk consulting		Lake Talik Configuration	
		Deep Ground Temperatures – Boston Mining Area	
Job No: 1CT022.004 Filename: BostonDeepGroundTemperatures.pptx	HOPE BAY PROJECT	Date: 2/12/2016	Approved: cws	Figure: **7**



Notes:

1. 2D analytical model of steady state talik configuration based on -2°C isotherm (solid lines)
2. Position of -2°C isotherm based on thermistor measurements (solid circles)
3. Depth indicated as vertical metres below ground surface (mbgs)
4. Mean annual ground surface temperature (MAGST)
5. Lake bottom temperature (LbT)

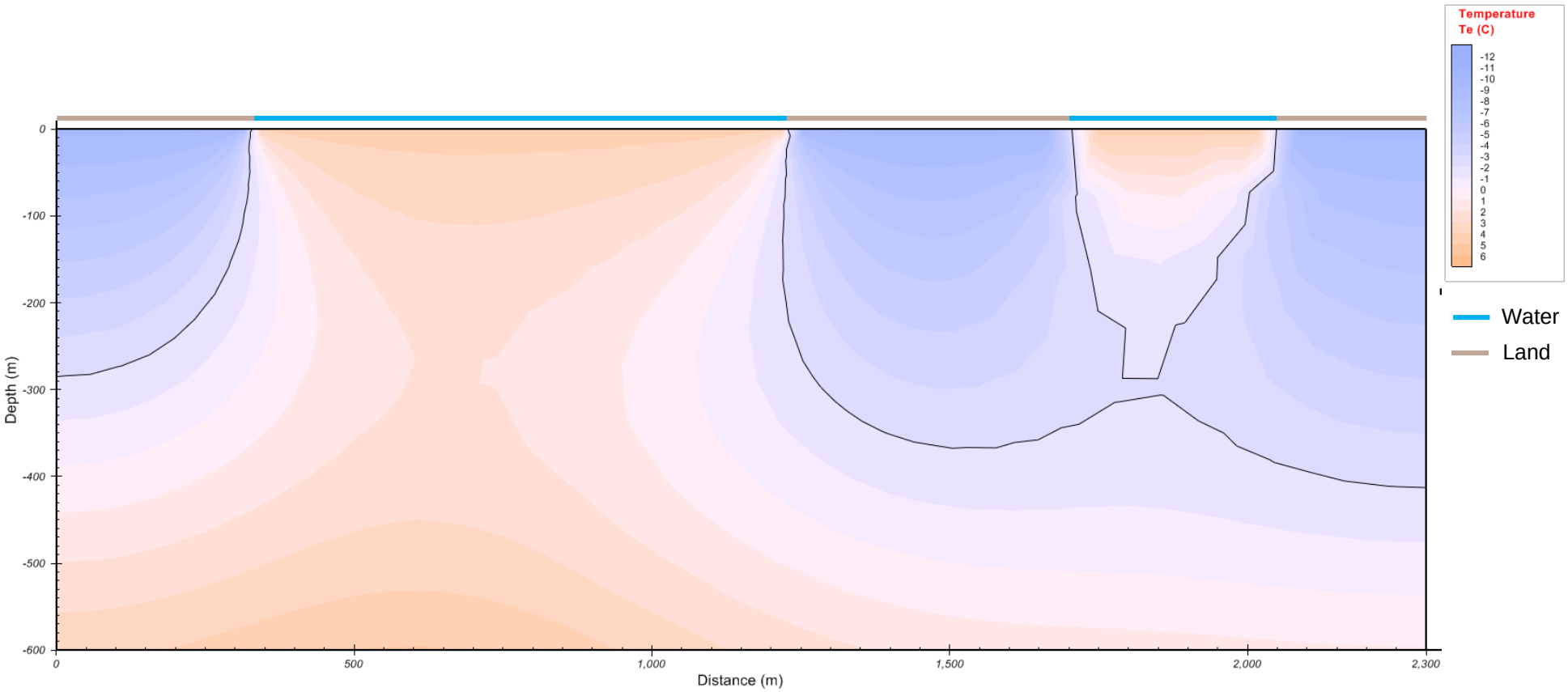
srk consulting	MAC RESOURCES	Lake Talik Configuration
Job No: 1CT022.004 Filename: BostonDeepGroundTemperatures.pptx	HOPE BAY PROJECT	**Steady State Model – Aimaokatalok Lake Talik**
		Date: 2/12/2016 | Approved: cws | Figure: **8**



Notes:

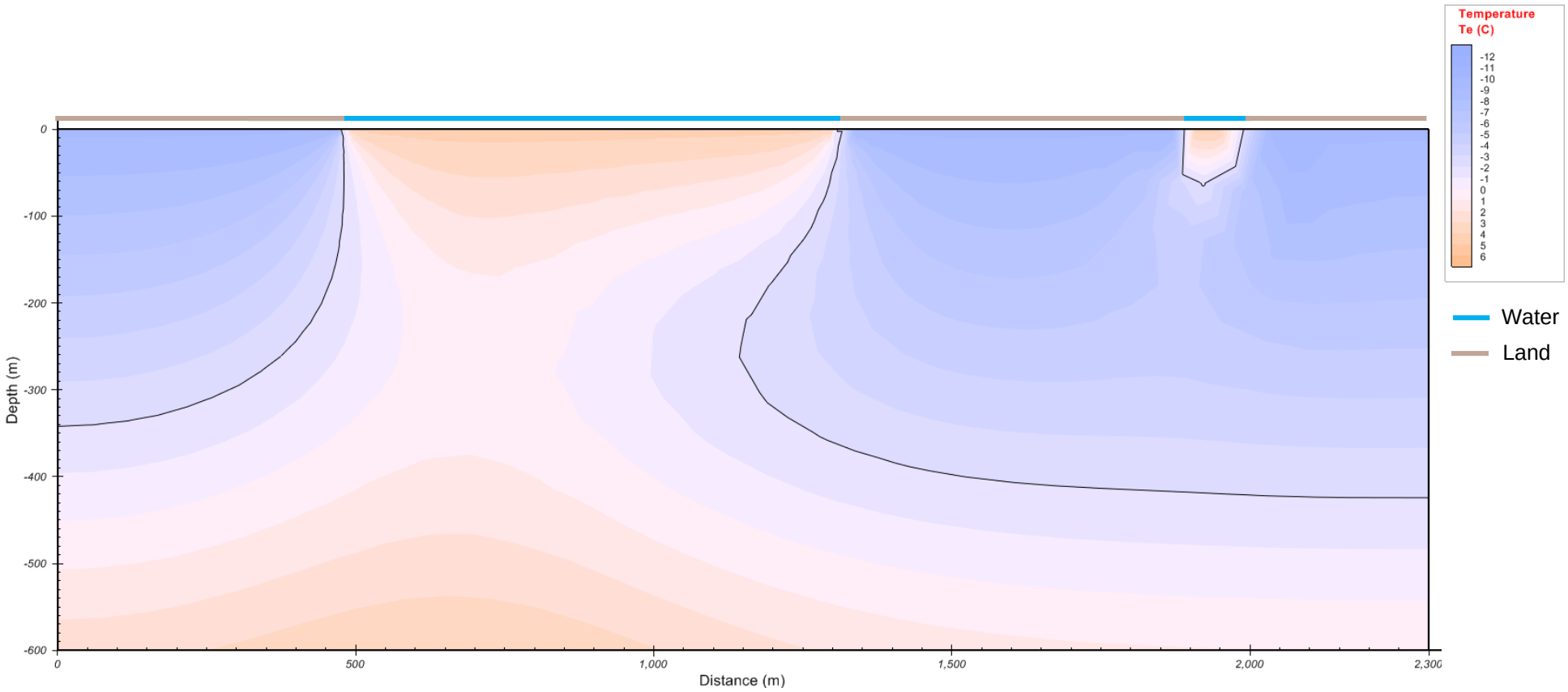
1. Solid line indicates water depth along model section
2. Section only shown for locations where ground temperature measurements extend beneath the lake
3. Dashed black line is two-thirds of the average late-winter ice thickness

srk consulting	MAC RESOURCES	Lake Talik Configuration
		Aimaokatalok Lake Water Bathymetry
Job No: 1CT022.004 Filename: WaterBathymetryModelTransects.pptx	HOPE BAY PROJECT	Date: 2/12/2016 | Approved: cws | Figure: **9**



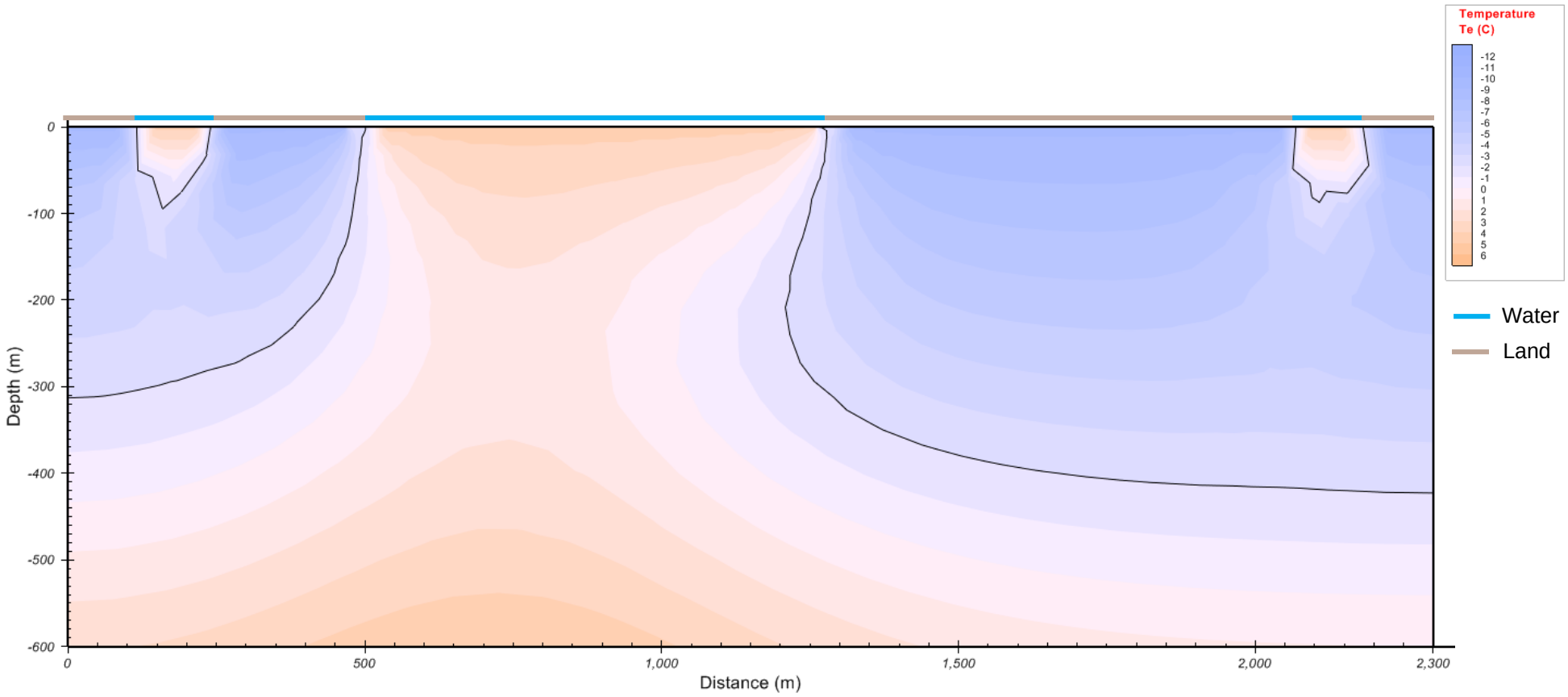
Notes:
1. -2°C isotherm indicated with solid black line
2. Model section extends from west to east

srk consulting	TMAC RESOURCES	Lake Talik Configuration		
		Boston Mining Area – 2D Model Section T1		
Job No: 1CT022.004 Filename: BostonDeepGroundTemperatures.pptx	HOPE BAY PROJECT	Date: 2/12/2016	Approved: cws	Figure: **10**



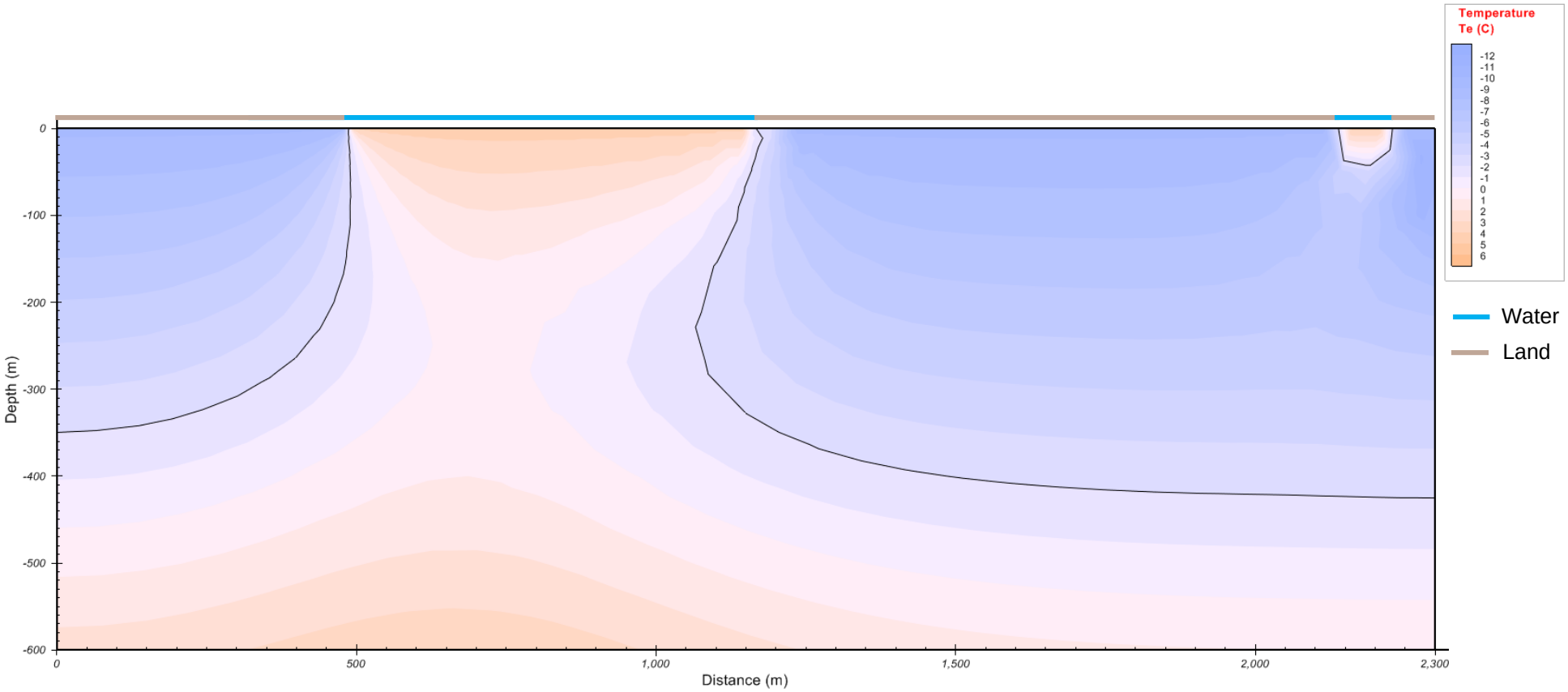
Notes:
1. -2°C isotherm indicated with solid black line
2. Model section extends from west to east

srk consulting	TMAC RESOURCES	Lake Talik Configuration
Job No: 1CT022.004 Filename: BostonDeepGroundTemperatures.pptx	HOPE BAY PROJECT	**Boston Mining Area – 2D Model Section T2**
		Date: 2/12/2016 | Approved: cws | Figure: **11**



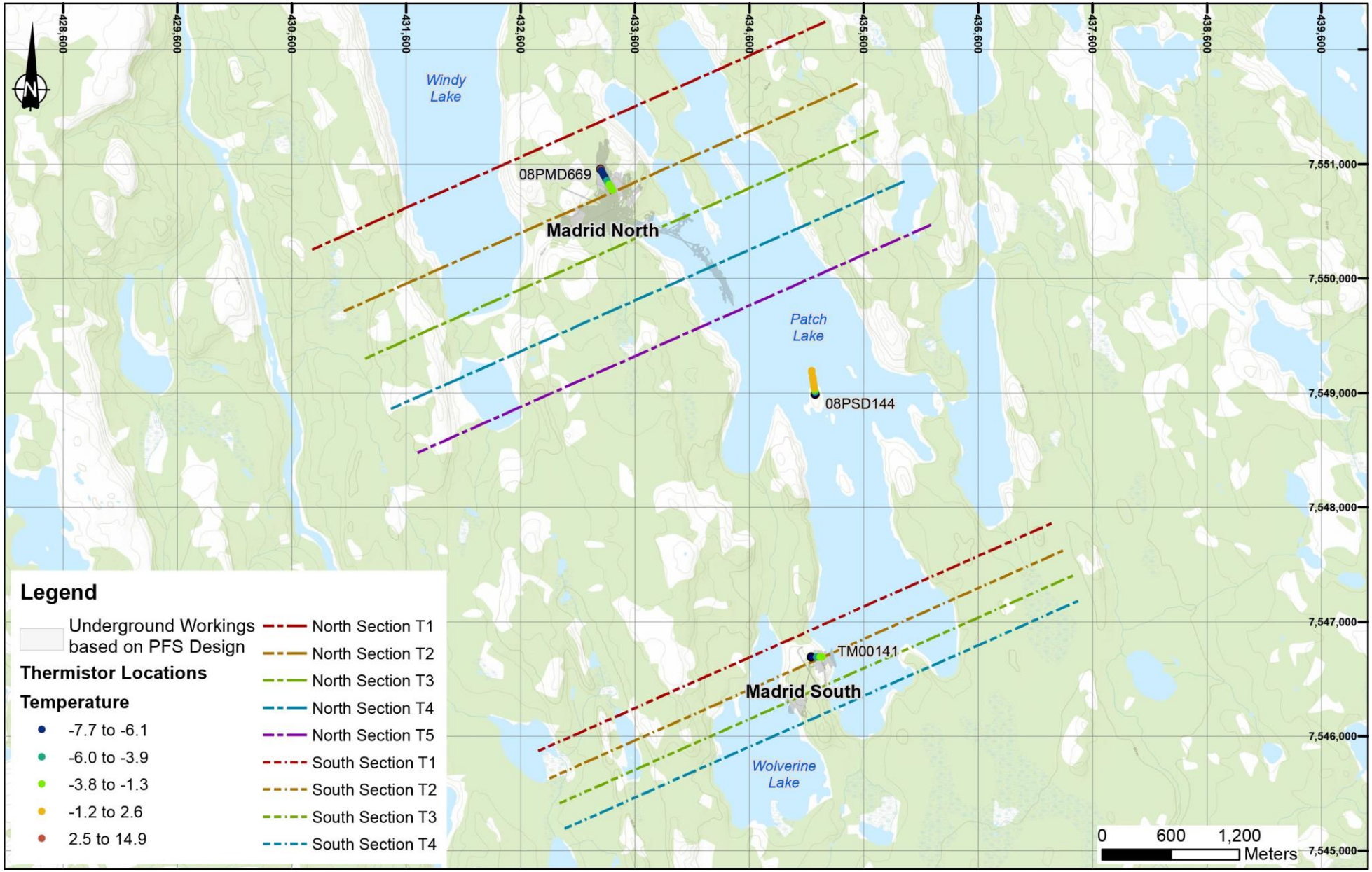
Notes:
1. -2°C isotherm indicated with solid black line
2. Model section extends from west to east

srk consulting	TMAC RESOURCES	Lake Talik Configuration
		Boston Mining Area – 2D Model Section T3
Job No: 1CT022.004 Filename: BostonDeepGroundTemperatures.pptx	HOPE BAY PROJECT	Date: 2/12/2016 | Approved: cws | Figure: **12**



Notes:
1. -2°C isotherm indicated with solid black line
2. Model section extends from west to east

srk consulting	TMAC RESOURCES	Lake Talik Configuration
		Boston Mining Area – 2D Model Section T4
Job No: 1CT022.004 Filename: BostonDeepGroundTemperatures.pptx	HOPE BAY PROJECT	Date: 2/12/2016 | Approved: cws | Figure: **13**



Notes:

1. Coordinate System: UTM NAD 83 Zone13
2. Basemap Credits: ERSI, DeLorme, TomTom, Intermap, NRCAN, GeoBase
3. Underground Workings based on PFS Design

srk consulting

Job No: 1CT022.004

Filename: BostonDeepGroundTemperatures.pptx

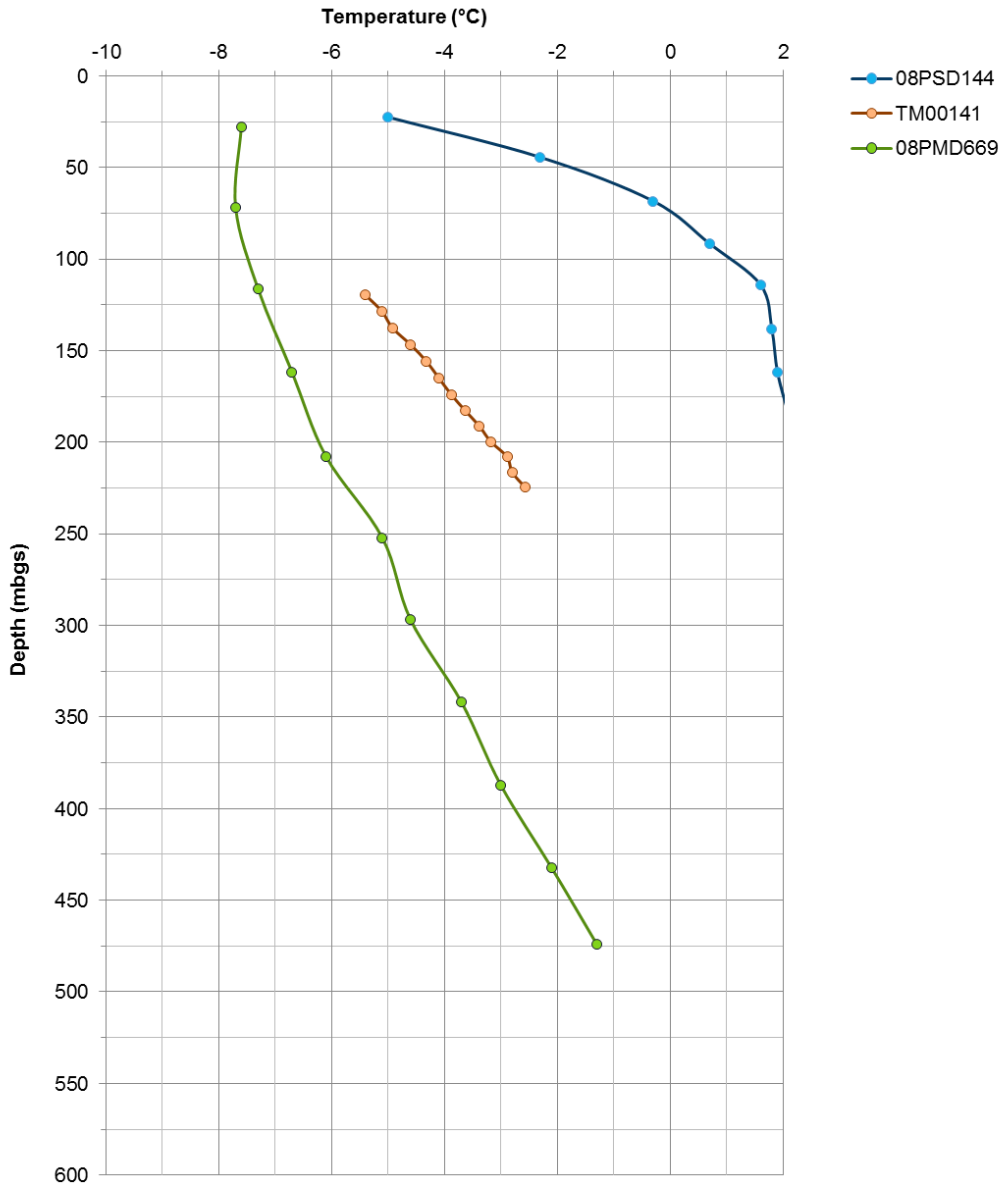
TMAC RESOURCES

HOPE BAY PROJECT

Lake Talik Configuration

Madrid North and South Mining Areas

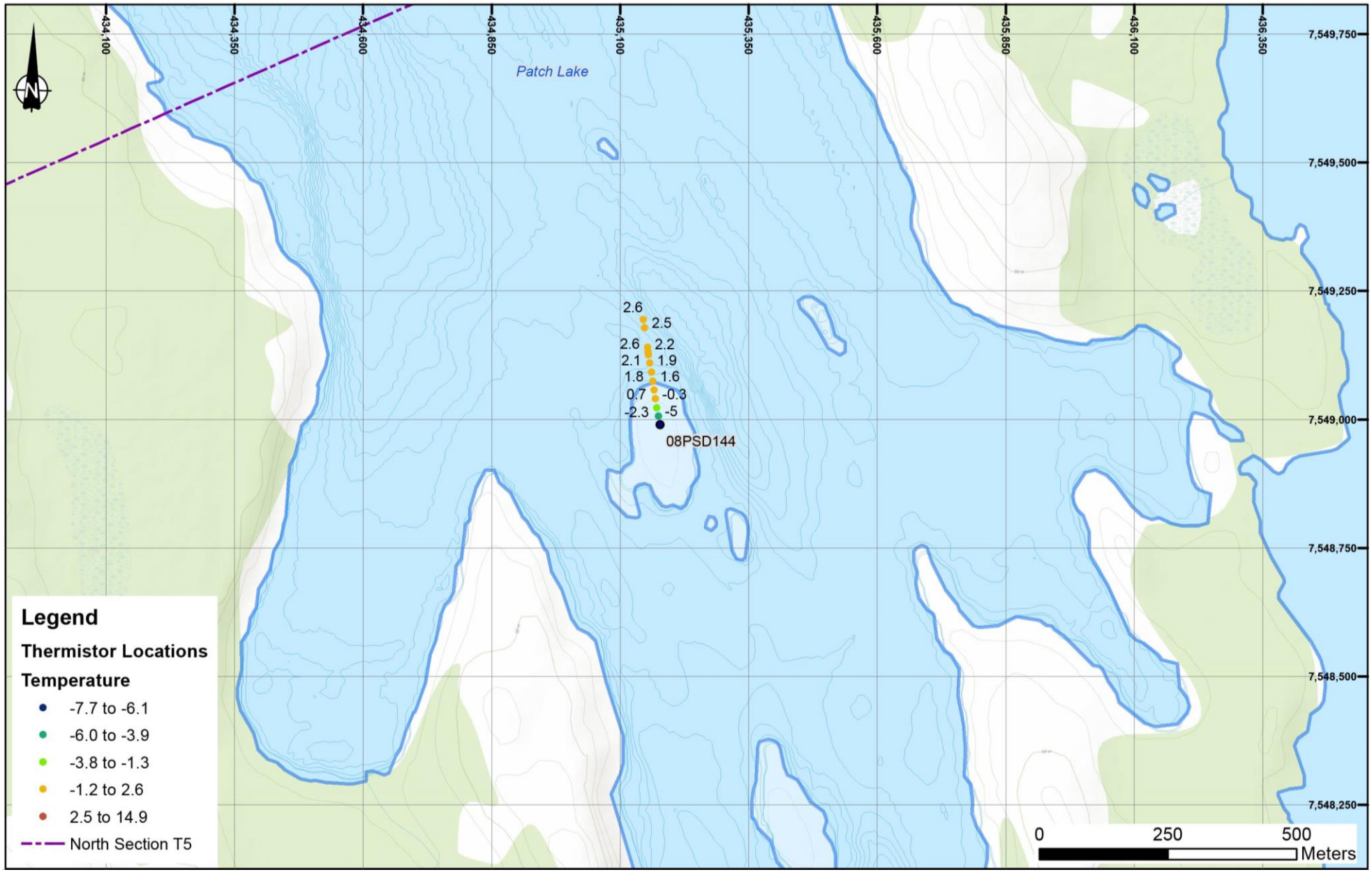
Date:	Approved:	Figure:
2/12/2016	cws	14



Notes:

1. Depth indicated as vertical metres below ground surface (mbgs)

srk consulting	TMAC RESOURCES	Lake Talik Configuration
Job No: 1CT022.004 Filename: BostonDeepGroundTemperatures.pptx	HOPE BAY PROJECT	**Deep Ground Temperatures – Madrid Mining Area**
		Date: 2/12/2016 | Approved: cws | Figure: **15**



Notes:

1. Coordinate System: UTM NAD 83 Zone13
2. Basemap Credits: ERSI, DeLorme, TomTom, Intermap, NRCAN, GeoBase
3. Underground Workings based on PFS Design

srk consulting

Job No: 1CT022.004

Filename: BostonDeepGroundTemperatures.pptx

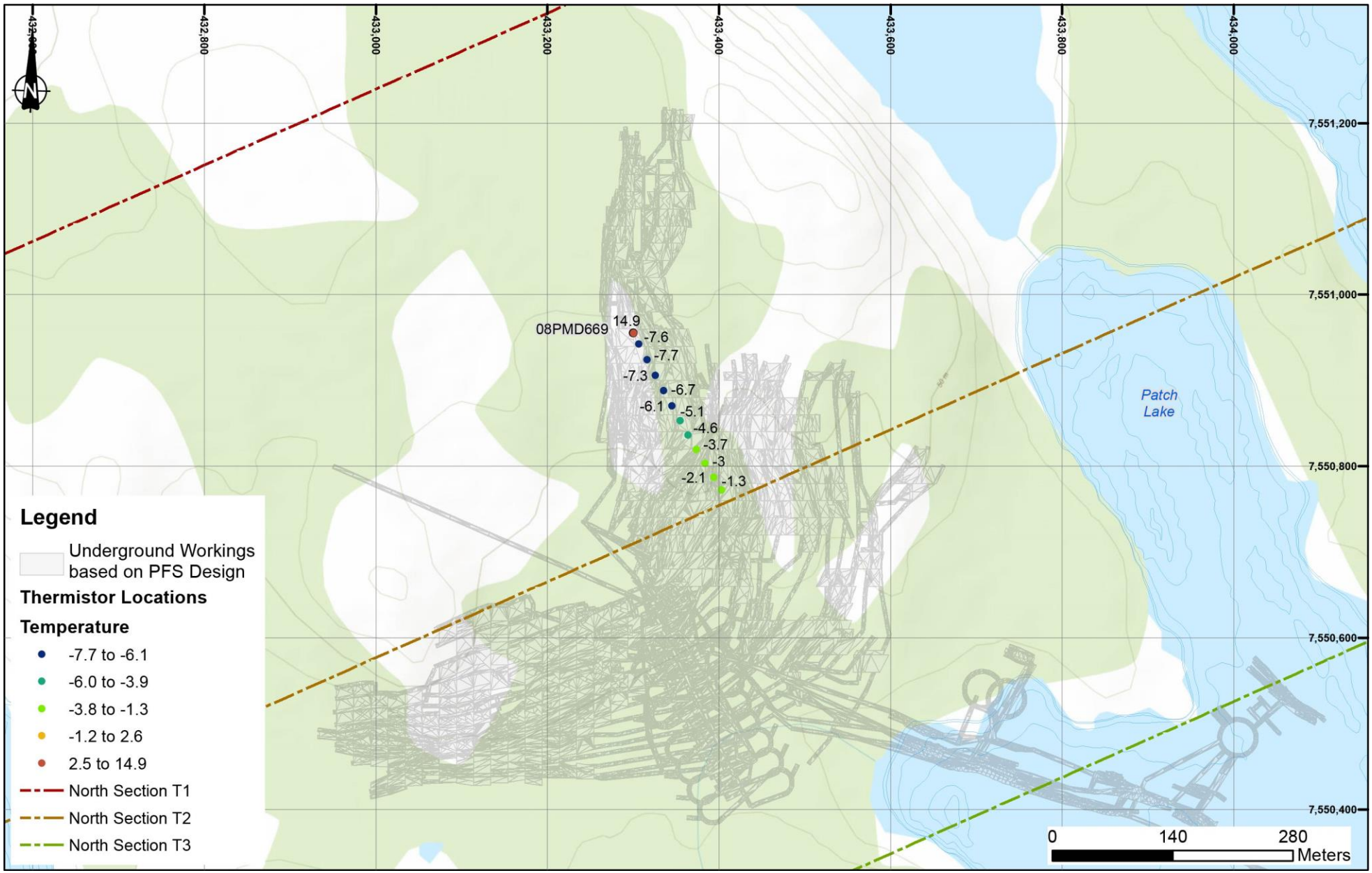
TMAC RESOURCES

HOPE BAY PROJECT

Lake Talik Configuration

Patch Island – Thermistor Site ID 08PSD144

Date:	Approved:	Figure:
2/12/2016	cws	**16**



Notes:

1. Coordinate System: UTM NAD 83 Zone13
2. Basemap Credits: ERSI, DeLorme, TomTom, Intermap, NRCAN, GeoBase
3. Underground Workings based on PFS Design

srk consulting

Job No: 1CT022.004

Filename: BostonDeepGroundTemperatures.pptx

TMAC RESOURCES

HOPE BAY PROJECT

Lake Talik Configuration

Madrid North Mining Area – Thermistor Site ID 08PMD669

Date:	Approved:	Figure:
2/12/2016	cws	17



Notes:

1. Coordinate System: UTM NAD 83 Zone13
2. Basemap Credits: ERSI, DeLorme, TomTom, Intermap, NRCAN, GeoBase
3. Underground Workings based on PFS Design

srk consulting

Job No: 1CT022.004

Filename: BostonDeepGroundTemperatures.pptx

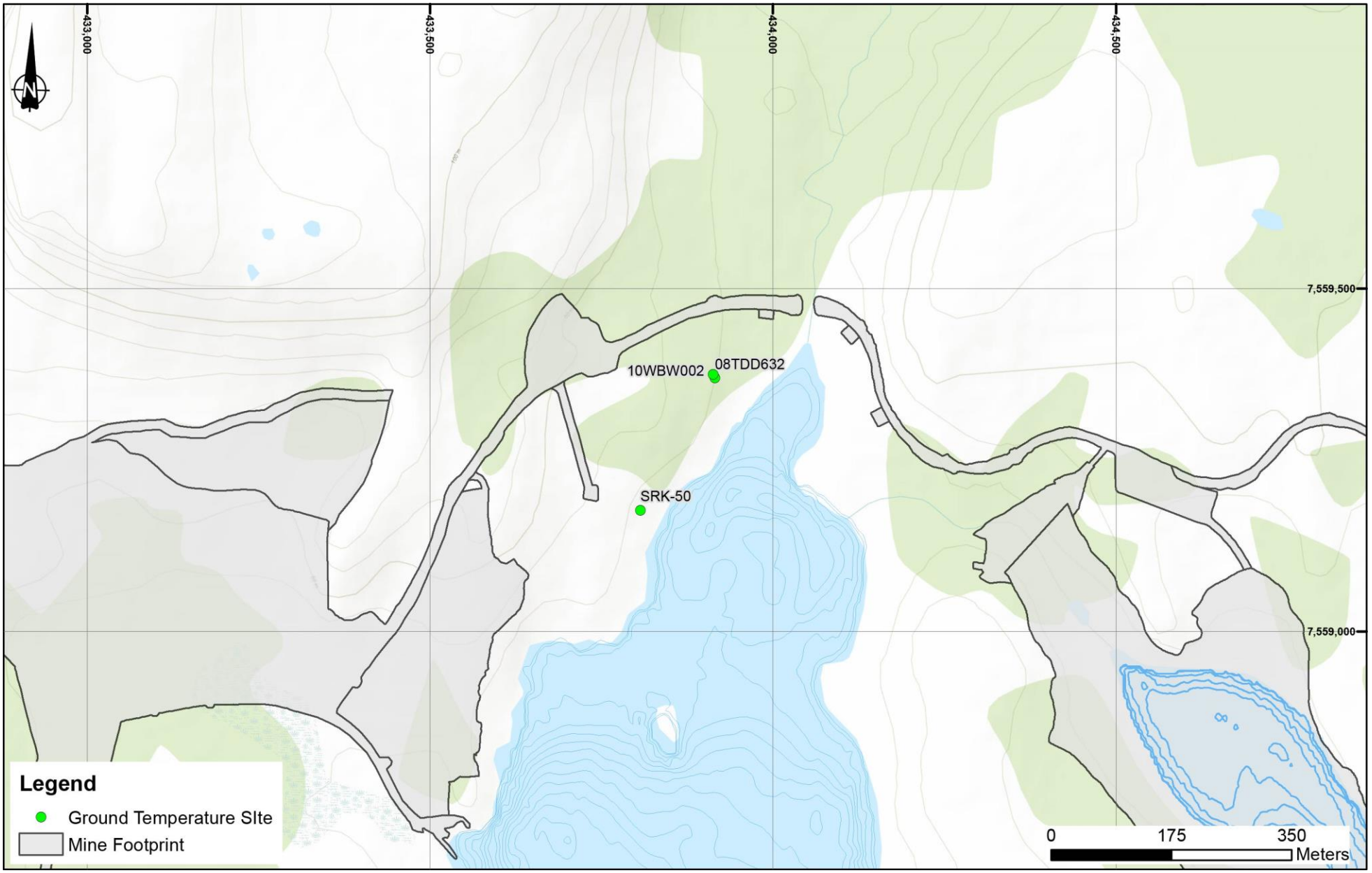
TMAC RESOURCES

HOPE BAY PROJECT

Lake Talik Configuration

Madrid South Mining Area – Thermistor Site ID TM00141

Date:	Approved:	Figure:
2/12/2016	cws	**18**



Notes:

1. Coordinate System: UTM NAD 83 Zone13
2. Basemap Credits: ERSI, DeLorme, TomTom, Intermap, NRCAN, GeoBase
3. Mine Footprint based on PFS Design

srk consulting

Job No: 1CT022.004

Filename: BostonDeepGroundTemperatures.pptx

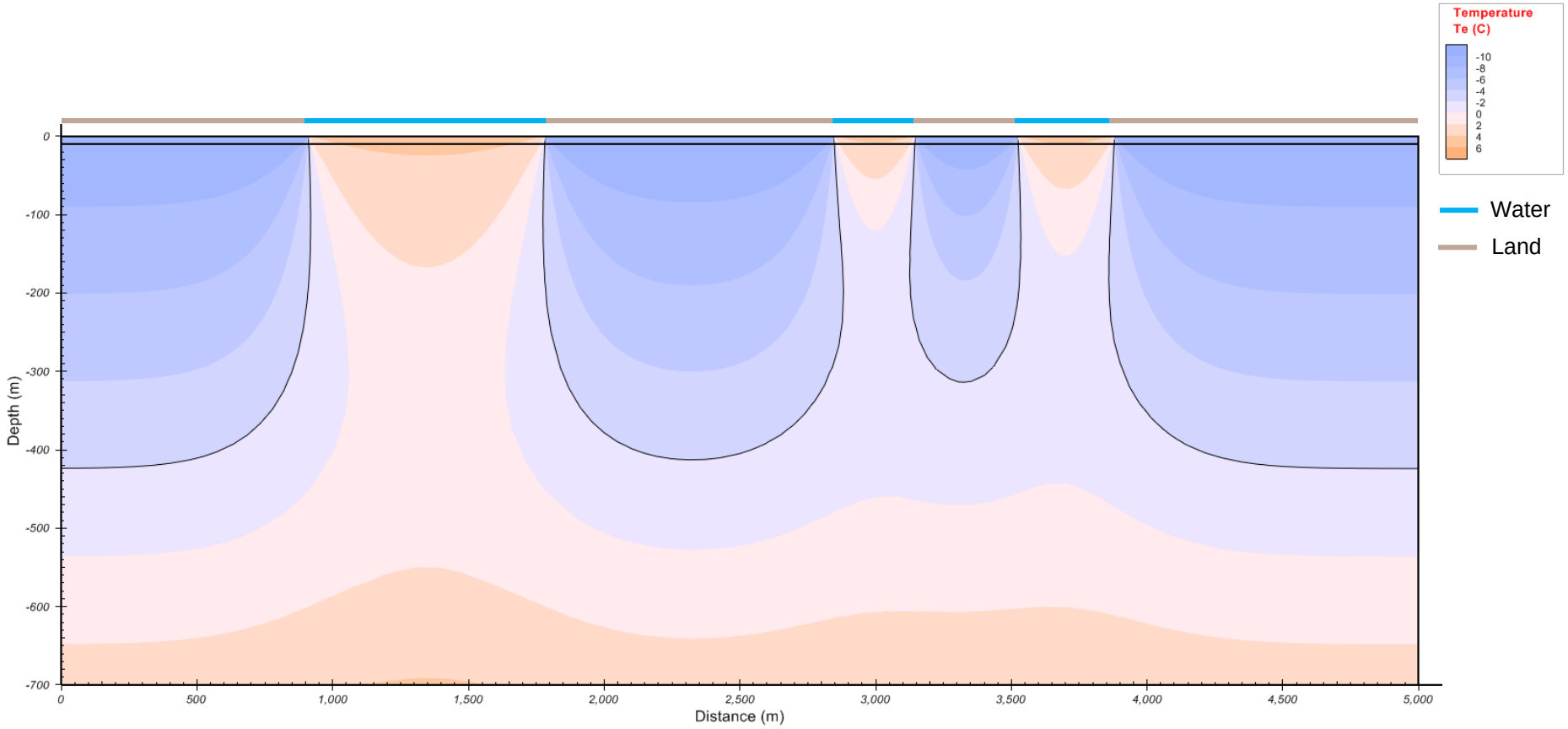
TMAC RESOURCES

HOPE BAY PROJECT

Lake Talik Configuration

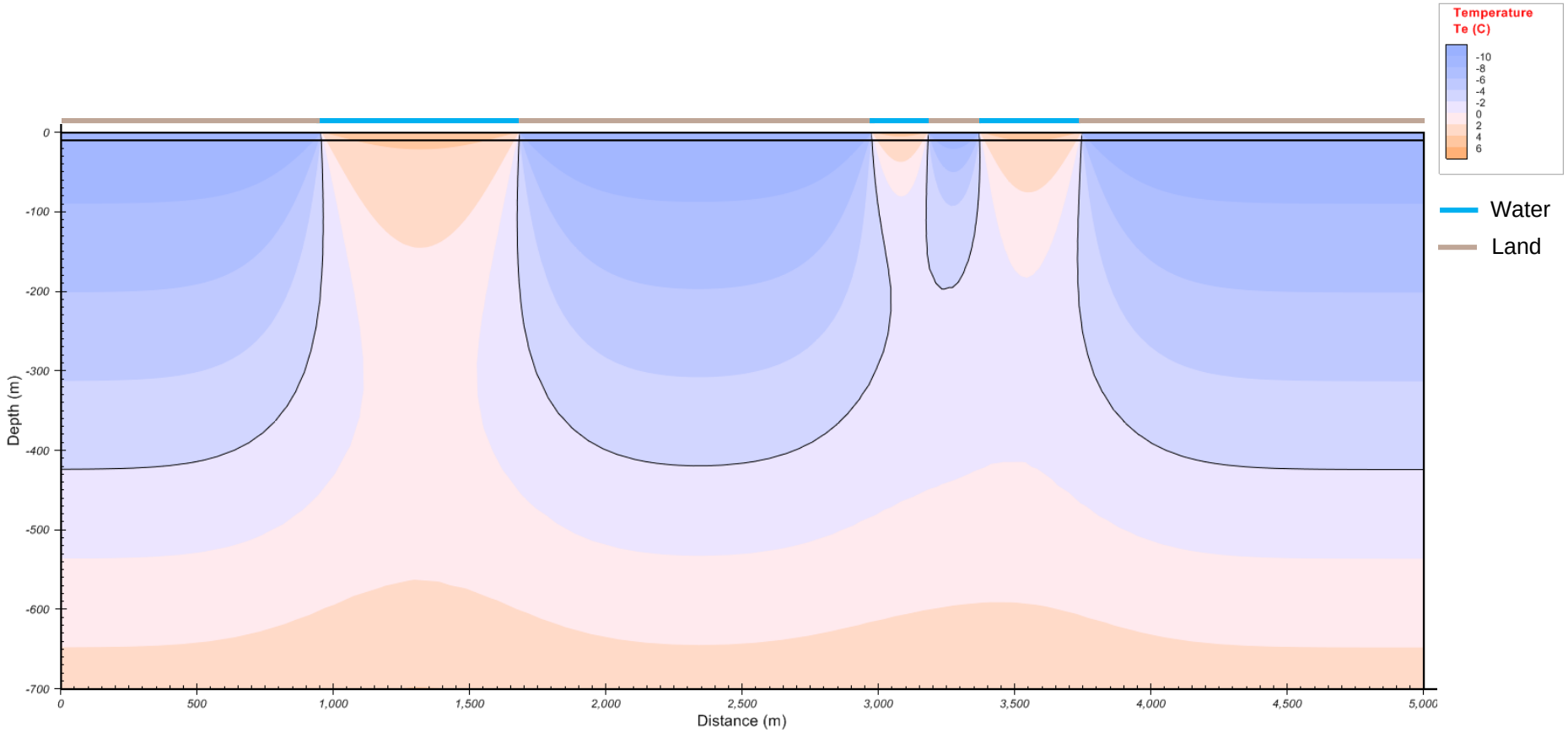
Madrid South Mining Area – Thermistor Site ID TM00141

Date:	Approved:	Figure:
2/12/2016	cws	**19**



Notes:
1. -2°C isotherm indicated with solid black line
2. Model section extends from west to east

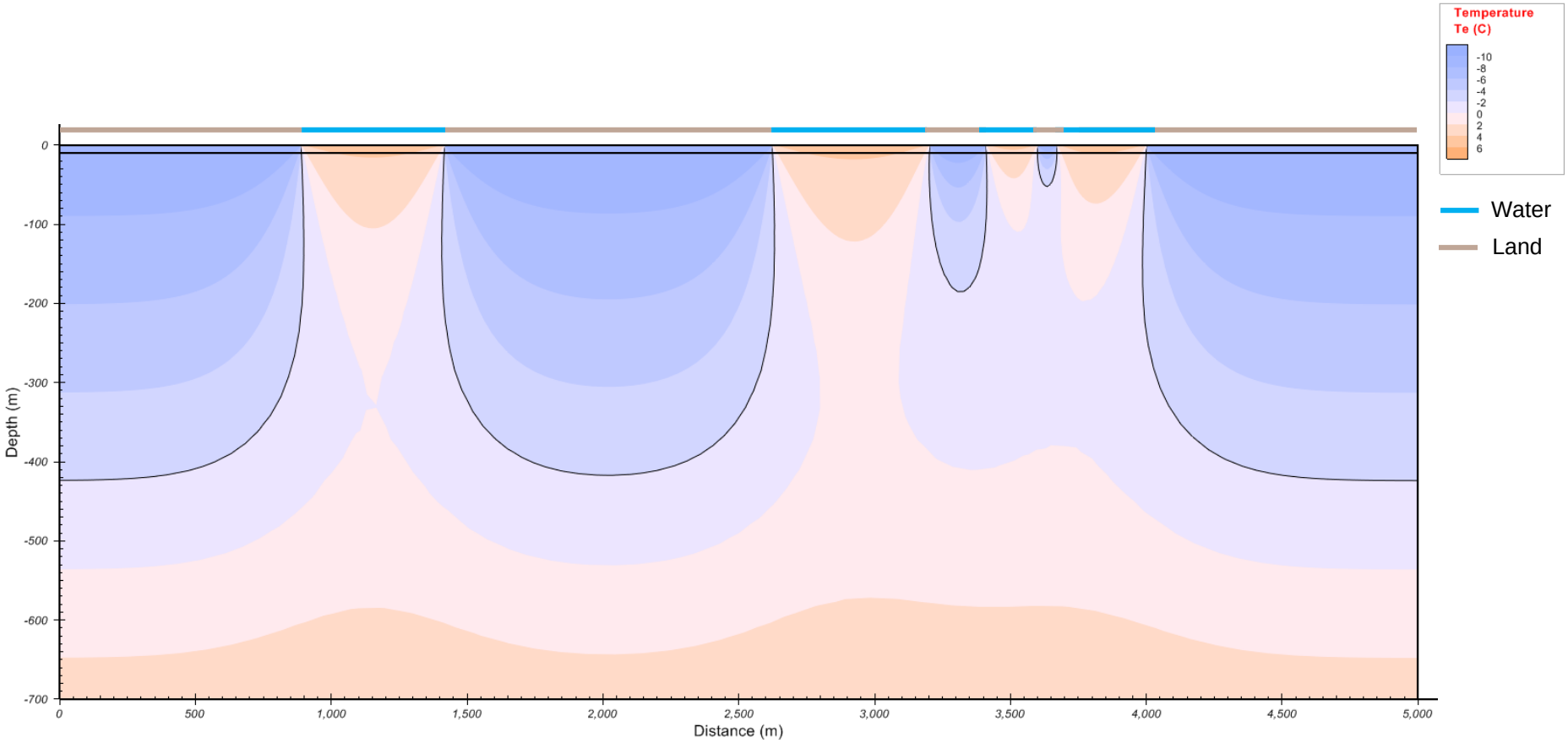
srk consulting	TMAC RESOURCES	Lake Talik Configuration
		Madrid North Mining Area – 2D Model Section T1
Job No: 1CT022.004 Filename: BostonDeepGroundTemperatures.pptx	HOPE BAY PROJECT	Date: 2/12/2016 | Approved: cws | Figure: **20**



Notes:

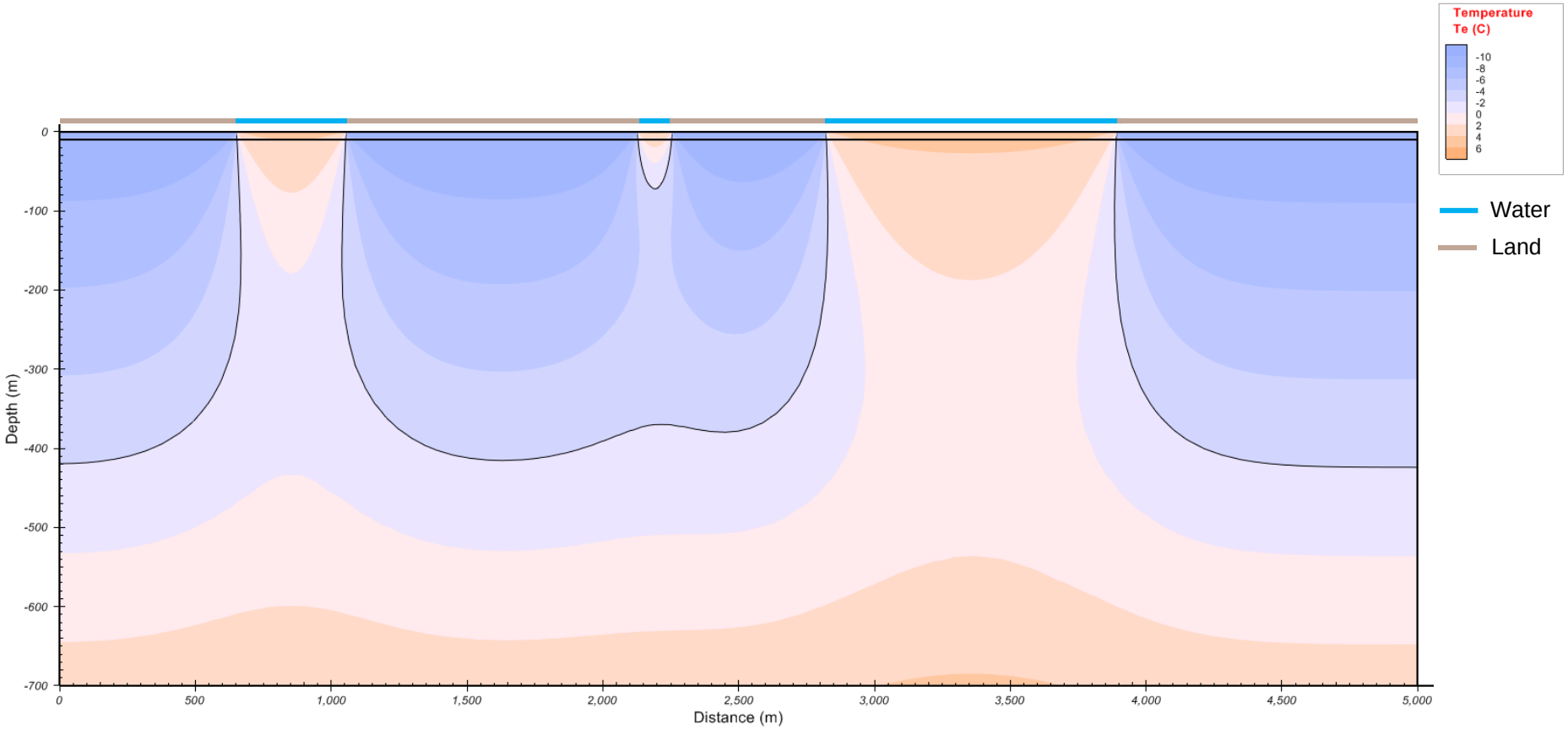
1. -2°C isotherm indicated with solid black line
2. Model section extends from west to east

srk consulting	TMAC RESOURCES	Lake Talik Configuration
		Madrid North Mining Area – 2D Model Section T2
Job No: 1CT022.004 Filename: BostonDeepGroundTemperatures.pptx	HOPE BAY PROJECT	Date: 2/12/2016 | Approved: cws | Figure: **21**



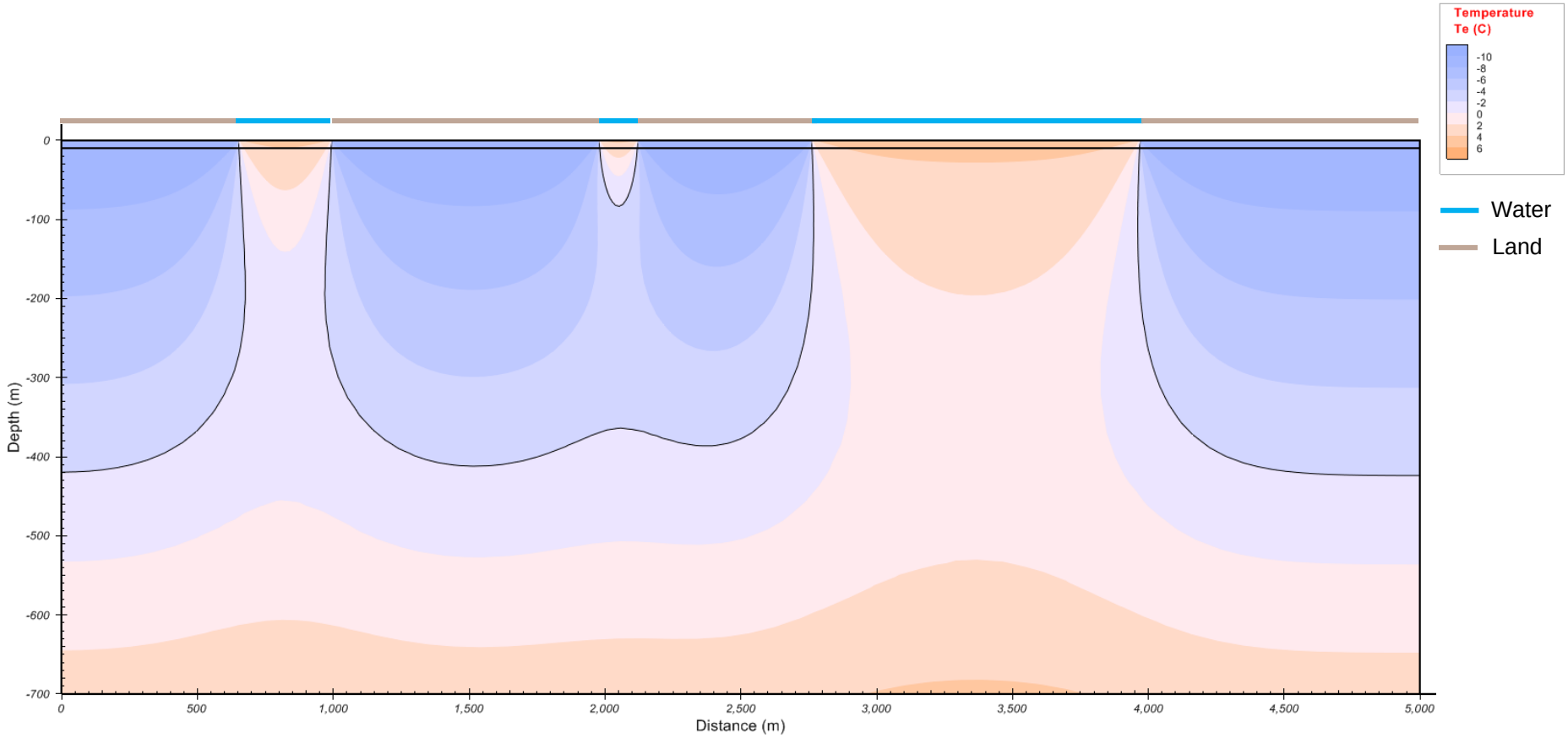
Notes:
1. -2°C isotherm indicated with solid black line
2. Model section extends from west to east

srk consulting	TMAC RESOURCES	Lake Talik Configuration
		Madrid North Mining Area – 2D Model Section T3
Job No: 1CT022.004 Filename: BostonDeepGroundTemperatures.pptx	HOPE BAY PROJECT	Date: 2/12/2016 | Approved: cws | Figure: **22**



Notes:
1. -2°C isotherm indicated with solid black line
2. Model section extends from west to east

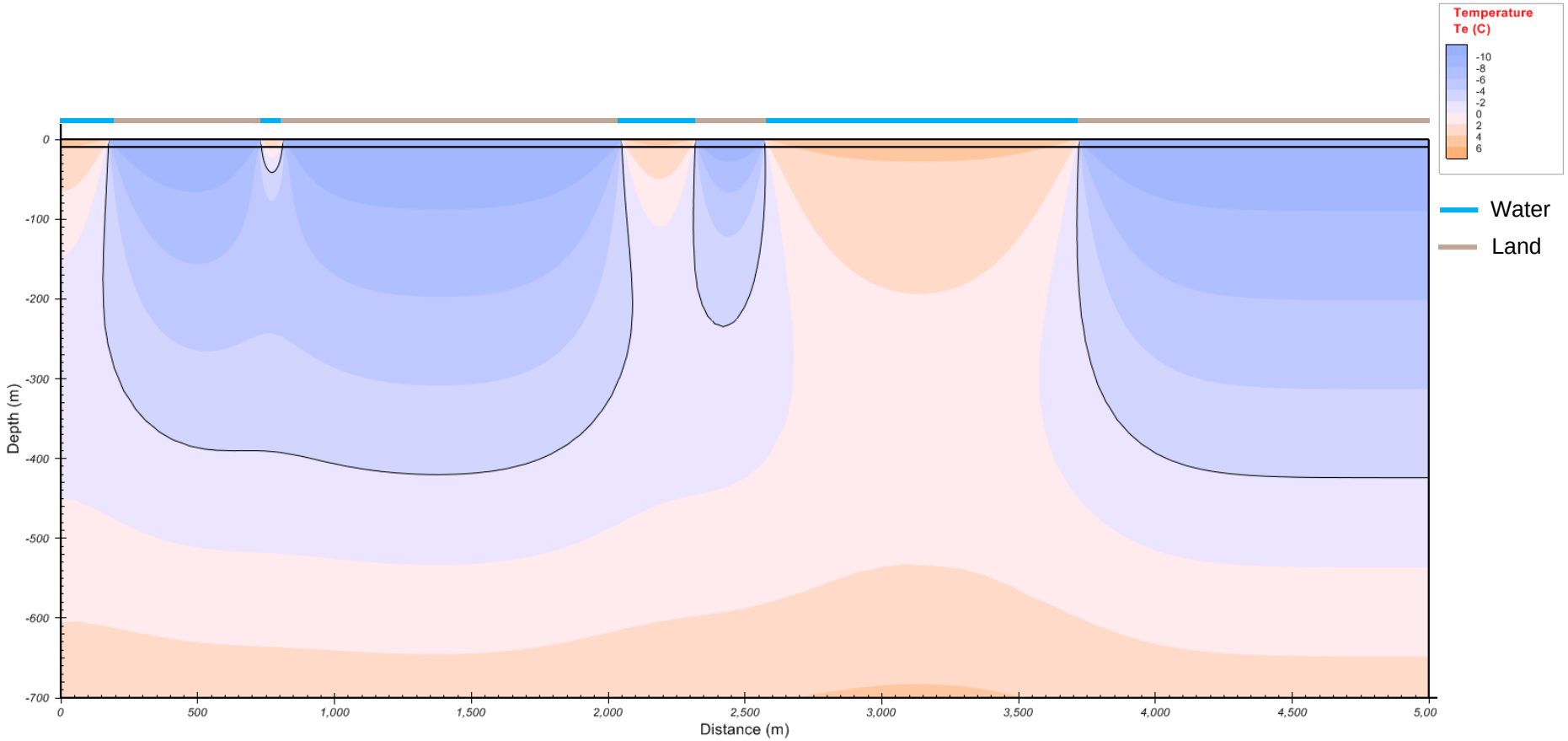
srk consulting	TMAC RESOURCES	Lake Talik Configuration
		Madrid North Mining Area – 2D Model Section T4
Job No: 1CT022.004 Filename: BostonDeepGroundTemperatures.pptx	HOPE BAY PROJECT	Date: 2/12/2016 | Approved: cws | Figure: **23**



Notes:

1. -2°C isotherm indicated with solid black line
2. Model section extends from west to east

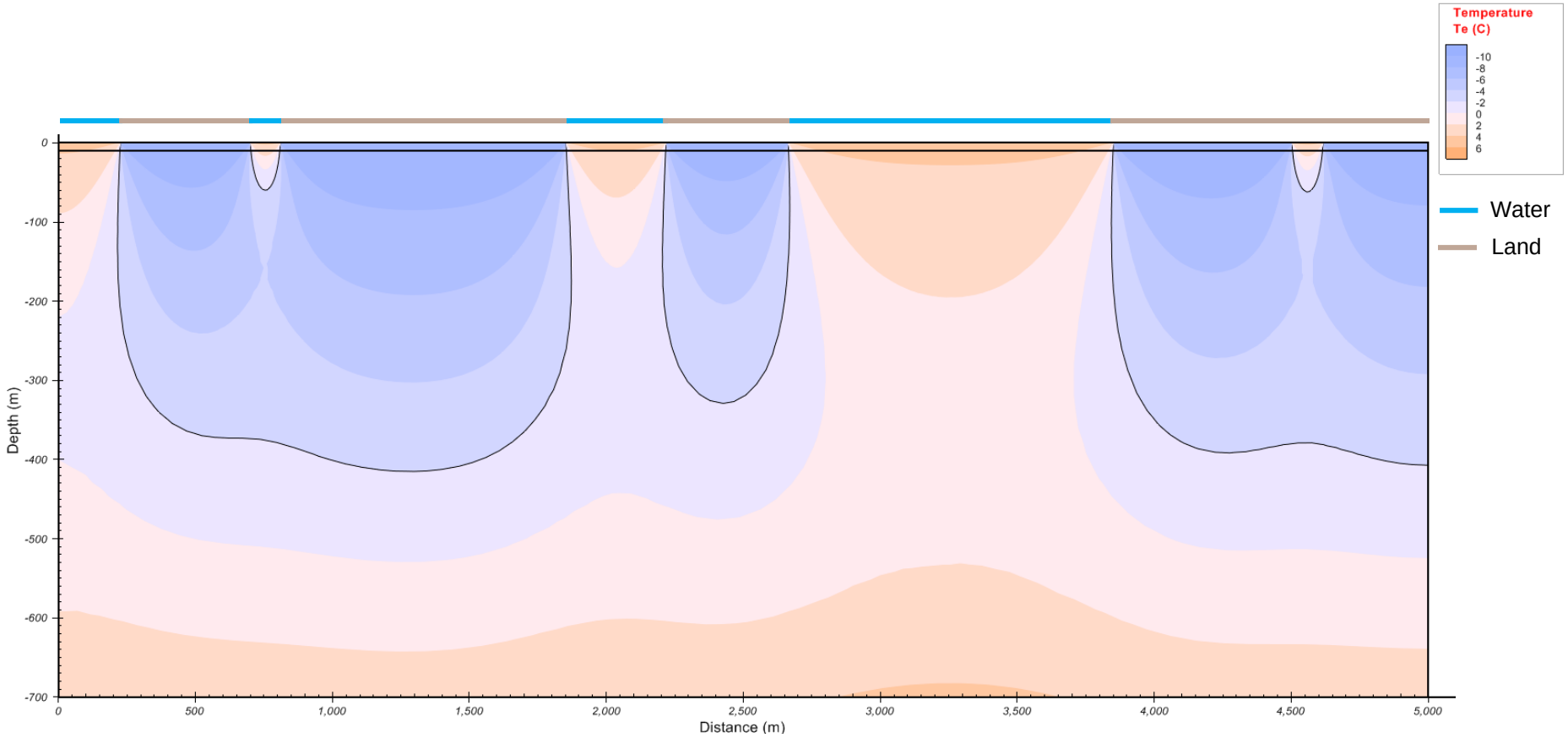
srk consulting	TMAC RESOURCES	Lake Talik Configuration
		Madrid North Mining Area – 2D Model Section T5
Job No: 1CT022.004 Filename: BostonDeepGroundTemperatures.pptx	HOPE BAY PROJECT	Date: 2/12/2016 | Approved: cws | Figure: **24**



Notes:

1. -2°C isotherm indicated with solid black line
2. Model section extends from west to east

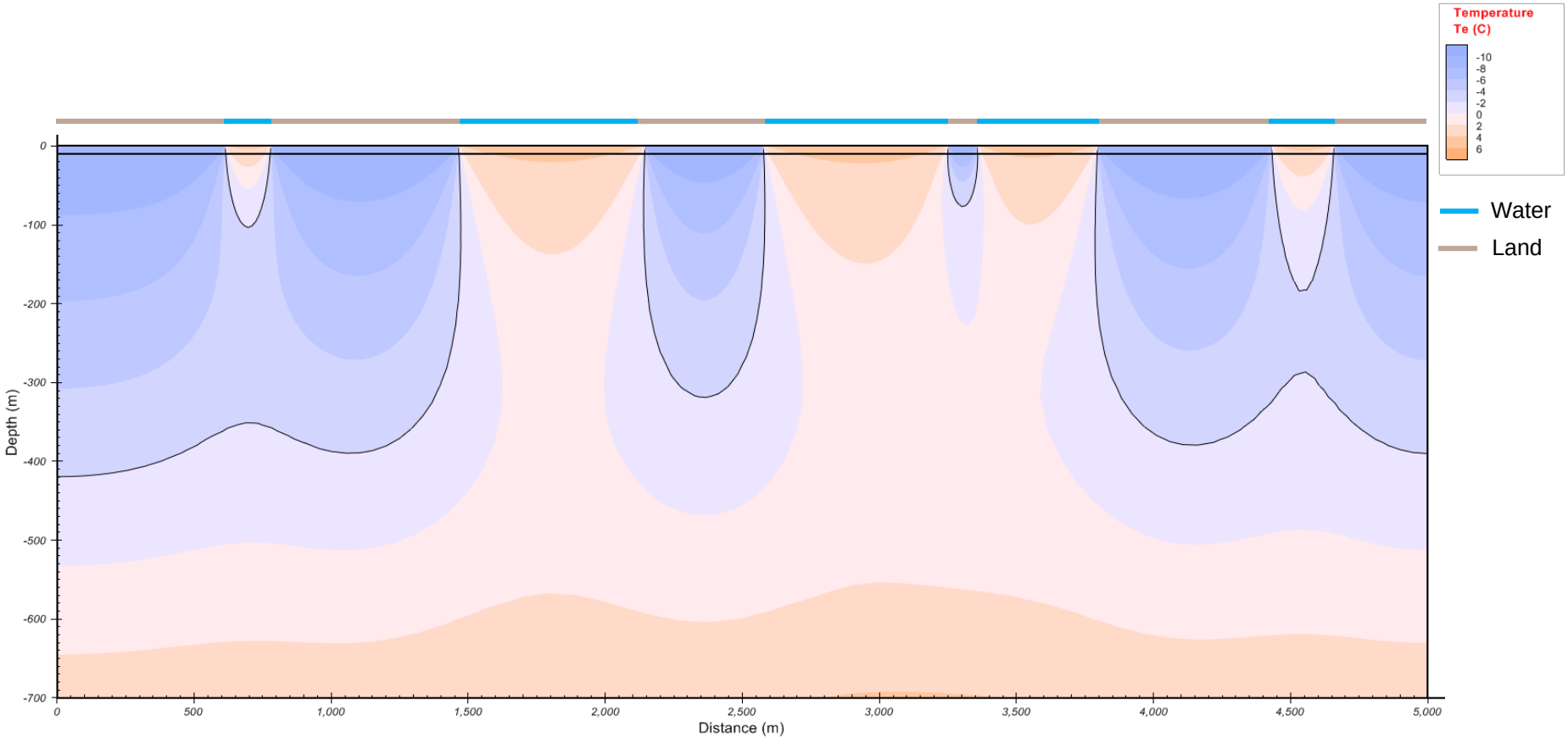
srk consulting	TMAC RESOURCES	Lake Talik Configuration
Job No: 1CT022.004 Filename: BostonDeepGroundTemperatures.pptx	HOPE BAY PROJECT	**Madrid South Mining Area – 2D Model Section T1**
		Date: 2/12/2016 | Approved: cws | Figure: **25**



Notes:

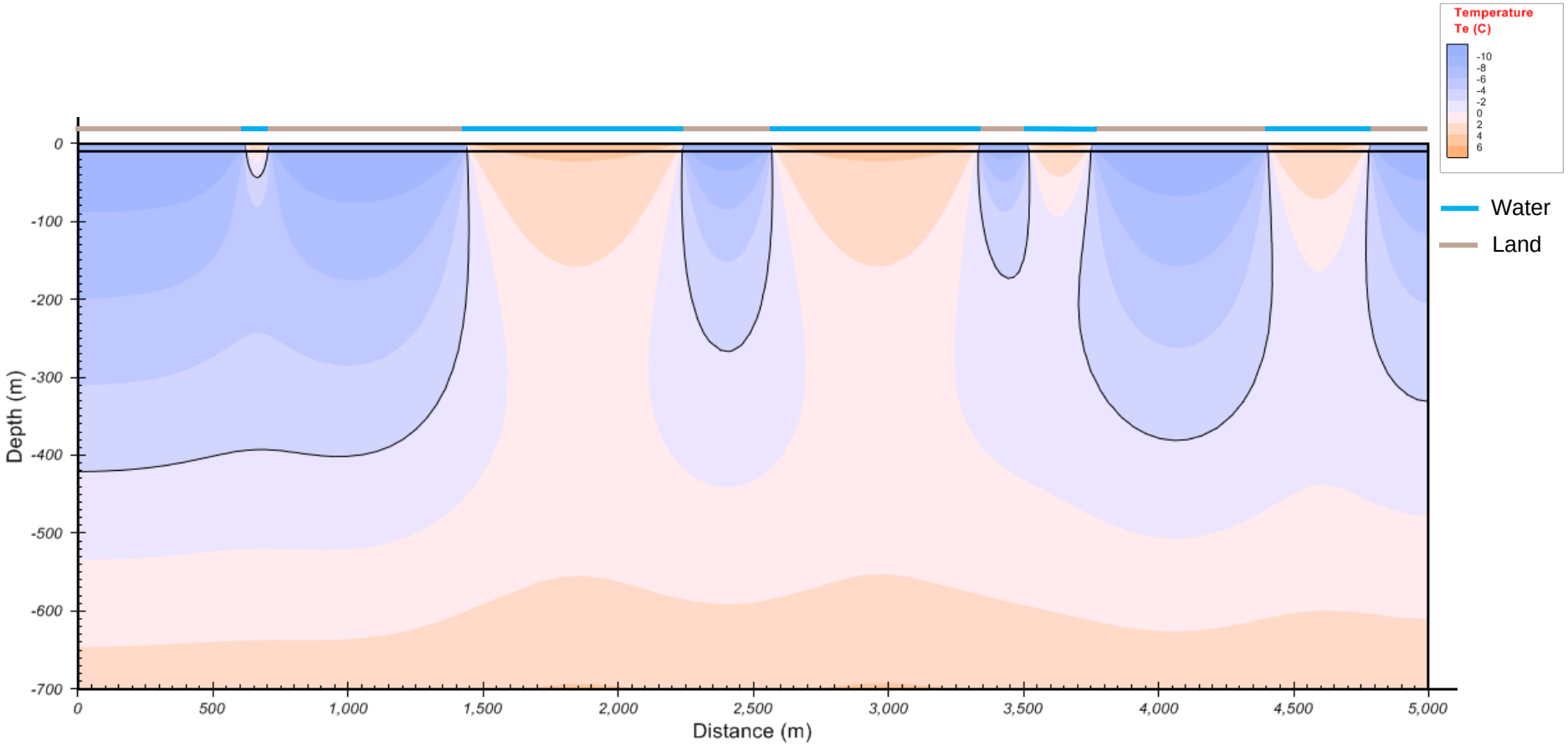
1. -2°C isotherm indicated with solid black line
2. Model section extends from west to east

srk consulting	TMAC RESOURCES	Lake Talik Configuration
		Madrid South Mining Area – 2D Model Section T2
Job No: 1CT022.004 Filename: BostonDeepGroundTemperatures.pptx	HOPE BAY PROJECT	Date: 2/12/2016 | Approved: cws | Figure: **26**



Notes:
1. -2°C isotherm indicated with solid black line
2. Model section extends from west to east

srk consulting	TMAC RESOURCES	Lake Talik Configuration
		Madrid South Mining Area – 2D Model Section T3
Job No: 1CT022.004 Filename: BostonDeepGroundTemperatures.pptx	HOPE BAY PROJECT	Date: 2/12/2016 | Approved: cws | Figure: **27**



Notes:
1. -2°C isotherm indicated with solid black line
2. Model section extends from west to east

srk consulting	MAC RESOURCES	Lake Talik Configuration
Job No: 1CT022.004 Filename: BostonDeepGroundTemperatures.pptx	HOPE BAY PROJECT	**Madrid South Mining Area – 2D Model Section T4**
		Date: 2/12/2016 | Approved: cws | Figure: **28**

Appendix H – 2020-2022 Doris Inflow Data

Project: Hope Bay Mine
Number: CAPR001915

Source: HopeBay_MineWaterSummary_CAPR001959_R00_ajb.xlsx
email from Andrea Bowie dated Dec14th 2022

Date	Total Doris Mine inflow (m^3/day)	Month Avg. Chloride (mg/L)	Month Avg. Chloride Load (kg/d)
01-Jan-18	0	20700	0
01-Feb-18	98	22575	2214
01-Mar-18	299	22100	6604
01-Apr-18	251	21767	5456
01-May-18	229	18400	4211
01-Jun-18	325	17860	5804
01-Jul-18	361	16975	6134
01-Aug-18	316	16440	5192
01-Sep-18	226	14665	3310
01-Oct-18	611	14125	8630
01-Nov-18	735	14700	10810
01-Dec-18	653	13650	8914
01-Jan-19	649	14350	9308
01-Feb-19	678	13000	8814
01-Mar-19	1091	12800	13966
01-Apr-19	781	12825	10017
01-May-19	828	12350	10221
01-Jun-19	912	10615	9684
01-Jul-19	914	10673	9760
01-Aug-19	947	11260	10664
01-Sep-19	1014	10923	11071
01-Oct-19	1016	11167	11344
01-Nov-19	1338	9890	13233
01-Dec-19	2352	9640	22671
01-Jan-20	2766	8690	24035
01-Feb-20	2171	8945	19417
01-Mar-20	2268	9345	21197
01-Apr-20	1979	10203	20194
01-May-20	1427	9173	13085
01-Jun-20	1201	9413	11305
01-Jul-20	1569	8730	13694
01-Aug-20	1258	8200	10314
01-Sep-20	1513	8053	12188
01-Oct-20	1607	8058	12946
01-Nov-20	1900	7788	14796
01-Dec-20	1348	7900	10650
01-Jan-21	1281	7300	9351
01-Feb-21	1540	7200	11088
01-Mar-21	1570	8473	13300
01-Apr-21	1822	7547	13752
01-May-21	1477	8906	13155
01-Jun-21	1934	8285	16027
01-Jul-21	1083	8028	8692
01-Aug-21	1106	7255	8023
01-Sep-21	729	6785	4946
01-Oct-21	1170	7677	8979
01-Nov-21	800	6740	5392
01-Dec-21	1577	6153	9705
01-Jan-22	1699	6735	11440
01-Feb-22	1720	6460	11113
01-Mar-22	1789	#N/A	#N/A
01-Apr-22	1618	#N/A	#N/A
01-May-22	1460	6193	9045
01-Jun-22	1535	4216	6472
01-Jul-22	1033	7030	7265
01-Aug-22	1360	6005	8169
01-Sep-22	1021	5293	5405